

# Twistor Inspired Methods in Perturbative Field Theory and Fuzzy Funnel

**Simon McNamara**

Thesis submitted for the degree of  
Doctor of Philosophy (PhD)  
of the University of London

Thesis Supervisor  
Prof. Bill Spence

Department of Physics,  
Queen Mary, University of London,  
Mile End Road,  
London, E1 4NS



August 2006

# Abstract

The first part of this thesis contains two new techniques for the calculation of scattering amplitudes in quantum field theories. These methods were inspired by the recent proposal of a correspondence between the weakly coupled regime of the maximally supersymmetric four dimensional gauge theory and a string theory in twistor space.

We show how generalised unitarity cuts in  $D=4-2\epsilon$  dimensions can be used to calculate efficiently complete one-loop scattering amplitudes in non-supersymmetric Yang-Mills theory. This approach naturally generates the rational terms in the amplitudes, as well as the cut-constructible parts. We then show that the ideas of the Britto, Cachazo, Feng and Witten tree-level on-shell recursion relation can also be applied to the calculation of finite one-loop amplitudes in pure Einstein gravity.

The second part of this thesis is a study of the nonabelian phenomena associated with  $D$ -branes. Specifically we study the nonabelian bionic brane intersection in which a stack of many coincident  $D1$ -branes expand via a non-commutative spherical configuration into a collection of higher dimensional  $D$ -branes orthogonal to the original stack of  $D1$ -branes.

We suggest a construction of monopoles in dimension  $2k+1$  from fuzzy funnels. We then perform two charge calculations related to this construction. This leads to a new formula for the symmetrised trace quantity. This new formula for the symmetrised trace is then used to study the collapse of a spherical bound state of  $D0$ -branes.

# Declaration

I declare that the work in this thesis is my own, unless otherwise stated and resulted from collaborations with Andreas Brandhuber, Costis Papageorgakis, Sanjaye Ramgoolam, Bill Spence and Gabriele Travaglini. Some of the content of this thesis has been published in the papers [1] and [2].

Simon McNamara

# Acknowledgements

It is a pleasure to thank my inspirational supervisor Bill Spence and collaborators Andreas Brandhuber, Costis Papageorgakis, Sanjaye Ramgoolam, and Gabriele Travaglini. Thank you for so many fun hours of doing research. You have taught me a huge number of fascinating things. Thank you for all your help.

A big thank you to my friends James Bedford, Samantha Bidwell, John Booth, Peter Brooks, Micheal Coad, Will Creedy, Aneta Dybek, Jannick Guillome, Paul Hafner, David Herbert, Xuan Kroeger, Fanny Lessous, Richard Lewis, Caroline Middleton-Hockin, David Mulryne, Simon Nickerson, Ronald Reid-Edwards, John Richards, John Ward, and Mark Wesker. Thanks also to all the members of Harpenden Cricket Club and the choir of St Martin-in-the-Fields.

Finally thank you Mum, Dad and Sarah for looking after me.

# Table of contents

ABSTRACT	2
DECLARATION	3
ACKNOWLEDGEMENTS	4
INTRODUCTION	12
1 PERTURBATIVE FIELD THEORY AND TWISTORS	14
1.1 Introduction . . . . .	14
1.2 Amplitudes in perturbative field theory . . . . .	17
1.2.1 Feynman rules . . . . .	17
1.2.2 Colour stripped amplitudes . . . . .	18
1.2.3 The spinor helicity formalism . . . . .	19
1.3 Twistors . . . . .	22
1.3.1 The twistor transform . . . . .	22
1.3.2 The MHV amplitude in twistor space . . . . .	23
1.3.3 Twistor string theory . . . . .	26
1.4 Field theoretic MHV rules . . . . .	27
1.4.1 The tree level CSW rules. . . . .	27
1.4.2 The one loop BST rules . . . . .	29
1.4.3 Mansfield's proof of the CSW rules . . . . .	30
1.5 BDDK's two-particle unitarity cuts . . . . .	31
1.6 Generalised Unitarity . . . . .	34
1.6.1 Quadruple cuts in $\mathcal{N}=4$ Super Yang-Mills . . . . .	35

1.6.2	Triple cuts in $\mathcal{N}=1$ Super Yang-Mills . . . . .	37
1.7	The BCFW recursion relation . . . . .	39
1.7.1	A four-point example . . . . .	40
1.7.2	Generalisations of BCFW recursion . . . . .	42
1.7.3	Risager's proof of the CSW rules . . . . .	43
2	GENERALISED UNITARITY FOR PURE YANG-MILLS . . . . .	45
2.1	Generalised Unitarity in $D = 4 - 2\epsilon$ Dimensions . . . . .	45
2.2	The one-loop $++++$ amplitude . . . . .	49
2.3	The one-loop $-+++$ amplitude . . . . .	52
2.4	The one-loop $--++$ amplitude . . . . .	58
2.5	The one-loop $-+-+$ amplitude . . . . .	61
2.6	The one-loop $++++$ amplitude . . . . .	66
2.7	Future directions . . . . .	69
2.7.1	Higher point QCD amplitudes . . . . .	69
2.7.2	Higher loops, integrability and the AdS/CFT correspondence . . . . .	70
3	ON-SHELL RECURSION RELATIONS FOR ONE-LOOP GRAVITY . . . . .	73
3.1	Introduction . . . . .	73
3.2	The all-plus amplitude . . . . .	76
3.2.1	The five-point all-plus amplitude . . . . .	77
3.2.2	The six-point all-plus amplitude . . . . .	80
3.3	The one-loop $-+++$ amplitude . . . . .	84
3.3.1	$-+++$ in Yang-Mills . . . . .	84
3.3.2	$-+++$ in Gravity . . . . .	85
3.4	The one-loop $-++++$ Gravity amplitude . . . . .	88
3.5	The description of nonstandard factorisations . . . . .	93
3.5.1	$-++++$ in Yang-Mills with $ 1\rangle,  3\rangle$ shifts . . . . .	93
3.5.2	$-+++$ in gravity with $ 1\rangle,  2\rangle,  3\rangle,  4\rangle$ shifts . . . . .	95
3.6	Avoiding nonstandard factorisations . . . . .	96
3.6.1	The $-++++$ Yang-Mills amplitude . . . . .	97

4	THE ADHM CONSTRUCTION AND D-BRANE CHARGES	100
4.1	Introduction . . . . .	100
4.2	The ADHM construction . . . . .	106
4.2.1	Review of Nahm's construction for $D1 \perp D3$ . . . . .	106
4.2.2	Generalisation to higher dimensions . . . . .	109
4.2.3	Construction of the Monopole . . . . .	110
4.3	Charge calculations . . . . .	111
4.3.1	Monopole charge calculation . . . . .	111
4.3.2	Proof of the identity involving $N(k, n)$ and $N(k - 1, n + 1)$ . . . . .	112
4.3.3	Fuzzy funnel charge calculation. . . . .	113
4.4	Symmetrised trace calculations . . . . .	115
4.4.1	Chord diagram calculations . . . . .	117
4.4.2	The large $n$ expansion of $\text{Str}(X_i X_i)^m$ . . . . .	121
4.4.3	An exact formula for the symmetrised trace . . . . .	124
5	FINITE $N$ EFFECTS ON THE COLLAPSE OF FUZZY SPHERES	126
5.1	Introduction . . . . .	126
5.2	Lorentz invariance and the physical radius . . . . .	127
5.3	The fuzzy $S^2$ at finite $n$ . . . . .	129
5.3.1	The $D1 \perp D3$ intersection at finite- $n$ . . . . .	131
5.3.2	Finite $N$ dynamics as a quotient of free multi-particle dynamics . . . . .	132
5.4	Physical properties of the finite $N$ solutions . . . . .	133
5.4.1	Special limits where finite $n$ and large $n$ formulae agree . . . . .	133
5.4.2	Finite $N$ effects . . . . .	135
5.4.3	Distance to blow-up in $D1 \perp D3$ . . . . .	138
5.5	Towards a generalisation to higher even-dimensional fuzzy-spheres . . . . .	139
5.6	Summary and Outlook . . . . .	141
A	INTEGRAL IDENTITIES	143
A.1	Scalar box, triangle and bubble integrals . . . . .	143
A.2	Scalar Integral Identities . . . . .	144
A.3	PV reduction . . . . .	145

B	GRAVITY AMPLITUDE CHECKS	148
B.1	The VegasShift[n] Mathematica command . . . . .	148
B.2	Other shifts of the $- + + + +$ gravity amplitude . . . . .	149
B.2.1	The $ 4\rangle,  5\rangle$ shifts . . . . .	149
B.2.2	The $ 2\rangle,  1\rangle$ shifts . . . . .	151
C	STR CALCULATIONS USING THE HIGHEST WEIGHT METHOD	152
C.1	Review of spin half for $SO(3)$ . . . . .	153
C.2	Derivation of symmetrised trace for minimal $SO(2l + 1)$ representation . . .	154
C.3	Derivation of spin one symmetrised trace for $SO(3)$ . . . . .	155
C.4	Derivation of next-to-minimal representation for $SO(2l + 1)$ . . . . .	156

# List of Figures

1.1	<i>The result that MHV amplitudes are supported on degree one, genus zero curves in twistor space is equivalent to the fact that the MHV amplitude is a function of only the <math>\lambda</math>s and not of the <math>\tilde{\lambda}</math>s. . . . .</i>	24
1.2	<i>The twistor space localisation of tree amplitudes. Diagram (a) shows the localisation of an amplitude with three negative helicity gluons and diagram (b) an amplitude with four negative helicity gluons. . . . .</i>	25
1.3	<i>The MHV diagrams associated with the CSW construction of the simplest next-to-MHV tree-level amplitude <math>A(1^-, 2^-, 3^-, 4^+, 5^+)</math>. It is conventional to consider amplitudes where all the momenta are outgoing, so an internal leg joining two amplitudes will have different helicities labels at each end. . . . .</i>	28
1.4	<i>The BST construction of the MHV one-loop amplitude in <math>\mathcal{N}=4</math> super Yang-Mills by sewing two tree-level MHV amplitudes together. . . . .</i>	29
1.5	<i>The <math>s</math> channel cut of a one-loop amplitude. . . . .</i>	32
1.6	<i>A simple quadruple cut to evaluate the coefficient of a one-mass box in the five-point MHV amplitude in <math>\mathcal{N}=4</math> Super Yang-Mills. . . . .</i>	35
1.7	<i>The diagrams in the triple cut of the one-loop MHV amplitude for <math>\mathcal{N}=1</math> Super-Yang Mills. . . . .</i>	38
1.8	<i>A diagrammatic representation of the BCFW recursion relation. The sum is over all factorisations into pairs of amplitudes and the possible helicity of the intermediate state. . . . .</i>	40
1.9	<i>The recursive diagram in the BCFW construction of <math>A(1^-, 2^+, 3^-, 4^+)</math>. . . . .</i>	41
2.1	<i>One of the two quadruple-cut diagrams for the amplitude <math>1^+2^+3^+4^+</math>. This diagram is obtained by sewing tree amplitudes (represented by the blue bubbles) with an external positive-helicity gluon and two internal scalars of opposite ‘helicities’. There are two such diagrams, which are obtained one from the other by flipping all the internal helicities. These diagrams are equal so that the full result is obtained by doubling the contribution from the diagram in this Figure. The same remark applies to all the other diagrams considered in this chapter. . . . .</i>	50

2.2	<i>One of the possible three-particle cut diagrams for the amplitude <math>1^+2^+3^+4^+</math>. The others are obtained from this one by cyclic relabelling of the external particles.</i>	51
2.3	<i>The quadruple cut for the amplitude <math>1^-2^+3^+4^+</math>.</i>	53
2.4	<i>The two inequivalent triple cuts for the amplitude <math>1^-2^+3^+4^+</math>.</i>	55
2.5	<i>The quadruple cut for the amplitude <math>1^-2^-3^+4^+</math>.</i>	59
2.6	<i>The two inequivalent triple cuts for the amplitude <math>1^-2^-3^+4^+</math>.</i>	60
2.7	<i>The quadruple cut for the amplitude <math>1^-2^+3^-4^+</math>.</i>	62
2.8	<i>The only independent triple cut for the amplitude <math>1^-2^+3^-4^+</math> (the others are obtained from this one by cyclic relabelling of the external gluons).</i>	63
2.9	<i>One of the quadruple cuts for the amplitude <math>1^+2^+3^+4^+5^+</math>.</i>	66
2.10	<i>A puzzling quadruple cut of the six point all-plus amplitude.</i>	69
3.1	<i>The diagram in the recursive expression for <math>M_5^{(1)}(1^+, 2^+, 3^+, 4^+, 5^+)</math> associated with the pole <math>\langle \hat{1}\hat{2} \rangle = 0</math>. The amplitude labelled by a <math>T</math> is a tree-level amplitude and the one labelled by <math>L</math> is a one-loop amplitude.</i>	78
3.2	<i>The diagram in the recursive expression for <math>M_5^{(1)}(1^+, 2^+, 3^+, 4^+, 5^+)</math> associated with the pole <math>\langle \hat{1}5 \rangle = 0</math>.</i>	79
3.3	<i>The diagram in the recursive expression for <math>M_5^{(1)}(1^+, 2^+, 3^+, 4^+, 5^+, 6^+)</math> associated with the pole <math>\langle \hat{2}\hat{3} \rangle = 0</math>.</i>	81
3.4	<i>The diagram in the recursive expression for <math>M_5^{(1)}(1^+, 2^+, 3^+, 4^+, 5^+, 6^+)</math> associated with the pole <math>\langle \hat{1}6 \rangle = 0</math>.</i>	82
3.5	<i>The recursive construction of <math>A_4^{(1)}(1^-, 2^+, 3^+, 4^+)</math> via shifting <math> 1\rangle</math> and <math> 2\rangle</math> involves this nonstandard factorisation diagram.</i>	85
3.6	<i>The recursive construction of <math>M_4^{(1)}(1^-, 2^+, 3^+, 4^+)</math> via shifting <math> 1\rangle</math> and <math> 2\rangle</math> involves these two nonstandard factorisation diagrams.</i>	87
3.7	<i>The diagram in the recursive expression for <math>M_5^{(1)}(1^-, 2^+, 3^+, 4^+, 5^+)</math> corresponding to a simple-pole associated with <math>[\hat{1}5] = 0</math>.</i>	89
3.8	<i>The diagram in the recursive expression for <math>M_5^{(1)}(1^-, 2^+, 3^+, 4^+, 5^+)</math> corresponding to a simple-pole associated with <math>\langle \hat{2}3 \rangle = 0</math>.</i>	90
3.9	<i>The diagram in the recursive expression for <math>M_5^{(1)}(1^-, 2^+, 3^+, 4^+, 5^+)</math> corresponding to the double-pole associated with <math>\langle \hat{2}3 \rangle = 0</math>.</i>	91
3.10	<i>The diagrams in the recursive expression for <math>A_5^{(1)}(1^-, 2^+, 3^+, 4^+, 5^+)</math> with shifts on <math> 1\rangle</math> and <math> 3\rangle</math>.</i>	94
3.11	<i>The diagrams in the <math> 1\rangle  2\rangle</math> shift of <math>A_5^{(1)}(1^-, 2^+, 3^+, 4^+, 5^+)</math>.</i>	97
3.12	<i>The diagram in the <math> 4\rangle  5\rangle</math> shift of <math>A_5^{(1)}(1^-, 2^+, 3^+, 4^+, 5^+)</math>.</i>	98

A.1	<i>Kinematics of the bubble and triangle integral functions studied in this Appendix.</i>	145
B.1	<i>The diagram associated with <math>\langle 1\hat{5} \rangle = 0</math>, with shifts on <math> 4\rangle,  5\rangle</math>.</i>	149
B.2	<i>The diagram associated with <math>[1\hat{4}] = 0</math>, with shifts on <math> 4\rangle,  5\rangle</math>.</i>	149
B.3	<i>The standard factorisation diagram associated with <math>\langle 2\hat{5} \rangle = 0</math>, with shifts on <math> 4\rangle,  5\rangle</math>.</i>	150
B.4	<i>The nonstandard factorisation diagram associated with <math>\langle 2\hat{5} \rangle = 0</math>, with shifts on <math> 4\rangle,  5\rangle</math>.</i>	150
B.5	<i>The diagram associated with <math>\langle \hat{1}5 \rangle = 0</math> with shifts on <math> 2\rangle,  1\rangle</math>.</i>	151

# Introduction

The first three chapters of this thesis are concerned with twistor inspired methods in perturbative quantum field theory. Chapter 1 contains an introduction to this subject. Chapter 2 shows that generalised unitarity in  $D$ -dimensions can be used to compute amplitudes in one-loop QCD. Chapter 3 shows that finite one-loop gravity amplitudes can be computed using on-shell recursion. The remaining two chapters are about fuzzy funnels. Chapter 4 contains a study of the duality between monopoles and fuzzy funnels. In Chapter 5 we consider finite  $n$  effects on the collapse of fuzzy spheres.

Chapter 1 provides an introduction to the remarkable recent progress in understanding perturbative quantum field theory which was initiated by Witten's proposal of a duality between weakly coupled  $\mathcal{N}=4$  Super Yang-Mills and a string theory in twistor space  $\mathbb{CP}^{3|4}$ . This duality explains the remarkable simplicity of certain amplitudes which is hidden by standard Feynman diagram calculations. The unexpected beauty of scattering amplitudes is exposed by writing colour stripped amplitudes in the spinor helicity formalism. The notion of a twistor and the twistor transform of the maximally helicity violating amplitude (MHV) are then reviewed. We then summarise the twistor space localisation of general amplitudes and describe the string theoretic proposal. The twistor string theory has inspired many new and efficient field theory techniques for the calculation of amplitudes. We review the remarkable new insight that tree and loop level amplitudes can be built by joining multiple MHV amplitudes together. Finally we review the twistor inspired field theory techniques of generalised unitarity and on-shell recursion.

In chapter 2 we show how generalised unitarity cuts in  $D = 4 - 2\epsilon$  dimensions can be used to calculate efficiently complete one-loop scattering amplitudes in non-supersymmetric Yang-Mills theory. This approach naturally generates the rational terms in the amplitudes, as well as the cut-constructible parts. We test the validity of our method by re-deriving the one-loop  $++++$ ,  $-+++$ ,  $--++$ ,  $-+-+$  and  $++++$  gluon scattering amplitudes using generalised quadruple cuts and triple cuts in  $D$  dimensions. We observe that triple cuts are sufficient to compute complete amplitudes. Thus we can avoid the calculation of two-particle cuts which are the most technically challenging to evaluate. In principle this new method can be applied to more complicated and currently unknown amplitudes which are important for the experimental programmes at hadron colliders.

In chapter 3 we show that the ideas of the Britto, Cachazo, Feng and Witten tree-level on-shell recursion relation can also be applied to the calculation of finite one-loop amplitudes in pure Einstein gravity. We show how to compute the five and six point all-plus one-loop gravity amplitudes without having to consider boundary terms. We then consider the recursive construction of the known one-loop  $-+++$  gravity amplitude and observe that the factorisation properties in complex momenta of this gravity amplitude are similar to those of the one-loop  $-+++$  amplitude in Yang-Mills. The new issue that arises for the amplitude with a single negative helicity is the appearance of the one-loop three-point all-plus nonstandard factorisation which gives single and double pole contributions to the amplitude. We then attempt to calculate the unknown one-loop  $-++++$  gravity amplitude using on-shell recursion. Unfortunately we do not understand the single pole under the double pole contributions of the three-point one-loop all-plus factorisation in this amplitude so are unable to calculate the full answer. We review an unsuccessful proposal for this missing term, and an unsuccessful attempt to avoid the nonstandard factorisations using auxiliary recursion relations.

In chapter 4 we consider the nonabelian bionic brane intersection in which a stack of many coincident  $D1$ -branes expand via a non-commutative spherical configuration into a collection of higher dimensional  $D$ -branes orthogonal to the original stack of  $D1$ -branes. We suggest a construction of monopoles in dimension  $2k + 1$  from fuzzy funnels. For  $k = 1$  this construction coincides with Nahm's construction of monopoles, which is an adaptation of the Atiyah, Drinfeld, Hitchin and Manin construction of instantons. For  $k = 1, 2, 3$  this gives a finite  $n$  realisation of the duality between  $D1$ -brane and  $D(2k + 1)$ -brane world-volume pictures of the non-commutative bionic brane intersection. We then perform two charge calculations related to this construction. First we calculate the charge of the monopole and get an answer in precise agreement with the size of the matrices in the fuzzy funnel. Secondly we calculate the charge of the fuzzy funnel. To get this charge to agree with the size of the matrices in the monopole beyond leading orders in  $1/n$ , we propose a speculative use of the symmetrised trace. A matching of the terms of the symmetrised trace with the number of branes expected from the charge calculation then leads to a new and surprisingly simple formula for the symmetrised trace quantity.

In chapter 5 we consider finite  $n$  effects on the time evolution of fuzzy 2-spheres moving in flat space-time. We use the new formula for the symmetrised trace found in chapter 4 to show that exotic bounces of the kind seen in the  $1/n$  expansion do not exist at finite  $n$ .

# CHAPTER 1

## PERTURBATIVE FIELD THEORY AND TWISTORS

### 1.1 Introduction

There are many interesting things yet to be understood about four-dimensional quantum gauge theories like QCD. It has long been thought that phenomena such as quark confinement were related to strings. In 1974 't Hooft [3] presented a purely diagrammatic argument suggesting that a gauge theory should have a dual description as a string theory. This proposal did not identify which string theory is equivalent to four-dimensional gauge theory and little progress was made until in 1997 Maldacena [4] proposed that the maximally supersymmetric gauge theory  $\mathcal{N}=4$  Super Yang-Mills was equivalent in the 't Hooft sense to Type IIB superstring theory on the target space  $\text{AdS}_5 \times \mathbb{S}^5$ .

The 't Hooft expansion relates the strongly-coupled regime of a gauge theory to a weakly-coupled string theory. The Maldacena correspondence therefore provides a perturbative window into non-perturbative physics. Other dualities including mirror symmetry and Montonen-Olive duality have demonstrated that the character of quantum field theories is radically different in different parameter regimes. It would therefore be fascinating both theoretically and phenomenologically to find a duality complementary to Maldacena's, giving a weakly-coupled string theoretic description of the weakly-coupled gauge theory. A key step in this direction was made in 2003 by Witten [5]. He suggested a remarkable duality between weakly-coupled  $\mathcal{N}=4$  super Yang Mills and a weakly-coupled  $B$ -model topological string theory on the super Calabi-Yau manifold  $\mathbb{CP}^{3|4}$ . Intriguingly, the target space  $\mathbb{CP}^{3|4}$  has six bosonic real dimensions which are related to the usual four dimensional space-time of the quantum field theory by the twistor construction of Penrose [6].

In principle the perturbative analysis of a gauge theory in terms of Feynman diagrams is under control, but in practice the number of such diagrams grows very rapidly with the number of external legs and the number of loops. Strikingly, after simplifying the huge number of Feynman diagrams, the final answer is often simple and elegant. This strongly hints at the existence of an underlying dual string theoretic description and was the challenge set by Parke and Taylor in 1986 [7] when they discovered the expression for the tree-level maximally helicity violating (MHV) amplitude. An MHV amplitude is one where all but

two of the external gluons have the same helicity. When the MHV amplitude is written in the spinor helicity formalism, it is given by a simple holomorphic function of just one of the two spinors needed to describe the massless particles. Witten observed that all tree-level gauge theory amplitudes, after a Fourier transform to twistor space, are supported on holomorphically embedded algebraic curves. For the case of MHV amplitudes these curves are simply straight lines. This beautiful geometrical localisation is totally hidden by the Feynman diagram expansion and led to the string theoretic proposal that gauge theory amplitudes could be obtained by integrating over the moduli space of  $D1$ -brane instantons.

Witten's insight has motivated a revolution in our understanding of perturbative gauge theory. Some of the most fruitful advances inspired by twistor string theory have been powerful new diagrammatic rules for field theory calculations. In March 2004, Cachazo, Svrček and Witten (CSW) [8] proposed elevating the MHV amplitude to an effective vertex in a new perturbative expansion of the tree-level Yang-Mills theory. They observed that amplitudes with more than two negative helicity gluons could be computed by joining these effective vertices together with scalar propagators. In twistor string theory there are several different prescriptions for integrating over curves. When calculating tree level gauge theory amplitudes, one can either use a single instanton of degree  $d$ , or alternatively  $d$  completely disconnected curves each of degree one connected by twistor propagators. The disconnected prescription gives the remarkably efficient MHV diagram construction. For example, the amplitude with three negative helicity and three positive helicity gluons involves 220 Feynman diagrams [9, 10], but can be reconstructed from just 6 diagrams in CSW's diagrammatic approach.

Despite its many successful achievements, twistor string theory leaves us with many interesting open questions. It is clear that the twistor string theory proposed by Witten fails at loop level because amplitudes receive contributions from closed string, conformal supergravity states [11]. Surprisingly, a formalism which glues tree-level MHV vertices together to form loops has been proposed by Brandhuber, Spence and Travaglini (BST) [12] and used to correctly reproduce the one-loop MHV amplitude in supersymmetric Yang-Mills. The twistor space localisation of gauge theory amplitudes therefore persists beyond tree level to the quantum theory. Their method unified the MHV vertex construction with the celebrated unitarity-based, cut-constructibility approach of Bern, Dixon, Dunbar and Kosower (BDDK) [13, 14]. This strongly suggests that there may be a version of twistor string theory dual to pure  $\mathcal{N} = 4$  super Yang-Mills at loop level. Another open problem associated with the duality at loop level is how the infrared singularities of the gauge theory amplitudes arise in the string theory. In the one-loop amplitude the infrared divergent terms are those where one of the MHV vertices is a four-particle vertex. In twistor space this corresponds to a localisation on a disjoint union of lines. So it is possible that the transformation to twistor space also disentangles the infra-red divergences of the amplitudes.

The rest of this chapter provides an introduction to the recent progress in understanding perturbative field theory. In the next section we define amplitudes via the Feynman rules. In sections 1.2.2 and 1.2.3 we introduce colour stripping and the spinor helicity formalism, which are two notational techniques that expose the hidden beauty of scattering amplitudes. The notion of a twistor and the twistor transform of the MHV amplitude are reviewed in section 1.3. We then summarise the twistor space localisation of amplitudes with more than two negative helicity gluons and briefly describe the string theoretic proposal that provides a natural framework for the twistor space properties of amplitudes. In section 1.4 we review the twistor string inspired MHV rules, which calculate tree-level amplitudes with more than two negative helicity gluons by sewing MHV amplitudes together and also correctly compute the one-loop MHV amplitude in supersymmetric theories by joining a pair of tree-level MHV amplitudes together to form a loop.

In addition to the MHV rules, the twistor string has inspired many new and efficient methods for the calculation of scattering amplitudes. One of these new techniques is the notion of generalised four-dimensional unitarity [15]. We review the background to this powerful tool in section 1.6. In Chapter 2 we present the new technique of  $D = 4 - 2\epsilon$  generalised unitarity. We show how generalised unitarity cuts in  $D = 4 - 2\epsilon$  dimensions can be used to calculate efficiently complete one-loop scattering amplitudes in non-supersymmetric Yang-Mills theory. This approach naturally generates the rational terms in the amplitudes, as well as the cut-constructible parts. Chapter 2 is based on the work [1].

The recursion relation of Britto, Cachazo, Feng and Witten (BCFW) [16, 17] is another elegant and systematic method for the computation of tree-level Yang-Mills amplitudes. In section 1.7 we review the proof of this recursion relation and some of its applications. In chapter 3 we show that the ideas of BCFW recursion extend with many complications to the finite amplitudes of one-loop pure Einstein gravity. This generalisation has a close connection with the use of recursion relations in the calculation of the rational parts of one-loop QCD amplitudes by Bern, Dixon and Kosower (BDK) [18]. This idea is remarkable because it enables one to calculate very efficiently at one-loop without really performing any loop integrals.

The calculation and understanding of scattering amplitudes is interesting because as well as uncovering the hidden beauty of field theory and linking gauge theory to string theory, it has also allowed us to calculate more efficiently in realistic theories of nature. Asymptotic freedom [19, 20] allows us to calculate scattering amplitudes as a perturbative expansion in the strong coupling constant  $\alpha_s(\mu)$ , evaluated at a large momentum scale  $\mu$  where the theory is weakly coupled. However, at hadron colliders the leading order tree-amplitudes do not suffice to get a reasonable uncertainty and corrections from next to leading order are important. A precise knowledge of QCD backgrounds for events involving several jets is needed for maximising the potential for the discovery of physics beyond the Standard Model at colliders like the Large Hadron Collider.

## 1.2 Amplitudes in perturbative field theory

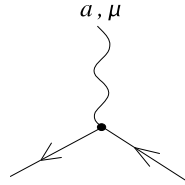
### 1.2.1 Feynman rules

The Lagrangian for a non-abelian gauge theory is

$$L = \bar{\psi}(i\gamma^\mu\partial_\mu - m)\psi - \frac{1}{4}(\partial_\mu A_\nu^a - \partial_\nu A_\mu^a)^2 + gA_\mu^a\bar{\psi}\gamma^\mu t^a\psi - gf^{abc}(\partial_\mu A_\nu^a)A^{\mu b}A^{\nu c} - \frac{1}{4}g^2(f^{cab}A_\mu^aA_\nu^b)(f^{ecd}A^{\mu a}A^{\nu d}) \quad (1.1)$$

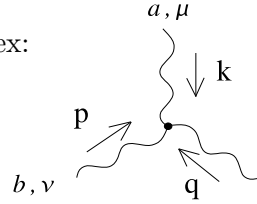
Observable quantities are then calculated using perturbation theory. The textbook technique for performing this procedure is to draw and then compute Feynman diagrams. The Feynman diagrams for a non-abelian gauge theory in Feynman gauge are given by:

Fermion vertex:



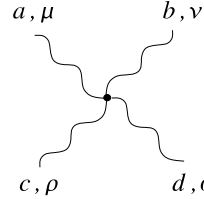
$$= ig\gamma^\mu t^a$$

Three-point gluon vertex:



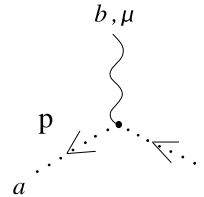
$$= gf^{abc}[g^{\mu\nu}(k-p)^\rho + g^{\nu\rho}(p-q)^\mu + g^{\rho\mu}(p-k)^\nu]$$

Four-point gluon vertex:



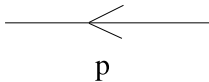
$$= -ig^2[f^{abe}f^{cde}(g^{\mu\rho}g^{\nu\sigma} - g^{\mu\sigma}g^{\nu\rho}) + f^{ace}f^{bde}(g^{\mu\nu}g^{\rho\sigma} - g^{\mu\sigma}g^{\nu\rho}) + f^{ade}f^{bce}(g^{\mu\nu}g^{\rho\sigma} - g^{\mu\rho}g^{\nu\sigma})]$$

Ghost vertex:



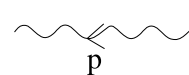
$$= -gf^{abc}p^\mu$$

Fermion propagator



$$= \frac{i(\gamma^\mu p_\mu + m)\delta_{ab}}{p^2 - m^2 + i\epsilon}$$

Gluon propagator



$$= \frac{-ig_{\mu\nu}\delta_{ab}}{p^2 + i\epsilon}$$

The first part of this thesis is about the calculation of amplitudes, however we will not use the Lagrangian or the Feynman rules very much at all. One of the themes of the thesis

is that the Feynman rules hide the simplicity of scattering amplitudes. In the next two sections we introduce colour stripping and the spinor helicity formalism. These are the formalisms which originally exposed the surprising simplicity of scattering amplitudes.

### 1.2.2 Colour stripped amplitudes

In pure Yang-Mills an  $n$ -point amplitude is a function of the  $i$ th gluon's momentum vector  $p_i$ , polarisation vector  $\epsilon_i$  and colour index  $a_i$ . At tree level, the interactions are planar, so a gluon amplitude can be written as a sum of single trace terms. This observation leads to the colour decomposition of the gluon tree amplitude [9, 10, 21].

$$A_n^{\text{tree}}(p_i, \epsilon_i, a_i) = g^{n-2} \sum_{\sigma \in S_n / \mathbf{Z}_n} \text{Tr}(T^{a_{\sigma(1)}} \dots T^{a_{\sigma(n)}}) A_n(\sigma(p_1, \epsilon_1), \dots, \sigma(p_n, \epsilon_n)) \quad (1.2)$$

where  $g$  is the gauge coupling and the  $A_n(p_i, \epsilon_i)$  are called colour-ordered partial amplitudes. These partial amplitudes do not carry any colour structure, but contain all the kinematic information of the amplitude.  $S_n$  is the group of permutations of  $n$  objects and  $\mathbf{Z}_n$  is the subgroup of cyclic permutations, which preserve the cyclic orderings in the trace.

It is simpler to study these partial amplitudes than the full amplitude because they only receive contributions from diagrams with cyclically ordered gluons. This is called colour ordering. In colour ordered amplitudes, the poles and cuts can only occur in momentum channels made out of sums of cyclically adjacent gluons. Hence the analytic structure of partial amplitudes is simpler than that of the full amplitude.

At one-loop both single trace and double trace structures are generated. The colour decomposition of the  $n$ -gluon one-loop amplitude is given by [22]:

$$A_n^{\text{one-loop}}(p_i, \epsilon_i, a_i) = g^n \left[ \sum_{\sigma \in S_n / \mathbf{Z}_n} N_c \text{Tr}(T^{a_{\sigma(1)}} \dots T^{a_{\sigma(n)}}) A_{n;1}(\sigma(p_1, \epsilon_1), \dots, \sigma(p_n, \epsilon_n)) \right. \\ \left. + \sum_{c=2}^{\lfloor n/2 \rfloor + 1} \sum_{\sigma \in S_n / S_{n;c}} \text{Tr}(T^{a_{\sigma(1)}} \dots T^{a_{\sigma(c-1)}}) (T^{a_{\sigma(c)}} \dots T^{a_{\sigma(n)}}) \right. \\ \left. \times A_{n;c}(\sigma(p_1, \epsilon_1), \dots, \sigma(p_n, \epsilon_n)) \right] \quad (1.3)$$

where  $A_{n;c}(p_i, \epsilon_i)$  are the partial amplitudes.  $\mathbf{Z}_n$  and  $S_{n;c}$  are the subgroups of  $S_n$  which preserve the single and double trace structures. The  $A_{n;1}$  are called primitive amplitudes. Just like the tree-level partial amplitudes the  $A_{n;1}$  are colour ordered. The  $A_{n;c}$  for  $c > 1$  can be written as sums of permutations of the primitive  $A_{n;1}$  amplitudes<sup>1</sup>. For the rest of this thesis, when studying Yang-Mills amplitudes, we will ignore colour structure and consider colour ordered amplitudes.

<sup>1</sup>See section 7 and appendix III of [13] for more details.

## 1.2.3 The spinor helicity formalism

In this section we review the spinor helicity formalism [23] for the description of quantities involving massless particles. This formalism is responsible for the existence of compact expressions for tree and loop amplitudes. It introduces a new set of kinematic objects, spinor products, which neatly capture the collinear behaviour of these amplitudes.

The complexified Lorentz group is locally isomorphic to

$$SO(3, 1, \mathbb{C}) \cong Sl(2, \mathbb{C}) \times Sl(2, \mathbb{C}) \quad (1.4)$$

so finite dimensional representations of the Lorentz group are classified by  $(p, q)$  where  $p$  and  $q$  are integer or half-integer valued. We write  $\lambda_a$ ,  $a = 1, 2$  for a spinor transforming in the  $(\frac{1}{2}, 0)$  representation and  $\tilde{\lambda}_{\dot{a}}$ ,  $\dot{a} = 1, 2$  for a spinor transforming in the  $(0, \frac{1}{2})$  representation. The spinor indices of type  $(\frac{1}{2}, 0)$  are raised and lowered using the antisymmetric tensors  $\epsilon_{ab}$  and  $\epsilon^{ab}$  which satisfy  $\epsilon_{12} = 1$  and  $\epsilon^{ac}\epsilon_{cb} = \delta^a_b$ . The  $\tilde{\lambda}$  spinors transforming in the representation  $(0, \frac{1}{2})$  are analogously raised and lowered using the antisymmetric tensor  $\epsilon_{\dot{a}\dot{b}}$  and its inverse  $\epsilon^{\dot{a}\dot{b}}$ .

$$\lambda^a = \epsilon^{ab}\lambda_b \quad , \quad \lambda_a = \epsilon_{ab}\lambda^b \quad \text{and} \quad \tilde{\lambda}^{\dot{a}} = \epsilon^{\dot{a}\dot{b}}\tilde{\lambda}_{\dot{b}} \quad , \quad \tilde{\lambda}_{\dot{a}} = \epsilon_{\dot{a}\dot{b}}\tilde{\lambda}^{\dot{b}} \quad (1.5)$$

There is a scalar product for two spinors  $\lambda$  and  $\lambda'$  in the  $(\frac{1}{2}, 0)$  representation and an analogous scalar product for two spinors  $\tilde{\lambda}$  and  $\tilde{\lambda}'$  in the  $(0, \frac{1}{2})$  representation

$$\langle \lambda \lambda' \rangle = \epsilon_{ab}\lambda^a\lambda'^b \quad \text{and} \quad [\tilde{\lambda} \tilde{\lambda}'] = \epsilon_{\dot{a}\dot{b}}\tilde{\lambda}^{\dot{a}}\tilde{\lambda}'^{\dot{b}} \quad (1.6)$$

These scalar products are antisymmetric in their two variables. Vanishing of the scalar product  $\langle \lambda \lambda' \rangle = 0$  implies  $\lambda \propto \lambda'$  and similarly  $[\tilde{\lambda} \tilde{\lambda}'] = 0$  implies  $\tilde{\lambda} \propto \tilde{\lambda}'$ . All the  $\lambda$ s and  $\tilde{\lambda}$ s in this formalism are commuting spinors. Note that they are not Grassmann variables.

The vector representation of  $SO(3, 1, \mathbb{C})$  is the  $(\frac{1}{2}, \frac{1}{2})$  representation. So a momentum vector  $p^\mu$ ,  $\mu = 0, \dots, 3$  can be represented as a bi-spinor  $p_{a\dot{a}}$  with two spinor indices  $a$  and  $\dot{a}$  transforming in the different spinor representations. More explicitly any four-vector  $p^\mu$  can be written as a  $2 \times 2$  matrix,

$$p_{a\dot{a}} = p_\mu \sigma_{a\dot{a}}^\mu \quad (1.7)$$

where  $\sigma^\mu = (1, \vec{\sigma})$  and  $\vec{\sigma}$  are the usual  $2 \times 2$  Pauli matrices. In this new notation we have

$$p^\mu p_\mu = \det(p_{a\dot{a}}) \quad (1.8)$$

If we now impose that the four-vector  $p^\mu$  is massless,  $p^2 = 0$ , then the determinant of the associated  $2 \times 2$  matrix is zero and the rank of this matrix is less than or equal to one. So a four-momentum  $p^\mu$  being massless is equivalent to the fact that it can be written as the

product of two (commuting) spinors

$$p_{a\dot{a}} = \lambda_a \tilde{\lambda}_{\dot{a}} \quad (1.9)$$

For a given massless vector  $p^\mu$  the spinors  $\lambda_a$  and  $\tilde{\lambda}_{\dot{a}}$  are unique up to a scaling.

$$(\lambda, \tilde{\lambda}) \rightarrow (t\lambda, t^{-1}\tilde{\lambda}) \quad \text{for } t \in \mathbb{C}, t \neq 0 \quad (1.10)$$

For real momenta in Minkowski space

$$\bar{\lambda} = \pm \tilde{\lambda} \quad (1.11)$$

where the  $\pm$  depends on whether the four-vector is future or past pointing. Thus the spinors  $\lambda$  are usually called ‘holomorphic’ and the spinors  $\tilde{\lambda}$  ‘anti-holomorphic’. If we use complex momenta then the spinors  $\lambda$  and  $\tilde{\lambda}$  are independent.

It is customary, when writing amplitudes, to shorten the spinor helicity notation for different particles  $i$  and  $j$  to  $\langle \lambda_i \lambda_j \rangle = \langle ij \rangle$  and  $[\tilde{\lambda}_i \tilde{\lambda}_j] = [ij]$ . It is common to shorten the spinor helicity formalism further using  $\langle ij \rangle [jk] = \langle i|j|k]$ .

We now introduce some useful identities for manipulating quantities written in the spinor helicity formalism. First we have the Schouten identity

$$\langle ij \rangle \langle kl \rangle = \langle ik \rangle \langle jl \rangle - \langle il \rangle \langle jk \rangle \quad (1.12)$$

Amplitudes are often written in terms of traces of Dirac  $\gamma$  matrices.

$$\langle ij \rangle [ji] = \text{tr} \left( \frac{1}{2} (1 + \gamma_5) \not{k}_i \not{k}_j \right) = 2k_i \cdot k_j \quad (1.13)$$

$$\langle ij \rangle [jl] \langle lm \rangle [mi] = \text{tr} \left( \frac{1}{2} (1 + \gamma_5) \not{k}_i \not{k}_j \not{k}_l \not{k}_m \right) \quad (1.14)$$

$$\langle ij \rangle [jl] \langle lm \rangle [mn] \langle np \rangle [pi] = \text{tr} \left( \frac{1}{2} (1 + \gamma_5) \not{k}_i \not{k}_j \not{k}_l \not{k}_m \not{k}_n \not{k}_p \right) \quad (1.15)$$

The Fierz rearrangement is:

$$\langle i | \gamma^\mu | j \rangle \langle k | \gamma_\mu | l \rangle = 2 \langle ik \rangle [lj] \quad (1.16)$$

Given a spinor helicity decomposition of the momentum  $p_{a\dot{a}} = \lambda_a \tilde{\lambda}_{\dot{a}}$ , we have enough information to determine the polarisation vector, up to a gauge transformation, of a gluon of specific helicity. For a positive helicity gluon we have the polarisation vector:

$$\epsilon_{a\dot{a}}^+ = \frac{\rho_a \tilde{\lambda}_{\dot{a}}}{\langle \rho \lambda \rangle} \quad (1.17)$$

where  $\rho$  is a negative chirality spinor that is not a multiple of  $\lambda$ . For a negative helicity

gluon we have the polarisation vector:

$$\epsilon_{a\dot{a}}^- = \frac{\lambda_a \tilde{\rho}_{\dot{a}}}{[\lambda, \rho]} \quad (1.18)$$

where  $\tilde{\rho}$  is any positive chirality spinor that is not a multiple of  $\tilde{\lambda}$ . With these definitions the polarisation vectors have no unphysical longitudinal modes as they obey the constraint  $p_\mu \epsilon^\mu = 0$ . The gauge invariance  $\epsilon^\mu \rightarrow \epsilon^\mu + w p^\mu$  of the polarisation vector is manifest in this description since  $\epsilon^+$  is independent of  $\rho$  up to a gauge transformation. To see this notice that the  $\rho$  lives in a two dimensional space spanned by  $\lambda$  and  $\rho$ , so a change in  $\rho$  is of the form  $\delta\rho = \alpha\rho + \beta\lambda$ . The polarisation vector  $\epsilon^+$  is invariant under the  $\alpha$  term and the  $\beta$  term corresponds to a gauge transformation of the polarisation vector:

$$\delta e_{a\dot{a}}^+ = \beta \frac{\lambda_a \tilde{\lambda}_{\dot{a}}}{\langle \rho \lambda \rangle} \quad (1.19)$$

Finally, calculating the linearised field strength  $F_{\mu\nu} = \partial_\mu A_\nu - \partial_\nu A_\mu$  for a particle of helicity +1 with  $A_{a\dot{a}} = \epsilon_{a\dot{a}}^+ \exp(ix_{c\dot{c}} \lambda^c \tilde{\lambda}^{\dot{c}})$  gives the answer:

$$F_{a\dot{a}b\dot{b}} = \epsilon_{ab} \tilde{\lambda}_{\dot{a}} \tilde{\lambda}_{\dot{b}} \exp(ix_{c\dot{c}} \lambda^c \tilde{\lambda}^{\dot{c}}) \quad (1.20)$$

In bi-spinor notation the field strength is  $F_{a\dot{a}b\dot{b}} = \epsilon_{ab} \tilde{f}_{\dot{a}\dot{b}} + \epsilon_{\dot{a}\dot{b}} f_{ab}$  where  $f_{ab}$  and  $\tilde{f}_{\dot{a}\dot{b}}$  are respectively the self-dual and anti-self-dual parts of  $F$ . So the polarisation vector  $\epsilon^+$  correctly gives an anti-self-dual field strength.

When an amplitude is written in the spinor helicity formalism it often takes a very simple form. The most famous example of this is the MHV amplitude. The tree-level Yang-Mills scattering amplitude with all outgoing gluons having positive helicity vanishes. The amplitudes with one negative helicity gluon and all the rest positive helicity also vanishes. In any supersymmetric Yang-Mills theory the vanishing of these amplitudes can be seen from a supersymmetric Ward identity [24,25]. The tree-level gluon amplitudes of a supersymmetric theory and a non-supersymmetric theory are, of course, the same, so these amplitudes also vanish in pure Yang-Mills. The first nonzero amplitude is called the maximally helicity violating (MHV) amplitude and has two negative helicity gluons with all the rest having positive helicity. Once the momentum conserving delta function has been stripped off the MHV amplitude it is a very simple function of only the holomorphic spinors  $\lambda_i$ .

$$A(1^+, 2^+, \dots, n-1^+, n^+) = 0 \quad (1.21)$$

$$A(1^+, 2^+, \dots, i^-, \dots, n-1^+, n^+) = 0 \quad (1.22)$$

$$A(1^+, 2^+, \dots, i^-, \dots, j^-, \dots, n-1^+, n^+) = i \frac{\langle ij \rangle^4}{\langle 12 \rangle \langle 23 \rangle \dots \langle n-1 n \rangle \langle n 1 \rangle} \quad (1.23)$$

### 1.3 Twistors

#### 1.3.1 The twistor transform

We define a twistor in the same way as Witten [5]. The spinor variables  $(\lambda, \tilde{\lambda})$  are related to the twistor variables  $(\lambda, \mu)$  by the following half Fourier transform:

$$\begin{aligned}\tilde{\lambda}_{\dot{a}} &\rightarrow i \frac{\partial}{\partial \mu^{\dot{a}}} \\ \frac{\partial}{\partial \tilde{\lambda}^{\dot{a}}} &\rightarrow i \mu_{\dot{a}}\end{aligned}\tag{1.24}$$

The choice to Fourier transform  $\lambda$  rather than  $\tilde{\lambda}$  is an arbitrary one. Writing things in twistor variables breaks the symmetry between positive and negative helicities. Later we will see that the holomorphicity of the MHV amplitude has a natural geometrical interpretation in twistor space. However with this choice of Fourier transform, the antiholomorphicity of the amplitude with two positive helicity gluons and all the rest negative helicity will be hidden. These anti-MHV amplitudes are usually called ‘googly’<sup>2</sup>.

This asymmetry will also be manifest in twistor inspired constructions such as the CSW rules which we will review in section 1.4.1. In this method the construction of MHV amplitudes is trivial, but the googly amplitudes are each constructed differently depending on the number of negative helicity gluons they contain. For example the five-point googly amplitude  $---++$  has one more negative helicity gluon than an MHV amplitude and is constructed by joining two MHV amplitudes together. The six-point googly amplitude is next-to, next-to MHV and constructed by sewing three MHV amplitudes together.

We now consider the effect of the transformation (1.24) on the representation of the Lorentz and conformal symmetry generators. In spinor variables the Lorentz generators are first order differential operators:

$$J_{ab} = \frac{i}{2} \left( \lambda_a \frac{\partial}{\partial \lambda^b} + \lambda_b \frac{\partial}{\partial \lambda^a} \right) \quad , \quad \tilde{J}_{\dot{a}\dot{b}} = \frac{i}{2} \left( \tilde{\lambda}_{\dot{a}} \frac{\partial}{\partial \tilde{\lambda}^{\dot{b}}} + \tilde{\lambda}_{\dot{b}} \frac{\partial}{\partial \tilde{\lambda}^{\dot{a}}} \right)\tag{1.25}$$

In twistor variables these generators remain first order:

$$J_{ab} = \frac{i}{2} \left( \lambda_a \frac{\partial}{\partial \lambda^b} + \lambda_b \frac{\partial}{\partial \lambda^a} \right) \quad , \quad \tilde{J}_{\dot{a}\dot{b}} = \frac{i}{2} \left( \mu_{\dot{a}} \frac{\partial}{\partial \mu^{\dot{b}}} + \mu_{\dot{b}} \frac{\partial}{\partial \mu^{\dot{a}}} \right)\tag{1.26}$$

In spinor variables the momentum and special conformal transformation generators are respectively a multiplication operator and a second order differential operator. In twistor

---

<sup>2</sup>The term googly is borrowed from cricket where it refers to the ball bowled out of the back of the hand by a leg spin bowler which spins the opposite way to the stock delivery.

variables, however, these generators take a more standard form both becoming first order:

$$P_{a\dot{s}} = \lambda_a \tilde{\lambda}_{\dot{a}} \quad , \quad K_{a\dot{a}} = \frac{\partial^2}{\partial \lambda^a \partial \tilde{\lambda}^{\dot{a}}} \quad (1.27)$$

$$P_{a\dot{s}} = i \lambda_a \frac{\partial}{\partial \mu^{\dot{a}}} \quad , \quad K_{a\dot{a}} = i \mu_{\dot{a}} \frac{\partial}{\partial \lambda^a} \quad (1.28)$$

Finally, the dilatation operator is an inhomogeneous operator in the spinor variables:

$$D = \frac{i}{2} \left( \lambda_a \frac{\partial}{\partial \lambda^a} + \tilde{\lambda}_{\dot{a}} \frac{\partial}{\partial \tilde{\lambda}^{\dot{a}}} + 2 \right) \quad (1.29)$$

In twistor variables the operator is homogeneous:

$$D = \frac{i}{2} \left( \lambda_a \frac{\partial}{\partial \lambda^a} - \mu_{\dot{a}} \frac{\partial}{\partial \mu^{\dot{a}}} \right) \quad (1.30)$$

This simple representation of the four dimensional conformal group in twistor variables is easy to understand. The conformal group of Minkowski space is  $SO(4, 2)$  which is the same as  $SU(2, 2)$ . The complexification of this group to  $Sl(4, \mathbb{C})$ , has an obvious four dimensional representation acting on the twistor  $Z = (\lambda^1, \lambda^2, \mu^1, \mu^2)$ . Twistor space is thus  $\mathbb{C}^4$ .

Tree amplitudes of gluons and more generally the quantum observables of  $\mathcal{N} = 4$  super Yang-Mills are conformally invariant quantities. So it is natural to hope that they will have a simple description in twistor variables.

### 1.3.2 The MHV amplitude in twistor space

Following Witten [5], we now consider the properties of amplitudes after they have been half Fourier transformed to twistor space.

$$A(\lambda_i, \tilde{\lambda}_i) \rightarrow A(\lambda_i, \mu_i) \equiv \frac{1}{(2\pi)^{2n}} \int \prod_{i=1}^n d^2 \tilde{\lambda}_i \exp \left( i \sum_{i=1}^n \mu_{i\dot{a}} \tilde{\lambda}_i^{\dot{a}} \right) A(\lambda_i, \tilde{\lambda}_i) \quad (1.31)$$

The simplest case is the MHV amplitude (1.23). The MHV amplitude only contains angle brackets and thus only has dependence on the space of  $\tilde{\lambda}_i$  spinors through the usual momentum-conserving  $\delta$ -function which multiplies the amplitude. Now recall the following identity for the Dirac delta function

$$\delta(x) = \frac{1}{2\pi} \int_{-\infty}^{\infty} dk e^{ikx} \quad (1.32)$$

We can use this to write the usual momentum conserving delta function as:

$$\delta^4 \left( \sum_{i=1}^n p_i \right) = \frac{1}{(2\pi)^4} \int d^4 x^{a\dot{a}} \exp \left( i x_{b\dot{b}} \sum_{j=1}^n \lambda_j^b \tilde{\lambda}_j^{\dot{b}} \right) \quad (1.33)$$

where the integral is over the ordinary four dimensional space time. Thus the twistor transform  $A(\lambda_i, \mu_i)$  of the MHV amplitude is:

$$\begin{aligned}
 &= \frac{1}{(2\pi)^{2n+4}} \int \prod_{i=1}^n d^2 \tilde{\lambda}_i \exp \left( i \sum_{i=1}^n \mu_{i\dot{a}} \tilde{\lambda}_i^{\dot{a}} \right) \int d^4 x^{a\dot{a}} \exp \left( i x_{b\dot{b}} \sum_{j=1}^n \lambda_j^b \tilde{\lambda}_j^{\dot{b}} \right) A_n^{\text{MHV}}(\lambda_i) \\
 &= \frac{1}{(2\pi)^{2n+4}} \int d^4 x^{a\dot{a}} A_n^{\text{MHV}}(\lambda_i) \int \prod_{i=1}^n d^2 \tilde{\lambda}_i \exp \left( i \sum_{i=1}^n \mu_{i\dot{a}} \tilde{\lambda}_i^{\dot{a}} + i x_{b\dot{b}} \sum_{j=1}^n \lambda_j^b \tilde{\lambda}_j^{\dot{b}} \right) \\
 &= A_n^{\text{MHV}}(\lambda_i) \frac{1}{(2\pi)^4} \int d^4 x \prod_{i=1}^n \delta^2(\mu_{i\dot{a}} + x_{a\dot{a}} \lambda_i^a) \tag{1.34}
 \end{aligned}$$

So we are led to consider the following equation:

$$\mu_{i\dot{a}} + x_{a\dot{a}} \lambda_i^a = 0 \tag{1.35}$$

This equation is familiar from the twistor literature, where it plays a central role and is known as the *incidence relation*. Traditionally the equation (1.35) is the definition of a twistor. For a given  $x$  the equation (1.35) is regarded as an equation for  $\lambda$  and  $\mu$  which defines a degree one, genus zero curve. Complexified Minkowski space is the moduli space of such curves. The transformed amplitude (1.34) will vanish unless (1.35) is satisfied for all the gluons. So all  $n$  points  $(\lambda_i, \mu_i)$  in an MHV amplitude must lie on a degree one, genus zero curve determined by  $x_{a\dot{a}}$ . See Figure 1.1. Alternatively, if  $\lambda$  and  $\mu$  are given, then equation (1.35) is an equation for  $x$ . The set of solutions is a two complex dimensional subspace of complexified Minkowski space that is null and self-dual. In the twistor literature this subspace is called an  $\alpha$ -plane. Twistor space is the moduli space of these  $\alpha$ -planes. An  $\alpha$ -plane being null means that any tangent vector to the  $\alpha$ -plane is null. An  $\alpha$ -plane being self-dual means that the tangent bi-vector is self-dual.

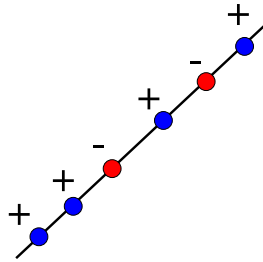


Figure 1.1: *The result that MHV amplitudes are supported on degree one, genus zero curves in twistor space is equivalent to the fact that the MHV amplitude is a function of only the  $\lambda$ s and not of the  $\tilde{\lambda}$ s.*

At this point we should be more precise about what we mean by twistor space. The space called twistor space in the last paragraph is in fact projective twistor space  $\mathbb{CP}^3$  and

not the full twistor space  $\mathbb{C}^4$ . The wave function of a massless particle with helicity  $h$  scales under  $(\lambda, \tilde{\lambda}) \rightarrow (t\lambda, t^{-1}\tilde{\lambda})$  as  $t^{-2h}$ . For example (1.20) describes a particle of helicity  $+1$  and scales like  $t^{-2}$ . So a scattering amplitude will obey the following differential equation for every particle  $i$  of helicity  $h_i$ :

$$\left( \lambda_i^a \frac{\partial}{\partial \lambda_i^a} - \tilde{\lambda}_i^{\dot{a}} \frac{\partial}{\partial \tilde{\lambda}_i^{\dot{a}}} \right) A(\lambda_i, \tilde{\lambda}_i, h_i) = -2h_i A(\lambda_i, \tilde{\lambda}_i, h_i) \quad (1.36)$$

Rewriting this equation in twistor variables it becomes:

$$\left( \lambda_i^a \frac{\partial}{\partial \lambda_i^a} + \mu_i^{\dot{a}} \frac{\partial}{\partial \mu_i^{\dot{a}}} \right) A(\lambda_i, \mu_i, h_i) = -(2h_i + 2) A(\lambda_i, \mu_i, h_i) \quad (1.37)$$

The operator on the left hand side of (1.37) is  $Z_i^I \frac{\partial}{\partial Z_i^I}$  where  $Z_i^I = (\lambda_i^1, \lambda_i^2, \mu_i^{\dot{1}}, \mu_i^{\dot{2}})$  is the twistor. So under  $Z_i^I \rightarrow tZ_i^I$  amplitudes transform like  $t^{-(2h_i+2)}$ . Since amplitudes are homogeneous functions of degree  $-(2h_i + 2)$  in the twistor variable  $Z_i^I$  we can identify points of twistor space  $\mathbb{C}^4$  projectively and consider projective twistor space  $\mathbb{CP}^3$ .

Witten [5] proposed that the localisation of the tree-level MHV amplitudes extends naturally to general amplitudes with  $q$  negative helicity gluons and  $l$  loops by suggesting that in twistor space they are supported on holomorphic curves of the degree  $d$  and genus  $g$ . Where  $d$  and  $g$  are given in terms of  $q$  and  $l$  by:

$$\begin{aligned} d &= q - 1 + l \\ g &\leq l \end{aligned} \quad (1.38)$$

The tree-level MHV amplitude is the case  $q = 2$  and  $l = 0$  corresponding to  $d = 1$  and  $g = 0$ .

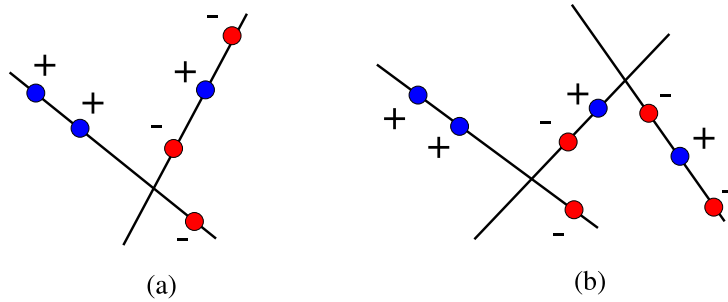


Figure 1.2: *The twistor space localisation of tree amplitudes. Diagram (a) shows the localisation of an amplitude with three negative helicity gluons and diagram (b) an amplitude with four negative helicity gluons.*

In general it is difficult to explicitly half Fourier transform amplitudes as was done for the MHV amplitude in (1.34). However the collinear and coplanar conditions on a set of

points in twistor space correspond via the twistor transform (1.24) to differential equations in the usual spinor variables [5]. For example the condition on three points  $Z_i^I, Z_j^I, Z_k^I$  in  $\mathbb{CP}^3$  to be collinear is that:

$$0 = F_{ijkL} = \epsilon_{IJKL} Z_i^K Z_j^K Z_k^K \quad , \quad L = 1, \dots, 4 \quad (1.39)$$

After twistor transforming this becomes a differential operator. For  $L = 4$  we have:

$$F_{ijk} = \langle ij \rangle \frac{\partial}{\partial \tilde{\lambda}_k^1} + \langle ki \rangle \frac{\partial}{\partial \tilde{\lambda}_j^1} + \langle jk \rangle \frac{\partial}{\partial \tilde{\lambda}_i^1} \quad (1.40)$$

Given a known amplitude differential operators can be applied to find the support of the amplitude in twistor space. This confirmed the picture in Figure (1.2).

### 1.3.3 Twistor string theory

In [5] Witten proposed that the weakly coupled  $\mathcal{N} = 4$  gauge theory was dual to a string theory with the super twistor space  $\mathbb{CP}^{3|4}$  as the target manifold. The target spaces  $\mathbb{CP}^{3|4}$  and  $\text{AdS}_5 \times \mathbb{S}^5$  both have the symmetry group  $PSU(2, 2|4)$  of  $\mathcal{N} = 4$  super Yang-Mills. The space  $\mathbb{CP}^{3|N}$  is also a Calabi-Yau super manifold if and only if  $N = 4$ . This enables one to define a topological B-model with target  $\mathbb{CP}^{3|4}$ . The topological string is quite different to the usual super string theory of Maldacena's duality [4] between strongly coupled  $\mathcal{N} = 4$  super Yang-Mills and type IIB super strings on  $\text{AdS}_5 \times \mathbb{S}^5$ . The B-model has fewer dynamical degrees of freedom than the full super string theories, having only massless states rather than a full tower of massive ones.

With space filling branes, the open strings on  $\mathbb{CP}^{3|4}$  reproduce the spectrum of  $\mathcal{N} = 4$  super Yang-Mills. However, the topological B-model does not give the full set of interactions of the gauge theory. While the  $++-$  vertex is present, the  $--+$  vertex is absent and one has to add  $D1$ -instantons to get this interaction. The closed strings of the B-model describe the variations of the complex structure in the target manifold. These closed strings give conformal supergravity [11], which is a non-unitary theory. It also appears that this gravitational theory cannot be decoupled from the gauge theory and thus the twistor string does not describe  $\mathcal{N} = 4$  gauge theory at loop level. Recently twistor strings involving Einstein gravity, rather than conformal supergravity, have been constructed [26]. It may also be possible to decouple the closed strings in these new models.

Despite these unsatisfactory elements of the duality, Rioban, Spradlin and Volovich have extracted tree amplitudes with many negative helicities from the B-model by integrating over connected curves [27–29]. It was shown that integrating over connected curves is equivalent to integrating over disconnected curves in [30]. The analysis of these disconnected curves led to the efficient CSW rules which are reviewed in the next section.

## 1.4 Field theoretic MHV rules

### 1.4.1 The tree level CSW rules.

The geometrical structure in twistor space of the amplitudes, drawn in Figure (1.2), was also the root of a further important development. In [8], Cachazo, Svrček and Witten (CSW) proposed a novel perturbative expansion for on-shell amplitudes in Yang-Mills, where the MHV amplitudes are lifted to vertices, joined by simple scalar propagators  $i/P^2$  in order to form amplitudes with an increasing number of negative helicities. It is natural to think of an MHV amplitude as a local interaction, since the line in twistor space on which an MHV amplitude localises corresponds to a point in Minkowski space via the incidence relation. All possible diagrams made of MHV amplitudes with a cyclic ordering of external legs have to be summed. Applications at tree level confirmed the validity of the method and led to the derivation of various new amplitudes in gauge theory [8, 31–37].

To generalise the MHV amplitude to a vertex we need to explain what is meant by  $\lambda_a$  when  $p_{a\dot{a}}$  is not massless, as is the case for all the internal legs that join the MHV amplitudes together. The CSW ‘off-shell’ prescription defining the  $\lambda_a$  for internal lines carrying momentum  $p_{a\dot{a}}$  is to use:

$$\lambda_a = p_{a\dot{a}}\eta^{\dot{a}} \quad (1.41)$$

where  $\eta^{\dot{a}}$  is an arbitrary negative chirality spinor. The same  $\eta$  is used for all ‘off-shell’ lines in all diagrams contributing to a given amplitude.

As an example of the CSW construction we now consider the five point  $---++$  amplitude. This amplitude is googly, so the amplitude is given by (1.23), but using  $\tilde{\lambda}$  spinors in place of the  $\lambda$  spinors:

$$A(1^-, 2^-, 3^-, 4^+, 5^+) = i \frac{[45]^3}{[12][23][34][51]} \quad (1.42)$$

In the twistor picture the  $---++$  amplitude is viewed as a next-to-MHV amplitude. In CSW’s construction, next-to-MHV amplitudes are made by joining two MHV amplitudes together. The diagrams in the CSW construction of this five-point next-to-MHV amplitude are given in Figure 1.3. The diagram in Figure 1.3a gives the following product of two tree amplitudes and a scalar propagator:

$$\left( i \frac{\langle 12 \rangle^3}{\langle 2k \rangle \langle k5 \rangle \langle 51 \rangle} \right) \frac{i}{\langle 34 \rangle [43]} \left( i \frac{\langle k3 \rangle^3}{\langle 34 \rangle \langle 4k \rangle} \right) \quad (1.43)$$

We now use the CSW ‘off-shell’ prescription (1.41) to define the brackets involving  $k$ .

$$\langle 2k \rangle \rightarrow \langle 2|k|\eta \rangle = \langle 2|3 + 4|\eta \rangle \quad (1.44)$$

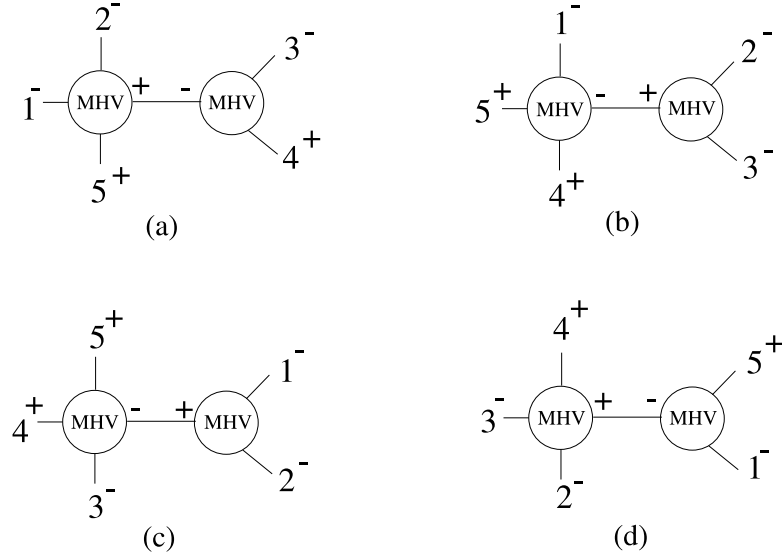


Figure 1.3: The MHV diagrams associated with the CSW construction of the simplest next-to-MHV tree-level amplitude  $A(1^-, 2^-, 3^-, 4^+, 5^+)$ . It is conventional to consider amplitudes where all the momenta are outgoing, so an internal leg joining two amplitudes will have different helicities labels at each end.

The brackets  $\langle k5 \rangle$ ,  $\langle k3 \rangle$ ,  $\langle 4k \rangle$  are similarly dealt with yielding the answer for Figure 1.3a:

$$i \frac{\langle 12 \rangle^3 \langle 34 | \eta \rangle^3}{\langle 15 \rangle \langle 34 \rangle^2 [34] \langle 2 | 3 + 4 | \eta \rangle \langle 5 | 3 + 4 | \eta \rangle \langle 4 | 3 | \eta \rangle} \quad (1.45)$$

The remaining three diagrams in Figure 1.3 are given by the three terms:

$$i \frac{\langle 23 \rangle^2 \langle 1 | 2 + 3 | \eta \rangle^3}{\langle 45 \rangle \langle 51 \rangle [23] \langle 4 | 2 + 3 | \eta \rangle \langle 2 | 3 | \eta \rangle \langle 3 | 2 | \eta \rangle} + i \frac{\langle 12 \rangle^2 \langle 3 | 1 + 2 | \eta \rangle^3}{\langle 34 \rangle \langle 45 \rangle [12] \langle 5 | 1 + 2 | \eta \rangle \langle 1 | 2 | \eta \rangle \langle 2 | 1 | \eta \rangle} + i \frac{\langle 23 \rangle^3 \langle 1 | 5 | \eta \rangle^3}{\langle 34 \rangle \langle 15 \rangle^2 [15] \langle 4 | 1 + 5 | \eta \rangle \langle 2 | 1 + 5 | \eta \rangle \langle 5 | 1 | \eta \rangle} \quad (1.46)$$

The sum of the four terms in (1.45) and (1.46) agree with the known answer (1.42). This can be checked numerically by taking the arbitrary spinor to be  $|\eta\rangle = |4\rangle + |5\rangle$  and using the `VegasShift[n]` Mathematica program in Appendix B. It can be also be shown that the construction is independent of the arbitrary reference spinor  $\eta$ .

The CSW construction can of course be applied to amplitudes which are neither MHV or googly. The first example of this is the next-to-MHV six point amplitude. This amplitude is constructed from six CSW diagrams, where as a Feynman rules calculation involves 220 diagrams [9, 10]. The efficient CSW construction including the ‘off-shell’ prescription for the internal legs can be proved simply and directly by realising that the CSW rules are an example of BCFW on shell recursion [38]. This will be reviewed in section 1.7.3.

## 1.4.2 The one loop BST rules

In [8], a heuristic derivation of the CSW method was given from the twistor string theory. Rather unfortunately, the latter only appears to describe the scattering amplitudes of Yang-Mills at tree level [11], as at one loop states of conformal supergravity enter the game, and cannot be decoupled in any known limit. The duality between gauge theory and twistor string theory is thus spoilt by quantum corrections. Surprisingly, it was found by Brandhuber, Spence and Travaglini (BST) that the MHV method does succeed in correctly reproducing the one-loop MHV scattering amplitude [12].

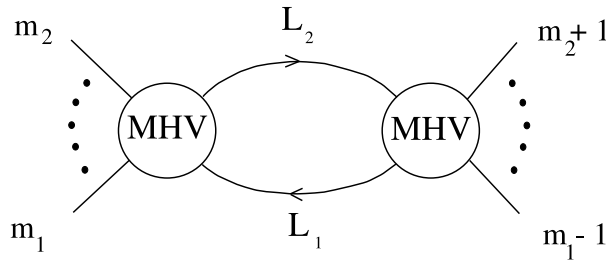


Figure 1.4: *The BST construction of the MHV one-loop amplitude in  $\mathcal{N} = 4$  super Yang-Mills by sewing two tree-level MHV amplitudes together.*

The BST method is given schematically by the diagram in Figure 1.4. The one-loop MHV amplitude is computed from:

$$A = \sum_{m_1 m_2} \int dM A_L(-l_1, m_1, \dots, m_2, l_2) A_R(-l_2, m_2 + 1, \dots, m_1 - 1, l_1) \quad (1.47)$$

where the full  $\mathcal{N} = 4$  multiplet can run in the loop.  $A_L$  and  $A_R$  are MHV amplitudes with the CSW ‘off shell’ prescription  $L_i = l_i + z_i \eta$ . The measure  $dM$  is given by

$$dM = (2\pi)^4 \delta^{(4)}(L_2 - l_1 + P_l) \frac{d^4 L_1}{L_1^2} \frac{d^4 L_2}{L_2^2} \quad (1.48)$$

Using the decomposition  $\frac{d^4 L}{L} = \frac{dz}{z} d^4 l \delta^{(+)}(l^2)$ , BST showed that the measure  $dM$  can be written as the product of two parts. The first part is a dispersive integral, which reconstructs the amplitude from its discontinuities. The second part is a Lorentz-invariant phase-space measure that computes the discontinuity of the diagram across the branch cut in the same way as the two-particle unitarity cuts method of BDDK [13, 14]. This method will be reviewed in section 1.5. The calculation of BST has many similarities to the unitarity based approach of BDDK. The main practical difference is that the MHV rules reproduce the cut-constructible parts of an amplitude directly without having to worry about over counting. In this sense the BST construction is a diagrammatic method.

The twistor space picture of one-loop amplitudes is now in complete agreement with that emerging from these MHV methods, which suggests that the amplitudes at one loop have localisation properties on unions of lines in twistor space in agreement with (1.38). An initial puzzle [39] was indeed clarified and explained in terms of a certain ‘holomorphic anomaly’, introduced in [40], and further analysed in [41–45]. A proof of the MHV method at tree level was given in [17] and more directly in [38]. At loop level it remains a (well-supported) conjecture. Further understanding of the loop level MHV construction via the Feynman tree theorem was gained in [46].

The initial successful application of the MHV method to  $\mathcal{N}=4$  SYM [12] was followed by calculations of MHV amplitudes in  $\mathcal{N}=1$  SYM [47, 48], and in pure Yang-Mills [49], where the four-dimensional cut-constructible part of the infinite sequence of MHV amplitudes was derived. However, amplitudes in non-supersymmetric Yang-Mills theory also have rational terms which escape analyses based on MHV diagrams at one loop [49] or four-dimensional unitarity [13, 14]. It would be interesting to extend the MHV construction to higher loops.

### 1.4.3 Mansfield’s proof of the CSW rules

It is possible to construct a canonical transformation that takes the usual Yang-Mills action into one whose Feynman diagram expansion generates the CSW rules. This transformation was found by Mansfield [50]. The light-front quantisation of Yang-Mills leads to a formulation of Yang-Mills in terms of only the physical degrees of freedom. There are no ghosts. If one chooses the gauge  $A_0 = 0$  in light-front coordinates and integrates out the remaining unphysical degree of freedom, one is left with a simple action:

$$S = \frac{4}{g^2} \int dx^0 d^3x \operatorname{tr} \left( A_z \partial_0 \partial_{\bar{0}} A_{\bar{z}} - [\mathcal{D}_{\bar{z}}, \partial_{\bar{0}} A_z] \partial_{\bar{0}}^{-2} [\mathcal{D}_z, \partial_{\bar{0}} A_{\bar{z}}] \right) \quad (1.49)$$

This Lagrangian can be written as a sum of four terms  $L_2 + L^{++-} + L^{--+} + L^{---+}$  where  $L_2$  is a kinetic term corresponding to a scalar propagator and the other three terms are interaction vertices labelled by their helicity content. Mansfield showed that it was possible to perform a transformation that eliminates the googly vertex  $L^{++-}$  and at the same time generate the missing MHV vertices of the CSW rules. This transformation writes the kinetic term and the three point googly interaction of the old field  $A$ , as the kinetic term of a new field  $B$ :

$$L_2[A] + L^{++-}[A] = L_2[B] \quad (1.50)$$

The transformation used by Mansfield is a canonical transformation in which  $B_+$  is a functional of  $A_z$  on the quantisation surface, but not  $A_{\bar{z}}$ . The remaining two terms of the Lagrangian  $L^{--+}[A] + L^{---+}[A]$  when written in terms of  $B_{\pm}$  give the infinite series of MHV vertices that occur in the CSW rules. Further developments in this area can be found in the papers [51, 52]. In principle this idea should generalise to the quantum theory.

## 1.5 BDDK's two-particle unitarity cuts

Unitarity is a well known and useful tool in quantum field theory. Unitarity applied at the level of Feynman diagrams usually goes under the name of the ‘Optical Theorem’. See for example [53–57]. If we write the S-matrix as  $S = 1 + iA$  then unitarity of the S-matrix implies, for example, that the imaginary part of a one loop amplitude can be found by considering the product of two tree amplitudes.

$$S^\dagger S = 1 \quad \Rightarrow \quad \text{Im}(A) \sim A^\dagger A \quad (1.51)$$

Each Feynman diagram contributing to an S-matrix element is real unless some denominator vanishes, so that the  $i\epsilon$  prescription for treating poles becomes relevant. Thus Feynman diagrams have an imaginary part only when the virtual particles in the diagram go on shell. Let  $F(s)$  be a Feynman diagram, where  $s$  is a momentum invariant. We now consider  $F(s)$  as an analytic function of the complex variable  $s$ , even though we are only interested in the result for external particles with real momentum. Let  $s_0$  be the threshold energy for the production of the lightest multi-particle state. For real  $s < s_0$  the intermediate state cannot go on shell, so  $F(s)$  is real:

$$F(s) = (F(s^*))^* \quad (1.52)$$

Both sides of this equation are analytic functions of  $s$ , so we can analytically continue to the entire complex  $s$  plane. For  $s > s_0$  this implies:

$$\text{Re}F(s + i\epsilon) = \text{Re}F(s - i\epsilon) \quad , \quad \text{Im}F(s + i\epsilon) = -\text{Im}F(s - i\epsilon) \quad (1.53)$$

Thus, there is a branch cut across the real axis for  $s > s_0$ . The  $i\epsilon$  prescription in the Feynman propagator means that the physical scattering amplitude should be evaluated above the cut at  $s + i\epsilon$ .

The simplicity of tree-level amplitudes in Yang-Mills was exploited by Bern, Dixon, Dunbar and Kosower (BDDK) in order to build one-loop scattering amplitudes [13, 14]. By applying unitarity at the level of amplitudes, rather than Feynman diagrams, these authors were able to construct many one-loop amplitudes in supersymmetric theories, such as the infinite sequence of MHV amplitudes in  $\mathcal{N} = 4$  and in  $\mathcal{N} = 1$  super Yang-Mills (SYM). The unitarity method of BDDK by-passes the use of Feynman diagrams and its related complications, and generates results of an unexpectedly simple form. For instance, the one-loop MHV amplitude in  $\mathcal{N} = 4$  SYM is simply given by the tree-level expression multiplied by a sum of ‘two-mass easy’ box functions, all with coefficient one.

Amplitudes in supersymmetric theories are of course special. They do contain rational terms, but these are uniquely linked to terms which have cuts in four dimensions.

In other words, these amplitudes can be reconstructed uniquely from their cuts in four-dimensions [13, 14] - a remarkable result. These cuts are of course four-dimensional tree-level amplitudes, whose simplicity is instrumental in allowing the derivation of analytic, closed-form expressions for the one-loop amplitudes.

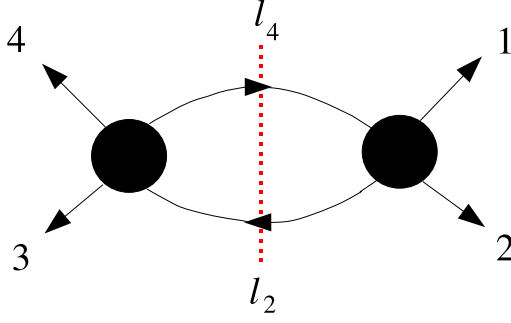


Figure 1.5: The  $s$  channel cut of a one-loop amplitude.

We now illustrate the computation of branch cut containing terms via the cutting procedure by considering the  $s$ -channel cut of a four point amplitude drawn in Figure 1.5.

$$\text{Im}A^{\text{one-loop}}(1, 2, 3, 4)\Big|_{\text{s-cut}} = \int d^{4-2\epsilon}l \delta^{(+)}(l_4^2)\delta^{(+)}(l_2^2) \times A^{\text{tree}}(-l_4, 1, 2, l_2)A^{\text{tree}}(-l_2, 3, 4, l_4) \quad (1.54)$$

Now suppose the amplitude has the form  $A^{\text{one-loop}} = c \log(-s) + \dots = c(\log|s| - i\pi) + \dots$ . The phase-space integral (1.54) computes the  $i\pi$  term. We want both terms, so we replace the phase-space integral by an unrestricted loop integral in which the delta functions have been replaced with propagators. This procedure is usually called ‘reconstruction of the Feynman integral’:

$$A(1, 2, 3, 4)\Big|_{\text{s-cut}} = \int d^{4-2\epsilon}l \frac{i}{l_4^2} \frac{i}{l_2^2} A^{\text{tree}}(-l_4, 1, 2, l_2)A^{\text{tree}}(-l_2, 3, 4, l_4)\Big|_{\text{s-cut}} \quad (1.55)$$

Equation (1.54) involves only the imaginary part, but equation (1.55) contains both the real and imaginary parts. This process of ‘reconstructing the Feynman integral’ will be pushed further in chapter 2 to understand the new D-dimensional generalised unitarity cuts. Equation (1.55) is only valid for terms with an  $s$ -channel branch cut. A similar cut must be performed to compute the terms with a  $t$ -channel cut. In this way all terms with cuts can be found. Combining the two cuts into a single function in a way that avoids over counting gives the complete amplitude.

In non-supersymmetric theories, amplitudes can still be reconstructed from their cuts, but on the condition of working in  $4 - 2\epsilon$  dimensions, with  $\epsilon \neq 0$  [58–60]. This is a powerful statement, but it also implies the rather unpleasant fact that one should in principle work with tree-level amplitudes involving gluons continued to  $4 - 2\epsilon$  dimensions, which are not simple.

An important simplification is offered by the well-known supersymmetric decomposition of one-loop amplitudes of gluons in pure Yang-Mills. Given a one-loop amplitude  $\mathcal{A}_g$  with gluons running the loop, one can re-cast it as

$$\mathcal{A}_g = (\mathcal{A}_g + 4\mathcal{A}_f + 3\mathcal{A}_s) - 4(\mathcal{A}_f + \mathcal{A}_s) + \mathcal{A}_s . \quad (1.56)$$

Here  $\mathcal{A}_f$  ( $\mathcal{A}_s$ ) is the amplitude with the same external particles as  $\mathcal{A}_g$  but with a Weyl fermion (complex scalar) in the adjoint of the gauge group running in the loop.

This decomposition is useful because the first two terms on the right hand side of (1.56) are contributions coming from an  $\mathcal{N} = 4$  multiplet and (minus four times) a chiral  $\mathcal{N} = 1$  multiplet, respectively; therefore, these terms are four-dimensional cut-constructible, which simplifies their calculation enormously. The last term in (1.56),  $\mathcal{A}_s$ , is the contribution coming from a scalar running in the loop. The key point here is that the calculation of this term is much easier than that of the original amplitude  $\mathcal{A}_g$ . It is this last contribution which is the focus of chapter 2 of this thesis.

The root of the simplification lies in the fact that a massless scalar in  $4 - 2\epsilon$  dimensions can equivalently be described as a massive scalar in four dimensions [59, 60]. Indeed, if  $L$  is the  $(4 - 2\epsilon)$ -dimensional momentum of the massless scalar ( $L^2 = 0$ ), decomposed into a four-dimensional component  $l_{(4)}$  and a  $-2\epsilon$ -dimensional component  $l_{(-2\epsilon)}$ ,  $L := l_{(4)} + l_{(-2\epsilon)}$ , one has  $L^2 := l_{(4)}^2 + l_{(-2\epsilon)}^2 = l_{(4)}^2 - \mu^2$ , where  $l_{(-2\epsilon)}^2 := -\mu^2$  and the four-dimensional and  $-2\epsilon$ -dimensional subspaces are taken to be orthogonal.

The tree-level amplitudes entering the  $(4 - 2\epsilon)$ -dimensional cuts of a one-loop amplitude with a scalar in the loop are therefore those involving a pair of massive scalars and gluons. Crucially, these amplitudes have a rather simple form. Some of these amplitudes appear in [59, 60]; furthermore, a recent paper [61] describes how to efficiently derive such amplitudes using a recursion relation similar to that of BCFW. This recursion relation will be reviewed in section 1.7.2.

Using two-particle cuts in  $4 - 2\epsilon$  dimensions, together with the supersymmetric decomposition mentioned above, various amplitudes in pure Yang-Mills were derived in recent years, starting with the pioneering works [59, 60]. In chapter 2 we show that this analysis can be performed with the help of an additional tool: generalised  $(4 - 2\epsilon)$ -dimensional unitarity.

## 1.6 Generalised Unitarity

The twistor string proposal of Witten [5] has inspired many new techniques for the calculation of scattering amplitudes in gauge theory and gravity. As reviewed in section 1.2.3 it is efficient to write amplitudes in the spinor-helicity formalism and many of these new techniques make use of an analytic continuation of these spinors to complex momenta at intermediate steps. For example the use of complex momenta allows for the use of on-shell three-point amplitudes at intermediate steps. For a three-point on shell amplitude we have the following kinematic constraints

$$\begin{aligned} 0 &= P_1^2 = 2P_2.P_3 = \langle 23 \rangle [32] \\ 0 &= P_2^2 = 2P_3.P_1 = \langle 31 \rangle [13] \\ 0 &= P_3^2 = 2P_1.P_2 = \langle 12 \rangle [21] \end{aligned}$$

For real momenta in Minkowski space, the spinors are also related by the additional constraint  $\tilde{\lambda} = \pm \bar{\lambda}$  and so any three-point amplitude must vanish. If we now use complex momenta the  $\lambda$  and  $\tilde{\lambda}$  are independent and thus only one of the conditions  $\lambda_1 \propto \lambda_2 \propto \lambda_3$  and  $\tilde{\lambda}_1 \propto \tilde{\lambda}_2 \propto \tilde{\lambda}_3$  could hold and we can use the other non-proportional spinors to formally define three-point amplitudes. For example, we can define the three-point on-shell tree-level Yang-Mills amplitudes by

$$\begin{aligned} A_3^{(\text{tree})}(1^-, 2^-, 3^+) &= i \frac{\langle 12 \rangle^3}{\langle 23 \rangle \langle 31 \rangle} \quad \text{and} \quad \tilde{\lambda}_1 \propto \tilde{\lambda}_2 \propto \tilde{\lambda}_3 \\ A_3^{(\text{tree})}(1^+, 2^+, 3^-) &= i \frac{[12]^3}{[23] [31]} \quad \text{and} \quad \lambda_1 \propto \lambda_2 \propto \lambda_3 \end{aligned} \tag{1.57}$$

Working with complex momenta has enabled a dramatic generalisation of the two-particle cut constructibility techniques to multiple cuts. [56, 57, 62–64] Constructing an amplitude using two-particle cuts can be quite complicated since there are often many functions which share the same branch cut. The various scalar integrals of the final amplitude also have many different branch cuts so one coefficient appears in multiple cut equations. Two-particle cuts also require complicated Passarino-Veltman reduction to write the tensor integrals of the cut integrals in terms of the scalar integrals of the final amplitude. This reduction results in large expressions for the rational coefficients of the scalar integrals. Often these complicated expressions are equivalent to simple formulae suggesting that there is a more elegant way of computing them [44].

The idea which realises this goal, is to simply cut more propagators than the two which are cut in a two-particle cut. This is called generalised unitarity. Just as a two-particle cut replaces two propagators by two delta functions, a generalised cut replaces more propagators by delta functions. Simultaneously cutting more legs reduces the overlap between the

various cuts, thus making the disentanglement of the coefficients from the various cuts much simpler. Since the additional delta functions give more on-shell conditions with which to manipulate the cut integrand, generalised unitarity also reduces the complexity of the required Passarino-Veltman reduction. In order to cut these extra legs it is crucial to use three point vertices and therefore complexified momenta.

### 1.6.1 Quadruple cuts in $\mathcal{N}=4$ Super Yang-Mills

Generalised cuts most dramatic application is to the one-loop amplitudes of  $\mathcal{N}=4$  Super Yang-Mills [15]. The one-loop amplitudes of  $\mathcal{N}=4$  Super Yang-Mills can be written as a linear combination of only scalar box integrals with rational coefficients [13]. There are no triangle and bubble integrals. The scalar box integrals can be thought of as the basis of a vector space. Each one-loop amplitude is then a vector which can be written as a linear combination of members of this basis. Performing the quadruple cut of an amplitude is then a way of projecting this vector onto a specific member of the basis computing the corresponding coefficient. Each scalar box integral is associated with a unique quadruple cut. So for  $\mathcal{N}=4$  Super Yang-Mills quadruple cuts can be thought of as a diagrammatic method. Replacing all of the four propagators of a scalar box integral with delta functions completely localises the integral onto the two solutions of the four on-shell conditions and no Passarino-Veltman reduction is required. Quadruple cuts have thus reduced the calculation of one-loop amplitudes in  $\mathcal{N}=4$  Super Yang-Mills to multiplication of four tree amplitudes.

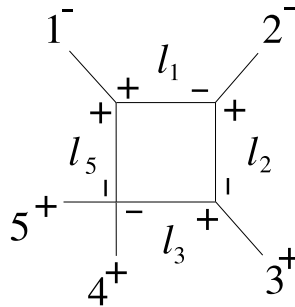


Figure 1.6: A simple quadruple cut to evaluate the coefficient of a one-mass box in the five-point MHV amplitude in  $\mathcal{N}=4$  Super Yang-Mills.

We now present an explicit example of the use of a quadruple cut in the calculation of the coefficient of a one-mass box integral in a one-loop MHV amplitude of  $\mathcal{N}=4$  super Yang-Mills. We consider the quadruple cut drawn in Figure 1.6. This particular example of a quadruple cut is simple because only gluons propagate in the loop. In general all the particles in the  $\mathcal{N}=4$  multiplet can run in the loop of a quadruple cut. The helicity assignments of the internal legs in a quadruple cut must be chosen so that the three point

vertices used do not give rise to unphysical constraints on the external momenta. For the particular one-mass box in Figure 1.6 the only possible helicity assignment is the one given in the diagram and with this helicity assignment it is only possible for gluons to propagate in the loop.

To calculate the coefficient of the one-mass box in the amplitude we simply multiply four on-shell gluon tree amplitudes together.

$$\begin{aligned}
 & A(l_5^+, 1^-, l_1^+) A(l_1^-, 2^-, l_2^+) A(l_2^-, 3^+, l_3^+) A(l_3^-, 4^+, 5^+, l_5^-) \\
 &= \left( i \frac{[l_1 l_5]^3}{[l_5 1][1 l_1]} \right) \left( i \frac{\langle l_1 2 \rangle^3}{\langle 2 l_2 \rangle \langle l_2 l_1 \rangle} \right) \left( i \frac{[3 l_3]^3}{[l_3 l_2][l_2 3]} \right) \left( i \frac{\langle l_3 l_5 \rangle^3}{\langle l_3 4 \rangle \langle 4 5 \rangle \langle 5 l_5 \rangle} \right) \quad (1.58)
 \end{aligned}$$

We now use momentum conservation and on-shell conditions to eliminate as many of the  $l$ s as possible. The numerator of (1.58) simplifies to:

$$\begin{aligned}
 \langle 2 | l_1 l_5 l_3 | 3 \rangle^3 &= \langle 2 | l_1 l_5 (4 + 5) | 3 \rangle^3 \\
 &= \langle 2 | l_1 1 (4 + 5) | 3 \rangle^3 \\
 &= -\langle 2 | l_1 1 2 | 3 \rangle^3 \\
 &= -\langle 2 | l_1 | 1 \rangle^3 \langle 1 2 \rangle^3 [2 3]^3
 \end{aligned}$$

The denominator of (1.58) simplifies to:

$$\begin{aligned}
 -\langle 4 | l_3 l_2 l_1 | 1 \rangle \langle 2 | l_2 | 3 \rangle \langle 5 | l_5 | 1 \rangle \langle 4 5 \rangle &= -\langle 4 | 3 2 l_1 | 1 \rangle \langle 2 | l_1 | 3 \rangle \langle 5 | l_1 | 1 \rangle \langle 4 5 \rangle \\
 &= -\langle 2 | l_1 | 1 \rangle^2 \langle 5 | l_1 | 3 \rangle \langle 4 3 \rangle [3 2] \langle 4 5 \rangle
 \end{aligned}$$

So the quadruple cut (1.58) has the value

$$\frac{\langle 1 2 \rangle^3 [2 3]^2 \langle 2 | l_1 | 1 \rangle}{\langle 3 4 \rangle \langle 4 5 \rangle \langle 5 | l_1 | 3 \rangle} \quad (1.59)$$

Now recall the conditions (1.57) on three point vertices in complex momenta. The three-point vertices involving the external legs 1 and 2 give the conditions  $\lambda_{l_1} \propto \lambda_1$  and  $\tilde{\lambda}_{l_1} \propto \tilde{\lambda}_2$  which can be used to eliminate the remaining dependence on the loop momenta:

$$\frac{\langle 2 | l_1 | 1 \rangle}{\langle 5 | l_1 | 3 \rangle} = \frac{\langle 2 1 \rangle [2 1]}{\langle 5 1 \rangle [2 3]} \quad (1.60)$$

Thus the quadruple cut (1.58) gives the coefficient of the scalar box integral to be:

$$A^{\text{tree}}(1^-, 2^-, 3^+, 4^+, 5^+) (p_1 + p_2)^2 (p_2 + p_3)^2 \quad (1.61)$$

This answer was originally calculated using two-particle unitarity cuts in [13]. It has also been calculated using loop-level MHV rules in [12]. In general it is not always possible to eliminate the loop momentum from the quadruple cut in such a simple fashion and one

has to explicitly solve the four on-shell conditions for the loop momentum in terms of the external particles [15]. There are generally two solutions to this problem and the amplitude is given by averaging over these two solutions.

The four dimensional quadruple cuts reviewed above have much in common with the  $D$ -dimensional quadruple cuts that are presented in chapter 2. However the four dimensional cuts only compute amplitudes to the leading orders in  $\epsilon$ , where as the  $D$ -dimensional cuts that will be introduced in chapter 2 correctly compute to all orders in  $\epsilon$ . For example the quadruple cut considered in Figure 1.6 should contain a pentagon term if true to all orders in  $\epsilon$ , but there is no pentagon term in (1.61). These higher order in  $\epsilon$  contributions are important in, for example, the study of iterative cross order relations that relate the higher order in  $\epsilon$  terms in the one-loop amplitude to higher loop amplitudes [65–68]. For MHV amplitudes in  $\mathcal{N} = 4$  super Yang-Mills the dimension shifting relationship of [60] can be used in conjunction with the  $D$ -dimensional generalised unitarity method in chapter 2 to compute to all orders in  $\epsilon$ .

### 1.6.2 Triple cuts in $\mathcal{N} = 1$ Super Yang-Mills

Generalised unitarity was also applied to  $\mathcal{N} = 1$  SYM, in particular to the calculation of the next-to-MHV amplitude with adjacent negative-helicity gluons [69]. These amplitudes can be expressed solely in terms of triangles, and were computed in [69] using triple cuts<sup>3</sup>.

We now consider the simple example of the triple cut of a the MHV amplitude in  $\mathcal{N} = 1$  Super Yang-Mills with the two negative helicity gluons adjacent. This example was instrumental in our understanding of the procedure of ‘reconstructing the Feynman integral’ which enabled us to understand how to compute the  $D$ -dimensional triple cuts of chapter 2. The MHV amplitude with adjacent negative helicity gluons has been computed using two particle cuts [59, 60] and MHV rules [47, 48] and is particularly simple as it does not contain any box integral terms. The absence of boxes can also be seen immediately by considering the quadruple cuts and realising that all helicity assignments result in an unphysical constraint on the external momenta.

The two helicity assignments contributing to this triple cut are given in Figure 1.7. The amplitudes in this cut involve many positive helicity gluons, a single negative helicity gluon and a pair of fermions  $f$  or a pair of scalars  $s$ . These amplitudes are related to the usual gluon amplitudes by:

$$A(\dots g_i^- \dots f_j^- \dots f_k^+) = \frac{\langle ik \rangle}{\langle ij \rangle} A^{\text{gluons}} \quad (1.62)$$

$$A(\dots g_i^- \dots s_j^- \dots s_k^+) = \frac{\langle ik \rangle^2}{\langle ij \rangle^2} A^{\text{gluons}} \quad (1.63)$$

---

<sup>3</sup>A new calculation based on localisation in spinor space was also introduced in [70].

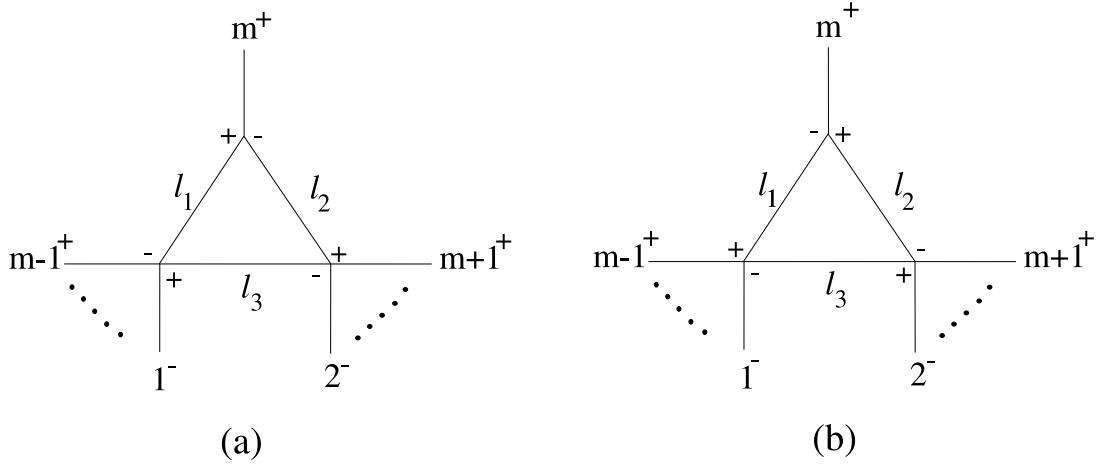


Figure 1.7: *The diagrams in the triple cut of the one-loop MHV amplitude for  $\mathcal{N}=1$  Super-Yang Mills.*

The triple cut contains four terms corresponding to a fermion and a scalar running in the loop of the two diagrams in Figure 1.7:

$$\begin{aligned}
 \text{triple cut} &= \frac{\langle 1|ml_1|2\rangle\langle 1|l_2l_3|1\rangle\langle 2|l_1l_3|2\rangle}{P^2Q^2\langle 23\rangle\dots\langle n1\rangle} - \frac{\langle 2|ml_1|2\rangle\langle 1|l_2l_3|1\rangle\langle 2|l_1l_3|1\rangle}{P^2Q^2\langle 23\rangle\dots\langle n1\rangle} \\
 &+ \frac{\langle 1|ml_1|2\rangle\langle 1|l_2l_3|1\rangle\langle 2|l_1l_3|2\rangle}{P^2Q^2\langle 23\rangle\dots\langle n1\rangle} - \frac{\langle 1|ml_1|1\rangle\langle 1|l_2l_3|2\rangle\langle 2|l_1l_3|2\rangle}{P^2Q^2\langle 23\rangle\dots\langle n1\rangle} \\
 &= \frac{A_n^{\text{tree}}(1^-, 2^-, 3^+, \dots, n^+)}{(p_1 + p_2)^2} \text{tr}_+(12 l_1 m)
 \end{aligned} \tag{1.64}$$

Unlike the quadruple cuts, which completely localise the integral, triple cuts cut only three of the propagators and there is still some integration left to do. In this example it appears we are left with the following integral:

$$\int d^{4-2\epsilon}l \delta^+(l_1^2)\delta^+(l_2^2)\delta^+(l_3^2) l_1^\mu \tag{1.65}$$

However, calculation of this integral reveals that it is proportional to  $m^\mu$  and therefore the triple cut (1.64) vanishes. So initially, it appears that triple cuts do not allow us to compute the amplitude. The correct procedure is to ‘reconstruct the Feynman integral’ by replacing the delta functions in (1.65) by propagators to give the integral:

$$\int d^{4-2\epsilon}l \frac{l_1^\mu}{l_1^2 l_2^2 l_3^2} \tag{1.66}$$

Inserting the result of this integral into (1.64) yields an answer in agreement with two-particle cuts [59, 60] and MHV rules [47, 48].

## 1.7 The BCFW recursion relation

Another new technique for calculating amplitudes is the Britto, Cachazo, Feng and Witten (BCFW) recursion relation for tree-level Yang-Mills amplitudes [16, 17]. This elegant technique is based on only two very general properties of amplitudes, analyticity [53, 57] and factorisation on multi-particle poles and hence the idea of BCFW recursion is applicable in many different contexts. Scattering amplitudes can be regarded as analytic functions of many complex variables, the (complexified) kinematic invariants they depend on. However, in order to fully use the powerful theorems of complex analysis, it is useful to map scattering amplitudes to a function of one complex variable. To this end, BCFW considered the following deformation of an amplitude which shifts the spinors of two of the  $n$  massless external particles labelled  $i$  and  $j$  and involves a complex parameter  $z$ :

$$\begin{aligned}\lambda_i &\rightarrow \lambda_i \\ \tilde{\lambda}_i &\rightarrow \tilde{\lambda}_i - z\tilde{\lambda}_j \\ \lambda_j &\rightarrow \lambda_j + z\lambda_i \\ \tilde{\lambda}_j &\rightarrow \tilde{\lambda}_j\end{aligned}\tag{1.67}$$

This deformation does not make sense for real momenta in Minkowski space which satisfy  $\tilde{\lambda} = \pm\bar{\lambda}$ , but is fine for complex momenta. Under this shift, the shifted momenta  $p_i(z)$  and  $p_j(z)$  remain on-shell for all  $z$  and  $p_i(z) + p_j(z) = p_i(0) + p_j(0)$ . So the shifted amplitude  $A(1, \dots, p_i(z), \dots, p_j(z), \dots, n)$  is an on-shell amplitude for all  $z$ . In BCFW recursion the deformed amplitude  $A(z)$  proves useful for calculating the undeformed amplitude of physical interest  $A(0)$ . It is possible and often useful to consider more general deformations than (1.67) which still preserve momentum conservation for all  $z$ . For example more exotic shifts have shown that the tree-level CSW rules [38] are an instance of BCFW recursion and multiple shifts have been used to eliminate boundary terms in a generalisation of BCFW recursion to one-loop QCD amplitudes [18].

The BCFW recursion relation emerges from considering the following integral where the contour of the integral  $C$  is the circle at infinity,

$$\frac{1}{2\pi i} \oint_C dz \frac{A(z)}{z}\tag{1.68}$$

Assuming that  $A(z) \rightarrow 0$  as  $z \rightarrow \infty$  then the Cauchy residue theorem writes the amplitude we wish to calculate  $A(0)$  as a sum of residues of  $A(z)/z$ ,

$$A(0) = - \sum_{\substack{\text{poles of } A(z)/z \\ \text{excluding } z=0}} \text{Res} \left\{ \frac{A(z)}{z} \right\}\tag{1.69}$$

For tree-level Yang-Mills,  $A(z)$  has only simple poles. The pole at  $z = z_{\text{pole}}$  is associated

with the shifted momentum invariant  $(p_a(z) + \dots + p_b(z))^2$  becoming zero. The residue at this pole is then given by factorising the shifted amplitude on this pole in the shifted momentum invariants,

$$\text{Res} \left\{ \frac{A(z)}{z} \right\} = \sum_h A_L^h(z=z_{pole}) \frac{i}{(p_a + \dots + p_b)^2} A_R^{-h}(z=z_{pole}) \quad (1.70)$$

where the sum is over the possible helicity  $h$  of the intermediate state. The left and right shifted amplitudes  $A_L$  and  $A_R$  are, of course, only defined for  $z = z_{pole}$  when the shifted momentum invariant  $(p_a(z) + \dots + p_b(z))^2$  is zero. The inverse squared momentum associated with the pole which appears between the left and right shifted amplitudes, is reminiscent of a scalar propagator and is evaluated with unshifted kinematics. Since a shifted momentum invariant involving both (or neither) of the shifted legs  $i$  and  $j$  will remain unshifted and not give rise to a pole, the shifted legs  $i$  and  $j$  will always appear on opposite sides of the factorisation. So this procedure constructs an  $n$ -point amplitude from amplitudes with fewer legs. The use of complex momenta is essential throughout for the shifts to make sense and also the factorisation onto three point amplitudes.

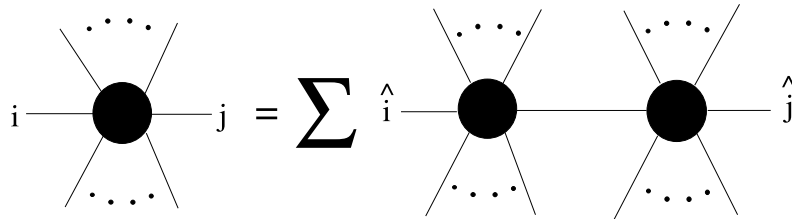


Figure 1.8: A diagrammatic representation of the BCFW recursion relation. The sum is over all factorisations into pairs of amplitudes and the possible helicity of the intermediate state.

### 1.7.1 A four-point example

In this section we review an explicit example of BCFW recursion. We show how to compute the tree-level four-point MHV Yang-Mills amplitude  $A(1^-, 2^+, 3^-, 4^+)$  from the three-point amplitudes given in equation (1.57). To do this we use the standard BCFW shifts in (1.67) with  $i = 1$  and  $j = 2$ . It is standard to denote the shifted spinors  $i$  and  $j$  with hats.

The first thing to do is to consider which shifted momentum invariants can vanish causing the shifted amplitude to develop singularities. In our case there is just one shifted momentum invariant which can vanish  $(\hat{1} + 4)^2 = (\hat{2} + 3)^2$ . In this four-point example the singularity in the shifted amplitude is caused by individual shifted spinor brackets vanishing.

The shifted brackets  $[\hat{1}4]$  and  $\langle\hat{2}3\rangle$  both vanish at the same point  $z_{pole}$  in the complex  $z$  plane.

$$z_{pole} = \frac{[14]}{[24]} = -\frac{\langle 23 \rangle}{\langle 13 \rangle} \quad (1.71)$$

Now we want to understand the factorisation at this pole. Recall the kinematic conditions for three point amplitudes in complex momenta given in (1.57). At the pole we have the condition  $[\hat{1}] \propto |4\rangle$ , which implies that the  $\hat{1}$  and 4 legs are part of a three-point  $A(\hat{1}^-, \hat{k}^-, 4^+)$  amplitude. Similarly,  $[\hat{2}] \propto |3\rangle$  at the pole implies that the  $\hat{2}$  and 3 legs are part of the three-point  $A(3^-, \hat{k}^+, \hat{2}^+)$  amplitude. So the single recursive diagram in this construction is the one given in Figure 1.9.

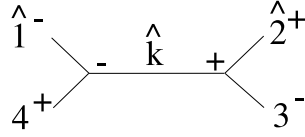


Figure 1.9: *The recursive diagram in the BCFW construction of  $A(1^-, 2^+, 3^-, 4^+)$ .*

To calculate the four point amplitude  $A(1^-, 2^+, 3^-, 4^+)$  we simply multiply the two three-point amplitudes, evaluated with shifted kinematics at  $z = z_{pole}$ , by the scalar propagator for the diagram,

$$\begin{aligned} A(1^-, 2^+, 3^-, 4^+) &= A(\hat{1}^-, \hat{k}^-, 4^+) \frac{i}{\langle 23 \rangle [32]} A(3^-, \hat{k}^+, \hat{2}^+) \\ &= \left( i \frac{\langle 1\hat{k} \rangle^3}{\langle \hat{k}4 \rangle \langle 41 \rangle} \right) \frac{i}{\langle 23 \rangle [32]} \left( i \frac{[2\hat{k}]^3}{[23] [3\hat{k}]} \right) \\ &= \frac{i}{\langle 41 \rangle \langle 23 \rangle [23]^2} \frac{\langle 1|\hat{k}|2 \rangle^3}{\langle 4|\hat{k}|3 \rangle} \\ &= \frac{i}{\langle 41 \rangle \langle 23 \rangle [23]^2} \frac{\langle 1|3|2 \rangle^3}{\langle 4|\hat{2}|3 \rangle} \\ &= i \frac{\langle 13 \rangle^3}{\langle 41 \rangle \langle 23 \rangle \langle \hat{2}4 \rangle} \end{aligned} \quad (1.72)$$

where we have eliminated  $\hat{k}$  using the momentum conservation formula  $\hat{k} = \hat{2} + 3$ . To remove the remaining hat from this expression we use the value of  $z$  at the pole (1.71),

$$\begin{aligned} \langle \hat{2}4 \rangle &= \langle 24 \rangle + z_{pole} \langle 14 \rangle \\ &= \langle 24 \rangle - \frac{\langle 23 \rangle \langle 14 \rangle}{\langle 13 \rangle} = \langle 24 \rangle - \frac{\langle 21 \rangle \langle 34 \rangle}{\langle 13 \rangle} + \frac{\langle 24 \rangle \langle 31 \rangle}{\langle 13 \rangle} = \frac{\langle 12 \rangle \langle 34 \rangle}{\langle 13 \rangle} \end{aligned} \quad (1.73)$$

where the simplification uses the Schouten identity (1.12). Using (1.73) in (1.72) gives a

result in agreement with (1.23):

$$A(1^-, 2^+, 3^-, 4^+) = i \frac{\langle 13 \rangle^4}{\langle 12 \rangle \langle 23 \rangle \langle 34 \rangle \langle 41 \rangle} \quad (1.74)$$

### 1.7.2 Generalisations of BCFW recursion

The idea of the BCFW recursion relation has been generalised to many other situations in perturbative field theory. These include tree-level amplitudes with fermions and scalars [71, 72] tree-level gravity amplitudes [73, 74] and tree-level amplitudes with massive particles [61]. The recursion relation has been generalised to compute the rational part of one-loop QCD amplitudes [18, 75–78]. On-shell recursion has also be used to determine the coefficients of integral functions appearing in one-loop scattering amplitudes of gauge theories [79].

Once the three-point vertices of a theory in complex momenta have been specified, no further information is required to use BCFW recursion to compute all the higher point tree-amplitudes. The generalisation of BCFW recursion to tree-level gravity [73, 74] uses the following three-point gravity amplitudes which are just the square of the Yang-Mills amplitudes:

$$M_3(1^-, 2^-, 3^+) = \left( i \frac{\langle 12 \rangle^3}{\langle 23 \rangle \langle 31 \rangle} \right)^2 \quad \text{and} \quad \tilde{\lambda}_1 \propto \tilde{\lambda}_2 \propto \tilde{\lambda}_3 \quad (1.75)$$

$$M_3(1^+, 2^+, 3^-) = \left( i \frac{[12]^3}{[23][31]} \right)^2 \quad \text{and} \quad \lambda_1 \propto \lambda_2 \propto \lambda_3 \quad (1.76)$$

A complication that arises in the generalisation of BCFW recursion to other field theories is understanding the behaviour of the shifted amplitude at large  $z$ . In [17] the vanishing at infinity of an appropriately shifted Yang-Mills amplitude was proved by analysing the Feynman diagrams. For tree-level gravity there is no complete proof of the absence of boundary terms. In the appendix of [74] the KLT relations were used to prove that  $A(z) \rightarrow 0$  as  $z \rightarrow \infty$  for amplitudes with up to eight gravitons. The KLT relations [80] relate tree-level Yang-Mills amplitudes to tree-level gravity amplitudes.

It is also possible to perform BCFW recursion for tree amplitudes with two adjacent massive scalars and many massless gluons [61]. These tree-level amplitudes will be important in the next chapter, as they are the building blocks of the new method of  $D$ -dimensional generalised unitarity for the calculation of complete one-loop QCD amplitudes. In this case the three-point amplitudes are given by:

$$A_3(l_1^+, k^+, l_2^-) = A_3(l_1^-, k^+, l_2^+) = \frac{\langle q_1 | l_1 | k \rangle}{\langle q_1 k \rangle} \quad (1.77)$$

$$A_3(l_1^+, k^-, l_2^-) = A_3(l_1^-, k^-, l_2^+) = \frac{\langle k | l_1 | q_2 \rangle}{[k q_2]} \quad (1.78)$$

Where  $l_1$  and  $l_2$  are the massive scalars and  $k$  is a massless gluon.  $q_1$  and  $q_2$  are arbitrary reference vectors that are not proportional to  $k$ . Higher point amplitudes can be built recursively from these three-point amplitudes using standard BCFW shifts on the massless external legs. As in the massless case the shifted amplitude has simple poles coming from internal propagators  $1/P(z)^2$ . The only difference in this case is that the propagator is now a massive one.

In chapter 3 we will present a generalisation of BCFW recursion to the one-loop finite amplitudes of pure Einstein gravity. This generalisation has much in common with the generalisation of BCFW recursion to the rational parts of one-loop QCD amplitudes of [18].

### 1.7.3 Risager's proof of the CSW rules

The CSW rules for Yang-Mills tree amplitudes are just one instance of BCFW recursion. This elegant proof of the CSW construction was discovered by Risager [38]. Instead of using the standard BCFW shifts (1.67) Risager used more exotic shifts that give precisely the CSW diagrammatics. These shifts were then used to provide a CSW style construction for tree-level gravity [81].

The choice of BCFW shifts that coincide with the CSW rules are those that affect the shifted momentum invariants corresponding to the propagators in the set of CSW diagrams and none of the others. To construct CSW rules for a next-to-MHV amplitude the shifted momentum invariants must contain at least one negative helicity gluon and the compliment of the shifted momentum invariants must also contain at least one negative helicity gluon. This set of invariants are affected by a shift on every negative helicity gluon. For the three-point googly amplitudes not to contribute only the anti-holomorphic spinors must be shifted.

For the CSW construction of a next-to-MHV amplitude, Risager found some explicit shifts. A next-to-MHV amplitude has three negative helicity gluons. These gluons will be labelled 1, 2, 3. We start by considering the following sum of three standard BCFW shifts:

$$\begin{aligned}
 \eta &\rightarrow \eta + z_1 r_1 \lambda_1 + z_2 r_2 \lambda_2 + z_3 r_3 \lambda_3 \\
 \tilde{\lambda}_1 &\rightarrow \tilde{\lambda}_1 - z_1 r_1 \tilde{\eta} \\
 \tilde{\lambda}_2 &\rightarrow \tilde{\lambda}_2 - z_2 r_2 \tilde{\eta} \\
 \tilde{\lambda}_3 &\rightarrow \tilde{\lambda}_3 - z_3 r_3 \tilde{\eta}
 \end{aligned} \tag{1.79}$$

This sum of shifts preserves momentum conservation. If we now choose  $z_1 = z_2 = z_3 = z$  and  $r_1 = \langle 23 \rangle$ ,  $r_2 = \langle 31 \rangle$ ,  $r_3 = \langle 12 \rangle$  then  $\eta$  becomes unshifted. This can be seen by contracting the

shifted  $\eta$  with an arbitrary spinor  $a$  and using the Schouten identity (1.12).

$$\begin{aligned}
 \langle \hat{\eta}a \rangle &= \langle \eta a \rangle + z(\langle 23 \rangle \langle a1 \rangle + \langle 31 \rangle \langle a2 \rangle + \langle 12 \rangle \langle a3 \rangle) \\
 &= \langle \eta a \rangle + z(\langle 2a \rangle \langle 31 \rangle - \langle 21 \rangle \langle 3a \rangle + \langle 31 \rangle \langle a2 \rangle + \langle 12 \rangle \langle a3 \rangle) \\
 &= \langle \eta a \rangle
 \end{aligned} \tag{1.80}$$

Thus we have the shifts that we require to split a next-to-MHV amplitude into a sum of diagrams containing all the possible pairs of MHV amplitudes:

$$\begin{aligned}
 \tilde{\lambda}_1 &\rightarrow \tilde{\lambda}_1 - z\langle 23 \rangle \tilde{\eta} \\
 \tilde{\lambda}_2 &\rightarrow \tilde{\lambda}_2 - z\langle 31 \rangle \tilde{\eta} \\
 \tilde{\lambda}_3 &\rightarrow \tilde{\lambda}_3 - z\langle 12 \rangle \tilde{\eta}
 \end{aligned} \tag{1.81}$$

where  $\tilde{\eta}$  is completely arbitrary spinor. Of course the  $\eta$  in these shifts is the same  $\eta$  as appeared in the CSW ‘off-shell’ prescription (1.41). BCFW recursion gives an on-shell explanation of CSW’s ‘off-shell’ prescription. The off-shell prescription is just the process of writing the shifted internal legs of the on-shell recursive diagram in terms of the unshifted external legs. For example if one is calculating the  $- - - + +$  amplitude using Risager’s shifts, one has the same diagrams as occur in Figure 1.3. Figure 1.3a gives the same algebra as (1.43) where the internal leg  $k$  is always on-shell and usually denoted by  $\hat{k}$ . One then eliminates the  $\hat{k}$  from the various brackets like this:

$$\begin{aligned}
 \langle 2\hat{k} \rangle &= \frac{\langle 2|\hat{k}|\eta \rangle}{[\hat{k}\eta]} \\
 &= \frac{\langle 2|\hat{3} + 4|\eta \rangle}{[\hat{k}\eta]} \\
 &= \frac{\langle 2|3 + 4|\eta \rangle}{[\hat{k}\eta]}
 \end{aligned} \tag{1.82}$$

where the  $[\hat{k}\eta]$  in the denominator of (1.82) will cancel overall since the expression (1.43) has the same number of  $\hat{k}$ s in the numerator as the denominator. So (1.82) exactly parallels the example of CSW’s ‘off-shell’ prescription in (1.44).

In chapter 3 we will use Risager’s shifts for a different purpose. In chapter 3 we will present a generalisation of BCFW recursion to the one-loop finite amplitudes in pure Einstein gravity. Using the standard BCFW shifts to calculate the all-plus one-loop amplitude in pure gravity recursively results in a boundary term, however using Risager’s shifts to shift only the holomorphic spinors does not involve a boundary term.

# CHAPTER 2

## GENERALISED UNITARITY FOR PURE YANG-MILLS

The main point of this chapter is the observation that generalised unitarity is actually a useful concept also in  $4 - 2\epsilon$  dimensions; in turn this means that generalised  $(4 - 2\epsilon)$ -dimensional unitarity is relevant for the calculation of non-supersymmetric amplitudes at one loop. In particular in this chapter we will be able to compute amplitudes in non-supersymmetric Yang-Mills by using quadruple and triple cuts in  $4 - 2\epsilon$  dimensions. This is advantageous for at least three reasons. First of all, working with multiple cuts simplifies considerably the algebra, because several on-shell conditions can be used at the same time; furthermore, for the case of quadruple cuts the integration is actually completely frozen [15] so that the coefficient of the relevant box functions entering the amplitude can be calculated without performing any integration at all. Lastly, the tree-level sub-amplitudes which are sewn together in order to form the multiple cut of the amplitude are simpler than those entering the two-particle cuts of the same amplitude. In principle further progress with this approach will not require major new conceptual advances, and the method will be directly applicable to more complicated and currently unknown amplitudes.

### 2.1 Generalised Unitarity in $D = 4 - 2\epsilon$ Dimensions

Conventional unitarity and generalised unitarity in *four dimensions* have been shown to be extremely powerful tools for calculating one-loop and higher-loop scattering amplitudes in supersymmetric gauge theories and gravity. At one-loop, conventional unitarity amounts to reconstructing the full amplitude from the knowledge of the discontinuity or imaginary part of the amplitude. In this process the amplitude is cut into two tree-level, on-shell amplitudes defined in four dimensions, and the two propagators connecting the two sub-amplitudes are replaced by on-shell delta-functions which reduce the loop integration to a phase space integration. In principle this cutting technique is only sensitive to terms in the amplitude that have discontinuities, like logarithms and polylogarithms, and in general any cut-free, rational terms are lost. However, in supersymmetric theories all rational terms turn out to be uniquely linked to terms with discontinuities, and therefore the full amplitudes can be reconstructed in this fashion [13, 14].

Furthermore, in supersymmetric theories the one-loop amplitudes are known to be linear combinations of scalar box functions, linear triangle functions and linear bubble functions, with the coefficients being rational functions in spinor products. So the task is really to find an efficient way to fix those coefficients with as few manipulations and/or integrations as possible.

The method based on conventional unitarity introduced by BDDK in [13, 14] does not evaluate the phase space integrals explicitly (from which the full amplitude would be obtained by performing a dispersion integral), rather it reconstructs the loop integrand from which one is able to read off the coefficients of the various integral functions. In practice this means that for a given momentum channel the integrand (which is a product of two tree amplitudes) is simplified as much as possible using the condition that the two internal lines are on-shell, and only in the last step the two delta-functions are replaced by the appropriate propagators which turn the integral from a phase space integral back to a fully-fledged loop integral. The resulting integral function will have the correct discontinuities in the particular channel, but, in general, it will also have additional discontinuities in other channels. Nevertheless, working channel by channel one can extract linear equations for the coefficients which allow us in the end to determine the complete amplitude. However, because of the problem of the additional, unwanted discontinuities, this does not provide a diagrammatic method, i.e. one cannot just sum the various integrals for each channel since different discontinuities might be counted with different weights.

It is natural to contemplate if there exist other complementary, or more efficient methods to extract the above mentioned rational coefficients of the various integral functions, and if in particular we can replace more than two propagators by delta functions, so that the loop integration is further restricted - or even completely localised. The procedure of replacing several internal propagators by  $\delta^{(+)}$ -functions is well known from the study of singularities and discontinuities of Feynman integrals, and goes under the name of *generalised unitarity* [56, 57]. What turns generalised unitarity into a powerful tool is the fact that generalised cuts of amplitudes can be evaluated with less effort than conventional two-particle cuts.

The most dramatic simplification arises from using quadruple cuts in one-loop amplitudes in  $\mathcal{N} = 4$  SYM. In this case it is known that the one-loop amplitudes are simply given by a sum of scalar box functions without triangles or bubbles [13]. Each quadruple cut singles out a unique box function, and because of the presence of the four  $\delta^{(+)}$ -functions the loop integration is completely frozen; hence, the coefficient of this particular box is simply given by the product of four tree-level scattering amplitudes [15]. An important subtlety arises here because quadruple cuts do not have solutions in real Minkowski space; therefore at intermediate steps one has to work with complexified momenta.

At this point we can push the analogy with the ‘reconstruction of the Feynman integrand’ a step further. Using the on-shell conditions we can pull out the prefactor which is just

the product of four tree-level amplitudes in front of the integral, and the integrand of the remaining loop integral becomes just a product of four  $\delta^{(+)}$ -functions. If we now promote the integral to a Feynman integral by replacing all  $\delta^{(+)}$ -functions by the corresponding propagators<sup>1</sup> we arrive at the integral representation of the appropriate box function. Note that no over-counting issue arises, because each quadruple cut selects a unique box function, and the final result is obtained by summing over all quadruple cuts. In some sense, one can really think of this as a true diagrammatic prescription.

As we reduce the amount of supersymmetry to  $\mathcal{N} = 1$ , life becomes a bit more complicated, since the one-loop amplitudes are linear combinations of scalar box, triangle and bubble integral functions. No ambiguities related to rational terms occur however, thanks to supersymmetry. It is therefore natural to attack the problem in two steps: First, use quadruple cuts to fix all the box coefficients as described in the previous paragraph. Second, use triple cuts to fix triangle and bubble coefficients. Note that the triple cuts also have contributions from the box functions which have been determined in the first step. The three  $\delta^{(+)}$ -functions are not sufficient to freeze the loop integration completely, and it is advantageous to use again the “reconstruction of the Feynman integrand” method, i.e. use the on-shell conditions to simplify the integrand as much as possible, and lift the integral to a full loop integral by reinstating three propagators. The resulting integrand can be written as a sum of (integrand of) scalar boxes, triangles and bubbles, after standard reduction techniques, like Passarino-Veltman, have been employed.

At this point it is useful to distinguish three types of triple cuts according to the number of external lines attached to each of the three tree-level amplitudes. If  $p$  of the three amplitudes have more than one external line attached, we call the cut a  $p$ -mass triple cut. Let us start with the 3-mass triple cut. The box terms can be dropped as they have been determined using quadruple cuts, the coefficients of three-mass triangles can be read off directly, and the remaining terms, which are bubbles or triangles with a different triple cut, are dropped as well. Special care is needed for 1-mass and 2-mass triple cuts. First let us note that any bubble can be written as a linear combination of scalar and linear 1-mass triangles or scalar and linear 2-mass triangles depending on whether the bubble depends on a two-particle invariant,  $t_i^{[2]} = (p_i + p_{i+1})^2$ , or on a  $r$ -particle invariant,  $t_i^{[r]} = (p_i + \dots + p_{i+r-1})^2$ , with  $r > 2$ . Therefore, what we want to argue is that two-particle cuts are not needed and that 1-mass, 2-mass *and* bubbles can be determined from the 1-mass and 2-mass triple cuts. Now every 1-mass triple cut is in one-to-one correspondence with a unique two-particle channel  $t_i^{[2]} = (p_i + p_{i+1})^2$  and allows us to extract the coefficients of 1-mass triangles and bubbles by only keeping terms in the integral depending on that particular  $t_i^{[2]}$  and dropping all boxes and triangles/bubbles not depending on that particular variable. The 2-mass triple cut is associated with two momentum invariants, say  $P^2$  and

---

<sup>1</sup>We thank David Kosower for discussions on this point.

$Q^2$ , and we only keep 2-mass triangles and bubbles that depend on those two invariants.

In non-supersymmetric theories we have to face the problem that the amplitudes contain additional rational terms that are not linked to terms with discontinuities. This statement is true if we only keep terms in the amplitude up to  $\mathcal{O}(\epsilon^0)$ . If we work however in  $D = 4 - 2\epsilon$  dimensions and keep higher orders in  $\epsilon$ , even rational terms  $R$  develop discontinuities of the form  $R(-s)^{-\epsilon} = R - \epsilon \log(-s)R + \mathcal{O}(\epsilon^2)$  and become cut-constructible<sup>2</sup>. In practice, this means that, in our procedure, whenever we cut internal lines by replacing propagators by  $\delta^{(+)}$ -functions we have to keep the cut lines in  $D$  dimensions, and in order to proceed we need to know tree-amplitudes with two legs continued to  $D$  dimensions. Because of the supersymmetric decomposition of one-loop amplitudes in pure Yang-Mills, which was reviewed in the Introduction, we only need to consider the case of a scalar running in the loop. Furthermore, the massless scalar in  $D$  dimensions can be thought of as a massive scalar in four dimensions  $L^2 = l_{(4)}^2 + l_{(-2\epsilon)}^2 = l_{(4)}^2 - \mu^2$  whose mass has to be integrated over [59, 60]. Interestingly, a term in the loop integral with the insertion of “mass” term  $(\mu^2)^m$  can be mapped to a higher-dimensional loop integral in  $4 + 2m - 2\epsilon$  dimensions with a massless scalar [59, 60]. Some of the required tree amplitudes with two massive scalars and all positive helicity gluons have been calculated in [59, 60] using Feynman diagrams and recursive techniques, and more recently all amplitudes with up to four arbitrary helicity gluons and two massive scalars have been presented in [61].

The comments in the last paragraph make it clear that generalised unitarity techniques can readily be generalised to  $D$  dimensions and be used to obtain complete amplitudes in pure Yang-Mills and, more generally, in massless, non-supersymmetric gauge theories. The integrands produced by the method described for four dimensional unitarity will now contain terms multiplied by  $(\mu^2)^m$  and, therefore, the set of integral functions appearing in the amplitudes includes, in addition to the four-dimensional functions, also higher-dimensional box, triangle and bubble functions (some explicit examples of higher-dimensional integral functions can be found in Appendix A). For example the one-loop ++++ gluon amplitude, which vanishes in SYM, is given by a rational function times a box integral with  $\mu^4$  inserted,  $I_4[\mu^4] = (-\epsilon)(1-\epsilon)I_4^{8-2\epsilon} = -1/6 + \mathcal{O}(\epsilon)$ . Hence this amplitude is a purely rational function in spinor variables.

In the following sections we will describe in detail how this procedure is applied in practice. Specifically, using generalised unitarity in  $4 - 2\epsilon$  dimensions we will re-calculate the all-orders in  $\epsilon$  expressions of all one-loop, four gluon scattering amplitudes in non-supersymmetric Yang-Mills, that is ++++, -+++, and the two MHV amplitudes --++ and +-+-; and finally, the five-gluon all-plus helicity amplitude +++++. These amplitudes have already been computed to all orders in  $\epsilon$  in [59], and we find in all cases complete agreement with the results of that paper. The examples we consider are comple-

---

<sup>2</sup>The idea of using unitarity in  $D = 4 - 2\epsilon$  dimensions goes back to [58], and was used in [59, 60].

mentary, as they show that this method can be applied to infrared finite amplitudes that are purely rational (whose supersymmetric counter parts vanish), as well as to infrared divergent amplitudes containing both rational and cut-constructible terms. These calculations are described in Section 3 and Section 4. In Appendix A we have collected some useful definitions and formulae.

## 2.2 The one-loop + + + + amplitude

The one-loop + + + + amplitude with a complex scalar running in the loop is the simplest of the all-plus gluon amplitudes, and was first derived in [82] using the string-inspired formalism. The expression in  $4 - 2\epsilon$  dimensions, valid to all-orders in  $\epsilon$ , is computed in [59] and is given by

$$\mathcal{A}_4^{\text{scalar}}(1^+, 2^+, 3^+, 4^+) = \frac{2i}{(4\pi)^{2-\epsilon}} \frac{[12][34]}{\langle 12 \rangle \langle 34 \rangle} K_4 \quad (2.1)$$

where<sup>3</sup>

$$K_4 := I_4[\mu^4] = -\epsilon(1 - \epsilon)I_4^{D=8-2\epsilon} = -\frac{1}{6} + \mathcal{O}(\epsilon) \quad (2.2)$$

In this chapter we closely follow the conventions of [59], with

$$I_n^{D=4-2\epsilon}[f(p, \mu^2)] := i(-)^{n+1}(4\pi)^{2-\epsilon} \int \frac{d^4 l}{(2\pi)^4} \frac{d^{-2\epsilon} \mu}{(2\pi)^{-2\epsilon}} \frac{f(l, \mu^2)}{(l^2 - \mu^2) \cdots [(l - \sum_{i=1}^{n-1} K_i)^2 - \mu^2]} \quad (2.3)$$

where  $K_i$  are external momenta (which, in colour-ordered amplitudes, are sums of adjacent null momenta of the external gluons) and  $f(l, \mu^2)$  is a generic function of the four-dimensional loop momentum  $l$  and of  $\mu^2$ .

The amplitude with four positive helicity gluons is part of the infinite sequence of all-plus helicity gluons, for which a closed expression was conjectured in [83, 84]. The result for all  $n$  is given by

$$\mathcal{A}_n(+, \dots, +) = -\frac{i}{48\pi^2} \sum_{1 \leq i_1 < i_2 < i_3 < i_4 \leq n} \frac{\langle i_1 i_2 \rangle [i_2 i_3] \langle i_3 i_4 \rangle [i_4 i_1]}{\langle 12 \rangle \langle 23 \rangle \cdots \langle n1 \rangle} \quad (2.4)$$

or alternatively

$$\mathcal{A}_n = -\frac{i}{96\pi^2} \sum_{1 \leq i_1 < i_2 < i_3 < i_4 \leq n} \frac{s_{i_1 i_2} s_{i_3 i_4} - s_{i_1 i_3} s_{i_2 i_4} + s_{i_1 i_4} s_{i_2 i_3} - 4i\epsilon(i_1 i_2 i_3 i_4)}{\langle 12 \rangle \langle 23 \rangle \cdots \langle n1 \rangle} \quad (2.5)$$

where  $\epsilon(abcd) := \epsilon_{\mu\nu\rho\sigma} a^\mu b^\nu c^\rho d^\sigma$ . As  $\epsilon \rightarrow 0$ , (2.1) becomes

$$\mathcal{A}_4 = \frac{i}{48\pi^2} \frac{s_{12}s_{23}}{\langle 12 \rangle \langle 23 \rangle \langle 34 \rangle \langle 41 \rangle} \quad (2.6)$$

---

<sup>3</sup>Notice also that  $[12][34]/(\langle 12 \rangle \langle 34 \rangle) = -s_{12}s_{23}/(\langle 12 \rangle \langle 23 \rangle \langle 34 \rangle \langle 41 \rangle)$ .

We see that this amplitude (2.1) consists of purely rational terms, which are cut-free in four dimensions. We now show how to derive (2.1) from quadruple cuts in  $D=4-2\epsilon$  dimensions.

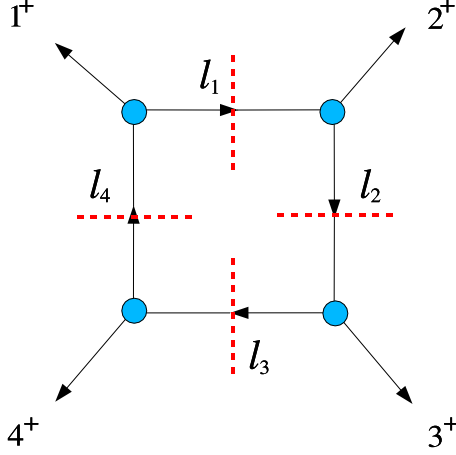


Figure 2.1: One of the two quadruple-cut diagrams for the amplitude  $1^+2^+3^+4^+$ . This diagram is obtained by sewing tree amplitudes (represented by the blue bubbles) with an external positive-helicity gluon and two internal scalars of opposite ‘helicities’. There are two such diagrams, which are obtained one from the other by flipping all the internal helicities. These diagrams are equal so that the full result is obtained by doubling the contribution from the diagram in this Figure. The same remark applies to all the other diagrams considered in this chapter.

Consider the quadruple-cut diagram in Figure 2.1, which is obtained by sewing four three-point scattering amplitudes<sup>4</sup> with one massless gluon and two massive scalars of mass  $\mu^2$ . From [61] we take the three-point amplitudes for one positive-helicity gluon and two scalars:

$$\mathcal{A}(l_1^+, k^+, l_2^-) = \mathcal{A}(l_1^-, k^+, l_2^+) = \frac{\langle q|l_1|k\rangle}{\langle qk\rangle} \quad (2.7)$$

where  $l_1 + l_2 + k = 0$ . Here  $|q\rangle$  is an arbitrary reference spinor not proportional to  $|k\rangle$ . It is easy to see [61] that (2.7) is actually independent of the choice of  $|q\rangle$ .

The  $D$ -dimensional quadruple cut of the amplitude  $++++$  is obtained by combining four three-point tree-level amplitudes,

$$\frac{\langle q_1|l_1|1\rangle}{\langle q_1 1\rangle} \frac{\langle q_2|l_2|2\rangle}{\langle q_2 2\rangle} \frac{\langle q_3|l_3|3\rangle}{\langle q_3 3\rangle} \frac{\langle q_4|l_4|4\rangle}{\langle q_4 4\rangle} \quad (2.8)$$

The reference momenta  $q_i, i = 1, \dots, 4$  in each of the four ratios in this expression may be

<sup>4</sup>In the following for the purpose of calculating the (generalised) cuts we drop factors of  $i$  appearing in the usual definition of tree-amplitudes and propagators. For quadruple and two-particle cuts this does not affect the final result, while for triple cuts this introduces an extra  $(-1)$  factor which we reinstate at the end of every calculation.

chosen arbitrarily. Then, using momentum conservation,

$$l_2 = l_1 - k_2 \quad , \quad l_4 = l_3 - k_4 \quad (2.9)$$

the fact that the external momenta are null, and that the internal momenta square to  $\mu^2$ , it is easy to see that

$$\frac{\langle q_1 | l_1 | 1 \rangle}{\langle q_1 1 \rangle} \frac{\langle q_2 | l_2 | 2 \rangle}{\langle q_2 2 \rangle} = -\mu^2 \frac{[12]}{\langle 12 \rangle} \quad (2.10)$$

and similarly

$$\frac{\langle q_3 | l_3 | 3 \rangle}{\langle q_3 3 \rangle} \frac{\langle q_4 | l_4 | 4 \rangle}{\langle q_4 4 \rangle} = -\mu^2 \frac{[34]}{\langle 34 \rangle} \quad (2.11)$$

so that the above expression (2.8) becomes simply

$$\mu^4 \frac{[12][34]}{\langle 12 \rangle \langle 34 \rangle} \quad (2.12)$$

Finally, we lift the quadruple-cut box to a box function by reinstating the appropriate Feynman propagators. These propagators then combine with the additional factor of  $\mu^4$  in (2.12) to yield the factor  $iK_4/(4\pi)^{2-\epsilon}$  which is proportional to the scalar box integral defined in (2.2). Including an additional factor of 2 due to the fact that there is a complex scalar propagating in the loop, the amplitude (2.1) is reproduced correctly.

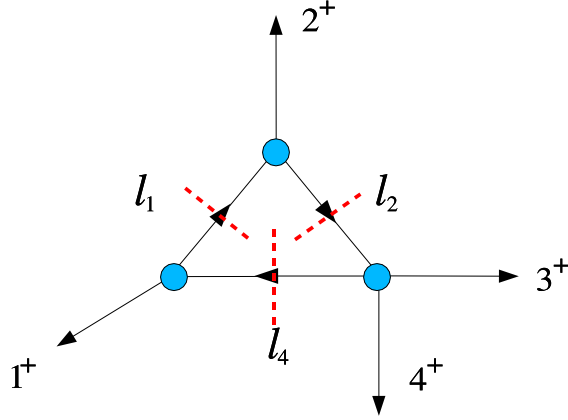


Figure 2.2: One of the possible three-particle cut diagrams for the amplitude  $1^+2^+3^+4^+$ . The others are obtained from this one by cyclic relabelling of the external particles.

Next we inspect three-particle cuts. One of the three tree-level amplitudes we saw in the triple-cut amplitude is an amplitude with two positive-helicity gluons and two scalars [60]

$$\mathcal{A}(l_1^+, 1^+, 2^+, l_2^-) = \mu^2 \frac{[12]}{\langle 12 \rangle [(l_1 + k_1)^2 - \mu^2]} \quad (2.13)$$

Consider, for example, the three-particle cut defined by  $1^+, 2^+, (3^+, 4^+)$ , see Figure 2.2.

Using (2.7) and (2.13), the product of the three tree-level amplitudes gives

$$\frac{\langle q_1|l_1|1\rangle}{\langle q_1 1\rangle} \frac{\langle q_2|l_1|2\rangle}{\langle q_2 2\rangle} \frac{\mu^2[34]}{\langle 34\rangle[(l_2 - k_3)^2 - \mu^2]} \quad (2.14)$$

with  $l_2 = l_1 - k_2$ . As for the quadruple cut, it is easily seen that, on this triple cut,

$$\frac{\langle q_1|l_1|1\rangle}{\langle q_1 1\rangle} \frac{\langle q_2|l_1|2\rangle}{\langle q_2 2\rangle} = -\mu^2 \frac{[12]}{\langle 12\rangle} \quad (2.15)$$

where we used  $l_1^2 = l_2^2 = l_4^2 = \mu^2$ . The triple-cut integrand then becomes

$$-\frac{[12][34]}{\langle 12\rangle\langle 34\rangle} \frac{\mu^4}{[(l_2 - k_3)^2 - \mu^2]} \quad (2.16)$$

which, after replacing the three  $\delta^{(+)}$  functions by propagators, integrates to (2.1), where we have included an additional  $(-1)$  factor following the comments in footnote 4 of this chapter. The factor of 2 in (2.1) comes from summing over the two ‘scalar helicities’. The same result comes from evaluating the remaining triple cuts.

We remark that in the case of the quadruple cut we did not even need to insert the solutions of the on-shell conditions for the loop momenta into the expression coming from the cut. This is not true in general; for example, for the five gluon amplitude discussed below the sum over solutions will be essential to obtaining the correct amplitude.

### 2.3 The one-loop $-+++$ amplitude

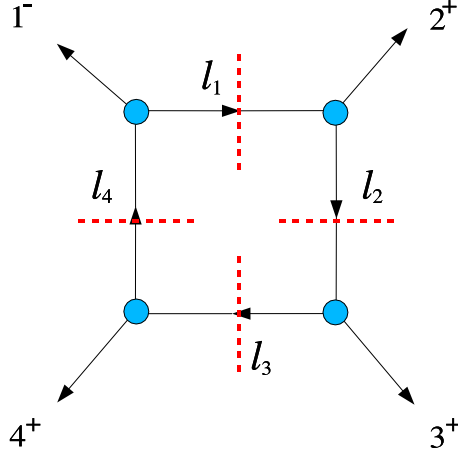
The one-loop four gluon scattering amplitude  $-+++$ , with a complex scalar running in the loop, is given to all orders in  $\epsilon$  by [59]

$$\begin{aligned} \mathcal{A}_4^{\text{scalar}}(1^-, 2^+, 3^+, 4^+) &= \frac{2i}{(4\pi)^{2-\epsilon}} \frac{[24]^2}{[12]\langle 23\rangle\langle 34\rangle[41]} \frac{st}{u} \left[ \frac{t(u-s)}{su} J_3(s) + \frac{s(u-t)}{tu} J_3(t) \right. \\ &\quad \left. - \frac{t-u}{s^2} J_2(s) - \frac{s-u}{t^2} J_2(t) + \frac{st}{2u} J_4 + K_4 \right] \end{aligned} \quad (2.17)$$

We will now show how to derive this result using generalised unitarity cuts.

First consider the quadruple cut (see Figure 2.3). The product of tree amplitudes gives

$$\frac{\langle 1|l_1|q_1\rangle}{[1q_1]} \frac{\langle q_2|l_2|2\rangle}{\langle q_2 2\rangle} \frac{\langle q_3|l_3|3\rangle}{\langle q_3 3\rangle} \frac{\langle q_4|l_4|4\rangle}{\langle q_4 4\rangle} \quad (2.18)$$


 Figure 2.3: *The quadruple cut for the amplitude  $1^- 2^+ 3^+ 4^+$ .*

It is straightforward to show that, on the quadruple cut,

$$\begin{aligned} \frac{\langle q_3 | l_3 | 3 \rangle \langle q_4 | l_4 | 4 \rangle}{\langle q_3 3 \rangle \langle q_4 4 \rangle} &= -\mu^2 \frac{[34]}{\langle 34 \rangle} \\ \frac{\langle 1 | l_1 | q_1 \rangle \langle q_2 | l_2 | 2 \rangle}{\langle 1 q_1 \rangle \langle q_2 2 \rangle} &= \frac{[23]}{[31]} \left( -\mu^2 \frac{\langle 31 \rangle}{\langle 23 \rangle} - [2 | l_1 | 1] \right) \end{aligned}$$

and hence the quadruple cut in Figure 2.3 gives

$$Q(1^+, 2^+, 3^+, 4^-) = \mu^2 \frac{[34]}{\langle 34 \rangle} \frac{[23]}{[31]} \left[ \mu^2 \frac{\langle 31 \rangle}{\langle 23 \rangle} + [2 | l_1 | 1] \right] \quad (2.19)$$

In order to compare with (2.17) it is useful to notice that

$$\frac{[34]}{\langle 34 \rangle} \frac{[23]}{[31]} \frac{\langle 31 \rangle}{\langle 23 \rangle} = \frac{[24]^2}{[12] \langle 23 \rangle \langle 34 \rangle [41]} \frac{st}{u} := \mathcal{N} \quad (2.20)$$

We conclude that the first term in (2.19) generates

$$\frac{i}{(4\pi)^{2-\epsilon}} \left( \frac{[24]^2}{[12] \langle 23 \rangle \langle 34 \rangle [41]} \frac{st}{u} \right) K_4 \quad (2.21)$$

where the prefactor in (2.21) comes from the definition (2.2) and (2.3) for the function  $K_4$ .

The second term in (2.19) corresponds to a linear box integral, which we examine now. We notice that the quadruple cut freezes the loop integration on the solution for the cut. In the linear box term in (2.19) we will then replace  $l_1$  in  $[2 | l_1 | 1]$  by the solutions of the cut, and sum over the different solutions.

Specifically, in order to solve for the cut-loop momentum  $l_1$  one has to require

$$\begin{aligned} l_1^2 &= l_2^2 = l_3^2 = l_4^2 = \mu^2, \\ l_1 &= l_4 - k_1, \quad l_2 = l_1 - k_2, \quad l_3 = l_2 - k_3, \quad l_4 = l_3 - k_4 \end{aligned} \quad (2.22)$$

In order to solve these conditions, it proves useful [15] to use the four linearly independent vectors  $k_1, k_2, k_3$  and  $K$ , where

$$K_\mu := \epsilon_{\mu\nu\rho\sigma} k_1^\nu k_2^\rho k_3^\sigma \quad (2.23)$$

Setting

$$l_1 = ak_1 + bk_2 + ck_3 + dK \quad (2.24)$$

one finds

$$\begin{aligned} a &= \frac{t}{2u}, \quad b = \frac{1}{2}, \quad c = -\frac{s}{2u}, \\ d &= \pm \sqrt{-\frac{st + 4\mu^2 u}{stu^2}} \end{aligned} \quad (2.25)$$

where

$$s = (k_1 + k_2)^2, \quad t = (k_2 + k_3)^2, \quad u = (k_1 + k_3)^2 \quad (2.26)$$

and  $s + t + u = 0$ . Then one has

$$[2|l_1|1] \longrightarrow [2|\frac{l_1^+ + l_1^-}{2}|1] = c \cdot [2|3|1] = -\frac{s}{2u} [23]\langle 31 \rangle \quad (2.27)$$

where  $l_1^\pm$  denotes the two solutions for the quadruple cut. The square root drops out of the calculation (as it should, given that the amplitude is a rational function). We conclude that the second term in (2.19) gives<sup>5</sup>

$$\frac{i}{(4\pi)^{2-\epsilon}} \left( \frac{[24]^2}{[12]\langle 23 \rangle \langle 34 \rangle [41]} \frac{st}{u} \right) \frac{st}{2u} J_4 \quad (2.28)$$

where

$$J_n := I_n[\mu^2] \quad (2.29)$$

Again, the prefactor in (2.28) arises from the definition (2.3). In total the quadruple cut (2.19) gives

$$\frac{2i}{(4\pi)^{2-\epsilon}} \mathcal{N} \left( K_4 + \frac{st}{2u} J_4 \right) \quad (2.30)$$

where we have again included a factor of two for the contribution of a complex scalar. This result matches exactly all the box functions appearing in (2.17).

---

<sup>5</sup>Recall that in our conventions  $t := \langle 23 \rangle [32]$ .

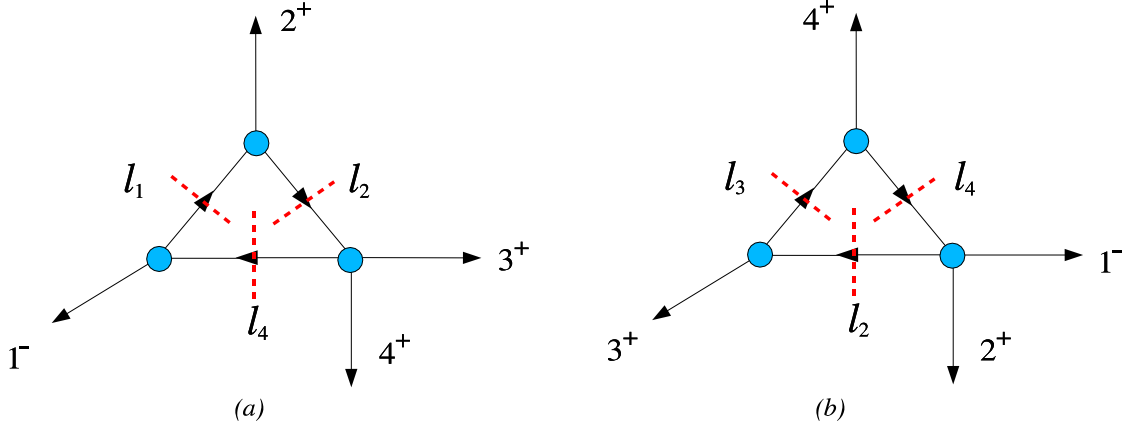


Figure 2.4: *The two inequivalent triple cuts for the amplitude  $1^- 2^+ 3^+ 4^+$ .*

We now move on to consider triple cuts. We start by considering the triple cut in Figure 2.4(a), which we label as  $(1^-, 2^+, (3^+, 4^+))$ . It may be shown that this triple cut yields the following expression:

$$\begin{aligned}
 TC(1^-, 2^+, (3^+, 4^+)) &= \mu^2 \frac{[34]}{\langle 34 \rangle} \frac{[23]}{[31]} \left( -\mu^2 \frac{\langle 31 \rangle}{\langle 23 \rangle} - [2|l_1|1] \right) \frac{1}{(l_2 - k_3)^2 - \mu^2} \\
 &\quad - \mu^2 \frac{[34]}{\langle 34 \rangle} \frac{[2|l_1|1]}{\langle 23 \rangle [31]}
 \end{aligned} \tag{2.31}$$

The first line in (2.31) clearly contains the (negative of the) term already studied with quadruple cuts – see (2.19) (For an explanation of the relative minus sign see again footnote 4 of this chapter).

We now reconsider the linear box term (second term in the first line of (2.31)), and study its Passarino-Veltman (PV) reduction. As we shall see, this box appears also in other triple cuts See (2.43). Let us consider the linear box integral

$$A^\mu := \int \frac{d^4 l_1}{(2\pi)^4} \frac{d^{-2\epsilon} \mu}{(2\pi)^{-2\epsilon}} \frac{\mu^2 l_1^\mu}{(l_1^2 - \mu^2)[(l_1 - k_2)^2 - \mu^2][(l_1 - k_2 - k_3)^2 - \mu^2][(l_1 + k_1)^2 - \mu^2]} \tag{2.32}$$

On general grounds the integral is a linear combination of three of the external momenta,

$$A^\mu = \alpha k_1^\mu + \beta k_2^\mu + \gamma k_3^\mu \tag{2.33}$$

For the coefficients we find

$$\begin{aligned}\alpha &= -\frac{i}{(4\pi)^{2-\epsilon}} \frac{1}{2u} \left[ -tJ_4 - 2J_3(s) + 2J_3(t) \right] \\ \beta &= \frac{i}{(4\pi)^{2-\epsilon}} \frac{1}{2} J_4 \\ \gamma &= -\frac{i}{(4\pi)^{2-\epsilon}} \frac{1}{2u} \left[ sJ_4 - 2J_3(s) + 2J_3(t) \right]\end{aligned}\quad (2.34)$$

Taken literally, this means that from the linear box in (2.31) we not only get the  $J_4$  function but, altogether:

$$\frac{i\mathcal{N}}{(4\pi)^{2-\epsilon}} \left( \frac{st}{2u} J_4 - \frac{t}{u} J_3(s) + \frac{t}{u} J_3(t) \right) \quad (2.35)$$

Summarising, the PV reduction of the first line of the triple cut (2.31), lifted to a Feynman integral, gives:

$$\frac{i\mathcal{N}}{(4\pi)^{2-\epsilon}} \left( K_4 + \frac{st}{2u} J_4 - \frac{t}{u} J_3(s) + \frac{t}{u} J_3(t) \right) \quad (2.36)$$

The last term in (2.36) is clearly spurious – it does not have the right triple cut, and has appeared because we lifted the cut-integral to a Feynman integral; hence we will drop it. In conclusion, the triple cut  $(1^-, 2^+, (3^+, 4^+))$  in Figure 4a leads to

$$\frac{i\mathcal{N}}{(4\pi)^{2-\epsilon}} \left( K_4 + \frac{st}{2u} J_4 - \frac{t}{u} J_3(s) \right) \quad (2.37)$$

We now consider the last term in (2.31), which generates a linear triangle, whose PV reduction we consider now. The linear triangle is proportional to

$$B^\mu := \int \frac{d^4 l_1}{(2\pi)^4} \frac{d^{-2\epsilon} \mu}{(2\pi)^{-2\epsilon}} \frac{\mu^2 l_1^\mu}{(l_1^2 - \mu^2)[(l_1 - k_2)^2 - \mu^2][(l_1 + k_1)^2 - \mu^2]} \quad (2.38)$$

On general grounds,

$$B^\mu = \theta k_1^\mu + \tau k_2^\mu \quad (2.39)$$

and hence

$$[2|B|1] = 0 \quad (2.40)$$

We conclude that the second line in (2.31) gives a vanishing contribution, so that the content of this triple cut is encoded in (2.37).

Next we consider the triple cut labelled by  $((1^-, 2^+), 3^+, 4^+)$  and represented in Figure 2.4b, which gives

$$\begin{aligned}TC((1^-, 2^+), 3^+, 4^+) &= \mu^2 \frac{[34][23]}{\langle 34 \rangle [31]} \left[ -\mu^2 \frac{\langle 31 \rangle}{\langle 23 \rangle} + \frac{\langle 12 \rangle}{\langle 23 \rangle} \langle 3|l_2|2 \rangle \right] \frac{1}{(l_2 + k_2)^2 - \mu^2} \\ &\quad + \mu^2 \frac{[34]}{\langle 34 \rangle} \frac{\langle 1|31l_2 - 23l_2|2 \rangle}{\langle 12 \rangle [12] \langle 23 \rangle [31]}\end{aligned}\quad (2.41)$$

The first term of (2.41) clearly corresponds to the function  $K_4$  already fixed using quadruple cuts. The second term can be rewritten as follows. Introducing  $l_1 := l_2 + k_2$ , we have

$$\frac{\langle 12 \rangle}{\langle 23 \rangle} \langle 3|l_2|2 \rangle = -[2|l_2|1] + \frac{\langle 13 \rangle}{\langle 23 \rangle} [(l_2 + k_2)^2 - \mu^2] \quad (2.42)$$

therefore we can rewrite (2.41) as

$$\begin{aligned} TC((1^-, 2^+), 3^+, 4^+) &= \mu^2 \frac{[34]}{\langle 34 \rangle} \frac{[23]}{[31]} \left( -\mu^2 \frac{\langle 31 \rangle}{\langle 23 \rangle} - [2|l_1|1] \right) \frac{1}{(l_2 + k_2)^2 - \mu^2} \\ &+ \mu^2 \frac{[34]}{\langle 34 \rangle} \left( \frac{\langle 1|31|l_2 - 23|l_2|2 \rangle}{\langle 12 \rangle [12] \langle 23 \rangle [31]} - \frac{[23] \langle 31 \rangle}{[31] \langle 23 \rangle} \right) \end{aligned} \quad (2.43)$$

We know already that the PV reduction of the first line of (2.43) corresponds to (2.36) – with the term containing  $J_3(t)$  removed – so we now study the second line, which will give new contributions.

The second term in the second line corresponds to a scalar triangle, more precisely it gives a contribution

$$-\frac{i\mathcal{N}}{(4\pi)^{2-\epsilon}} J_3(s) \quad (2.44)$$

The first term corresponds to a linear triangle, and now we perform its PV reduction. The relevant integral is

$$C^\mu := \int \frac{d^4 l_2}{(2\pi)^4} \frac{d^{-2\epsilon} \mu}{(2\pi)^{-2\epsilon}} \frac{\mu^2 l_2^\mu}{(l_2^2 - \mu^2)[(l_2 - k_3)^2 - \mu^2][(l_2 + k_1 + k_2)^2 - \mu^2]} \quad (2.45)$$

On general grounds,

$$C^\mu = \lambda k_3^\mu + \kappa (k_1 + k_2)^\mu \quad (2.46)$$

A quick calculation shows that

$$\lambda = -\frac{i}{(4\pi)^{2-\epsilon}} \left[ J_3(s) - \frac{2}{s} J_2(s) \right], \quad \kappa = \frac{i}{(4\pi)^{2-\epsilon}} \frac{1}{s} J_2(s) \quad (2.47)$$

The first term in the second line of (2.43) gives then

$$\frac{i\mathcal{N}}{(4\pi)^{2-\epsilon}} \left( -\frac{u}{s} J_3(s) + \frac{u-t}{s} J_2(s) \right) \quad (2.48)$$

where  $\mathcal{N}$  is defined in (2.20). Altogether, the second line of (2.43) gives

$$\frac{i\mathcal{N}}{(4\pi)^{2-\epsilon}} \left( -\left(1 + \frac{u}{s}\right) J_3(s) + \frac{u-t}{s} J_2(s) \right) \quad (2.49)$$

whereas from the first line of the same equation we get

$$\frac{i\mathcal{N}}{(4\pi)^{2-\epsilon}} \left( K_4 + \frac{st}{2u} J_4 - \frac{t}{u} J_3(s) \right) \quad (2.50)$$

where we have dropped the term  $J_3(t)$  for reasons explained earlier.

We conclude that the function which incorporates all the right cuts in the channels considered so far is equal to the sum of (2.49) and (2.50), which gives

$$\frac{i\mathcal{N}}{(4\pi)^{2-\epsilon}} \left( K_4 + \frac{st}{2u} J_4 - \frac{t}{u} J_3(s) - \left(1 + \frac{u}{s}\right) J_3(s) + \frac{u-t}{s^2} J_2(s) \right) \quad (2.51)$$

Using  $-t/u - 1 - u/s = s/u - u/s$ , (2.51) becomes

$$\frac{i\mathcal{N}}{(4\pi)^{2-\epsilon}} \left( K_4 + \frac{st}{2u} J_4 + \left(\frac{s}{u} - \frac{u}{s}\right) J_3(s) + \frac{u-t}{s^2} J_2(s) \right) \quad (2.52)$$

To finish the calculation one has to consider the two remaining triple cuts. The remaining cuts are  $(4^+, 1^-, (2^+, 3^+))$  and  $((4^+, 1^-), 2^+, 3^+)$ . These cuts can be obtained from the previously considered cuts by exchanging  $s$  with  $t$ .

Our conclusion is therefore that the function (including the usual factor of 2) with the correct quadruple and triple cuts is:

$$\begin{aligned} \frac{2i\mathcal{N}}{(4\pi)^{2-\epsilon}} \left( K_4 + \frac{st}{2u} J_4 + \left(\frac{s}{u} - \frac{u}{s}\right) J_3(s) + \frac{u-t}{s^2} J_2(s) \right. \\ \left. + \left(\frac{t}{u} - \frac{u}{t}\right) J_3(t) + \frac{u-s}{t^2} J_2(t) \right) \end{aligned} \quad (2.53)$$

This agrees precisely with (2.1) using the identities

$$\frac{t(u-s)}{su} = \frac{s}{u} - \frac{u}{s}, \quad \frac{s(u-t)}{tu} = \frac{t}{u} - \frac{u}{t} \quad (2.54)$$

## 2.4 The one-loop $--++$ amplitude

We now turn our attention to the one-loop four point amplitudes with two negative helicity gluons. We start by considering the one-loop amplitude  $\mathcal{A}_4^{\text{scalar}}(1^-, 2^-, 3^+, 4^+)$ , which is given by [59]<sup>6</sup>

$$\mathcal{A}_4^{\text{scalar}}(1^-, 2^-, 3^+, 4^+) = 2 \frac{\mathcal{A}_4^{\text{tree}}}{(4\pi)^{2-\epsilon}} \left( -\frac{t}{s} K_4 + \frac{1}{s} J_2(t) + \frac{1}{t} I_2^{6-2\epsilon}(t) \right) \quad (2.55)$$

---

<sup>6</sup>Here for simplicity we drop the functions  $I_1$  and  $I_2(0)$ , which are zero in the massless case [59]. We also include a factor of two as we are considering complex scalars.

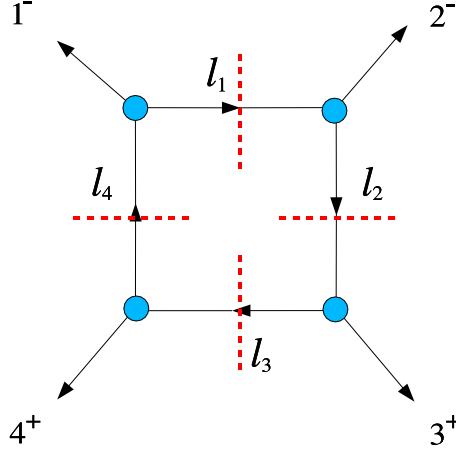


Figure 2.5: *The quadruple cut for the amplitude  $1^-2^-3^+4^+$ .*

To begin with, we consider the quadruple cut of the amplitude in Figure 2.5. It is given by

$$\frac{\langle 1|l_1|q_1\rangle}{[1q_1]} \frac{\langle 2|l_1|q_2\rangle}{[2q_2]} \frac{\langle q_3|l_3|3\rangle}{\langle q_33\rangle} \frac{\langle q_4|l_4|4\rangle}{\langle q_44\rangle} \quad (2.56)$$

By choosing  $q_1 = 2$ ,  $q_2 = 1$ ,  $q_3 = 4$ ,  $q_4 = 3$ , (2.56) can be rewritten as

$$i \frac{t}{s} \mathcal{A}_4^{\text{tree}} \mu^4 \quad (2.57)$$

where

$$\mathcal{A}_4^{\text{tree}} = i \frac{\langle 12\rangle^3}{\langle 23\rangle\langle 34\rangle\langle 41\rangle} \quad (2.58)$$

Reinstating the four cut propagators and integrating over the loop momentum, (2.57) gives

$$-\frac{\mathcal{A}_4^{\text{tree}}}{(4\pi)^{2-\epsilon}} \left( \frac{t}{s} K_4 \right) \quad (2.59)$$

where  $K_4$  is defined in (2.2).

Next we consider triple cuts. We begin our analysis with the triple cut in Figure 2.6(a). This yields

$$\frac{\mu^2[34]}{\langle 34\rangle 2(l_2 \cdot 3)} \frac{\langle 1|l_1|q_1\rangle}{[1q_1]} \frac{\langle 2|l_1|q_2\rangle}{[2q_2]} = -\mu^4 \frac{\langle 12\rangle[34]}{[12]\langle 34\rangle} \frac{1}{2(l_2 \cdot 3)} \quad (2.60)$$

which, upon reinstating the cut propagators and performing the loop momentum integration gives

$$-\frac{\mathcal{A}_4^{\text{tree}}}{(4\pi)^{2-\epsilon}} \left( \frac{t}{s} K_4 \right) \quad (2.61)$$

This function had already been detected with the quadruple cut, as discussed earlier.

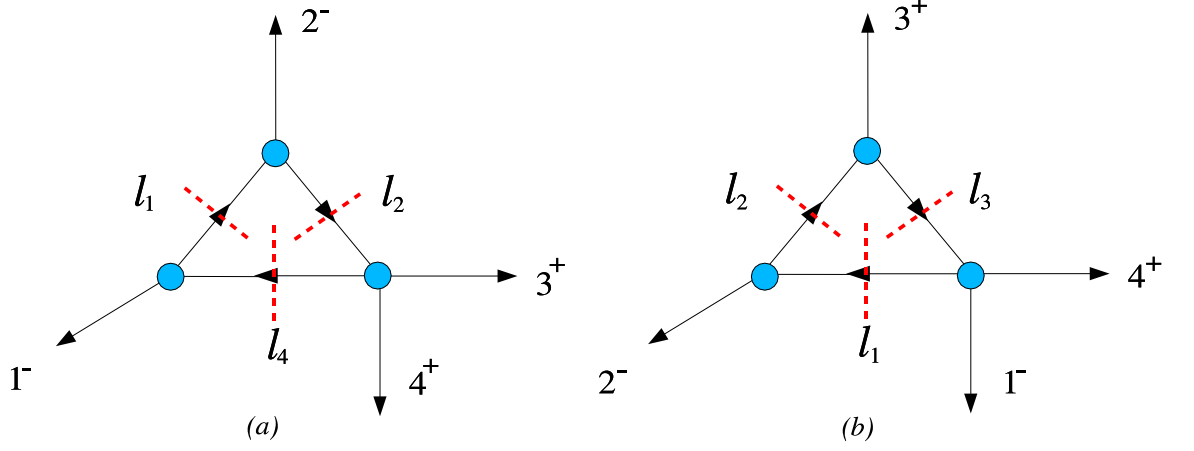


Figure 2.6: The two inequivalent triple cuts for the amplitude  $1^- 2^- 3^+ 4^+$ .

Next we move on to consider the triple cut in Figure 2.6(b). This yields

$$\frac{\langle 1|l_3|4\rangle^2}{2t(l_3 \cdot 4)} \frac{\langle 2|l_1|q_1\rangle}{[2q_1]} \frac{\langle q_2|l_2|3\rangle}{\langle q_2 3\rangle} \quad (2.62)$$

We can re-cast (2.62) as follows. Firstly, we write

$$\frac{\langle 1|l_3|4\rangle \langle q_2|l_2|3\rangle}{\langle q_2 3\rangle} = \mu^2 \frac{\langle 1|4|3\rangle}{\langle 3 4\rangle} - \frac{2(l_3 \cdot 4) \langle 1|l_3|3\rangle}{\langle 3 4\rangle} \quad (2.63)$$

and secondly

$$\frac{\langle 1|l_3|4\rangle \langle 2|l_1|q_1\rangle}{[2q_1]} = \mu^2 \frac{\langle 2|1|4\rangle}{[12]} - \frac{2(l_3 \cdot 4) \langle 2|1|4\rangle}{[12]} + \frac{2(l_3 \cdot 4) \langle 2|l_3|4\rangle}{[12]} \quad (2.64)$$

The expression (2.62) becomes a sum of six terms  $T_i$ ,  $i = 1, \dots, 6$ , where

$$\begin{aligned} T_1 &= \frac{\langle 1|4|3\rangle \langle 2|1|4\rangle \mu^4}{t \langle 3 4\rangle [12] 2(l_3 \cdot 4)} \\ T_2 &= -\frac{\langle 1|4|3\rangle \langle 2|1|4\rangle \mu^2}{t \langle 3 4\rangle [12]} \\ T_3 &= \frac{\langle 1|4|3\rangle \langle 2|l_3|4\rangle \mu^2}{t \langle 3 4\rangle [12]} \end{aligned}$$

$$\begin{aligned}
 T_4 &= -\frac{\langle 2|1|4\rangle\langle 1|l_3|3\rangle\mu^2}{t\langle 34\rangle[12]} \\
 T_5 &= \frac{\langle 2|1|4\rangle\langle 1|l_3|3\rangle 2(l_3 \cdot 4)}{t\langle 34\rangle[12]} \\
 T_6 &= -\frac{\langle 1|l_3|3\rangle\langle 2|l_3|4\rangle 2(l_3 \cdot 4)}{t\langle 34\rangle[12]} \tag{2.65}
 \end{aligned}$$

Next we replace the delta functions with propagators, and integrate over the loop momentum. To evaluate the integrals, we use the linear, quadratic and cubic triangle integrals in  $4 - 2\epsilon$  dimensions listed in the Appendix. The integration of the expressions gives

$$\begin{aligned}
 T_1 &\rightarrow -\frac{\mathcal{A}_4^{\text{tree}}}{(4\pi)^{2-\epsilon}} \left( \frac{t}{s} K_4 \right) \\
 T_2 &\rightarrow -\frac{\mathcal{A}_4^{\text{tree}}}{(4\pi)^{2-\epsilon}} \left( -\frac{t}{s} J_3(t) \right) \\
 T_3 &\rightarrow -\frac{\mathcal{A}_4^{\text{tree}}}{(4\pi)^{2-\epsilon}} \left( \frac{t}{s} J_3(t) - \frac{1}{s} J_2(t) \right) \\
 T_4 &\rightarrow -\frac{\mathcal{A}_4^{\text{tree}}}{(4\pi)^{2-\epsilon}} \left( -\frac{1}{s} J_2(t) \right) \\
 T_5 &\rightarrow -\frac{\mathcal{A}_4^{\text{tree}}}{(4\pi)^{2-\epsilon}} \left( \frac{t}{2s} I_2(t) + \frac{u}{s} I_3^{6-2\epsilon}(t) \right) \\
 T_6 &\rightarrow -\frac{\mathcal{A}_4^{\text{tree}}}{(4\pi)^{2-\epsilon}} \left( -\frac{t}{4s} I_2(t) - \left( \frac{3}{2s} + \frac{1}{t} \right) I_2^{6-2\epsilon}(t) - \frac{u}{s} I_3^{6-2\epsilon}(t) \right) \tag{2.66}
 \end{aligned}$$

We now use (A.26) in [59] or (A.7) of this thesis, relating  $J_2(t)$  to  $I_2(t)$  and  $I_2^{6-2\epsilon}(t)$ . This gives:

$$T_5 + T_6 \rightarrow -\mathcal{A}_4^{\text{tree}} \left( \frac{1}{s} J_2(t) - \frac{1}{t} I_2^{6-2\epsilon}(t) \right) \tag{2.67}$$

Adding up the six  $T_i$  terms, and including the usual factor of two, we obtain

$$-\frac{2\mathcal{A}_4^{\text{tree}}}{(4\pi)^{2-\epsilon}} \left( \frac{t}{s} K_4 - \frac{1}{s} J_2(t) - \frac{1}{t} I_2^{6-2\epsilon}(t) \right) \tag{2.68}$$

which precisely agrees with (2.55).

## 2.5 The one-loop $-+++$ amplitude

Now we consider the one-loop amplitude with a complex scalar in the loop,  $\mathcal{A}_4^{\text{scalar}}(1^-, 2^+, 3^-, 4^+)$ , which is given by [59]

$$\begin{aligned}
 \mathcal{A}_4^{\text{scalar}}(1^-, 2^+, 3^-, 4^+) &= -2 \frac{1}{(4\pi)^{2-\epsilon}} \mathcal{A}_4^{\text{tree}} \left( \frac{st}{u^2} K_4 - \frac{s^2 t^2}{u^3} I_4^{6-2\epsilon} + \frac{st}{u^2} I_3^{6-2\epsilon}(t) \right. \\
 &+ \frac{st}{u^2} I_3^{6-2\epsilon}(s) - \frac{st(s-t)}{u^3} J_3(t) - \frac{st(t-s)}{u^3} J_3(s) + \frac{s}{u^2} J_2(t) + \frac{t}{u^2} J_2(s) \\
 &\left. + \frac{s}{tu} I_2^{6-2\epsilon}(t) + \frac{t}{su} I_2^{6-2\epsilon}(s) + \frac{ts^2}{u^3} I_2(t) + \frac{st^2}{u^3} I_2(s) \right) \quad (2.69)
 \end{aligned}$$

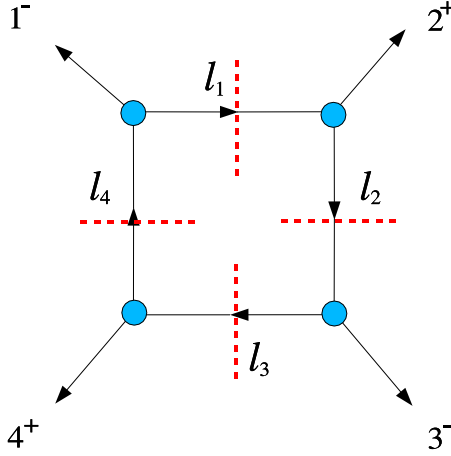


Figure 2.7: *The quadruple cut for the amplitude  $1^- 2^+ 3^- 4^+$ .*

The relevant quadruple cut is represented in Figure 2.7, and gives:

$$\begin{aligned}
 &\frac{\langle 1|l_1|q_1 \rangle}{[1 q_1]} \frac{\langle q_2|l_2|2 \rangle}{\langle q_2 2 \rangle} \frac{\langle 3|l_3|q_3 \rangle}{[3 q_3]} \frac{\langle q_4|l_4|q_4 \rangle}{\langle q_4 4 \rangle} \\
 &= \frac{1}{[1 3] \langle 2 4 \rangle} \left( \langle 1 3 \rangle \mu^2 + \langle 1 2 \rangle \langle 3|l_1|2 \rangle \right) \left( [2 4] \mu^2 - [3 4] \langle 3|l_1|2 \rangle \right) \\
 &= i \mathcal{A}_4^{\text{tree}} \left( \frac{st\mu^4}{u^2} + \frac{2s^2 t \langle 3|l_1|2 \rangle \mu^2}{u^2 \langle 3|1|2 \rangle} + \frac{s^3 t \langle 3|l_1|2 \rangle^2}{u^2 \langle 3|1|2 \rangle^2} \right) \quad (2.70)
 \end{aligned}$$

where

$$\mathcal{A}_4^{\text{tree}} = i \frac{\langle 13 \rangle^4}{\langle 12 \rangle \langle 23 \rangle \langle 34 \rangle \langle 41 \rangle} \quad (2.71)$$

Averaging over the two solutions of the quadruple cut we obtain the following expression:

$$i \mathcal{A}_4^{\text{tree}} \left( \frac{st}{u^2} \mu^4 + \frac{2s^2 t^2}{u^3} \mu^2 + \frac{s^3 t^3}{2u^4} \right) \quad (2.72)$$

After reinstating the four cut propagators and integrating over the loop momentum, (2.72)

gives

$$\frac{1}{(4\pi)^{2-\epsilon}} \mathcal{A}_4^{\text{tree}} \left( -\frac{st}{u^2} K_4 - \frac{2s^2 t^2}{u^3} J_4 - \frac{s^3 t^3}{2u^4} I_4 \right) \quad (2.73)$$

We now use the identity (A.26) in [59] or see (A.5) of this thesis. We ignore all functions that do not have a quadruple cut to write this quadruple cut as:

$$\frac{1}{(4\pi)^{2-\epsilon}} \mathcal{A}_4^{\text{tree}} \left( -\frac{st}{u^2} K_4 + \frac{s^2 t^2}{u^3} I_4^{6-2\epsilon} \right) \quad (2.74)$$

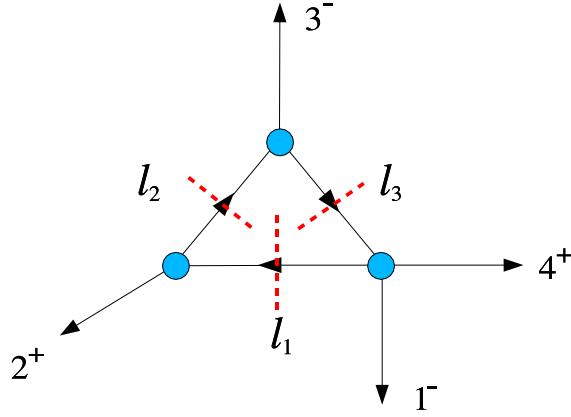


Figure 2.8: *The only independent triple cut for the amplitude  $1^- 2^+ 3^- 4^+$  (the others are obtained from this one by cyclic relabelling of the external gluons).*

We now consider triple cuts. There is only one independent triple cut, and we consider, for instance, the triple cut in Figure 2.8, which gives

$$\frac{\langle 1|l_3|4\rangle^2}{2t(l_3 \cdot 4)} \frac{\langle 3|l_3|q_2\rangle}{[3q_2]} \frac{\langle q_1|l_1|2\rangle}{\langle q_1 2\rangle} \quad (2.75)$$

Using straightforward spinor manipulations, and taking into account properties of the cut momenta, one finds that the above expression may be expanded as a product of two sets of terms. The first is

$$\frac{\langle 1|l_3|4\rangle \langle 3|l_3|q_2\rangle}{[3q_2]} = \frac{\mu^2 \langle 3|1|4\rangle}{[13]} - \frac{t \langle 3|l_3|4\rangle}{[13]} + \frac{2(l_3 \cdot 4) \langle 3|l_3|4\rangle}{[13]} \quad (2.76)$$

whereas the second is

$$\frac{\langle 1|l_3|4\rangle \langle q_1|l_1|2\rangle}{\langle q_1 2\rangle} = \frac{\mu^2 \langle 1|4|2\rangle}{\langle 24\rangle} + \frac{\langle 4|1|2\rangle \langle 1|l_3|4\rangle}{\langle 24\rangle} - \frac{2(l_3 \cdot 4) \langle 1|l_3|2\rangle}{\langle 24\rangle} \quad (2.77)$$

The expression (2.75) becomes then a sum of nine terms  $R_i$ ,  $i = 1, \dots, 9$ , where

$$\begin{aligned}
 R_1 &= \frac{\langle 1|4|2\rangle\langle 3|1|4\rangle\mu^4}{t[1\ 3]\langle 2\ 4\rangle 2(l_3 \cdot 4)} \\
 R_2 &= \frac{\langle 4|1|2\rangle\langle 3|1|4\rangle\langle 1|l_3|4\rangle\mu^2}{t[1\ 3]\langle 2\ 4\rangle 2(l_3 \cdot 4)} \\
 R_3 &= -\frac{\langle 3|1|4\rangle\langle 1|l_3|2\rangle\mu^2}{t[1\ 3]\langle 2\ 4\rangle} \\
 R_4 &= -\frac{\langle 1|4|2\rangle\langle 3|l_3|4\rangle\mu^2}{[1\ 3]\langle 2\ 4\rangle 2(l_3 \cdot 4)} \\
 R_5 &= -\frac{\langle 4|1|2\rangle\langle 3|l_3|4\rangle\langle 1|l_3|4\rangle}{[1\ 3]\langle 2\ 4\rangle 2(l_3 \cdot 4)} \\
 R_6 &= \frac{\langle 3|l_3|4\rangle\langle 1|l_3|2\rangle}{[1\ 3]\langle 2\ 4\rangle} \\
 R_7 &= \frac{\langle 1|4|2\rangle\langle 3|l_3|4\rangle\mu^2}{t[1\ 3]\langle 2\ 4\rangle} \\
 R_8 &= \frac{\langle 4|1|2\rangle\langle 3|l_3|4\rangle\langle 1|l_3|4\rangle}{t[1\ 3]\langle 2\ 4\rangle} \\
 R_9 &= -\frac{\langle 3|l_3|4\rangle\langle 1|l_3|2\rangle 2(l_3 \cdot 4)}{t[1\ 3]\langle 2\ 4\rangle} \tag{2.78}
 \end{aligned}$$

The term  $R_5$  becomes a quadratic box integral when the three delta functions are replaced with propagators. We can use the properties of the cut momenta to re-write  $R_5$  as a sum of terms which will give a box integral, a linear box integral and a linear triangle integral as follows,

$$R_5 = -\frac{\langle 4|1|2\rangle[4|3\ 1|4]\mu^2}{[1\ 3]^2\langle 2\ 4\rangle 2(l_3 \cdot 4)} + \frac{t\langle 4|1|2\rangle[4|3\ l_3|4]}{[1\ 3]^2\langle 2\ 4\rangle 2(l_3 \cdot 4)} - \frac{\langle 4|1|2\rangle[4|3\ l_3|4]}{[1\ 3]^2\langle 2\ 4\rangle} \tag{2.79}$$

We now replace the delta functions with propagators and integrate over the cut momenta. Note that one must drop any terms without cuts in the  $t$ -channel. This must be used for all the linear box integrals that appear above. Using the results for the linear box and the linear, quadratic and cubic triangle integrals in  $4 - 2\epsilon$  dimensions listed in the Appendix

gives

$$\begin{aligned}
 R_1 &\rightarrow -\frac{\mathcal{A}_4^{\text{tree}}}{(4\pi)^{2-\epsilon}} \left( \frac{st}{u^2} K_4 \right) \\
 R_2 &\rightarrow -\frac{\mathcal{A}_4^{\text{tree}}}{(4\pi)^{2-\epsilon}} \left( \frac{s^2 t^2}{2u^3} J_4 - \frac{s^2 t}{u^3} J_3(t) \right) \\
 R_3 &\rightarrow -\frac{\mathcal{A}_4^{\text{tree}}}{(4\pi)^{2-\epsilon}} \left( -\frac{st}{u^2} J_3(t) + \frac{s}{u^2} J_2(t) \right) \\
 R_4 &\rightarrow -\frac{\mathcal{A}_4^{\text{tree}}}{(4\pi)^{2-\epsilon}} \left( \frac{s^2 t^2}{2u^3} J_4 + \frac{st^2}{u^3} J_3(t) \right) \\
 R_5 &\rightarrow -\frac{\mathcal{A}_4^{\text{tree}}}{(4\pi)^{2-\epsilon}} \left( \frac{s^2 t^2}{u^3} J_4 + \frac{s^3 t^3}{2u^4} I_4 + \frac{s^2 t^3}{u^4} I_3(t) + \frac{s^2 t}{u^3} I_2(t) \right) \\
 R_6 &\rightarrow -\frac{\mathcal{A}_4^{\text{tree}}}{(4\pi)^{2-\epsilon}} \left( \frac{st}{2u^2} I_2(t) \right) \\
 R_7 &\rightarrow -\frac{\mathcal{A}_4^{\text{tree}}}{(4\pi)^{2-\epsilon}} \left( \frac{s}{u^2} J_2(t) \right) \\
 R_8 &\rightarrow -\frac{\mathcal{A}_4^{\text{tree}}}{(4\pi)^{2-\epsilon}} \left( -\frac{s^2}{u^2} I_3^{6-2\epsilon}(t) \right) \\
 R_9 &\rightarrow -\frac{\mathcal{A}_4^{\text{tree}}}{(4\pi)^{2-\epsilon}} \left( -\frac{st}{4u^2} I_2(t) + \left( \frac{s}{2u^2} - \frac{s^2}{u^2 t} \right) I_2^{6-2\epsilon}(t) + \frac{s^2}{u^2} I_3^{6-2\epsilon}(t) \right) \quad (2.80)
 \end{aligned}$$

Now we use (A.26) in [59] or see (A.5),(A.6) and (A.7) of this thesis. Ignoring all terms without cuts in the  $t$ -channel, it is easy to show that the sum of these nine terms leads to the result

$$\begin{aligned}
 \mathcal{A}^{\text{t-cut}}(1^-, 2^+, 3^-, 4^+) &= -\frac{1}{(4\pi)^{2-\epsilon}} \mathcal{A}_4^{\text{tree}} \left( \frac{st}{u^2} K_4 - \frac{s^2 t^2}{u^3} I_4^{6-2\epsilon} + \frac{st}{u^2} I_3^{6-2\epsilon}(t) \right. \\
 &\quad \left. - \frac{st(s-t)}{u^3} J_3(t) + \frac{s}{u^2} J_2(t) + \frac{s}{tu} I_2^{6-2\epsilon}(t) + \frac{ts^2}{u^3} I_2(t) \right) \quad (2.81)
 \end{aligned}$$

Next, one must also include the corresponding terms coming from the  $s$ -channel version of the of triple cut in Figure 8. This just yields (2.81) with  $t$  replaced by  $s$ . Combining these two expressions, without double-counting the box contributions (which appear in both cuts), and including the usual factor of two, one precisely reproduces the amplitude for this process (2.69)

## 2.6 The one-loop +++++ amplitude

The five-gluon all-plus one loop amplitude, with a scalar in the loop, is given by [85]

$$\mathcal{A}_5(1^+, 2^+, 3^+, 4^+, 5^+) = \frac{i}{96\pi^2 C_5} \left[ s_{12}s_{23} + s_{23}s_{34} + s_{34}s_{45} + s_{45}s_{51} + s_{51}s_{12} + 4i\epsilon(1234) \right] \quad (2.82)$$

where  $C_5 := \langle 12 \rangle \langle 23 \rangle \langle 34 \rangle \langle 45 \rangle \langle 51 \rangle$  and  $\epsilon(abcd) := \epsilon_{\mu\nu\rho\sigma} a^\mu b^\nu c^\rho d^\sigma$ .

An expression for the five-gluon amplitude valid to all orders in  $\epsilon$  appears in [60],

$$\begin{aligned} \mathcal{A}_{5;1}^{\text{scalar}}(1^+, 2^+, 3^+, 4^+, 5^+) &= \frac{i}{C_5} \frac{\epsilon(1-\epsilon)}{(4\pi)^{2-2\epsilon}} \left[ s_{23}s_{34} I_4^{(1),8-2\epsilon} + s_{34}s_{45} I_4^{(2),8-2\epsilon} \right. \\ &\quad + s_{45}s_{51} I_4^{(3),8-2\epsilon} + s_{51}s_{12} I_4^{(4),8-2\epsilon} + s_{12}s_{23} I_4^{(5),8-2\epsilon} \\ &\quad \left. + 4i(4-2\epsilon)\epsilon(1234) I_5^{10-2\epsilon} \right] \quad (2.83) \end{aligned}$$

The result (2.82) is obtained from (2.83) by taking the  $\epsilon \rightarrow 0$  limit, where [60]

$$\epsilon(1-\epsilon) I_4^{8-2\epsilon} \rightarrow \frac{1}{6}, \quad \epsilon(1-\epsilon) I_5^{10-2\epsilon} \rightarrow \frac{1}{24}, \quad \epsilon(1-\epsilon) I_6^{10-2\epsilon} \rightarrow 0 \quad (2.84)$$

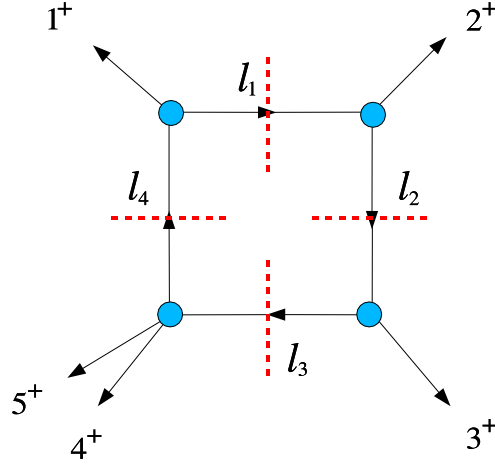


Figure 2.9: *One of the quadruple cuts for the amplitude  $1^+2^+3^+4^+5^+$ .*

Here we will find that we can reproduce the full amplitude using only quadruple cuts in  $4 - 2\epsilon$  dimensions. Let us start by considering the diagram in Figure 2.9, which represents the quadruple cut where gluons 4 and 5 enter the same tree amplitude. The momentum

constraints on this quadruple cut are given by

$$\begin{aligned} l_1^2 &= l_2^2 = l_3^2 = l_4^2 = \mu^2, \\ l_1 &= l_4 - k_1, \quad l_2 = l_1 - k_2, \quad l_3 = l_2 - k_3, \quad l_4 = l_3 - k_4 - k_5 \end{aligned} \quad (2.85)$$

It will prove convenient to solve for the momentum  $l_3$ , which we expand in the basis of vectors  $k_1, k_2, k_3$  and  $K$ , where  $K$  is defined in (2.23). One finds that the solution of (2.85) is given by<sup>7</sup>

$$l_3 = ak_1 + bk_2 + ck_3 + dK \quad (2.86)$$

with

$$\begin{aligned} a &= \frac{t}{2u}, \quad b = -\frac{1}{2}, \quad c = -1 - \frac{s}{2u}, \\ d &= \pm \sqrt{-\frac{st + 4\mu^2 u}{stu^2}} \end{aligned} \quad (2.87)$$

where the kinematical invariants  $s, t, u$  are again defined by (2.26), but now  $s + t + u = (k_4 + k_5)^2$ .

Considering the diagram in Figure 9, the product of tree-level amplitudes entering the quadruple cut can be written as

$$\frac{\langle q_1 | l_1 | 1 \rangle \langle q_2 | l_2 | 2 \rangle \langle q_3 | l_3 | 3 \rangle}{\langle q_1 1 \rangle \langle q_2 2 \rangle \langle q_3 3 \rangle} \frac{\mu^2 [45]}{\langle 45 \rangle [(l_3 - k_4)^2 - \mu^2]} \quad (2.88)$$

Using (2.10), and choosing  $q_3 = 2$ , (2.88) can be recast as

$$\begin{aligned} & - \mu^4 \frac{[12] [45] 1}{\langle 12 \rangle \langle 45 \rangle \langle 23 \rangle} \frac{\langle 2 | l_3 | 3 \rangle}{(l_3 - k_4)^2 - \mu^2} = \frac{\mu^4}{\langle 12 \rangle \langle 23 \rangle \langle 34 \rangle \langle 45 \rangle \langle 51 \rangle} \frac{\text{Tr}_-(5123l_34)}{(l_3 - k_4)^2 - \mu^2} \\ & = - \frac{\mu^4}{\langle 12 \rangle \langle 23 \rangle \langle 34 \rangle \langle 45 \rangle \langle 51 \rangle} \frac{\text{Tr}_+(123l_343) + \text{Tr}_+(123l_342)}{(l_3 - k_4)^2 - \mu^2} \end{aligned} \quad (2.89)$$

Using momentum conservation, and

$$\text{Tr}_+(abcd) = 2 \left[ (ab)(cd) - (ac)(bd) + (ad)(bc) + i\epsilon(abcd) \right] \quad (2.90)$$

it is easy to see that

$$\frac{\text{Tr}_+(123l_343) + \text{Tr}_+(123l_342)}{(l_3 \cdot k_4)} = 4(12)(23) - 4i \frac{(34)\epsilon(12l_33) - (12)\epsilon(234l_3)}{(l_3 \cdot k_4)} \quad (2.91)$$

---

<sup>7</sup>We notice that, had we solved for  $l_1$ , the solution would have taken the form (2.24) with the same coefficients  $a, b, c, d$  of (2.25) - but with  $u$  defined by  $u = -s - t - (k_4 + k_5)^2$ .

We set

$$V(l_3) = i\epsilon(12l_33)(3 \cdot 4) - i\epsilon(234l_3)(1 \cdot 2) \quad (2.92)$$

Now we wish to sum the expression (2.89) over the solutions (2.87), including a factor of  $1/2$ . Writing these solutions as  $l_3^\pm = x \pm y$ , where  $y$  contains the term involving the momentum  $K$ , it is straightforward to show that

$$\frac{1}{2} \sum_{l_3^\pm} \frac{\text{Tr}_+(123l_343) + \text{Tr}_+(123l_342)}{(l_3 \cdot k_4)} = 4(1 \cdot 2)(2 \cdot 3) - 4 \frac{V(x)(x \cdot 4) - V(y)(y \cdot 4)}{(x \cdot 4)^2 - (y \cdot 4)^2} \quad (2.93)$$

and

$$\frac{V(x)(x \cdot 4) - V(y)(y \cdot 4)}{(x \cdot 4)^2 - (y \cdot 4)^2} = -\frac{i}{2} \mu^2 \epsilon(1234) \left[ \frac{1}{(l_3^+ \cdot 4)} + \frac{1}{(l_3^- \cdot 4)} \right] \quad (2.94)$$

Summarising, we have found that

$$\begin{aligned} & \frac{1}{2} \sum_{l_3^\pm} \frac{\text{Tr}_+(123l_343) + \text{Tr}_+(123l_342)}{(l_3 \cdot k_4)} \\ &= 4(1 \cdot 2)(2 \cdot 3) + 2i\mu^2 \epsilon(1234) \left[ \frac{1}{(l_3^+ \cdot 4)} + \frac{1}{(l_3^- \cdot 4)} \right] \\ &= s_{12} s_{23} - 4i\mu^2 \epsilon(1234) \left[ \frac{1}{(l_3^+ - k_4)^2 - \mu^2} + \frac{1}{(l_3^- - k_4)^2 - \mu^2} \right] \end{aligned} \quad (2.95)$$

From (2.89), we see that the full amplitude in the quadruple cut is obtained by multiplying (2.95) by  $-\mu^4/C_5$ . Next, we lift the cut integral to a full Feynman integral, and get

$$\begin{aligned} & -2 \frac{\mu^4}{C_5} \left[ s_{12} s_{23} - 4i\mu^2 \epsilon(1234) \left( \frac{1}{(l_3^+ - k_4)^2 - \mu^2} + \frac{1}{(l_3^- - k_4)^2 - \mu^2} \right) \right] \\ & \rightarrow -\frac{i}{C_5 (4\pi)^{2-\epsilon}} \left[ I_4^{(5),4-2\epsilon} [\mu^4] s_{12} s_{23} + 8i I_5^{4-2\epsilon} [\mu^6] \epsilon(1234) \right] \\ & = \frac{i}{C_5} \frac{\epsilon(1-\epsilon)}{(4\pi)^{2-\epsilon}} \left[ s_{12} s_{23} I_4^{(5),8-2\epsilon} + 4i(4-2\epsilon) \epsilon(1234) I_5^{10-2\epsilon} \right] \end{aligned} \quad (2.96)$$

where the factor of 2 in the first line of (2.96) comes from adding, as usual, the two possible quadruple cuts of the amplitude (which are equal, since they are obtained one from the other by simply flipping all the internal ‘scalar helicities’).

Let us now discuss the result we have found. The first term in the last line of (2.96) gives the  $s_{12}s_{23}$  term in (2.83). The other quadruple cut diagrams, which come from cyclic relabelling of the external legs, will similarly generate the other  $\epsilon(1234)$ -independent terms in (2.83). Finally, the  $\epsilon(1234)$  term in (2.96) – a pentagon integral term – matches the  $\epsilon(1234)$  term in (2.83).

Thus we have shown that the five gluon amplitude  $++++$  may be reconstructed directly using quadruple cuts in  $4 - 2\epsilon$  dimensions.

## 2.7 Future directions

### 2.7.1 Higher point QCD amplitudes

Recently there has been much interest in techniques which enable efficient calculation of the unknown six point gluon amplitudes. See [77, 78, 86]. It would be useful to understand, at next-to-leading order, events such as the  $W + 4$  jet background to top-quark production for the experimental program at the Large Hadron Collider. It is therefore important to push the  $D$ -dimensional generalised unitarity technique to higher point amplitudes.

Using  $D$ -dimensional generalised unitarity to compute higher point amplitudes involves some subtleties that it would be interesting to understand. In this section we give a concrete example which involves the six point all-plus one-loop amplitude. This amplitude has been calculated using  $D$ -dimensional two-particle unitarity cuts in [60].

$$\begin{aligned}
 A_6^{\text{scalar}}(1^+, 2^+, 3^+, 4^+, 5^+, 6^+) &= \frac{\epsilon(1-\epsilon)}{2(4\pi)^{2-\epsilon}} \frac{i}{\langle 12 \rangle \langle 23 \rangle \langle 34 \rangle \langle 45 \rangle \langle 56 \rangle \langle 61 \rangle} \\
 &\times \left[ - \sum_{1 \leq i_1 < i_2 \leq 6} \text{tr}[k_{i_1} k_{i_1+1, i_2-1} k_{i_2} k_{i_2+1, i_1-1}] I_{4:i_1, i_2}^{8-2\epsilon} \right. \\
 &\quad + (4-2\epsilon) \sum_{i=1}^6 \epsilon(i+1, i+2, i+3, i+4) I_5^{(i), 10-2\epsilon} \\
 &\quad \left. + (4-2\epsilon) \text{tr}[123456] I_6^{10-2\epsilon} \right] \quad (2.97)
 \end{aligned}$$

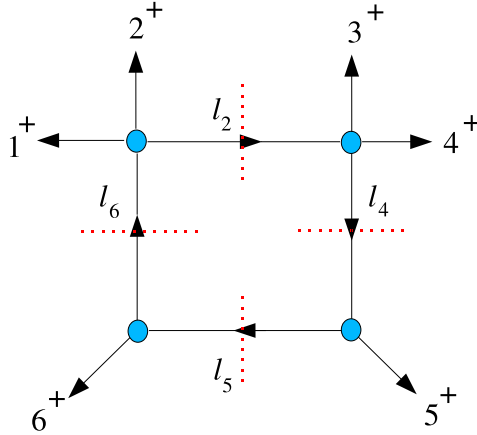


Figure 2.10: A puzzling quadruple cut of the six point all-plus amplitude.

The quadruple cut in Figure 2.10 gives the answer:

$$\begin{aligned} & \frac{\mu^2[12]}{\langle 12 \rangle [(l_6 - k_1)^2 - \mu^2]} \frac{\mu^2[34]}{\langle 34 \rangle [(l_2 - k_3)^2 - \mu^2]} \frac{\langle q_1 | l_5 | 5 \rangle \langle q_2 | l_6 | 6 \rangle}{\langle q_1 5 \rangle \langle q_2 6 \rangle} \\ &= \mu^6 \frac{[12][34][56]}{\langle 12 \rangle \langle 34 \rangle \langle 56 \rangle} \frac{1}{[(l_6 - k_1)^2 - \mu^2][(l_2 - k_3)^2 - \mu^2]} \end{aligned} \quad (2.98)$$

It is tempting to interpret the quadruple cut in (2.98) as giving a just hexagon integral term. At first sight this appears to be different to the known amplitude (2.97), which gives a different coefficient for the hexagon integral and also involves a pentagon term that appears to be absent from this quadruple cut. It would be interesting to understand how the equations (2.98) and (2.97) are consistent with each other.

We have observed in this chapter that full amplitudes can be computed by just considering quadruple cuts and triple cuts and that ordinary two-particle cuts are not needed. This surprising result is very significant, since two-particle cuts are by far the most technically challenging to calculate. It would be very interesting to understand the more general systematics of when triple cuts are sufficient.

### 2.7.2 Higher loops, integrability and the AdS/CFT correspondence

Maldacena's correspondence [4] relates the seemingly intractable planar limit of  $\mathcal{N}=4$  super Yang-Mills at strong coupling to free strings in  $\text{AdS}_5 \times \mathbb{S}^5$ . Supersymmetry protects some quantities, but it is less clear how the simplicity of the strongly coupled regime might be manifested in the perturbative series of unprotected quantities like amplitudes. A strong hint of this simplicity has been observed in iterative cross-order relations in higher-loop amplitudes [65, 66]. Remarkably the two-loop four-point amplitude can be written in terms of the one-loop amplitude.

$$M_n^{(2)}(\epsilon) = \frac{1}{2} \left[ M_n^{(1)} \right]^2 + f^{(2)}(\epsilon) M_n^{(1)}(2\epsilon) + C^{(2)} + E_n^{(2)}(\epsilon) \quad (2.99)$$

where  $M_n^{(l)}$  is the  $n$ -point  $l$ -loop MHV gluon amplitude divided by the tree amplitude. There is a similar iterative formula which writes the three-loop four-point amplitude in terms of the two-loop and one-loop four-point amplitudes [67]. This led to the conjecture that the formula for the all-loop MHV amplitude is the exponential of the one-loop answer:

$$M_n = \exp \left[ \sum_{l=1}^{\infty} a_\epsilon^l \left( f^{(l)}(\epsilon) M_n^{(1)}(l\epsilon) + C^{(l)} + E_n^{(l)}(\epsilon) \right) \right] \quad (2.100)$$

These formulae are based on sophisticated four-point and five-point, two-loop and three-loop unitarity computations.

These iterative gluon amplitude relations involve the function  $f^{(l)}(\epsilon)$ . This function is in fact related to the large spin anomalous dimension of the leading-twist operator in the gauge theory:

$$\text{Tr}(\mathcal{D}^s \mathcal{Z}^2) + \dots \quad (2.101)$$

where  $s$  is the spin of the operator and the leading-twist refers to the 2. In the limit  $s \rightarrow \infty$  this anomalous dimension is expected to scale logarithmically:

$$\Delta = s + f(g)\log(s) + \mathcal{O}(s^0) \quad (2.102)$$

The function  $f(g)$  is the  $\epsilon^0$  term in  $f^{(l)}(\epsilon)$  of the iterative gluon amplitude formula. The function  $f(g)$  is only a function of the 't Hooft coupling  $g^2 = g_{\text{YM}}^2 N$ . In a remarkable calculation [87] the anomalous dimension of the leading-twist operator, for arbitrary spin, was calculated to three loops in QCD. It appears that the most transcendental part of this QCD answer is the  $\mathcal{N}=4$  super Yang-Mills result [88]. The large  $s$  anomalous dimensions calculated using the iterative gluon amplitude technique are in agreement with this answer.

The anomalous dimensions of operators in  $\mathcal{N}=4$  super Yang-Mills are believed to be integrable and can be calculated using the Bethe ansatz. See for example [89]. At one-loop, the leading-twist spin  $s$  anomalous dimension is given by:

$$\Delta = \sum_{k=1}^s \frac{1}{u_k^2 + \frac{1}{4}} \quad , \quad \left( \frac{u_k + \frac{i}{2}}{u_k - \frac{i}{2}} \right)^2 = \prod_{\substack{j=1 \\ j \neq k}}^s \frac{u_k - u_j - i}{u_k - u_j + i} \quad (2.103)$$

It is conjectured that the one-loop Bethe ansatz can be extended to all loops via the following deformation of the spectral parameter  $u$ :

$$u = x + \frac{g^2}{2x} \quad , \quad x^\pm = x(u \pm \frac{i}{2}) \quad (2.104)$$

The all loop Bethe ansatz is:

$$\Delta = \sum_{k=1}^s \frac{i}{x_k^+} - \frac{i}{x_k^-} \quad , \quad \left( \frac{x_k^+}{x_k^-} \right)^2 = \prod_{\substack{j=1 \\ j \neq k}}^s \frac{u_k - u_j - i}{u_k - u_j + i} \quad (2.105)$$

Remarkably Eden and Staudacher [90] have managed to write these equations, for large  $s$ , in terms of an integral equation. This allows explicit calculation of the  $f(g)$  function:

$$f(g) = 4g^2 + 16g^4 \int_0^\infty dt \frac{J_1(gt)}{gt} \sigma(t) \quad (2.106)$$

where  $J$  is a Bessel function and the density of the Bethe roots  $\sigma(t)$  satisfies the integral

equation:

$$\sigma(t) = -\frac{t}{e^{t/\sqrt{2}} - 1} \left[ \frac{1}{2} \frac{J_1(gt)}{gt} + g^2 \int_0^\infty dt' \left( \frac{J_1(gt)J_0(gt') - J_0(gt)J_1(gt')}{gt - gt'} \right) \sigma(t') \right] \quad (2.107)$$

These equations can be easily be solved order by order to a very high number of loops using a program such as Mathematica. The answer to four loops is:

$$\begin{aligned} f(g) = & 4g^2 - 4\zeta(2)g^4 + (4\zeta(2)^2 + 12\zeta(4))g^6 \\ & - (4\zeta(2)^3 + 24\zeta(2)\zeta(4) + 4\zeta(3)^2 + 50\zeta(6))g^8 + \dots \end{aligned} \quad (2.108)$$

The first three loops are in agreement with the result derived from QCD using the transcendentality principle [88]. The four loop result is new and Bern et al. have announced that they are currently testing it using unitarity techniques and the iterative gluon amplitude approach. If (2.108) breaks down, then BMN scaling and the transcendentality principle both breakdown at four loops [90]. It would also be very interesting to understand the Eden Staudacher equation for large  $g$  to see if it matches the energy of the appropriate spinning string as predicted by Maldacena's AdS/CFT correspondence [91]:

$$\text{energy} = f(g) = 2\sqrt{2}g + \frac{3}{\pi} \log(2) + \mathcal{O}\left(\frac{1}{g}\right) \quad (2.109)$$

The AdS/CFT correspondence tells us that certain field theories reorganise themselves into a higher-dimensional dual description, but we do not really understand how this happens. It is thought that the underlying mechanism is open/closed string duality in which the stack of  $D$ -branes in the open string theory are traded for a warped geometry with only closed strings. The duality between Chern-Simons gauge theory on  $\mathbb{S}^3$  and topological strings on the resolved conifold is an example in which the holes in the open string description explicitly close up to form closed string world-sheets [92]. Unfortunately the 't Hooft expansion of  $\mathcal{N} = 4$  super Yang-Mills has not yet been understood explicitly in such terms. Greater understanding of the twistor string proposal and of open/closed string duality, along the lines of [93], will perhaps enable us to also view the large  $N$  duality of  $\mathcal{N} = 4$  super Yang-Mills in a manner close to the well understood topological examples.

# CHAPTER 3

## ON-SHELL RECURSION RELATIONS FOR ONE-LOOP GRAVITY

### 3.1 Introduction

The idea of the BCFW recursion relation [16, 17] was introduced in section 1.7. BCFW recursion exploits a complex deformation of an amplitude and the Cauchy residue theorem to construct an amplitude from a set of factorisations which involve amplitudes with fewer legs. BCFW recursion was originally considered in the context of tree-level Yang-Mills amplitudes. As BCFW recursion is based on the very general properties of analyticity [53–57] and factorisation on multi-particle poles, it is applicable in many different contexts in perturbative field theory [61, 71–74]. In this chapter we consider the generalisation of BCFW recursion to one-loop finite amplitudes in pure gravity. Pure gravity is renormalisable at one-loop [94]. See the review [95] for what is known about the renormalisability of (super)gravity theories in various dimensions.

In the last chapter we presented the method of  $D$ -dimensional generalised unitarity which calculates an amplitude to all orders in  $\epsilon$  where the dimensional regularisation parameter is defined to be  $4 - 2\epsilon$ . In the  $\epsilon \rightarrow 0$  limit these amplitudes contain two types of term: Those which have a branch cut and those which are purely rational functions, independent of  $\epsilon$ . This can be seen explicitly using the formulae in equation (A.4) of appendix A. As reviewed in section 1.5 of the introduction, calculating with four dimensional unitarity cuts only gives the terms of the nonsupersymmetric amplitude which have cuts in four dimensions, but misses the rational parts of the amplitude (which are not linked to the cut containing terms).

Remarkably, the ideas of BCFW recursion can be applied to the calculation of these rational parts of QCD amplitudes. This has been studied in the series of papers [18, 75–78]. A low point one-loop amplitude calculated using Feynman rules, unitarity or even the generalised unitarity of the last chapter, can be used to compute the rational terms of the higher point amplitudes recursively. Calculating the rational terms of an amplitude in this way avoids many of the complications of  $D$ -dimensional unitarity, including the disentangling of the various cuts, the complicated Passarino-Veltman reduction, and the involvement of higher-point integral functions such as pentagons. In this way BCFW recursion offers the

remarkable possibility of calculating loop amplitudes without really performing the loop integrations.

In [18], Bern Dixon and Kosower (BDK) initiated the use of BCFW recursion to calculate the rational parts of one-loop amplitudes by considering the QCD all-plus amplitude and the amplitude with a single negative helicity gluon. Since these amplitudes vanish at tree-level, they are infrared finite at one-loop. So these one-loop amplitudes are purely rational functions, as tree-level amplitudes are.

In tree-level Yang-Mills, the structure of multi-particle factorisation means that in general only simple-poles result from performing shifts on an amplitude [17]. As explained in [18] the same is almost true for the rational terms of one-loop QCD amplitudes. The splitting amplitudes in all helicity configurations except  $(+++)$  and  $(---)$  only involve lone powers of spinor products and hence only single-poles. The  $(+++)$  splitting function has the form  $[ab]/\langle ab \rangle^2$  [13]. So the three-point one-loop all-plus factorisations will give rise to double poles, when the shifted  $\langle ab \rangle$  vanishes. These factorisations, along with all the other three-point one-loop factorisations, are called *nonstandard factorisations* and are the main complicating factor in the extension of BCFW recursion to one-loop.

Since QCD tree-level amplitudes with more than three legs and less than two negative helicity gluons vanish, the one-loop all-plus amplitude is finite and also has no multi-particle poles. So the shifted all-plus amplitude only has simple-poles coming from the collinear singularity of the tree-level  $(-; ++)$  splitting amplitude. Once shifts without a boundary term have been found, the all-plus amplitudes can be constructed recursively by sewing all-plus loop amplitudes with fewer legs to tree amplitudes [18]. In section 3.2 we show that the all-plus one-loop gravity amplitudes behave in a similar way.

Remarkably the ideas of BCFW recursion can be extended to more general QCD one-loop amplitudes such as the amplitude with a single negative-helicity gluon [18]. As can be seen by, for example, performing the BCFW shifts on a known amplitude, there is an added complication in this one-loop recursion as performing a shift results in the appearance of a double pole. As explained in [18] these double poles are precisely due to the appearance of three-point all-plus one-loop vertices. BCFW's use of the Cauchy residue theorem does, of course, extend to this case since although the double-pole in  $A(z)$  does not have a residue, recall that we are integrating  $A(z)/z$  which does have a residue

$$\text{Res}_{z=a} \left\{ \frac{1}{z(z-a)^2} \right\} = -\frac{1}{a^2} \quad (3.1)$$

Factorisation at a double pole will therefore take the form:

$$A_L \frac{1}{(P^2)^2} A_R \quad (3.2)$$

It is clear even on dimensional grounds that  $A_L$  and  $A_R$  cannot both be amplitudes. So the three-point one-loop all-plus factorisation will involve a vertex with the dimensions of an amplitude times a momentum squared. As pointed out in [18] this may seem puzzling at first sight, but it can be understood from the structure of the one-loop three-vertex used for obtaining, one-loop splitting amplitudes [13, 96, 97]:

$$A_3^{(1)}(1^+, 2^+, 3^+) = -i \frac{N_p}{96\pi^2} \frac{[12][23][31]}{K_{12}^2} \quad (3.3)$$

So the three-point one-loop all-plus amplitude is either zero or infinite even in complex momenta as it involves both the  $\lambda$  and  $\tilde{\lambda}$  variables. To compute the recursive double pole terms associated with the three-point all-plus factorisations, BDK propose the use of the following vertex, which has the right dimensions and is only a function of the  $\tilde{\lambda}$  variables:

$$V_3^{(1)}(1^+, 2^+, 3^+) = -\frac{i}{96\pi^2} [12][23][31] \quad (3.4)$$

In section 3.3 we will observe that the double poles in the one-loop  $- + ++$  pure gravity amplitude can be understood in an analogous way. For one-loop gravity we use the vertex:

$$W_3^{(1)}(1^+, 2^+, 3^+) = C([12][23][31])^2 \quad (3.5)$$

where we will fix the numerical coefficient  $C$  of this vertex by comparison with the known  $- + ++$  gravity amplitude. This amplitude was calculated using  $D$ -dimensional two-particle unitarity cuts in [98]. These three-point all-plus gravity factorisations are only double poles in complex momenta. In real momenta the double pole terms in the  $- + + + +$  gravity amplitude look like  $[ab]^4/\langle ab \rangle^2$ , so there is no pole at all. The one-loop gravity splitting functions vanish.

The three-point one-loop all-plus factorisation also contains a single pole term [18]. The description of this ‘single pole under the double pole term’ is more tricky. In [18] BDK arrived at a candidate single pole under the double pole by proposing that the single pole differed from the double pole by a factor of the form:

$$S(a_1, \hat{K}^+, a_2) K^2 S(b_1, -\hat{K}^-, b_2) \quad (3.6)$$

In this factor,  $K^2$  is the propagator that is responsible for the pole in the shifted amplitude. This factor, when multiplying the double pole, cancels one of the two  $K^2$  in the double pole term to give a single-pole term. The legs  $b_1$  and  $b_2$  are the external legs on the three-point all-plus vertex. In [18] experimentation revealed that the legs  $a_1$  and  $a_2$  are to be identified with the external legs of the tree amplitude part of the recursive diagram which are colour adjacent to the propagator. The ‘soft factors’ are given by:

$$S(a, s^+, b) = \frac{\langle ab \rangle}{\langle as \rangle \langle sb \rangle}, \quad S(a, s^-, b) = -\frac{[ab]}{[as][sb]} \quad (3.7)$$

In section 3.3.1 we will explicitly review this construction for the simplest case of the four-point one-loop  $-+++$  Yang-Mills amplitude. We demonstrate in section 3.3.2 that a remarkably similar procedure can also be applied to the single poles in the  $-+++$  one-loop gravity amplitude.

We then attempt to construct the unknown one-loop  $++++$  gravity amplitude using on shell recursion in section 3.4. Unfortunately our understanding of the three-point all-plus nonstandard factorisations gained from studying the known  $-+++$  one-loop gravity amplitude has not allowed us to generalise to this unknown case yet. We have been unable to find ‘single pole under the double pole’ terms which are consistent with the symmetries and limits of the amplitude. A method for calculating Yang-Mills amplitudes avoiding all nonstandard factorisations was given in [77]. We review this method in section 3.6 and calculate the  $-+++$  Yang-Mills amplitude using only standard factorisations. Unfortunately, extension of these ideas to the  $++++$  one-loop gravity amplitude does not immediately work, but we are hopeful that ideas along these lines will soon enable the construction of this amplitude.

### 3.2 The all-plus amplitude

An ansatz for the  $n$  point one-loop amplitude in pure Einstein gravity in which all the external gravitons have the same outgoing helicity was presented in [99]. This ansatz agrees with explicit computations via  $D$ -dimensional unitarity cuts for  $n \leq 6$  [100]. This amplitude corresponds to self-dual configurations of the field strength. The amplitude is also related to the one-loop ‘maximally helicity-violating’ (MHV) amplitude in  $N=8$  supergravity via the ‘dimension-shifting’ relation of [100]. The explicit expression for this amplitude is:

$$M_n^{(1)}(1^+, 2^+, \dots, n^+) = -\frac{i}{(4\pi)^2} \frac{1}{960} \sum_{\substack{1 \leq a < b \leq n \\ M, N}} h(a, M, b) h(b, N, a) \text{tr}[\not{k}_a \not{k}_M \not{k}_b \not{k}_N] \quad (3.8)$$

In this formula,  $a$  and  $b$  are massless legs and  $M$  and  $N$  are two sets forming a distinct nontrivial partition of the remaining  $n-2$  legs. The first few half soft functions  $h(a, S, b)$  are given by

$$\begin{aligned} h(a, \{1\}, b) &= \frac{1}{\langle a1 \rangle^2 \langle 1b \rangle^2} \\ h(a, \{1, 2\}, b) &= \frac{[12]}{\langle 12 \rangle \langle a1 \rangle \langle 1b \rangle \langle a2 \rangle \langle 2b \rangle} \\ h(a, \{1, 2, 3\}, b) &= \frac{[12][23]}{\langle 12 \rangle \langle 23 \rangle \langle a1 \rangle \langle 1b \rangle \langle a3 \rangle \langle 3b \rangle} + \frac{[23][31]}{\langle 23 \rangle \langle 31 \rangle \langle a2 \rangle \langle 2b \rangle \langle a1 \rangle \langle 1b \rangle} \\ &\quad + \frac{[31][12]}{\langle 31 \rangle \langle 12 \rangle \langle a3 \rangle \langle 3b \rangle \langle a2 \rangle \langle 2b \rangle} \end{aligned} \quad (3.9)$$

In the following sections we show that the five and six point amplitudes can be constructed recursively. Inspection of the all-plus amplitude (3.8) shows that the standard BCFW shifts [17] give a boundary term. The following shifts, which first appeared in [38], eliminate a boundary term for suitable choices of  $\eta$

$$\begin{aligned}\hat{\lambda}_1 &= \lambda_1 + z[23]\eta \\ \hat{\lambda}_2 &= \lambda_2 + z[31]\eta \\ \hat{\lambda}_3 &= \lambda_3 + z[12]\eta\end{aligned}\tag{3.10}$$

When we construct the five-point all-plus gravity amplitude recursively from the four point we use  $\eta = \lambda_4 + \lambda_5$ . For construction of the six-point all-plus amplitude from the five-point amplitude we use  $\eta = \lambda_4 + \lambda_5 + \lambda_6$ . We choose the shifts (3.10) because they do not give any boundary term, but these shifts were invented for another purpose. In [38] they were used to show that the CSW rules [8] for tree-level gauge theory are just a specific instance of the BCFW [17] recursion relation. See section 1.7.3 of this thesis. These shifts were then used to obtain a CSW-style formalism for calculating graviton scattering amplitudes in [81]. Applying the shifts (3.10) to the all-plus amplitude (3.8) gives a shifted amplitude  $M_n^{(1)}(z)$  with only simple-poles. In the next sections we show that the residues at these poles can be computed from standard recursion relation diagrams.

### 3.2.1 The five-point all-plus amplitude

In this section we use on-shell one-loop recursion to recompute the known five-point all-plus amplitude from the known four-point all-plus amplitude. The four-point all-plus amplitude (3.8) is given explicitly by

$$M_4^{(1)}(1^+, 2^+, 3^+, 4^+) = -\frac{i}{(4\pi)^2} \frac{1}{60} \left( \frac{[12][34]}{\langle 12 \rangle \langle 34 \rangle} \right)^2 (s^2 + st + t^2)\tag{3.11}$$

Where  $s = (p_1 + p_2)^2$  and  $t = (p_2 + p_3)^2$ . This four-point all-plus amplitude was first computed using  $D$ -dimensional unitarity-cuts in [98].

In the construction of the five-point all-plus amplitude, the shifts (3.10) give rise to nine different diagrams corresponding to the nine different angle brackets that the shifts can make singular. Using the symmetric choice of  $\eta = \lambda_4 + \lambda_5$  there are only two distinct types of diagram to compute and then the remaining diagrams are straight forward permutations of these two diagrams. All the recursive diagrams contain a four-point one-loop amplitude joined to a tree-level  $++-$  amplitude. The first type of diagram has two shifted external legs attached to the tree-level  $++-$  diagram. There are three of these diagrams associated with the three simple-poles  $\langle \hat{1}\hat{2} \rangle = \langle \hat{2}\hat{3} \rangle = \langle \hat{3}\hat{1} \rangle = 0$  in the shifted amplitude. The diagram associated with the pole  $\langle \hat{1}\hat{2} \rangle = 0$  is given in Figure 3.1. The second type of diagram has a

shifted and an unshifted leg attached to the tree-level  $++-$  amplitude. There are six of this type of diagram associated with the simple-poles  $\langle \hat{1}4 \rangle = \langle \hat{1}5 \rangle = \langle \hat{2}4 \rangle = \langle \hat{2}5 \rangle = \langle \hat{3}4 \rangle = \langle \hat{3}5 \rangle = 0$  in the shifted amplitude. The diagram associated with  $\langle \hat{1}5 \rangle = 0$  is given in Figure 3.2.

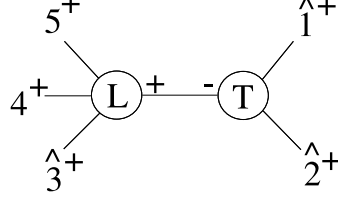


Figure 3.1: The diagram in the recursive expression for  $M_5^{(1)}(1^+, 2^+, 3^+, 4^+, 5^+)$  associated with the pole  $\langle \hat{1}2 \rangle = 0$ . The amplitude labelled by a  $T$  is a tree-level amplitude and the one labelled by  $L$  is a one-loop amplitude.

The diagram in Figure 3.1 contributes

$$M_4^{(1)}(\hat{3}^+, 4^+, 5^+, \hat{K}_{12}^+) \frac{i}{\hat{K}_{12}} M_3^{(0)}(\hat{1}^+, \hat{2}^+, -\hat{K}_{12}^-) \quad (3.12)$$

Where the three-point tree amplitude is given by

$$M_3^{(0)}(1^+, 2^+, 3^-) = -i \left( i \frac{[12]^3}{[23][31]} \right)^2 \quad (3.13)$$

substituting this tree-level amplitude and the one-loop result (3.11) into (3.12) yields

$$\frac{i}{(4\pi)^2} \frac{1}{60} \frac{[34]^4 [12]^5}{\langle 12 \rangle} \frac{(\langle \hat{3}4 \rangle^2 [34]^2 + \langle \hat{3}4 \rangle [34] \langle 45 \rangle [45] + \langle 45 \rangle^2 [45]^2)}{\langle 5|\hat{K}|1\rangle^2 \langle 5|\hat{K}|2\rangle^2}$$

We can eliminate  $\hat{K}_{12}$  from this expression using

$$\langle 5|\hat{K}|1\rangle^2 = \langle \hat{2}5 \rangle^2 [12]^2 \quad \text{and} \quad \langle 5|\hat{K}|2\rangle^2 = \langle \hat{1}5 \rangle^2 [12]^2$$

Figure 3.1 gives  $\langle \hat{1}2 \rangle = 0$  which corresponds to a pole in the complex  $z$ -plane at

$$z = -\frac{\langle 12 \rangle}{\langle \eta|1 + 2|3 \rangle}$$

It is then easy to show that

$$\begin{aligned} \langle \hat{2}5 \rangle &= \frac{[34] \langle 45 \rangle \langle \eta 2 \rangle}{\langle \eta|1 + 2|3 \rangle} \\ \langle \hat{1}5 \rangle &= \frac{[34] \langle 45 \rangle \langle \eta 1 \rangle}{\langle \eta|1 + 2|3 \rangle} \\ \langle \hat{3}4 \rangle &= \langle 34 \rangle - \frac{\langle 12 \rangle [12] \langle \eta 4 \rangle}{\langle \eta|1 + 2|3 \rangle} \end{aligned}$$

using  $\eta = \lambda_4 + \lambda_5$  gives the final contribution from Figure 3.1 and (3.12).

$$-\frac{i}{(4\pi)^2} \frac{1}{60} \frac{[12]([34] - [35])^4}{\langle 12 \rangle (\langle 14 \rangle + \langle 15 \rangle)^2 (\langle 24 \rangle + \langle 25 \rangle)^2} \left\{ \left( \langle 34 \rangle - \frac{\langle 12 \rangle [12]}{[34] - [35]} \right)^2 [34]^2 + \left( \langle 34 \rangle - \frac{\langle 12 \rangle [12]}{[34] - [35]} \right) [34] \langle 45 \rangle [45] + \langle 45 \rangle^2 [45]^2 \right\} \quad (3.14)$$

The contributions from the diagrams corresponding to the poles  $\langle \hat{2}\hat{3} \rangle = 0$  and  $\langle \hat{3}\hat{1} \rangle = 0$  are given by cyclically permuting the external legs  $\{1, 2, 3\}$ .

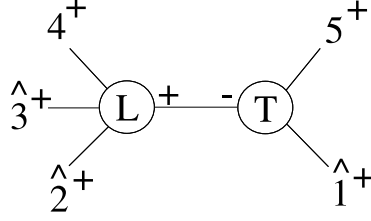


Figure 3.2: The diagram in the recursive expression for  $M_5^{(1)}(1^+, 2^+, 3^+, 4^+, 5^+)$  associated with the pole  $\langle \hat{1}\hat{5} \rangle = 0$ .

We now consider the second type of diagram. Figure 3.2 contributes

$$M_4^{(1)}(\hat{2}^+, \hat{3}^+, 4^+, \hat{K}_{15}^+) \frac{i}{\hat{K}_{15}} M_3^{(0)}(5^+, \hat{1}^+, -\hat{K}_{15}^-) \quad (3.15)$$

again using (3.11) this yields

$$-\frac{i}{(4\pi)^2} \frac{1}{60} \frac{[23]^4 [15]^5 (\langle \hat{2}\hat{3} \rangle^2 [23]^2 + \langle \hat{2}\hat{3} \rangle [23] \langle \hat{3}\hat{4} \rangle [34] + \langle \hat{3}\hat{4} \rangle^2 [34]^2)}{\langle 15 \rangle \langle 4|\hat{K}|1\rangle^2 \langle 4|\hat{K}|5\rangle^2}$$

We can eliminate  $\hat{K}_{15}$  from this expression using

$$\langle 4|\hat{K}|1\rangle^2 = \langle 45 \rangle^2 [15]^2 \quad \text{and} \quad \langle 4|\hat{K}|5\rangle^2 = \langle \hat{1}\hat{4} \rangle^2 [15]^2$$

Figure 3.1 gives  $\langle \hat{1}\hat{5} \rangle = 0$  which corresponds to a pole in the complex  $z$ -plane at

$$z = -\frac{\langle 15 \rangle}{[23] \langle \eta 5 \rangle}$$

It is then easy to show that

$$\begin{aligned} \langle \hat{1}\hat{4} \rangle &= \frac{\langle 45 \rangle \langle \eta 1 \rangle}{\langle \eta 5 \rangle} \\ \langle \hat{2}\hat{3} \rangle &= \langle 23 \rangle - \frac{\langle 15 \rangle \langle \eta | 2 + 3 | 1 \rangle}{[23] \langle \eta 5 \rangle} \end{aligned}$$

$$\langle \hat{3}4 \rangle = \langle 34 \rangle - \frac{\langle 15 \rangle [12] \langle \eta 4 \rangle}{[23] \langle \eta 5 \rangle}$$

using  $\eta = \lambda_4 + \lambda_5$  gives the final contribution from Figure 3.2 and (3.15).

$$\begin{aligned} -\frac{i}{(4\pi)^2} \frac{1}{60} \frac{[15][23]^4}{\langle 15 \rangle \langle 45 \rangle^2 (\langle 14 \rangle + \langle 15 \rangle)^2} & \left\{ \left( \langle 23 \rangle [23] + \langle 15 \rangle ([14] - [15]) \right)^2 \right. \\ & + \left( \langle 23 \rangle [23] + \langle 15 \rangle ([14] - [15]) \right) \left( \langle 34 \rangle [34] + \frac{\langle 15 \rangle [12] [34]}{[23]} \right) \\ & \left. + \left( \langle 34 \rangle [34] + \frac{\langle 15 \rangle [12] [34]}{[23]} \right)^2 \right\} \end{aligned} \quad (3.16)$$

The contributions from the diagrams corresponding to the poles  $\langle \hat{2}5 \rangle = 0$  and  $\langle \hat{3}5 \rangle = 0$  are obtained by cyclically permuting the external legs  $\{1, 2, 3\}$ . The diagram corresponding to the pole  $\langle \hat{1}4 \rangle = 0$  is obtained from the  $\langle \hat{1}5 \rangle = 0$  diagram by interchanging legs 4 and 5. The remaining diagrams corresponding to the poles  $\langle \hat{2}4 \rangle = 0$  and  $\langle \hat{3}4 \rangle = 0$  are then obtained by cyclically permuting the external legs  $\{1, 2, 3\}$  of the  $\langle \hat{1}4 \rangle = 0$  diagram.

We have checked numerically that each of the terms in the recursion relation agree with the residues of the shifted known answer (3.8) and so the sum of the nine recursion relation terms are in agreement with the thirty terms of the known answer (3.8).

See Appendix B for a Mathematica program that can be used to compare amplitudes numerically. The command `evalnormal[X]` can be used for this purpose. The Appendix also contains a command, `evalshift[X]` that can be used to compare the individual residues of amplitudes under various shifts.

### 3.2.2 The six-point all-plus amplitude

In this section we recompute the known six-point all-plus amplitude from the five-point all-plus amplitude. We again use Risager shifts (3.10), but now choose  $\eta = \lambda_4 + \lambda_5 + \lambda_6$ . Just like the previous five-point case all diagrams contain a one-loop all-plus amplitude and a  $++-$  tree-level amplitude. There are again two types of diagram. The first type of diagram corresponds to having two shifted legs attached to the three-point tree-level amplitude. There are three of these diagrams associated with the three poles  $\langle \hat{1}\hat{2} \rangle = \langle \hat{2}\hat{3} \rangle = \langle \hat{3}\hat{1} \rangle = 0$ . The diagram associated with the pole  $\langle \hat{2}\hat{3} \rangle = 0$  is given in Figure 3.3. The second type of diagram corresponds to having a shifted and an unshifted leg attached to the three-point tree-level amplitude. There are nine of these diagrams associated with the nine poles  $\langle \hat{1}4 \rangle = \langle \hat{1}5 \rangle = \langle \hat{1}6 \rangle = \langle \hat{2}4 \rangle = \langle \hat{2}5 \rangle = \langle \hat{2}6 \rangle = \langle \hat{3}4 \rangle = \langle \hat{3}5 \rangle = \langle \hat{3}6 \rangle = 0$ . The diagram associated with the pole  $\langle \hat{1}6 \rangle = 0$  is given in Figure 3.4.

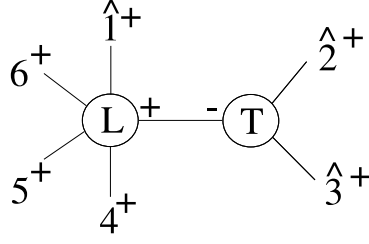


Figure 3.3: The diagram in the recursive expression for  $M_5^{(1)}(1^+, 2^+, 3^+, 4^+, 5^+, 6^+)$  associated with the pole  $\langle \hat{2}\hat{3} \rangle = 0$ .

The first type of recursive diagram is given in Figure 3.3. This contributes:

$$M_5^{(1)}(4^+, 5^+, 6^+, \hat{1}^+, \hat{K}_{23}^+) \frac{i}{K_{23}} M_3^{(0)}(\hat{2}^+, \hat{3}^+, -\hat{K}_{23}^-) \quad (3.17)$$

The  $M_5^{(1)}(+++++)$  amplitude contains thirty terms (3.8). Fortunately the symmetries in the shifts and the choice for  $|\eta\rangle = |4\rangle + |5\rangle + |6\rangle$  reduce these thirty terms to the following ten terms plus the two cyclic permutations involving  $\{4, 5, 6\}$  of these ten terms.

$$\begin{aligned} & \frac{8i}{(4\pi)^2} \left[ - \frac{[23]\langle 46 \rangle [46]^3 \langle 56 \rangle [56]^3 (\langle 45 \rangle [45] + \langle 56 \rangle [56] + \langle 46 \rangle [46])}{\langle 23 \rangle \langle \hat{1}4 \rangle \langle \hat{1}5 \rangle \langle \hat{2}4 \rangle \langle \hat{2}5 \rangle} \right. \\ & - \frac{[23][14]^3 [15]^3 \langle \hat{1}4 \rangle \langle \hat{1}5 \rangle (\langle \hat{1}4 \rangle [14] + \langle \hat{1}5 \rangle [15] + \langle 45 \rangle [45])}{\langle 23 \rangle \langle 46 \rangle \langle 56 \rangle \langle \hat{2}4 \rangle \langle \hat{2}5 \rangle \langle \hat{3}6 \rangle^2} \\ & - \frac{[23][16] (\langle \hat{2}4 \rangle [24] + \langle \hat{3}4 \rangle [34])^3 (\langle \hat{2}5 \rangle [25] + \langle \hat{3}5 \rangle [35])^3}{\langle 23 \rangle \langle 46 \rangle \langle 56 \rangle \langle \hat{1}4 \rangle \langle \hat{1}5 \rangle \langle \hat{1}6 \rangle \langle \hat{3}4 \rangle^2 \langle \hat{2}5 \rangle^2} \\ & + \frac{[23]\langle 45 \rangle [45]^3 [15]^3 \langle \hat{1}5 \rangle (\langle \hat{1}4 \rangle [14] + \langle \hat{1}5 \rangle [15] + \langle 45 \rangle [45])}{\langle 23 \rangle \langle 46 \rangle \langle \hat{1}6 \rangle \langle \hat{2}4 \rangle \langle \hat{1}2 \rangle \langle \hat{3}6 \rangle^2} \\ & + \frac{[23]\langle 46 \rangle [46]^3 [16]^3 \langle \hat{1}6 \rangle (\langle \hat{1}4 \rangle [14] + \langle \hat{1}6 \rangle [16] + \langle 46 \rangle [46])}{\langle 23 \rangle \langle 45 \rangle \langle \hat{1}5 \rangle \langle \hat{2}4 \rangle \langle \hat{1}2 \rangle \langle \hat{3}5 \rangle^2} \\ & - \frac{[23][56] (\langle 45 \rangle [45] + \langle 56 \rangle [56] + \langle 46 \rangle [46])^3 (\langle \hat{2}4 \rangle [24] + \langle \hat{3}4 \rangle [34])^3}{\langle 23 \rangle \langle 45 \rangle \langle 46 \rangle \langle 56 \rangle \langle \hat{1}5 \rangle \langle \hat{1}6 \rangle \langle \hat{3}1 \rangle^2 \langle \hat{2}4 \rangle^2} \\ & - \frac{[23][16] \langle 45 \rangle [45]^3 (\langle \hat{2}5 \rangle [25] + \langle \hat{3}5 \rangle [35])^3}{\langle 23 \rangle \langle 46 \rangle \langle \hat{1}4 \rangle \langle \hat{1}6 \rangle \langle \hat{2}6 \rangle \langle \hat{1}2 \rangle \langle \hat{3}5 \rangle^2} \\ & - \frac{[23][15] \langle 46 \rangle [46]^3 (\langle \hat{2}6 \rangle [26] + \langle \hat{3}6 \rangle [36])^3}{\langle 23 \rangle \langle 45 \rangle \langle \hat{1}4 \rangle \langle \hat{1}5 \rangle \langle \hat{2}5 \rangle \langle \hat{1}2 \rangle \langle \hat{3}6 \rangle^2} \\ & - \frac{[23][56][14]^3 \langle \hat{1}4 \rangle (\langle 45 \rangle [45] + \langle 56 \rangle [56] \langle 46 \rangle [46])^3}{\langle 23 \rangle \langle 45 \rangle \langle 46 \rangle \langle 56 \rangle \langle \hat{2}5 \rangle \langle \hat{2}6 \rangle \langle \hat{3}1 \rangle^2} \\ & \left. - \frac{[23][56][14]^3 \langle \hat{1}4 \rangle (\langle \hat{2}4 \rangle [24] + \langle \hat{3}4 \rangle [34])^3}{\langle 23 \rangle \langle 56 \rangle \langle \hat{1}5 \rangle \langle \hat{1}6 \rangle \langle \hat{2}5 \rangle \langle \hat{2}6 \rangle \langle \hat{3}4 \rangle^2} \right] \quad (3.18) \end{aligned}$$

The diagram in Figure 3.3 is associated with  $\langle \hat{2}\hat{3} \rangle = 0$  or equivalently with

$$z = -\frac{\langle 23 \rangle}{\langle \eta | 2 + 3 | 1 \rangle} \quad (3.19)$$

using this value for  $z$  it is then simple to rewrite the brackets containing hats in (3.18) in terms of the external legs. We have checked numerically that the expression (3.18) plus the permutations agrees with the residue at  $\langle \hat{2}\hat{3} \rangle = 0$  of the known amplitude (3.8)

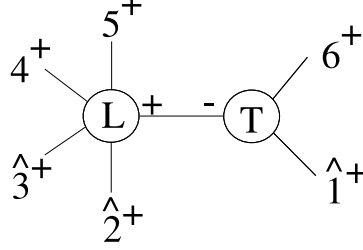


Figure 3.4: The diagram in the recursive expression for  $M_5^{(1)}(1^+, 2^+, 3^+, 4^+, 5^+, 6^+)$  associated with the pole  $\langle \hat{1}\hat{6} \rangle = 0$ .

The second type of recursive diagram is given in Figure 3.4. This contributes:

$$M_5^{(1)}(\hat{2}^+, \hat{3}^+, 4^+, 5^+, \hat{K}_{16}^+) \frac{i}{K_{16}} M_3^{(0)}(6^+, \hat{1}^+, -\hat{K}_{16}^-) \quad (3.20)$$

Just like the other term, the  $M_5^{(1)}(+++++)$  amplitude contains thirty terms, but the symmetries of the shifts and the choice of  $|\eta\rangle = |4\rangle + |5\rangle + |6\rangle$  reduce these thirty terms to the following set of terms and permutations:

$$\begin{aligned} & \frac{8i}{(4\pi)^2} \left[ -\frac{[16][23]^3[34]^3\langle \hat{2}\hat{3} \rangle\langle \hat{3}\hat{4} \rangle(\langle \hat{1}\hat{5} \rangle[15] + \langle 56 \rangle[56])}{\langle 16 \rangle\langle 45 \rangle\langle 56 \rangle^2\langle \hat{2}\hat{5} \rangle\langle \hat{1}\hat{2} \rangle\langle \hat{1}\hat{4} \rangle} \right. \\ & + \frac{[16][25]^3[45]^3\langle 45 \rangle\langle \hat{2}\hat{5} \rangle(\langle \hat{3}\hat{1} \rangle[31] + \langle \hat{3}\hat{6} \rangle[36])}{\langle 16 \rangle\langle \hat{2}\hat{3} \rangle\langle \hat{3}\hat{4} \rangle\langle \hat{1}\hat{4} \rangle\langle \hat{1}\hat{2} \rangle\langle \hat{3}\hat{6} \rangle^2} \\ & + \frac{[16][35][24]^3\langle \hat{2}\hat{4} \rangle(\langle \hat{1}\hat{4} \rangle[14] + \langle 46 \rangle[46])^3}{\langle 16 \rangle\langle 46 \rangle^2\langle \hat{3}\hat{5} \rangle\langle \hat{2}\hat{5} \rangle\langle \hat{2}\hat{3} \rangle\langle \hat{1}\hat{5} \rangle\langle \hat{3}\hat{1} \rangle} \\ & - \frac{[16][35][24]^3\langle \hat{2}\hat{4} \rangle(\langle \hat{1}\hat{2} \rangle[12] + \langle \hat{2}\hat{6} \rangle[26])^3}{\langle 16 \rangle\langle 45 \rangle\langle \hat{3}\hat{4} \rangle\langle \hat{3}\hat{5} \rangle\langle \hat{2}\hat{6} \rangle^2\langle \hat{3}\hat{1} \rangle\langle \hat{1}\hat{5} \rangle} \\ & \left. + \frac{[16][35](\langle \hat{1}\hat{4} \rangle[14] + \langle 46 \rangle[46])^3(\langle \hat{1}\hat{2} \rangle[12] + \langle \hat{2}\hat{6} \rangle[26])^3}{\langle 16 \rangle\langle 45 \rangle\langle \hat{3}\hat{5} \rangle\langle \hat{2}\hat{3} \rangle\langle \hat{2}\hat{5} \rangle\langle \hat{3}\hat{4} \rangle\langle \hat{2}\hat{6} \rangle^2\langle \hat{1}\hat{4} \rangle^2} \right] \quad (3.21) \end{aligned}$$

We also include three other sets of terms which are the same as (3.21) but with 2, 3 swapped,

4, 5 swapped and with 2, 3 and 4, 5 swapped

$$\frac{8i}{(4\pi)^2} \left[ \frac{[16][45][23]^3 \langle \hat{2}\hat{3} \rangle \langle \hat{3}\hat{1} \rangle [31] + \langle \hat{3}\hat{6} \rangle [36]^3}{\langle 16 \rangle \langle 45 \rangle \langle \hat{2}\hat{4} \rangle \langle \hat{2}\hat{5} \rangle \langle \hat{1}\hat{4} \rangle \langle \hat{1}\hat{5} \rangle \langle \hat{3}\hat{6} \rangle^2} - \frac{[16][24]^3 [25]^3 \langle \hat{2}\hat{4} \rangle \langle \hat{2}\hat{5} \rangle \langle \hat{3}\hat{1} \rangle [31] + \langle \hat{3}\hat{6} \rangle [36]^3}{\langle 16 \rangle \langle \hat{3}\hat{4} \rangle \langle \hat{3}\hat{5} \rangle \langle \hat{1}\hat{4} \rangle \langle \hat{1}\hat{5} \rangle \langle \hat{3}\hat{6} \rangle^2} \right] \quad (3.22)$$

We also include another set of terms which are the same as (3.22) but with 2, 3 swapped.

$$\frac{8i}{(4\pi)^2} \left[ \frac{[16][24]^3 [34]^3 \langle \hat{2}\hat{4} \rangle \langle \hat{3}\hat{4} \rangle \langle \hat{1}\hat{5} \rangle [15] + \langle 56 \rangle [56]}{\langle 16 \rangle \langle 56 \rangle^2 \langle \hat{2}\hat{5} \rangle \langle \hat{3}\hat{5} \rangle \langle \hat{1}\hat{2} \rangle \langle \hat{3}\hat{1} \rangle} + \frac{[16][23][45]^3 \langle \hat{4}\hat{5} \rangle \langle \hat{1}\hat{5} \rangle [15] + \langle 56 \rangle [56]^3}{\langle 16 \rangle \langle 56 \rangle^2 \langle \hat{2}\hat{4} \rangle \langle \hat{3}\hat{4} \rangle \langle \hat{2}\hat{3} \rangle \langle \hat{1}\hat{2} \rangle \langle \hat{3}\hat{1} \rangle} \right] \quad (3.23)$$

We also include another set of terms which are the same as (3.23) but with 4, 5 swapped.

$$\frac{8i}{(4\pi)^2} \left[ \frac{[16][45] \langle \hat{1}\hat{2} \rangle [12] + \langle \hat{2}\hat{6} \rangle [26]^3 \langle \hat{3}\hat{1} \rangle [31] + \langle \hat{3}\hat{6} \rangle [36]^3}{\langle 16 \rangle \langle 45 \rangle \langle \hat{2}\hat{4} \rangle \langle \hat{2}\hat{5} \rangle \langle \hat{3}\hat{4} \rangle \langle \hat{3}\hat{5} \rangle \langle \hat{2}\hat{6} \rangle^2 \langle \hat{3}\hat{1} \rangle^2} - \frac{[16][23] \langle \hat{1}\hat{4} \rangle [14] + \langle 46 \rangle [46] \langle \hat{1}\hat{5} \rangle [15] + \langle 56 \rangle [56]}{\langle 16 \rangle \langle 46 \rangle^2 \langle \hat{2}\hat{4} \rangle \langle \hat{2}\hat{5} \rangle \langle \hat{3}\hat{4} \rangle \langle \hat{3}\hat{5} \rangle \langle \hat{1}\hat{5} \rangle^2 \langle \hat{2}\hat{3} \rangle} \right] \quad (3.24)$$

So (3.21) plus permutations contributes 20 terms, (3.22) plus permutations contributes 4 terms, (3.23) plus permutations contributes 4 terms and (3.24) contributes 2 terms. So we correctly have a contribution from all 30 terms in the five-point all-plus amplitude. The diagram in Figure 3.4 is associated with  $\langle \hat{1}\hat{6} \rangle = 0$ , or equivalently with:

$$z = -\frac{\langle 16 \rangle}{[23] \langle \eta 6 \rangle} \quad (3.25)$$

We have checked numerically that the sum of these terms agrees with the residue of the shifted known amplitude (3.8).

We have shown that the five and six point all-plus amplitudes can be calculated using on-shell recursion. It would be interesting if it were possible to find some shifts that left the structure of the all-plus one-loop amplitudes (3.8) written in terms of the half soft functions (3.9) explicit. The half soft functions satisfy the recursion relation [100]:

$$\sum_{\substack{ACC \\ B \equiv C - A}} h(q, A, r) h(q, B, r) \langle q | K_A K_B | q \rangle \langle r | K_A K_B | r \rangle = -K_C^2 h(q, C, r) \quad (3.26)$$

It would be interesting if it were possible to find some shifts that exploited this recursion relation in some way. It would be good to use BCFW recursion to calculate the  $n$ -point all-plus gravity amplitude for all  $n$ .

### 3.3 The one-loop $-+++$ amplitude

#### 3.3.1 $-+++$ in Yang-Mills

In [18] the five, six and seven-point one-loop Yang-Mills amplitudes with a single negative helicity gluon were derived from on-shell recursion. Unlike the all-plus amplitude of the previous section these amplitudes contain the significant complication of the three-point all-plus nonstandard factorisation from which there is both a double pole and a single pole contribution. In this section we review their construction for the simplest four-point case. The  $-+++$  amplitude was first calculated by other methods in [82].

$$A_4^{(1)}(1^-, 2^+, 3^+, 4^+) = \frac{i}{96\pi^2} \frac{\langle 24 \rangle [24]^3}{[12] \langle 23 \rangle \langle 34 \rangle [41]} \quad (3.27)$$

We will consider recursion based on the standard BCFW shifts on  $|1\rangle$  and  $|2\rangle$ :

$$\begin{aligned} \lambda_1 &\rightarrow \lambda_1 \\ \tilde{\lambda}_1 &\rightarrow \tilde{\lambda}_1 - z\tilde{\lambda}_2 \\ \lambda_2 &\rightarrow \lambda_2 + z\lambda_1 \\ \tilde{\lambda}_2 &\rightarrow \tilde{\lambda}_2 \end{aligned} \quad (3.28)$$

These shifts applied to the amplitude do not give a boundary term and give a shifted amplitude which is singular at a single point in the complex  $z$ -plane.

$$\begin{aligned} \langle \hat{2}3 \rangle &= \langle 13 \rangle (z - b) \quad , \quad [\hat{1}4] = [42] (z - b) \\ \text{where } b &= -\frac{\langle 23 \rangle}{\langle 13 \rangle} = \frac{[14]}{[24]} \end{aligned} \quad (3.29)$$

So applying the shifts (3.28) to the known amplitude (3.27) yields:

$$A_4^{(1)}(\hat{1}^-, \hat{2}^+, 3^+, 4^+)(z) = \frac{i}{96\pi^2} \frac{\langle 12 \rangle [24]}{\langle 34 \rangle \langle 31 \rangle} \left( \frac{1}{(z - b)^2} + \frac{\langle 13 \rangle \langle 14 \rangle}{\langle 34 \rangle \langle 12 \rangle} \frac{1}{(z - b)} \right) \quad (3.30)$$

We can now write the original amplitude  $A_4^{(1)}(\hat{1}^-, \hat{2}^+, 3^+, 4^+)(0)$  as a sum of residues of the poles that occur in the function  $A_4^{(1)}(\hat{1}^-, \hat{2}^+, 3^+, 4^+)(z)/z$ . In this case there is only one pole at  $z = b$ . Following [18] this single residue will be explained recursively by splitting it up into two parts. The first part comes from the double pole in (3.30) and the second part comes from the single pole in (3.30). There will be a one-to-one map between the terms of this expansion and the terms of a recursion relation based on the shifts (3.28).

$$A_4^{(1)}(1^-, 2^+, 3^+, 4^+) = \frac{i}{96\pi^2} \left[ \frac{\langle 12 \rangle \langle 13 \rangle [24]}{\langle 23 \rangle^2 \langle 34 \rangle} + \frac{\langle 12 \rangle \langle 13 \rangle [24]}{\langle 23 \rangle^2 \langle 34 \rangle} \frac{\langle 14 \rangle \langle 23 \rangle}{\langle 12 \rangle \langle 34 \rangle} \right] \quad (3.31)$$

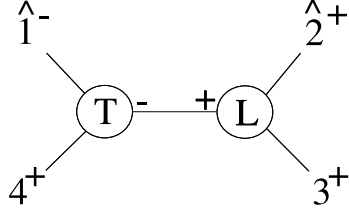


Figure 3.5: The recursive construction of  $A_4^{(1)}(1^-, 2^+, 3^+, 4^+)$  via shifting  $|1\rangle$  and  $|2\rangle$  involves this nonstandard factorisation diagram.

We now review the origin of the two terms in (3.31) from a BCFW recursion relation. Recalling that both terms are associated with  $\langle \hat{2}3 \rangle = [\hat{1}4] = 0$  the corresponding diagram is in Figure 3.5.

BDK [18] reproduced the double-pole term in (3.31) recursively from Figure 3.5 using the one-loop all-plus vertex  $V_3^{(1)}(+++)$  which was introduced in (3.4).

$$\begin{aligned} A_3^{(0)}(4^+, \hat{1}^+, \hat{K}_{23}^-) \frac{i}{(K_{23}^2)^2} V_3^{(1)}(-\hat{K}_{23}^+, \hat{2}^+, 3^+) &= \frac{i}{96\pi^2} \frac{\langle 1|\hat{K}|2\rangle \langle 1|\hat{K}|3\rangle \langle \hat{K}1\rangle}{\langle 14\rangle \langle 23\rangle^2 [23] \langle \hat{K}4\rangle} \\ &= \frac{i}{96\pi^2} \frac{\langle 12\rangle \langle 13\rangle [24]}{\langle 23\rangle^2 \langle 34\rangle} \end{aligned} \quad (3.32)$$

The ‘single pole under the double pole’ term in (3.31) differs from the double pole term by the factor:

$$\frac{\langle 14\rangle \langle 23\rangle}{\langle 12\rangle \langle 34\rangle} \quad (3.33)$$

As reviewed in the introduction, the candidate explanation (3.6) for this factor given in [18] uses the ‘soft factors’ given in equation (3.7) with the following prescription:

$$S(\hat{1}, \hat{K}_{23}^+, 4) K_{23}^2 S(\hat{2}, -\hat{K}_{23}^-, 3) = \frac{\langle 14\rangle \langle 23\rangle [23]^2}{\langle 1|\hat{K}|3\rangle \langle 4|\hat{K}|2\rangle} = \frac{\langle 14\rangle \langle 23\rangle}{\langle 12\rangle \langle 34\rangle} \quad (3.34)$$

### 3.3.2 $-+++$ in Gravity

The  $-+++$  one-loop gravity amplitude was calculated using two-particle unitarity cuts with a  $D$ -dimensional scalar running in the loop in [98]. We use the normalisation conventions of [100].

$$M_4^{(1)}(1^-, 2^+, 3^+, 4^+) = \frac{i}{(4\pi)^2} \frac{1}{180} \left( \frac{\langle 12\rangle [23] [24]}{[12] \langle 23\rangle \langle 24\rangle} \right)^2 (s^2 + st + t^2) \quad (3.35)$$

Remarkably the recursive procedure for Yang-Mills which was reviewed in the last section extends very simply to this gravity case. Just as in the Yang-Mills case we consider the standard BCFW shifts on  $|1\rangle$  and  $|2\rangle$  given in (3.28). Applying these shifts to the known

amplitude does not give a boundary term and introduces singularities at two different points in the complex  $z$ -plane.

$$\langle \hat{2}4 \rangle = \langle 14 \rangle (z - a) \quad \text{where} \quad a = -\frac{\langle 24 \rangle}{\langle 14 \rangle} \quad (3.36)$$

$$\langle \hat{2}3 \rangle = \langle 13 \rangle (z - b) \quad \text{where} \quad b = -\frac{\langle 23 \rangle}{\langle 13 \rangle} \quad (3.37)$$

When we later reconstruct this amplitude from a recursion relation the residues at these two points will come from different diagrams. It is not a surprise that there are more recursive diagrams in gravity than there are in Yang-Mills, because in gravity there is no cyclic ordering of legs like there is for the colour ordered amplitudes of Yang-Mills. Under the shifts (3.28) the amplitude (3.35) becomes

$$M_4^{(1)}(\hat{1}^-, \hat{2}^+, 3^+, 4^+)(z) = \frac{i}{(4\pi)^2} \frac{1}{180} \left[ \frac{\langle 12 \rangle^4 [23]^2 [24]^2}{\langle 13 \rangle^2 \langle 14 \rangle^2} \frac{1}{(z-a)^2 (z-b)^2} + \frac{\langle 12 \rangle^3 [23]^3 [24]^2}{\langle 13 \rangle \langle 14 \rangle^2 [12]} \frac{1}{(z-a)^2 (z-b)} + \frac{\langle 12 \rangle^2 [23]^4 [24]^2}{\langle 14 \rangle^2 [12]^2} \frac{1}{(z-a)^2} \right] \quad (3.38)$$

We now separate out the different poles using the following partial fraction expansions:

$$\begin{aligned} \frac{1}{(z-a)^2 (z-b)^2} &= \frac{1}{(a-b)^2 (z-a)^2} - \frac{2}{(a-b)^3 (z-a)} \\ &\quad + \frac{1}{(a-b)^2 (z-b)^2} + \frac{2}{(a-b)^3 (z-b)} \\ \frac{1}{(z-a)^2 (z-b)} &= \frac{1}{(a-b)(z-a)^2} - \frac{1}{(a-b)^2 (z-a)} + \frac{1}{(a-b)^2 (z-b)} \end{aligned}$$

where  $a - b$  can be simplified using the Schouten identity:

$$a - b = -\frac{\langle 24 \rangle}{\langle 14 \rangle} + \frac{\langle 23 \rangle}{\langle 13 \rangle} = -\frac{\langle 12 \rangle \langle 34 \rangle}{\langle 13 \rangle \langle 14 \rangle} \quad (3.39)$$

We can now write the shifted amplitude as a sum of terms associated with the various different types of pole at different locations.

$$M_4^{(1)}(\hat{1}^-, \hat{2}^+, 3^+, 4^+)(z) = \frac{i}{(4\pi)^2} \frac{1}{180} \left[ \frac{\langle 12 \rangle^2 [23]^2 [24]^2}{\langle 34 \rangle^2} \frac{1}{(z-a)^2} + \frac{\langle 12 \rangle \langle 13 \rangle \langle 14 \rangle [23]^2 [24]^2}{\langle 43 \rangle^3} \frac{1}{z-a} + \frac{\langle 12 \rangle^2 [23]^2 [24]^2}{\langle 34 \rangle^2} \frac{1}{(z-b)^2} + \frac{\langle 12 \rangle \langle 13 \rangle \langle 14 \rangle [23]^2 [24]^2}{\langle 34 \rangle^3} \frac{1}{z-b} \right] \quad (3.40)$$

Finally we can write the original amplitude  $M_4^{(1)}(\hat{1}^-, \hat{2}^+, 3^+, 4^+)(0)$  as a sum of residues of the function  $M_4^{(1)}(\hat{1}^-, \hat{2}^+, 3^+, 4^+)(z)/z$  at the poles of various types and locations in complex  $z$ -plane.

$$M_4^{(1)} = \frac{i}{(4\pi)^2} \frac{1}{180} \left[ \frac{\langle 12 \rangle^2 \langle 14 \rangle^2 [23]^2 [24]^2}{\langle 24 \rangle^2 \langle 34 \rangle^2} \right. \quad \text{double-pole, } z = a \quad (3.41)$$

$$+ \frac{\langle 12 \rangle^2 \langle 14 \rangle^2 [23]^2 [24]^2}{\langle 24 \rangle^2 \langle 34 \rangle^2} \left( -\frac{\langle 13 \rangle \langle 24 \rangle}{\langle 12 \rangle \langle 43 \rangle} \right) \quad \text{single-pole, } z = a \quad (3.42)$$

$$+ \frac{\langle 12 \rangle^2 \langle 13 \rangle^2 [23]^2 [24]^2}{\langle 23 \rangle^2 \langle 34 \rangle^2} \quad \text{double-pole, } z = b \quad (3.43)$$

$$+ \left. \frac{\langle 12 \rangle^2 \langle 13 \rangle^2 [23]^2 [24]^2}{\langle 23 \rangle^2 \langle 34 \rangle^2} \left( -\frac{\langle 14 \rangle \langle 23 \rangle}{\langle 12 \rangle \langle 34 \rangle} \right) \right] \quad \text{single-pole, } z = b \quad (3.44)$$

We will now reconstruct these four terms from the diagrams of a recursion relation. There will be two diagrams corresponding to the two locations, in the complex  $z$ -plane, where there are poles in the shifted amplitude  $M_4^{(1)}(\hat{1}^-, \hat{2}^+, 3^+, 4^+)(z)$ . The pole at  $z = a$  is associated with  $[\hat{1}3] = \langle \hat{2}4 \rangle = 0$  and corresponds to Figure 3.6a. The other pole at  $z = b$  is associated with  $[\hat{1}4] = \langle \hat{2}3 \rangle = 0$  and corresponds to Figure 3.6b.

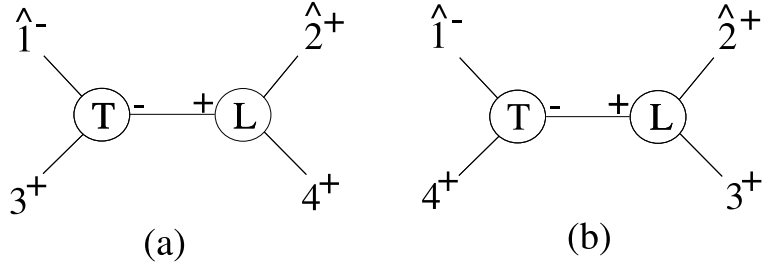


Figure 3.6: *The recursive construction of  $M_4^{(1)}(1^-, 2^+, 3^+, 4^+)$  via shifting  $|1\rangle$  and  $|2\rangle$  involves these two nonstandard factorisation diagrams.*

The double-pole term in (3.43) can be reconstructed recursively from Figure 3.6b using the new three-point one-loop all-plus gravity vertex  $W_3^{(1)}(+++)$  which up to a constant is the square of the Yang-Mills vertex and was introduced in (3.5)

$$M_3^{(0)}(\hat{1}^-, \hat{K}_{23}^-, 4^+) \frac{i}{(K_{23}^2)^2} W_3^{(1)}(\hat{2}^+, 3^+, -\hat{K}_{23}^+) = -C \frac{\langle 1|\hat{K}|3\rangle^2 \langle 1|\hat{K}|2\rangle^2 \langle 1\hat{K}\rangle^2}{(23)^2 \langle 41\rangle^2 \langle 4\hat{K}\rangle^2} \quad (3.45)$$

We will later fix the numerical constant  $C$  by comparison with the known answer (3.43). We now use the following relations to write the  $\hat{K}$  in terms of the external legs.

$$\begin{aligned} \langle 1|\hat{K}|3\rangle^2 &= \langle 1|\hat{2} + 3|3\rangle^2 = \langle 12 \rangle^2 [23]^2 \\ \langle 1|\hat{K}|2\rangle^2 &= \langle 1|\hat{2} + 3|2\rangle^2 = \langle 13 \rangle^2 [23]^2 \\ \frac{\langle 1\hat{K}\rangle^2}{\langle 4\hat{K}\rangle^2} &= \frac{\langle 1|\hat{K}|2\rangle^2}{\langle 4|\hat{K}|2\rangle^2} = \frac{\langle 1|\hat{2} + 3|2\rangle^2}{\langle 4|\hat{2} + 3|2\rangle^2} = \frac{\langle 13 \rangle^2}{\langle 34 \rangle^2} \end{aligned} \quad (3.46)$$

So (3.45) reproduces the spinor algebra of the known double pole residue at  $z = b$  (3.43).

$$-C \frac{\langle 12 \rangle^2 \langle 13 \rangle^2 [23]^2 [24]^2}{\langle 23 \rangle^2 \langle 34 \rangle^2} \quad (3.47)$$

By comparison with (3.43) we can fix  $C$  in the new vertex  $W_3^{(1)}(+ + +)$  to be:

$$C = -\frac{i}{(4\pi)^2} \frac{1}{180} \quad (3.48)$$

The other term (3.44) corresponding to Figure 3.6b is the residue of the single-pole underneath the double pole at  $z = b$ . This single-pole term differs from the double-pole term (3.43) and (3.45) up to a sign in the same way as in the Yang-Mills amplitude (3.31):

$$-\frac{\langle 14 \rangle \langle 23 \rangle}{\langle 12 \rangle \langle 34 \rangle} = -S(\hat{1}, \hat{K}_{23}^+, 4) K_{23}^2 S(\hat{2}, -\hat{K}_{23}^-, 3) \quad (3.49)$$

where the ‘soft factors’ are the same as were used for Yang-Mills (3.7). This suggests the following candidate for the single pole under the double pole in gravity:

$$-M_3^{(0)}(\hat{1}^-, \hat{K}_{23}^-, 4^+) S(\hat{1}, \hat{K}_{23}^+, 4) \frac{i}{K_{23}^2} S(\hat{2}, -\hat{K}_{23}^-, 3) W_3^{(1)}(\hat{2}^+, 3^+, -\hat{K}_{23}^+) \quad (3.50)$$

Figure 3.6a is the same as figure 3.6b, but with the external legs 3 and 4 interchanged. The two terms (3.41) and (3.42), associated with the point  $z = a$ , correspond to the Figure 3.6a and are similarly found by interchanging legs 3 and 4.

### 3.4 The one-loop $- + + + +$ Gravity amplitude

The  $- + + + +$  one-loop gravity amplitude is unknown. We now attempt to construct it using on-shell recursion. We use the shifts (3.28) on  $|1\rangle$  and  $|2\rangle$  and hope that they will not involve a boundary term. In Yang-Mills, shifts of the form  $[-, +\rangle$  have been observed to be free of large-parameter contributions [77, 101]. This observation extends to the  $- + + +$  gravity amplitude and we hope that it extends further to the  $- + + + +$  gravity amplitude.

The shifts (3.28) give nine different recursive diagrams. The shifted amplitude has simple-poles associated with  $[\hat{1}3] = [\hat{1}4] = [\hat{1}5] = 0$ . The simple pole associated with  $[\hat{1}5] = 0$  corresponds to the standard recursive diagram in Figure 3.7. The shifted amplitude will also have simple-pole associated with  $\langle \hat{2}3 \rangle = \langle \hat{2}4 \rangle = \langle \hat{2}5 \rangle = 0$ . The simple pole associated with  $\langle \hat{2}3 \rangle = 0$  corresponds to the standard factorisation diagram in Figure 3.8. Finally there are also nonstandard factorisations in the shifted amplitude corresponding to the poles associated with  $\langle \hat{2}3 \rangle = \langle \hat{2}4 \rangle = \langle \hat{2}5 \rangle = 0$ . These nonstandard factorisations contain a one-loop three-point all-plus vertex and contribute double poles and also single poles under these double poles. The diagram for the nonstandard factorisation associated with the a pole at

$\langle \hat{2}3 \rangle = 0$  is given in Figure 3.9. There are just three types of diagram to calculate; Figures 3.7, 3.8 and 3.9. The remaining diagrams can be obtained from these by permuting the external legs  $\{3, 4, 5\}$ .

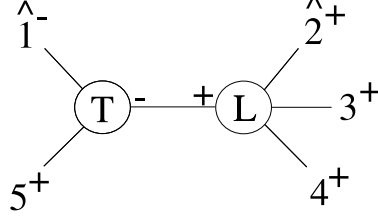


Figure 3.7: The diagram in the recursive expression for  $M_5^{(1)}(1^-, 2^+, 3^+, 4^+, 5^+)$  corresponding to a simple-pole associated with  $[\hat{1}5] = 0$ .

First consider Figure 3.7. This contributes:

$$M_3^{(0)}(\hat{1}^-, \hat{K}_{15}^-, 5^+) \frac{i}{K_{15}^2} M_4^{(1)}(\hat{2}^+, 3^+, 4^+, -\hat{K}_{15}^+) \quad (3.51)$$

where the  $M_3^{(0)}(- - +)$  amplitude is given by the square of the Yang-mills amplitude times  $-i$  and the  $M_4^{(1)}(+ + + +)$  amplitude was given in (3.11). So (3.51) yields:

$$-\frac{i}{(4\pi)^2} \frac{1}{60} \frac{[23]^2}{\langle 51 \rangle^3 [51]} \langle 1 | \hat{K} | 4 \rangle^2 \left( \frac{\langle 1 \hat{K} \rangle \langle 1 \hat{K} \rangle}{\langle 5 \hat{K} \rangle \langle 4 \hat{K} \rangle} \right)^2 \left( [23]^2 + \frac{[23] \langle 34 \rangle [34]}{\langle \hat{2}3 \rangle} + \frac{\langle 34 \rangle^2 [34]^2}{\langle \hat{2}3 \rangle^2} \right)$$

We now use the following relations to eliminate  $\hat{K}_{15}$ .

$$\begin{aligned} \langle 1 | \hat{K} | 4 \rangle^2 &= \langle 15 \rangle^2 [45]^2 \\ \frac{\langle 1 \hat{K} \rangle^2}{\langle 5 \hat{K} \rangle^2} &= \frac{[25]^2}{[12]^2} \\ \frac{\langle 1 \hat{K} \rangle^2}{\langle 4 \hat{K} \rangle^2} &= \frac{\langle 15 \rangle^2 [25]^2}{\langle 34 \rangle^2 [23]^2} \end{aligned}$$

Figure 3.7 is associated with  $0 = [\hat{1}5]$ , or equivalently to a pole located at  $z = [15]/[25]$ . It is then easy to show that:

$$\langle \hat{2}3 \rangle = \frac{\langle 34 \rangle [45]}{[25]}$$

So the final contribution of Figure 3.7 resulting from (3.51) is:

$$-\frac{i}{(4\pi)^2} \frac{1}{60} \frac{\langle 15 \rangle [25]^4}{\langle 34 \rangle^2 [12]^2 [15]} \left( [23]^2 [45]^2 + [23] [34] [45] [25] + [34]^2 [25]^2 \right) \quad (3.52)$$

There is no colour ordering in gravity, so Figure 3.7 is invariant under swapping the external legs labelled 3 and 4. Use of the Schouten identity shows that the result (3.52) is also

invariant under swapping 3 and 4.

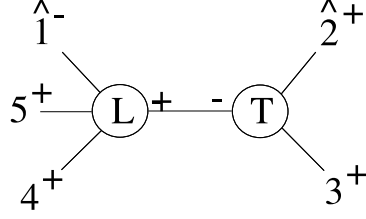


Figure 3.8: The diagram in the recursive expression for  $M_5^{(1)}(1^-, 2^+, 3^+, 4^+, 5^+)$  corresponding to a simple-pole associated with  $\langle \hat{2}3 \rangle = 0$ .

Next we consider Figure 3.8. This contributes:

$$M_4^{(1)}(\hat{1}^-, 4^+, 5^+, \hat{K}_{23}^+) \frac{i}{K_{23}^2} M_3^{(0)}(\hat{2}^+, 3^+, -\hat{K}_{23}^-) \quad (3.53)$$

Where the  $M_3^{(0)}(+ + -)$  amplitude is the square of the Yang-Mills one times  $-i$  and the  $M_4^{(1)}(- + ++)$  amplitude was given in (3.35). So (3.53) yields:

$$\frac{i}{(4\pi)^2} \frac{1}{180} \frac{\langle 14 \rangle^2 [45]^2 [23]^5}{\langle 45 \rangle^2 \langle 23 \rangle} \frac{1}{\langle 4 | \hat{K} | 2 \rangle^2} \left( \frac{[4\hat{K}]}{[3\hat{K}]} \right)^2 \left( \langle 14 \rangle^2 + \frac{\langle 14 \rangle \langle 45 \rangle [45]}{[\hat{1}4]} + \frac{\langle 45 \rangle^2 [45]^2}{[\hat{1}4]^2} \right) \quad (3.54)$$

We use the following relations to eliminate  $\hat{K}_{23}$

$$\begin{aligned} \langle 4 | \hat{K} | 2 \rangle^2 &= \langle 34 \rangle^2 [23]^2 \\ \frac{[4\hat{K}]}{[3\hat{K}]} &= \frac{\langle 15 \rangle^2 [45]^2}{\langle 12 \rangle^2 [23]^2} \end{aligned}$$

Figure 3.8 is associated with  $0 = \langle \hat{2}3 \rangle$ , or equivalently to a pole located at  $z = -\langle 23 \rangle / \langle 13 \rangle$ . It is then easy to show that:

$$[\hat{1}4] = -\frac{\langle 35 \rangle [45]}{\langle 13 \rangle}$$

So the final contribution of Figure 3.8 resulting from (3.53) is:

$$\frac{i}{(4\pi)^2} \frac{1}{180} \frac{\langle 14 \rangle^2 \langle 15 \rangle^2 [23] [45]^4}{\langle 12 \rangle^2 \langle 23 \rangle \langle 35 \rangle^2 \langle 34 \rangle^2 \langle 45 \rangle^2} \left( \langle 14 \rangle^2 \langle 35 \rangle^2 + \langle 14 \rangle \langle 45 \rangle \langle 53 \rangle \langle 13 \rangle + \langle 45 \rangle^2 \langle 13 \rangle^2 \right) \quad (3.55)$$

Figure 3.8 is invariant under swapping the external legs labelled 4 and 5. Use of the Schouten identity shows that the result (3.55) is also invariant under swapping 4 and 5.

Finally we consider contributions from the diagram in Figure 3.9. This diagram contains a three-point all-plus vertex so there will be two contributions from this diagram. As we saw in the four-point example the three-point all-plus vertex gives a single and a double

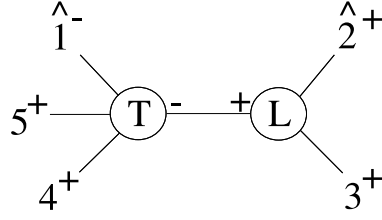


Figure 3.9: The diagram in the recursive expression for  $M_5^{(1)}(1^-, 2^+, 3^+, 4^+, 5^+)$  corresponding to the double-pole associated with  $\langle \hat{2}3 \rangle = 0$ .

pole term. First consider the double-pole term.

$$M_4^{(0)}(\hat{1}^-, \hat{K}_{23}^-, 4^+, 5^+) \frac{i}{(K_{23}^2)^2} W_3^{(1)}(\hat{2}^+, 3^+, -\hat{K}_{23}^+) \quad (3.56)$$

where the one-loop three-point all-plus vertex  $W_3^{(1)}(+++)$  is the new vertex which was introduced in (3.5) and the  $M_4^{(0)}(- - + +)$  amplitude is given via the following KLT relation:

$$\begin{aligned} M_4^{(0)}(1^-, 2^-, 3^+, 4^+) &= i \langle 12 \rangle [12] A_4^{(0)}(1^-, 2^-, 3^+, 4^+) A_4^{(0)}(1^-, 2^-, 4^+, 3^+) \\ &= -i \frac{\langle 12 \rangle^7 [12]}{\langle 13 \rangle \langle 14 \rangle \langle 23 \rangle \langle 24 \rangle \langle 34 \rangle^2} \end{aligned} \quad (3.57)$$

So (3.56) yields:

$$C \frac{\langle 1|\hat{K}|2\rangle^2 \langle 1|\hat{K}|3\rangle^2}{\langle 14 \rangle \langle 15 \rangle \langle 23 \rangle^2 \langle 45 \rangle^2} \langle 1|\hat{K}|\hat{1}\rangle \frac{\langle 1\hat{K} \rangle \langle 1\hat{K} \rangle}{\langle 4\hat{K} \rangle \langle 5\hat{K} \rangle}$$

We now use the following relations to eliminate the hats.

$$\begin{aligned} \langle 1|\hat{K}|2\rangle^2 &= \langle 13 \rangle^2 [23]^2, & \langle 1|\hat{K}|3\rangle^2 &= \langle 12 \rangle^2 [23]^2, & \langle 1|\hat{K}|\hat{1}\rangle &= \langle 45 \rangle [45] \\ \frac{\langle 1\hat{K} \rangle}{\langle 4\hat{K} \rangle} &= -\frac{\langle 13 \rangle}{\langle 34 \rangle}, & \frac{\langle 1\hat{K} \rangle}{\langle 5\hat{K} \rangle} &= -\frac{\langle 13 \rangle}{\langle 35 \rangle} \end{aligned}$$

So the double-pole contribution (3.56) from Figure 3.9 is:

$$C \frac{\langle 12 \rangle^2 \langle 13 \rangle^4 [23]^4 [45]}{\langle 14 \rangle \langle 15 \rangle \langle 23 \rangle^2 \langle 34 \rangle \langle 35 \rangle \langle 45 \rangle} \quad (3.58)$$

We fixed the coefficient  $C$  in (3.48) by comparison with the known  $- + + +$  one-loop gravity amplitude. Figure 3.9 is invariant under swapping the external legs labelled 4 and 5. The result (3.58) is also invariant under swapping 4 and 5.

The other contribution from Figure 3.9 is from the ‘single-pole underneath the double-pole’ term. Unfortunately this final term poses a problem. Inspired by the corresponding term (3.44) in the known  $- + + +$  gravity amplitude we might guess that this ‘single-pole under the double-pole’ term differs from the double-pole term by a now familiar factor of

the form introduced in (3.6). Recall that this factor has the form:

$$S(a_1, \hat{K}^+, a_2) K^2 S(b_1, -\hat{K}^-, b_2) \quad (3.59)$$

Experimentation in Yang-Mills [18] led to  $a_1$  and  $a_2$  being the legs colour adjacent to the propagator in the tree-level amplitude of the recursive diagram. This prescription cannot extend to gravity since there is no colour ordering of the external legs. If we are to use a factor of this form in gravity we have to choose two of the three external legs attached to the tree diagram in Figure 3.9 to be  $a_1$  and  $a_2$ . In the  $-+++$  gravity amplitude we did not encounter this decision because the tree amplitude in the recursive diagram only has two external legs. However, since a factor of this form is antisymmetric under swapping  $a_1$  and  $a_2$ , even in the  $-+++$  gravity example, the lack of ordering of the external particles means that this factor has an ambiguous sign. For Figure 3.9 there are three possible choices:

$$S(\hat{1}, \hat{K}_{23}^+, 4) K_{23}^2 S(\hat{2}, -\hat{K}_{23}^-, 3) = -\frac{\langle 14 \rangle \langle 23 \rangle [23]^2}{\langle 1 | \hat{K} | 3 \rangle \langle 4 | \hat{K} | 2 \rangle} = \frac{\langle 14 \rangle \langle 23 \rangle}{\langle 12 \rangle \langle 34 \rangle} \quad (3.60)$$

$$S(\hat{1}, \hat{K}_{23}^+, 5) K_{23}^2 S(\hat{2}, -\hat{K}_{23}^-, 3) = -\frac{\langle 15 \rangle \langle 23 \rangle [23]^2}{\langle 1 | \hat{K} | 3 \rangle \langle 5 | \hat{K} | 2 \rangle} = \frac{\langle 15 \rangle \langle 23 \rangle}{\langle 12 \rangle \langle 35 \rangle} \quad (3.61)$$

$$S(5, \hat{K}_{23}^+, 4) K_{23}^2 S(\hat{2}, -\hat{K}_{23}^-, 3) = \frac{\langle 23 \rangle \langle 45 \rangle [23]^2}{\langle 5 | \hat{K} | 2 \rangle \langle 4 | \hat{K} | 3 \rangle} = -\frac{\langle 13 \rangle \langle 23 \rangle \langle 45 \rangle}{\langle 12 \rangle \langle 34 \rangle \langle 35 \rangle} \quad (3.62)$$

It is perhaps natural to guess that a sum of these terms might give the correct ‘single pole under the double pole’ term. Figure 3.9 is symmetric under swapping legs 4 and 5, so we require a sum of factors which share this symmetry. An appropriate sum of factors is:

$$\pm \left( \frac{\langle 14 \rangle \langle 23 \rangle}{\langle 12 \rangle \langle 34 \rangle} + \frac{\langle 15 \rangle \langle 23 \rangle}{\langle 12 \rangle \langle 35 \rangle} \right) \quad (3.63)$$

However this proposal is incorrect as it does not give an amplitude which is symmetric under the interchange of legs 2 and 3. It is usually believed that an amplitude with the correct collinear and soft behaviour is the correct amplitude, but we have been unable to find a guess of this final term with the correct properties.

There are at least three possible ways that we might be able to calculate the missing ‘double pole under single pole’ terms. We could learn how to describe these factorisations by studying the factorisations of known amplitudes in Yang-Mills and then hope to extend these ideas to gravity. Some further examples of ‘single pole under double pole’ terms in Yang-Mills and gravity can be found in the next section. In section 3.6 we will review an unsuccessful attempt to use auxiliary recursions to completely avoid these problematic non-standard factorisations. Finally we could calculate the amplitude using traditional unitarity based techniques.

### 3.5 The description of nonstandard factorisations

Any recursive diagram containing a three-point one-loop part is termed a nonstandard factorisation [77]. Nonstandard factorisations are the complicating feature in the extension of the BCFW recursion relation from tree level amplitudes to the rational parts of one-loop amplitudes. For example factorisations involving the three-point all-plus amplitude give two types of term, a double pole term and a single pole under the double pole term. While the description of the double pole in terms of a three-point all-plus vertex appears to be independent of the choice of shifts, the description of the ‘single pole under the double pole’ as differing from the double pole term by a single factor of the form  $SP^2S$  is not universal, even in Yang-Mills. It only seems to work for the simplest BCFW shift on  $|1\rangle$  and  $|2\rangle$ .

#### 3.5.1 $-++++$ in Yang-Mills with $|1\rangle, |3\rangle$ shifts

The  $-++++$  Yang-Mills amplitude is given by

$$A_5^{(1)}(1^-, 2^+, 3^+, 4^+, 5^+) = i \frac{N_p}{96\pi^2} \frac{1}{\langle 34 \rangle^2} \left[ -\frac{[25]^3}{[12][51]} + \frac{\langle 14 \rangle^3 [45] \langle 35 \rangle}{\langle 12 \rangle \langle 23 \rangle \langle 45 \rangle^2} - \frac{\langle 13 \rangle^3 [32] \langle 42 \rangle}{\langle 15 \rangle \langle 54 \rangle \langle 23 \rangle^2} \right] \quad (3.64)$$

We now consider the standard BCFW shifts on  $|1\rangle$  and  $|3\rangle$ . We apply these shifts to the amplitude and use partial fractions to separate the various poles. If we then put  $z=0$  we have rewritten the amplitude in a form where there is a one to one correspondence between terms in this expansion of the amplitude and the terms of the recursion relation associated with the shifts.

$$A = i \frac{N_p}{96\pi^2} \left[ \frac{[35]^3}{\langle 24 \rangle^2 [15] [13]} \right] \quad (3.65)$$

$$+ \frac{[23]^3}{\langle 45 \rangle^2 [12] [13]} \quad (3.66)$$

$$+ \frac{\langle 25 \rangle \langle 14 \rangle^3 [45]}{\langle 13 \rangle \langle 23 \rangle \langle 45 \rangle^2 \langle 24 \rangle^2} \quad (3.67)$$

$$- \frac{\langle 12 \rangle^2 \langle 13 \rangle [23]}{\langle 45 \rangle \langle 51 \rangle \langle 24 \rangle \langle 23 \rangle^2} \left( 1 + 2 \frac{\langle 14 \rangle \langle 23 \rangle}{\langle 13 \rangle \langle 24 \rangle} \right) \quad (3.68)$$

$$- \frac{\langle 25 \rangle \langle 14 \rangle^3 [25]}{\langle 13 \rangle \langle 34 \rangle \langle 24 \rangle^2 \langle 45 \rangle^2} \quad (3.69)$$

$$- \frac{\langle 13 \rangle \langle 14 \rangle^3 [43]}{\langle 12 \rangle \langle 51 \rangle \langle 24 \rangle \langle 54 \rangle \langle 34 \rangle^2} \left( 1 - 2 \frac{\langle 12 \rangle \langle 34 \rangle}{\langle 13 \rangle \langle 42 \rangle} + \frac{\langle 15 \rangle \langle 34 \rangle}{\langle 13 \rangle \langle 45 \rangle} \right) \quad (3.70)$$

The terms in this expansion are in one-to-one correspondence with the diagrams in Figure 3.10. The term (3.65) corresponds to diagram 3.10(a). The term (3.66) corresponds to diagram 3.10(b). The term (3.67) corresponds to diagram 3.10(c). The term (3.68) corresponds to diagram 3.10(d). The term (3.69) corresponds to diagram 3.10(e). The term

(3.70) corresponds to diagram 3.10(f).

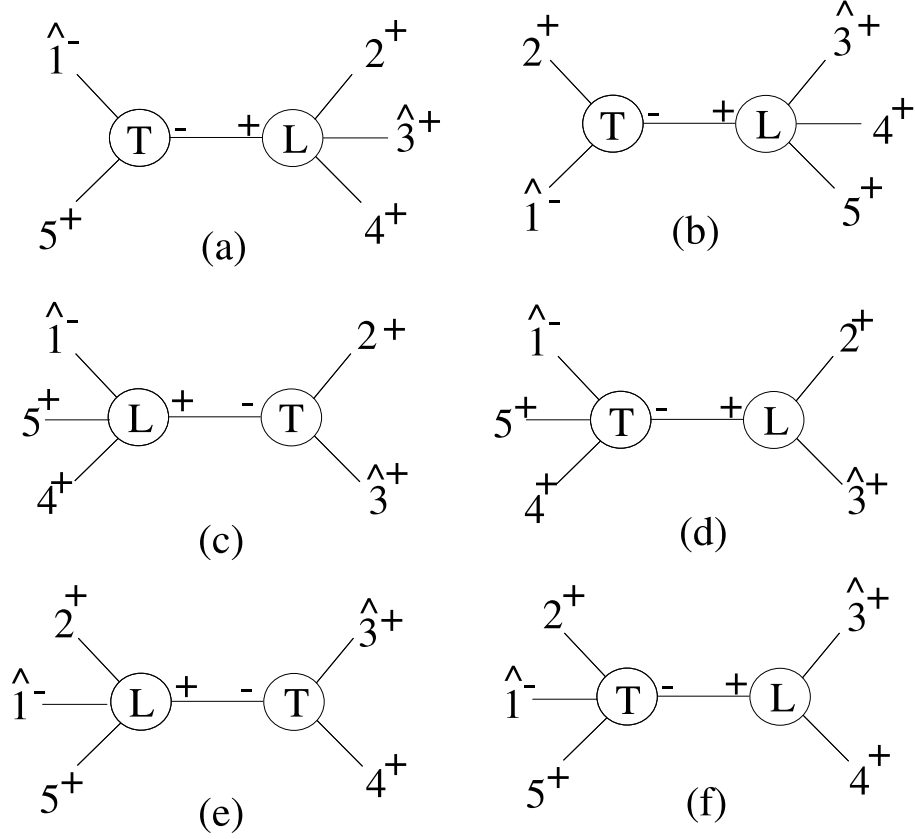


Figure 3.10: *The diagrams in the recursive expression for  $A_5^{(1)}(1^-, 2^+, 3^+, 4^+, 5^+)$  with shifts on  $|1\rangle$  and  $|3\rangle$ .*

The recursive description of the terms (3.65) to (3.70) is well understood with the exception of the two factors relating the ‘single pole under double pole’ terms to the corresponding double pole terms. Thus we require a full explanation of the factors in (3.68) and (3.70). These factors can be explained as a sum of BDK style  $SP^2S$  terms.

The ‘single pole under double pole’ factor in the term (3.68) is ‘explained’ in a BDK fashion by looking at the diagram in Figure 3.10(d) and considering the legs colour adjacent to the propagator:

$$\begin{aligned}
 \pm S(\hat{1}, k^+, 4) K_{23} S(2, k^-, \hat{3}) &= \pm \frac{\langle 14 \rangle}{\langle 1\hat{k} \rangle \langle \hat{k}4 \rangle} \langle 23 \rangle [23] \frac{[23]}{[2\hat{k}] [\hat{k}3]} \\
 &= \pm \frac{\langle 14 \rangle \langle 23 \rangle [23]^2}{\langle 1|\hat{k}|2 \rangle \langle 4|\hat{k}|3 \rangle} \\
 &= \pm \frac{\langle 14 \rangle \langle 23 \rangle}{\langle 13 \rangle \langle 24 \rangle} \tag{3.71}
 \end{aligned}$$

where  $\pm$  is included as we are unsure of the correct way to assign a sign to this term. We

cannot think of an explanation or rule for the factor of 2 that must appear in (3.68).

The spinor algebra that appears in factors in (3.70) can be similarly ‘explained’, but for the diagram in Figure 3.10(f) we do not consider the colour adjacent legs to the propagator. The first factor in (3.70) is equal to:

$$\begin{aligned}
 \pm S(\hat{1}, k^+, 2) K_{34} S(\hat{3}, k^-, 4) &= \pm \frac{\langle 12 \rangle}{\langle 1\hat{k} \rangle \langle \hat{k}2 \rangle} \langle 34 \rangle [34] \frac{[34]}{[3\hat{k}][\hat{k}4]} \\
 &= \pm \frac{\langle 12 \rangle \langle 34 \rangle [34]^2}{\langle 1|\hat{k}|4 \rangle \langle 2|\hat{k}|3 \rangle} \\
 &= \pm \frac{\langle 12 \rangle \langle 34 \rangle}{\langle 13 \rangle \langle 24 \rangle}
 \end{aligned} \tag{3.72}$$

We cannot think of a sensible explanation for the factor of 2 that appears in front of this first term in (3.70). The second factor in (3.70) is equal to:

$$\begin{aligned}
 \pm S(\hat{1}, k^+, 5) K_{34} S(\hat{3}, k^-, 4) &= \pm \frac{\langle 15 \rangle}{\langle 1\hat{k} \rangle \langle \hat{k}2 \rangle} \langle 34 \rangle [34] \frac{[34]}{[3\hat{k}][\hat{k}4]} \\
 &= \pm \frac{\langle 15 \rangle \langle 34 \rangle [34]^2}{\langle 1|\hat{k}|4 \rangle \langle 5|\hat{k}|3 \rangle} \\
 &= \pm \frac{\langle 15 \rangle \langle 34 \rangle}{\langle 13 \rangle \langle 45 \rangle}
 \end{aligned} \tag{3.73}$$

It would be interesting to find an explanation for the factors in (3.68) and (3.70).

### 3.5.2 $- + ++$ in gravity with $|1\rangle, |2\rangle, |3\rangle, |4\rangle$ shifts

In this section we give an example of a set of shifts for which the ‘single pole under the double pole’ in the  $- + ++$  gravity amplitude (3.35) are not of the form  $SP^2S$ :

$$\begin{aligned}
 |1] &\rightarrow |1] - z(|2] + |3] + |4]) \\
 |a\rangle &\rightarrow |a\rangle + z|1\rangle \quad \text{for } a = 2, 3, 4
 \end{aligned} \tag{3.74}$$

The ‘single pole under the double pole’ associated with  $\langle \hat{2}\hat{3} \rangle = 0$  differs from the double pole by a factor of the form:

$$\frac{\langle 14 \rangle \langle 23 \rangle}{\langle 12 \rangle \langle 13 \rangle} \frac{1}{\langle 23 \rangle + \langle 34 \rangle + \langle 42 \rangle} \left( -2 \frac{\langle 13 \rangle}{\langle 14 \rangle} (\langle 21 \rangle + \langle 14 \rangle) + (\langle 21 \rangle + \langle 13 \rangle) \right) \tag{3.75}$$

In these shifts  $SP^2S$  is equal to:

$$S(\hat{1}, \hat{k}^+, \hat{4}) k_{23} S(\hat{2}, \hat{k}^-, \hat{3}) = \frac{\langle 14 \rangle \langle 23 \rangle}{\langle 13 \rangle \langle 12 \rangle} \frac{\langle 21 \rangle + \langle 13 \rangle}{\langle 23 \rangle + \langle 34 \rangle + \langle 42 \rangle} \tag{3.76}$$

So in these shifts the ‘single pole under the double pole’ does not have the form  $SP^2S$ .

### 3.6 Avoiding nonstandard factorisations

It is possible to calculate amplitudes in Yang-Mills without having to consider nonstandard factorisations [77]. See also the review [101] of this remarkable method. These papers point out that it is possible to find shifts which avoid non-standard factorisations, but that these shifts will generically have a boundary term. Using a pair of shifts in two independent complex parameters the authors then exploited this fact to calculate complete amplitudes avoiding the consideration of any nonstandard factorisations. We now briefly review their method for the simple case of a purely rational amplitude. The pair of shifts are called the primary shift and the auxiliary shift:

$$\text{primary shift: } [j, l] \quad \begin{cases} \tilde{\lambda}_j \rightarrow \tilde{\lambda}_j - z\tilde{\lambda}_l \\ \lambda_l \rightarrow \lambda_l + z\lambda_j \end{cases} \quad (3.77)$$

$$\text{auxiliary shift: } [a, b] \quad \begin{cases} \tilde{\lambda}_a \rightarrow \tilde{\lambda}_a - w\tilde{\lambda}_b \\ \lambda_b \rightarrow \lambda_b + w\lambda_a \end{cases} \quad (3.78)$$

The primary shift is chosen to have no nonstandard factorisations, but it will have a boundary term and the auxiliary shift will have no boundary term, but it will include non-standard factorisations. These two shifts give rise to two recursion relations for the amplitude:

$$A_n^{(1)}(0) = \text{Inf}_{[j,l]} A_n + R_n^{\text{D,recursive } [j,l]} \quad (3.79)$$

$$A_n^{(1)}(0) = R_n^{\text{D,recursive } [a,b]} + R_n^{\text{D,non-standard } [a,b]} \quad (3.80)$$

We now apply the primary shift to the recursion relation for the auxiliary shift (3.80) to extract the large  $z$  behaviour of the primary shift:

$$\text{Inf}_{[j,l]} A_n = \text{Inf}_{[j,l]} R_n^{\text{D,recursive } [a,b]} + \text{Inf}_{[j,l]} R_n^{\text{D,non-standard } [a,b]} \quad (3.81)$$

where the Inf operation is defined to be the constant term in the expansion of the shifted term about  $z = \infty$ . We wish to avoid calculating terms involving nonstandard factorisations so we will assume that the following condition holds.

$$\text{Inf}_{[j,l]} R_n^{\text{D,non-standard } [a,b]} = 0 \quad (3.82)$$

Since we do not, in general, know how to calculate the terms involving nonstandard factorisations it is, of course, difficult to check explicitly if the condition (3.82) holds for a given pair of shifts. However, if one calculates an amplitude assuming that (3.82) holds and the resulting amplitude has the correct collinear and soft behaviour, then the amplitude is correct and the condition (3.82) must have been true. Thus if we assume the condition (3.82) and use (3.81) to calculate the boundary term in (3.79) we can calculate the amplitude

without considering any nonstandard factorisations:

$$A_n(0) = \text{Inf}_{[j,l]} R_n^{\text{D,recursive}} [a,b] + R_n^{\text{D,recursive}} [j,l] \quad (3.83)$$

### 3.6.1 The $- + + + +$ Yang-Mills amplitude

The following simple example exhibiting the possibility of calculating an amplitude using auxiliary recursions to avoid all nonstandard factorisations is not mentioned in [77], but is closely related to examples that they do consider in their paper. First recall that the known answer for the amplitude is

$$A_5^{(1)}(1^-, 2^+, 3^+, 4^+, 5^+) = i \frac{N_p}{96\pi^2} \frac{1}{\langle 34 \rangle^2} \left[ -\frac{[25]^3}{[12][51]} + \frac{\langle 14 \rangle^3 [45] \langle 35 \rangle}{\langle 12 \rangle \langle 23 \rangle \langle 45 \rangle^2} - \frac{\langle 13 \rangle^3 [32] \langle 42 \rangle}{\langle 15 \rangle \langle 54 \rangle \langle 23 \rangle^2} \right]$$

The three terms above will be called term 1, term 2 and term 3 for the purposes of this section. As shown in [18], if we consider the standard BCFW shifts on  $|1\rangle$  and  $|2\rangle$  then term 1 and term 2 come from standard factorisations and term 3 comes from a nonstandard factorisation. See Figure 3.11. Term 1 comes from the pole associated with  $[\hat{1}5] = 0$ . Term 2 and term 3 both come from the pole associated with  $\langle \hat{2}3 \rangle = 0$ . Term 2 is a standard factorisation, but term 3 involves the nonstandard three-point one-loop all-plus vertex. In [18] term 3 was computed by understanding this nonstandard factorisation as a sum of two terms called a double pole term and single pole under the double pole term.

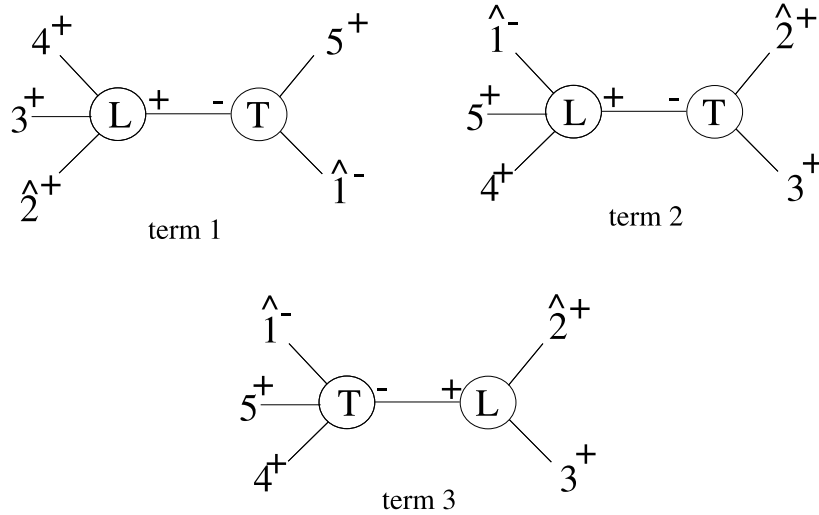


Figure 3.11: The diagrams in the  $|1\rangle|2\rangle$  shift of  $A_5^{(1)}(1^-, 2^+, 3^+, 4^+, 5^+)$ .

In this section we show how to use auxiliary recursions to calculate the amplitude without considering either of the two types of term associated with the three-point one-loop all-plus nonstandard factorisations. We will consider the following pair of shifts. The primary  $[j, l]$

shift is on  $|4\rangle$  and  $|5\rangle$ . This shift has no nonstandard factorisations, but does have boundary term. The auxiliary  $[a, b\rangle$  shift is on  $|1\rangle$  and  $|2\rangle$ . This shift has no boundary term, but does have nonstandard factorisations. From the discussion in the previous paragraph we know that

$$R_n^{\text{D,recursive } [a, b\rangle} = \text{term 1} + \text{term 2} \quad (3.84)$$

$$R_n^{\text{D,non-standard } [a, b\rangle} = \text{term 3} \quad (3.85)$$

Since we are recalculating a known amplitude we can explicitly check if the condition (3.82) is satisfied. If we perform the  $[j, l\rangle$  shift on term 3 (put hats on  $|4\rangle$  and  $|5\rangle$ ) and then consider large  $z$  then the term is  $O(1/z)$  so the condition (3.82) is satisfied:

$$\text{Inf}_{[j, l\rangle} R_n^{\text{D,non-standard } [a, b\rangle} = \text{Inf}_{[j, l\rangle} \text{term 3} = 0 \quad (3.86)$$

So it will be possible to calculate the  $- + + + +$  Yang-Mills amplitude without considering any nonstandard factorisations using this pair of shifts.

Now we summarise the details of actually calculating the amplitude. First we use (3.84) to calculate the first term in (3.83):

$$\text{Inf}_{[j, l\rangle} R_n^{\text{D,recursive } [a, b\rangle} = \text{Inf}_{[j, l\rangle} (\text{term 1} + \text{term 2}) = \text{term 1} + \text{term 2} \quad (3.87)$$

As explained in the previous section, this part should be thought of as the boundary term in the primary shift. Finally we have to calculate the recursive diagrams in the primary  $[j, l\rangle$  shift on  $|4\rangle$  and  $|5\rangle$ . There is only one diagram associated with these shifts. This is the diagram corresponding to a pole at  $\langle 1\hat{5} \rangle = 0$ . See Figure 3.12. Calculating this diagram gives the second term in (3.83).

$$R_n^{\text{D,recursive } [j, l\rangle} = \text{term 3} \quad (3.88)$$

So putting (3.87) and (3.88) into the equation (3.83) constructs the full amplitude.

$$A_n(0) = \text{term 1} + \text{term 2} + \text{term 3} \quad (3.89)$$

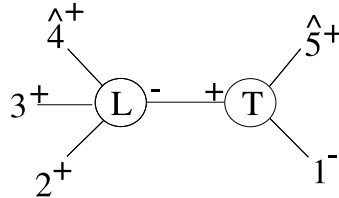


Figure 3.12: The diagram in the  $[4] |5\rangle$  shift of  $A_5^{(1)}(1^-, 2^+, 3^+, 4^+, 5^+)$ .

Unfortunately trying to follow this example directly to calculate the one-loop  $-++++$  gravity amplitude does not work. In gravity a shift generally involves more factorisations since in gravity there is no cyclic ordering condition on the external legs like there is in Yang-Mills. Using the primary shift on  $|4\rangle$  and  $|5\rangle$  will not work for gravity since some of these extra factorisations are nonstandard. The shift on  $|4\rangle$  and  $|5\rangle$  involves the poles associated with  $\langle\hat{5}2\rangle = 0$  and  $\langle\hat{5}3\rangle = 0$ . These include contributions from the three-point one-loop all-plus factorisation.

Despite the fact that the procedure for avoiding nonstandard factorisations in Yang-Mills does not immediately extend to gravity, we are hopeful that the results from various shifts can be combined in some way to compute the unknown ‘single pole under double pole’ terms in  $-++++$  gravity amplitude. The results for the other simple BCFW shifts of the  $-++++$  are collected in appendix B.2. Appendix B.2.1 contains the recursive diagrams in the  $|4\rangle, |5\rangle$  shift. Appendix B.2.2 contains the diagram in the  $|2\rangle, |1\rangle$  shift.

Calculating the  $-++++$  amplitude using old methods such as  $D$ -dimensional unitarity, or  $D$ -dimensional generalised unitarity would tell us the answer for the missing ‘single-pole underneath the double pole’ terms. Understanding the  $-++++$  gravity example would perhaps shed light on the general description of this type of nonstandard factorisation term.

# CHAPTER 4

## THE ADHM CONSTRUCTION AND D-BRANE CHARGES

In this chapter we suggest a construction of monopoles in dimension  $2k + 1$  from fuzzy funnels. For  $k = 1$  this construction coincides with Nahm's construction of monopoles [102], which is an adaptation of the Atiyah, Drinfeld, Hitchin and Manin (ADHM) construction of instantons [103]. For  $k = 1, 2, 3$  this gives a finite  $n$  realisation of the duality between D1-brane and D( $2k + 1$ )-brane world-volume pictures of the non-commutative bionic brane intersection [104–106]. We then perform two charge calculations related to this construction. First we calculate the charge of the monopole and get an answer in precise agreement with the size of the matrices in the fuzzy funnel. Secondly we calculate the charge of the fuzzy funnel. To get this charge to agree with the size of the matrices in the monopole beyond leading orders in  $1/n$  we propose a speculative use of the symmetrised trace. A matching of the terms of the symmetrised trace with the number of branes expected from the charge calculation then leads to a new and surprisingly simple formula for the symmetrised trace quantity.

### 4.1 Introduction

It is well known that the world-volume theory of  $N$  coincident  $D$ -branes, arising from open strings stretching between the  $D$ -branes, is a nonabelian  $U(N)$  gauge theory [107]. The massless world-volume theory of the  $D$ -branes also contains scalar fields describing the transverse fluctuations of the branes. For many coincident  $D$ -branes these coordinates are matrix-valued in the adjoint of the  $U(N)$  gauge group. The matrix-valued coordinates can be interpreted in terms of non-commutative geometry. The world-volume dynamics of these  $D$ -branes has revealed the phenomena of the dielectric effect [108, 109], where  $D$ -branes expand via non-commutative configurations into higher dimensional  $D$ -branes. The first example of the dielectric effect was that  $D0$ -branes in an external RR four-form field expand into a non-commutative two-sphere. This configuration is interpreted as a bound state of  $D0$  and  $D2$ -branes. For a review of nonabelian phenomena on  $D$ -branes see [110]. An introduction to the large subject of  $D$ -brane physics can be found in [111].

In this chapter we consider the static configurations of many coincident  $D1$ -branes expanding along their world-line into an orthogonal collection of coincident  $D(2k + 1)$ -branes.

In contrast to the dielectric effect this configuration has no nontrivial background fields. There are two different world-volume descriptions of this brane configuration, one coming from a solution to the world-volume theory of the  $D1$ -branes and the other from a solution to the world-volume theory of the  $D(2k+1)$ -branes. The duality between these different descriptions of the same configuration of branes was considered in the limit where the number of  $D1$ -branes is large in the references [104], [105], [106] for the cases  $k = 1, 2, 3$  respectively.

The  $D1$ -brane world-volume picture of this configuration is to consider solutions with only  $2k+1$  of the transverse scalars  $\Phi_i(s)$  turned on, where  $0 < s < \infty$  is the world-volume coordinate on the set of coincident straight semi-infinite  $D1$ -branes. As shown in [104–106] there is a solution called a fuzzy funnel which involves the ansatz

$$\Phi_i(s) = f(s)X_i(k, n) \quad (4.1)$$

where the  $X_i(k, n)$ , with  $i = 1, \dots, 2k+1$ , are the matrix coordinates of the fuzzy  $S^{2k}$  at level  $n = 1, 2, 3, \dots$ . The Fuzzy two-sphere was first introduced in [112]. Generalisation to the fuzzy four-sphere appeared in [113, 114]. Extension to higher dimensions occurred in [115, 116].

For the fuzzy two sphere, the matrix coordinates  $X_i$  are simply a representation of the lie algebra of  $SU(2)$ . The use of non-abelian coordinates rather than the normal commutative coordinates reduces the infinite space of functions on the ordinary sphere to a finite dimensional subset defining a *fuzzy* sphere. The space of functions on the two-sphere can be written as a polynomial expansion in the three coordinates on three dimensional flat space  $x_i$ , with the additional two-sphere constraint  $x_i x_i = 1$ , giving a set of functions of the form:

$$f(x_i) = f^{(0)} + f_{i_1}^{(1)} x_{i_1} + f_{i_1 i_2}^{(2)} x_{i_1} x_{i_2} + \dots + f_{i_1 \dots i_r}^{(r)} x_{i_1} \dots x_{i_r} + \dots \quad (4.2)$$

where the coefficients  $f_{i_1 \dots i_r}^{(r)}$  are totally symmetric and traceless. Just as the commutative coordinates satisfy the constraint  $x_i x_i = 1$ , the matrices in the representations of  $SU(2)$  satisfy a similar condition:

$$X_i X_i = n(n+2) \quad (4.3)$$

where the  $X_i$  are matrices of dimension  $n+1$ . If we normalise the  $X_i$  so that they satisfy  $X_i X_i = 1$ , then the commutator of the  $X_i$  will vanish in the large  $n$  limit and we will recover ordinary commuting coordinates. The emergence of the ordinary sphere as the dimension of the representation of  $SU(2)$  increases, can also be seen from the space of functions. The effect of changing the commutative coordinates to noncommutative coordinates is to truncate the set of functions (4.2). For example, if we use the two dimensional representation of  $SU(2)$ , given by the Pauli matrices, then any polynomial in these matrices which is quadratic or higher degree, can be written in terms of a single Pauli matrix using the relation  $\sigma_i \sigma_j = 2\delta_{ij} + i\epsilon_{ijk} \sigma_k$ . Thus the space of functions is reduced to a set given by

just the  $f^{(0)}$  and  $f_i^{(1)}$  terms of the expansion (4.2). This space of function has dimension  $1 + 3 = 4$ . In general [112] the  $n+1$  dimensional representation truncates the expansion (4.2) at the  $n$ th term. The functions  $f^{(r)}$  for  $r > n$  will be absent. We now count the size of this space of functions. The number of degrees of freedom in the symmetric traceless  $f_{i_1 \dots i_r}^{(r)}$  is given by:

$$\frac{1}{r!} \prod_{i=1}^r (i+2) - \frac{1}{(r-2)!} \prod_{i=1}^{r-2} (i+2) = 2r+1 \quad (4.4)$$

We now add up the degrees of freedom in  $f^{(0)}$  to  $f^{(n)}$  to get dimension of the truncated space of functions:

$$\sum_{r=0}^n (2r+1) = (n+1)^2 \quad (4.5)$$

So the space of functions of the fuzzy two-sphere at level  $n$  has dimension  $N^2 = (n+1)^2$  which is the same as the size of the matrices in the fuzzy sphere.

The generalisation of the fuzzy two-sphere to the fuzzy  $2k$ -sphere [115, 116] involves the matrices  $X_i$ , which are related to the representation of  $SO(2k+1)$  with  $k$  dimensional highest weight state  $(\frac{n}{2}, \frac{n}{2}, \dots, \frac{n}{2})$ . For  $n$  an even integer this representation corresponds to the Young tableaux which is rectangular with  $k$  rows and  $\frac{n}{2}$  columns. The dimension of the representation of  $SO(2k+1)$  with highest weight vector  $(\lambda_1, \dots, \lambda_k)$  is given by the Weyl character formula<sup>1</sup>:

$$\dim_{2k+1} = \prod_{1 \leq i < j \leq k} \frac{l_i^2 - l_j^2}{m_i^2 - m_j^2} \prod_{i=1}^k \frac{l_i}{m_i} \quad (4.6)$$

where

$$l_i = \lambda_i + k - i + \frac{1}{2}, \quad m_i = k - i + \frac{1}{2} \quad (4.7)$$

The fuzzy sphere  $X_i$  [115, 116] correspond to the representation with highest weight state  $(\frac{n}{2}, \frac{n}{2}, \dots, \frac{n}{2})$  and thus their dimension is given by:

$$N(k, n) = \prod_{1 \leq i < j \leq k} \frac{n+2k-(i+j)+1}{2k-(i+j)+1} \prod_{l=1}^k \frac{n+2k-2l+1}{2k-2l+1} \quad (4.8)$$

Just like the fuzzy two-sphere case, the use of these noncommutative coordinates truncates the space of functions on the classical  $2k$ -sphere to a subset defining the *fuzzy* sphere. In the limit  $n \rightarrow \infty$  the full infinite set of functions on the sphere is recovered, but for  $n$  finite the space of functions has dimension  $N(k, n)^2$  [115]. In fact in the large  $n$  limit, a space of higher dimension than a sphere emerges [118]. Since the size of the fuzzy sphere matrices  $X_i$  grows like  $N(k, n) \sim n^{\frac{k(k+1)}{2}}$ , this higher dimensional space is  $k(k+1)$ -dimensional and given by the coset space<sup>2</sup>  $SO(2k+1)/U(k)$  [118]. The generalisation of the relation (4.3)

<sup>1</sup>See for example page 408 of [117].

<sup>2</sup>This coset space is actually the twistor space of the  $2k$ -sphere. See for example [119].

to these higher dimensional spheres takes the form:

$$X_i(k, n)X_i(k, n) = c(k, n)1_{N(k, n)} \quad , \quad c(k, n) = n(n + 2k) \quad (4.9)$$

where the quantity  $c(k, n)$  is usually referred to as the quadratic Casimir since:

$$[X_i, X_j][X_j, X_i] = 2k c(k, n)1_{N(k, n)} \quad (4.10)$$

The alternative picture of this brane configuration comes from the  $D(2k + 1)$ -brane world-volume theory and is a monopole solution. This involves turning on a gauge field and a single matrix valued transverse scalar field. The original papers on the  $D3$ -brane spike are [120–122]. For the  $D5$ -brane monopole see appendix B of [105]. The generalisation to higher dimensional branes appeared in [123]. It was argued in the papers [104–106] that these different descriptions should agree for large  $n$ . The arguments for this appear in, for example, the discussion at the end of [104]. The nature of the agreement is that the number of branes in the two descriptions match at large  $n$ . The two descriptions are valid in complementary regions of the configuration. The solution to the  $D1$ -brane world-volume is valid far from the position of the  $D(2k + 1)$ -brane when the radius of the spike is small. The  $D(2k + 1)$ -brane solution is a good description in regions of the  $D(2k + 1)$ -brane world-volume a long way from the centre of the monopole.

However, there are indications that a more precise relationship should hold. For the  $D1$ -branes expanding into a  $D3$ -brane (the  $k = 1$  case) there are three excited matrix valued transverse scalar fields. The condition for minimum energy, coming from the action of [110], is that they satisfy Nahm’s equation:

$$\frac{\partial \Phi_i}{\partial \sigma} = i\epsilon_{ijk}[\Phi_j, \Phi_k] \quad (4.11)$$

See section 2 of [105]. One can also derive this equation from the requirement that some supersymmetry is preserved [104]. Since the work of Nahm [102] it has been known that there is an invertible transform that takes the matrix solutions to Nahm’s equation and constructs a monopole solution in a gauge theory with a precise gauge group and with a precise charge. The charge of the monopole is simply given by the size of the  $\Phi_i$  matrices. Nahm’s construction of monopoles is an adaptation of the ADHM construction of instantons [103]. This was shown to be relevant to D-brane intersections in the papers [124–127]. In [128] Nahm’s adaptation of the ADHM construction was identified with a bound state of  $D1$ -branes and  $D3$ -branes. The ADHM construction was used to understand the AdS/CFT correspondence in [129–131]. More recently there has been work explaining that the ADHM construction is Tachyon condensation [132–134].  $D$ -brane and M theory inspired generalisations of Nahm’s equation have also been considered in [135–138].

In Section 4.2.1 we review Nahm’s construction for the  $k = 1$  configuration, where the

$D1$ -branes expand into  $D3$ -branes. This example of Nahm's construction is well known. See for example section 4.5 of [139]. In this case the Nahm data, or solution to the  $D1$ -brane world-volume theory, is a fuzzy funnel made of fuzzy two-spheres. For the fuzzy two-sphere the  $X_i$  are just the lie algebra of  $SU(2)$  times a radial profile function:

$$\Phi_i(s) = \frac{1}{s} X_i \quad i = 1, 2, 3 \quad (4.12)$$

Nahm's construction takes these  $N$  by  $N$  matrices and constructs of a  $U(1)$  Dirac monopole with charge  $N = n + 1$  from them. The step from Nahm data to the monopole involves finding the space of normalisable solutions to a certain Dirac operator which depends on the Nahm data. The monopole gauge field is then constructed from this space of normalisable solutions. For fuzzy two-sphere Nahm data, this Dirac equation has a single normalisable solution. The single eigenvector means that the monopole will have gauge group  $U(1)$  and its charge will be the size of the matrices in the Nahm data which is  $N = n + 1$ .

In this  $D1 \perp D3$  example, the single normalisable solution of the Dirac equation corresponds to the eigenvector of the following matrix, which has eigenvalue  $nf - r$ :

$$fX_i(1, n) \otimes X_i(1, 1) + 1_{N(1, n) \times N(1, n)} \otimes x_i X_i(1, 1) \quad (4.13)$$

where in this  $k = 1$  case, the  $x_i$  for  $i = 1, 2, 3$  are the world volume coordinates on the flat orthogonal  $D3$ -brane and  $r = \sqrt{(x_1^2 + x_2^2 + x_3^2)}$ . We would now like to guess what to do for  $k \geq 2$ . It is natural that the construction of the monopole in the higher dimensional cases involves finding the space of eigenvectors with eigenvalues  $nf - r$  of the matrix:

$$fX_i(k, n) \otimes X_i(k, 1) + 1_{N(k, n) \times N(k, n)} \otimes x_i X_i(k, 1) \quad (4.14)$$

Where the  $x_i$  for  $i = 1, \dots, 2k + 1$  are the world-volume coordinates on the  $D(2k + 1)$ -brane and now  $r = \sqrt{(x_1^2 + \dots + x_{2k+1}^2)}$ . The  $D$ -brane duality studies in [104–106] strongly suggest that Nahm's construction for the  $D1 \perp D3$  system, which starts from the fuzzy two sphere, should generalise to the higher dimensional cases. That is, monopoles in higher dimensions can be constructed from higher dimensional fuzzy spheres.

It turns out that the matrix (4.14) does have  $nf - r$  as an eigenvalue and the dimension of the eigenspace is  $N(k - 1, n + 1)$ . Arguments to show this are given in section 4.2.2. This leads us to construct a monopole from the space of  $N(k - 1, n + 1)$  eigenvectors. The constructed gauge field is given by:

$$A_\mu(x_i) = \frac{1}{2r(r + x_{2k+1})} \Gamma_{\mu\nu}(k, n) x_\nu \quad , \quad A_{2k+1}(x_i) = 0 \quad (4.15)$$

where the indices  $\mu, \nu = 1, \dots, 2k$ . The matrices  $\Gamma_{\mu\nu}(k, n)$  are defined by:

$$\begin{aligned}\Gamma_{ab}(k, n) &= -\frac{i}{2}[X_a(k-1, n+1), X_b(k-1, n+1)] \\ \Gamma_{c2k}(k, n) &= X_c(k-1, n+1)\end{aligned}\tag{4.16}$$

where the indices  $a, b, c = 1, \dots, 2k-1$ . This monopole has appeared in [123], but now it is proposed to be linked precisely with the Nahm data for the fuzzy sphere (4.1).

We then perform two charge calculations as a consistency check of the proposed construction. The first charge calculation is the  $k$ th Chern class of the  $D(2k+1)$ -brane world-volume monopole:

$$\frac{1}{k!} \left(\frac{1}{2\pi}\right)^k \int_{S^{2k}} \text{Tr}(F^k)\tag{4.17}$$

This counts the number of  $D1$ -branes in the monopole solution to the  $D(2k+1)$ -branes world-volume theory since the Ramond-Ramond two-form couples to the  $k$ th Chern class in the Chern-Simons part of the world-volume action. As in the usual ADHM construction, consistency requires that the charge of the monopole must equal the size of the Nahm data matrices  $X_i$  from which it was constructed. So the monopole charge should be  $N(k, n)$ . We show that this is the case in section 4.3.1 using an identity that relates  $N(k, n)$  to  $N(k-1, n+1)$ , which we prove in section 4.3.2.

The other charge calculation we consider is for the fuzzy funnel solution of the  $D1$ -branes world-volume theory. This appears in section 4.3.3. We compute the coupling of the  $N(k, n)$   $D1$ -branes to the Ramond-Ramond potential  $C^{2k+2}$ . This counts the number of  $D(2k+1)$ -branes in the fuzzy funnel solution to the  $D1$ -branes world-volume theory. The relevant term comes for the Chern-Simons term in the action of [108, 109]:

$$\frac{i^k \lambda^k \mu_1}{k!} \int \text{StrP}[(i_\Phi i_\Phi)^k C^{2k+2}]\tag{4.18}$$

The consistency of the ADHM construction requires that the number of  $D(2k+1)$ -branes is  $N(k-1, n+1)$  which in the ADHM construction was the dimension of the eigenspace with eigenvector  $nf-r$ . The dimension of this eigenspace is equal to the size of the matrices in the monopole that gets constructed.

This second charge calculation does not yield precisely  $N(k-1, n+1)$ , but does agree for the first two orders in the  $1/n$  expansion. This appears to be a non-trivial check of the  $n+1$  argument in the  $N(k-1, n+1)$ . We then observe a possible mechanism for corrections to the sub-leading terms of this charge calculation so that there is agreement with the answer  $N(k-1, n+1)$ . The details of this suggestion are at the start of section 4.4. The  $1/n$  corrections proposed come from the symmetrised trace and were first calculated for the fuzzy two-sphere in [140]. The symmetrised trace quantity first appeared in [141]. The observation of a matching between the required corrections and the first few orders of

the symmetrised trace suggests an all orders prediction for the symmetrised trace quantity. It is surprising that this is possible given the apparent complexity of the symmetrised trace quantity when written in terms of chord diagrams [140]. This prompted a guess of an exact formula for the symmetrised trace. For the fuzzy two-sphere the proposed answer is very simple:

$$\frac{1}{N} \text{Str}(X_i X_i)^m = \begin{cases} \frac{2(2m+1)}{n+1} \sum_{i=1}^{\frac{n}{2}} (2i)^{2m} & \text{for } n \text{ even} \\ \frac{2(2m+1)}{n+1} \sum_{i=1}^{\frac{n+1}{2}} (2i-1)^{2m} & \text{for } n \text{ odd} \end{cases} \quad (4.19)$$

The existence of a systematic construction of the general term in the symmetrised trace was anticipated on page 9 of [104]. We have checked that (4.19) is true up to  $m = 6$ , but have no general proof. The dynamics of fuzzy two-spheres will be studied using this formula in chapter 5.

In summary, the proposal is that a fuzzy  $S^{2k}$  funnel made of  $N(k, n)$  D1-branes expands into a collection of precisely  $N(k-1, n+1)$  D(2k+1)-branes. This is an extension of the previous results that appeared in [104–106] which proposed the leading large  $n$  terms of this relation.

## 4.2 The ADHM construction

### 4.2.1 Review of Nahm's construction for $D1 \perp D3$

In this section we review Nahm's construction of Monopoles [102]. A useful review on monopoles can be found in [142]. We consider the case of the construction that takes a representation of  $SU(2)$  and constructs a  $U(1)$  monopole. This example is well known in the literature, see for example section 4.5 of [139]. The brane configuration that corresponds to this construction is  $D1 \perp D3$  bion [104].

The starting point for Nahm's construction consists of one dimensional scalar fields  $\Phi_i(s)$  where  $i = 1, 2, 3$  which satisfy Nahm's equation (4.11). In  $D$ -brane language this is a solution to the world-volume theory of many coincident  $D1$ -branes. The construction of the Monopole then proceeds in two steps. The first step is to calculate all the normalisable solutions to the following Dirac equation:

$$(\Phi_i(s) + x_i) \otimes X_i(1, 1) |u(x_i, s)\rangle = \frac{\partial}{\partial s} |u(x_i, s)\rangle \quad (4.20)$$

where we have used the fuzzy sphere notation  $X_i(1, 1)$  for the usual Pauli matrices to save

having multiple notations for the same matrices. The normalisable condition is that:

$$\int_0^\infty ds \langle u(x_i, s) | u(x_i, s) \rangle < \infty \quad (4.21)$$

The normalisable solutions to the (4.20) form a vector space with an orthonormal basis  $\{|u_\alpha(x_i, s)\rangle\}$  where the index  $\alpha$  runs over the elements of the basis. The second step in Nahm's construction is to calculate the fields of the monopole using the formula:

$$\begin{aligned} (\phi(x_i))_{\alpha\beta} &= \int_0^\infty ds \langle u_\alpha(x_i, s) | s | u_\beta(x_i, s) \rangle \\ (A_i(x_i))_{\alpha\beta} &= i \int_0^\infty ds \langle u_\alpha(x_i, s) | \frac{\partial}{\partial x_i} | u_\beta(x_i, s) \rangle \end{aligned} \quad (4.22)$$

We now consider the  $D1 \perp D3$  bion case in which a  $U(1)$  monopole is constructed from the following Nahm data which is just the fuzzy two sphere representation of  $SU(2)$ :

$$\Phi_i(s) = \frac{1}{s} X_i(1, n) \quad (4.23)$$

To explicitly construct the monopole corresponding to this Nahm data, we have to first find the solutions to the Dirac equation (4.20). As we have already pointed out in the introduction this amounts to finding the eigenvalues of the matrix (4.13). Recall that this matrix has the form:

$$f X_i(1, n) \otimes X_i(1, 1) + 1_{N(1, n) \times N(1, n)} \otimes x_i X_i(1, 1)$$

To calculate the eigenvalues of (4.13), we first use spherical symmetry to rotate this matrix into the following matrix:

$$f X_i(1, n) \otimes X_i(1, 1) + r 1 \otimes X_3(1, 1) \quad (4.24)$$

where  $r = \sqrt{(x_1^2 + x_2^2 + x_3^2)}$ . The standard way to label the irreducible representations of  $SU(2)$  is in terms of the representations spin  $j$ , where  $2j = n$ . The states of the spin  $j$  representation are then  $|j, m\rangle$  where  $m = j, j-1, \dots, -j$ .

$$\begin{aligned} J^2 |j, m\rangle &= j(j+1) |j, m\rangle \\ J_3 |j, m\rangle &= m |j, m\rangle \end{aligned} \quad (4.25)$$

The matrix (4.24) is a product of two representations of  $SU(2)$  which can be decomposed as a sum of two irreducible representations as follows:

$$\text{spin}(j) \otimes \text{spin}(\frac{1}{2}) = \text{spin}(j + \frac{1}{2}) \oplus \text{spin}(j - \frac{1}{2}) \quad (4.26)$$

Two of the eigenvectors and eigenvalues of the matrix are easily found:

$$\begin{aligned} \left( fX_i(1, n) \otimes X_i(1, 1) + r1 \otimes X_3(1, 1) \right) |j + \frac{1}{2}, j + \frac{1}{2}\rangle &= (nf + r) |j + \frac{1}{2}, j + \frac{1}{2}\rangle \\ \left( fX_i(1, n) \otimes X_i(1, 1) + r1 \otimes X_3(1, 1) \right) |j + \frac{1}{2}, -j - \frac{1}{2}\rangle &= (nf - r) |j + \frac{1}{2}, j + \frac{1}{2}\rangle \end{aligned}$$

The eigenvector with eigenvalue  $nf - r$  will be the single normalisable solution to the Dirac equation from which we will construct the monopole. The remaining eigenvalues can be found by considering the following pair of vectors:

$$\begin{aligned} |j + \frac{1}{2}, m\rangle &= a |j, m - \frac{1}{2}\rangle | \frac{1}{2}, \frac{1}{2} \rangle + b |j, m + \frac{1}{2}\rangle | \frac{1}{2}, -\frac{1}{2} \rangle \\ |j - \frac{1}{2}, m\rangle &= -b |j, m - \frac{1}{2}\rangle | \frac{1}{2}, \frac{1}{2} \rangle + a |j, m + \frac{1}{2}\rangle | \frac{1}{2}, -\frac{1}{2} \rangle \end{aligned} \quad (4.27)$$

where

$$a = \left( \frac{j + m + \frac{1}{2}}{2j + 1} \right)^{\frac{1}{2}}, \quad b = \left( \frac{j - m + \frac{1}{2}}{2j + 1} \right)^{\frac{1}{2}} \quad (4.28)$$

The second part of the matrix (4.24) acts on these states as follows:

$$\begin{aligned} 1 \otimes X_3(1, 1) |j + \frac{1}{2}, m\rangle &= a |j, m - \frac{1}{2}\rangle | \frac{1}{2}, \frac{1}{2} \rangle - b |j, m + \frac{1}{2}\rangle | \frac{1}{2}, -\frac{1}{2} \rangle \\ &= (a^2 - b^2) |j + \frac{1}{2}, m\rangle - 2ab |j - \frac{1}{2}, m\rangle \\ 1 \otimes X_3(1, 1) |j - \frac{1}{2}, m\rangle &= -b |j, m - \frac{1}{2}\rangle | \frac{1}{2}, \frac{1}{2} \rangle - a |j, m + \frac{1}{2}\rangle | \frac{1}{2}, -\frac{1}{2} \rangle \\ &= -2ab |j + \frac{1}{2}, m\rangle - (a^2 - b^2) |j + \frac{1}{2}, m\rangle \end{aligned} \quad (4.29)$$

thus the eigenvalue problem has been reduced to finding the eigenvalues of the following two by two matrix:

$$\begin{pmatrix} 2jf + (a^2 - b^2)r & -2abr \\ -2abr & -2(j + 1)f - (a^2 - b^2)r \end{pmatrix} \quad (4.30)$$

The eigenvalues of this matrix are:

$$\begin{aligned} &-f \pm \sqrt{((2j + 1)^2 f^2 + r^2 + 2(2j + 1)(a^2 - b^2)fr)} \\ &= -f \pm \sqrt{((2j + 1)^2 f^2 + r^2 + 4mfr)} \end{aligned} \quad (4.31)$$

The only normalisable solution of the Dirac equation is the one corresponding to the eigenvector with eigenvalue  $nf - r$ . It is then simple to use this eigenvector and the integrals (4.22) to get the gauge field of a  $U(1)$  monopole with charge  $n + 1$ .

### 4.2.2 Generalisation to higher dimensions

As explained in the introduction there is a natural generalisation of the  $D1 \perp D3$  case to the higher dimensional  $D1 \perp D(2k+1)$  situation. This involves finding the eigenvectors of the matrix (4.14) which has the form:

$$fX_i(k, n) \otimes X_i(k, 1) + 1 \otimes x_i X_i(k, 1)$$

The eigenvalues of this matrix are:

$$nf - r \quad , \quad nf + r \quad , \quad (-1)^p f \pm \sqrt{((n+p)^2 f^2 + r^2 + 2frq)} \quad (4.32)$$

where  $p = 1, \dots, k$  and  $q = n-1, n-3, \dots, -n+1$ . This claim is based on the following group representation decomposition. The matrix (4.14) is formed from a product of two representations of  $SO(2k+1)$  which can be written as a sum of irreducible representations of  $SO(2k+1)$ . This is where the possible values for  $p$  in (4.32) come from. Each of these irreducible representations of  $SO(2k+1)$  can be written as a sum of irreducible representations of  $SO(2k)$ . This is where the possible values of  $q$  in (4.32) come from. Writing the matrix (4.14) with respect to a suitable ordering of this basis of  $SO(2k)$  representations makes it block diagonal. The largest blocks in this block diagonal form are two by two, so the eigenvalue problem is reduced to a set of at worst quadratic equations. The two by two blocks are made from two vectors from copies of the same representation of  $SO(2k)$  coming from different representations of  $SO(2k+1)$ .

We now explain why the eigenspace with eigenvalue  $nf - r$  has dimension  $N(k-1, n+1)$ . To do this we need the Weyl character formula [117] for  $SO(2k)$ . This formula tells us the dimension of representation of  $SO(2k)$  with highest weight vector  $(\lambda_1, \dots, \lambda_k)$ :

$$\dim_{2k} = \prod_{1 \leq i < j \leq k} \frac{l_i^2 - l_j^2}{m_i - m_j} \quad (4.33)$$

where  $l_i = \lambda_i + k - i$  and  $m_i = k - i$ . The product of the representations of  $SO(2k+1)$  with  $k$  dimensional highest weight vectors  $(\frac{n}{2}, \dots, \frac{n}{2})$  and  $(\frac{1}{2}, \dots, \frac{1}{2})$  contains the representation with highest weight vector  $(\frac{n+1}{2}, \dots, \frac{n+1}{2})$ . This representation of  $SO(2k+1)$  contains two copies of the representation of  $SO(2k)$  with  $k$  dimensional highest weight vector  $(\frac{n+1}{2}, \dots, \frac{n+1}{2})$ . The eigenvectors of the matrix (4.14) with eigenvalue  $nf - r$  are precisely one of these representations of  $SO(2k)$ . The other copy of this representation are the eigenvectors with eigenvalue  $nf + r$ . As can be seen from (4.33) the dimension of the representation of  $SO(2k)$  with  $k$  dimensional highest weight vector  $(\frac{n+1}{2}, \dots, \frac{n+1}{2})$  is equal to the dimension of the representation of  $SO(2k-1)$  with  $k-1$  dimensional highest weight vector  $(\frac{n+1}{2}, \dots, \frac{n+1}{2})$  which is the definition of  $N(k-1, n+1)$ .

## 4.2.3 Construction of the Monopole

For  $n = 0$ , the Nahm data is trivial  $\Phi_i(s) = 0$ . It is well known that trivial Nahm data results in the construction of a non trivial Monopole [142]. For  $n = 0$  the Dirac equation reduces to:

$$x_i X_i(k, 1) |u(x_i, s)\rangle = \frac{\partial}{\partial s} |u(x_i, s)\rangle \quad (4.34)$$

The matrix  $x_i X_i(k, 1)$  has  $2^{k-1}$  eigenvectors  $|v_\alpha^+(x_i)\rangle$  ( $\alpha = 1, \dots, 2^{k-1}$ ) of eigenvalue  $r$  and  $2^{k-1}$  eigenvectors  $|v_\alpha^-(x_i)\rangle$  of eigenvalue  $-r$ . The vectors  $|u_\alpha(x_i, s)\rangle = g(x_i) e^{\pm rs} |v_\alpha^\pm(x_i)\rangle$  then solve (4.34) where  $g(x_i)$  is an arbitrary function of the  $x_i$ . However, the solutions with the factor  $e^{+rs}$  are not normalisable whilst those with the factor  $e^{-rs}$  are. Thus the normalisable solutions to (4.34) are:

$$|u_\alpha(x_i, s)\rangle = (2r)^{\frac{1}{2}} e^{-rs} |v_\alpha^-(x_i)\rangle \quad (4.35)$$

where  $g(x_i) = (2r)^{\frac{1}{2}}$  was determined by choosing unit normalisation. We now find a explicit form for the  $|v_\alpha^-(x_i)\rangle$ . The matrix  $x_i X_i(k, 1)$  can be written in terms of  $X_a(k-1, 1)$ :

$$x_i X_i(k, 1) = \begin{pmatrix} x_{2k+1} \mathbb{1}_{2^{k-1}} & x_{2k} \mathbb{1}_{2^{k-1}} - i x_a X_a(k-1, 1) \\ x_{2k} \mathbb{1}_{2^{k-1}} + i x_a X_a(k-1, 1) & -x_{2k+1} \mathbb{1}_{2^{k-1}} \end{pmatrix} \quad (4.36)$$

Thus an orthonormal set of the  $2^{k-1}$  eigenvectors of  $x_i X_i(k, 1)$  with eigenvalue  $-r$  is given explicitly in terms of  $X_a(k-1, 1)$  by:

$$|v_\alpha^-(x_i)\rangle = \begin{pmatrix} -\left(\frac{1}{2r(r+x_{2k+1})}\right)^{\frac{1}{2}} (x_{2k} \mathbb{1}_{2^{k-1}} - i x_a X_a(k-1, 1)) w_\alpha \\ \left(\frac{r+x_{2k+1}}{2r}\right)^{\frac{1}{2}} w_\alpha \end{pmatrix} \quad (4.37)$$

where  $\{w_\alpha\}$  are a set of  $2^{k-1}$  vectors each of dimension  $2^{k-1}$  with components  $(w_\alpha)_\beta = \delta_{\alpha\beta}$ . The second step in the construction is to compute the Monopole gauge field from these normalised solutions to (4.34)

$$(\phi(x_i))_{\alpha\beta} = \int_0^\infty ds \langle u_\alpha(x_i, s) | s | u_\beta(x_i, s) \rangle = \frac{1}{2r} \delta_{\alpha\beta} \quad (4.38)$$

$$(A_i(x_i))_{\alpha\beta} = i \int_0^\infty ds \langle u_\alpha(x_i, s) | \frac{\partial}{\partial x_i} | u_\beta(x_i, s) \rangle = i \langle v_\alpha^-(x_i) | \frac{\partial}{\partial x_i} | v_\beta^-(x_i) \rangle \quad (4.39)$$

It is then simple to show that:

$$A_\mu(x_i) = \frac{1}{2r(r+x_{2k+1})} \Gamma_{\mu\nu}(k, 0) x_\nu \quad , \quad A_{2k+1}(x_i) = 0 \quad (4.40)$$

Unfortunately we have been unable to find an argument for the construction of the general case, but checking a few examples has confirmed (4.15).

### 4.3 Charge calculations

#### 4.3.1 Monopole charge calculation

In this section we calculate the  $k$ th Chern class of the monopole. We hope the the charge of the monopole we have constructed (4.15) is equal to the size of the fuzzy sphere matrices which provided the starting point for the construction. This is what normally occurs in the Nahm or ADHM construction. So we hope that the charge of the monopole defined on a stack of  $N(k-1, n+1)$   $D(2k+1)$ -branes will yield precisely  $N(k, n)$ . This calculation extends the work in [123].

$$\frac{1}{k!} \left( \frac{1}{2\pi} \right)^k \int_{S^{2k}} \text{Tr}(F^k) \quad (4.41)$$

The field strength for the Monopole is given in the appendix of [123]. At the point  $x_\mu = 0$ ,  $x_{2k+1} = r$  it has the form:

$$\begin{aligned} F_{\mu\nu} &= \frac{1}{4r^2} \Gamma_{\mu\nu}(k, n) \\ F_{\mu 2k+1} &= 0 \end{aligned} \quad (4.42)$$

To calculate the  $k$ th Chern class, we first consider the matrix:

$$\begin{aligned} M &= \epsilon_{\mu_1 \dots \mu_{2k}} \Gamma_{\mu_1 \mu_2}(k, n) \dots \Gamma_{\mu_{2k-1} \mu_{2k}}(k, n) \\ &= 2\epsilon_{a_1 2k a_2 a_3 \dots a_{2k-2} a_{2k-1}} \Gamma_{a_1 2k}(k, n) \Gamma_{a_1 a_2}(k, n) \dots \Gamma_{a_{2k-2} a_{2k-1}}(k, n) \\ &\quad + 2\epsilon_{a_1 a_2 a_3 2k \dots a_{2k-2} a_{2k-1}} \Gamma_{a_1 a_2}(k, n) \Gamma_{a_3 2k}(k, n) \dots \Gamma_{a_{2k-2} a_{2k-1}}(k, n) \\ &\quad + \dots \\ &\quad + 2\epsilon_{a_1 a_2 a_3 a_4 \dots a_{2k-1} 2k} \Gamma_{a_1 a_2}(k, n) \Gamma_{a_3 a_4}(k, n) \dots \Gamma_{a_{2k-1} 2k}(k, n) \\ &= 2k(-i)^{k-1} \epsilon_{a_1 \dots a_{2k-1}} X_{a_1}(k-1, n+1) \dots X_{a_{2k-1}}(k-1, n+1) \end{aligned} \quad (4.43)$$

Now recall an identity from the appendix of [116].

$$\epsilon_{i_1 \dots i_{2k+1}} X_{i_1}(k, n) \dots X_{i_{2k+1}}(k, n) = C(k, n) X_i(k, n) X_i(k, n) \quad (4.44)$$

where

$$C(k, n) = -(2i)^k k! \prod_{l=1}^{k-1} (n+2l) \quad (4.45)$$

Now recalling the fuzzy sphere constraint equation (4.9) from the introduction to this chapter, we see that the matrix  $M$  is a multiple of the identity matrix:

$$M = -2^k k! \prod_{l=1}^k (n+2l-1) 1_{N(k-1, n+1)} \quad (4.46)$$

The volume of a  $2k$ -sphere is:

$$\Omega_{2k} = 2^{k+1} \pi^k \prod_{l=1}^k \frac{1}{2l-1} \quad (4.47)$$

Thus the monopole charge is:

$$-\frac{1}{4^k k!} \left( \frac{1}{2\pi} \right)^k \Omega_{2k} \text{Tr}(M) = N(k-1, n+1) \left( \prod_{l=1}^k \frac{n+2l-1}{2l-1} \right) 2^{1-k} \quad (4.48)$$

It turns out that the right hand side of the above equation is equal to  $N(k, n)$ , as we had hoped for. This identity is proved in the next section.

#### 4.3.2 Proof of the identity involving $N(k, n)$ and $N(k-1, n+1)$

In this section we show that the following identity is true.

$$N(k, n) = N(k-1, n+1) \left( \prod_{l=1}^k \frac{n+2l-1}{2l-1} \right) 2^{1-k} \quad (4.49)$$

$N(k, n)$  is given by the formula (4.8).

$$N(k-1, n+1) = \prod_{1 \leq i < j \leq k-1} \frac{n+2k-(i+j)}{2k-(i+j)-1} \prod_{l=1}^{k-1} \frac{n+2k-2l}{2k-2l-1} \quad (4.50)$$

The first product in  $N(k-1, n+1)$  can be written as

$$\prod_{1 \leq i < j \leq k-1} \frac{n+2k-(i+j+1)+1}{2k-(i+j+1)} = \prod_{(i,j) \in S_1} \frac{n+2k-(i+j)+1}{2k-(i+j)} \quad (4.51)$$

Where  $S_1 = \{(i, j) \mid 1 \leq i < j \leq k \text{ and } j-i \neq 1\}$ . The second product in  $N(k-1, n+1)$  can be written as

$$\prod_{l=1}^{k-1} \frac{n+2k-(l+l+1)+1}{2k-(l+l+1)} = \prod_{(i,j) \in S_2} \frac{n+2k-(i+j)+1}{2k-(i+j)} \quad (4.52)$$

Where  $S_2 = \{(i, j) \mid 1 \leq i < j \leq k \text{ and } j-i = 1\}$ . So we can now write  $N(k-1, n+1)$  as a single product

$$N(k-1, n+1) = \prod_{1 \leq i < j \leq k} \frac{n+2k-(i+j)+1}{2k-(i+j)} \quad (4.53)$$

This expression has the same numerator as the first product in  $N(k, n)$ , see (4.8), so we can write

$$N(k, n) = N(k-1, n+1) \prod_{1 \leq i < j \leq k} \frac{2k - (i+j)}{2k - (i+j) + 1} \prod_{l=1}^k \frac{n + 2k - 2l + 1}{2k - 2l + 1} \quad (4.54)$$

We can evaluate the first product on the right hand side of (4.54)

$$\begin{aligned} \prod_{1 \leq i < j \leq k} \frac{2k - (i+j)}{2k - (i+j) + 1} &= \begin{array}{l} \frac{k-1}{k} \times \frac{k}{k+1} \times \frac{k+1}{k+2} \times \dots \times \frac{2k-4}{2k-3} \times \frac{2k-3}{2k-2} \\ \times \frac{k-2}{k-3} \times \frac{k-3}{k-4} \times \frac{k-4}{k-5} \times \dots \times \frac{2k-5}{2k-4} \\ \vdots \quad \quad \quad \vdots \quad \quad \quad \vdots \\ \times \frac{2}{3} \times \frac{3}{4} \\ \times \frac{1}{2} \end{array} \\ &= \frac{(k-1)(k-2) \dots 1}{(2k-2)(2k-4) \dots 2} \\ &= 2^{1-k} \end{aligned} \quad (4.55)$$

We can rewrite the second product on the right hand side of (4.54)

$$\prod_{l=1}^k \frac{n + 2k - 2l + 1}{2k - 2l + 1} = \prod_{l=1}^k \frac{n + 2l - 1}{2l - 1} \quad (4.56)$$

The identity (4.49) now follows from putting (4.55) and (4.56) into (4.54).

### 4.3.3 Fuzzy funnel charge calculation.

In this section we calculate the number of higher dimensional branes in the stack of  $D1$ -branes that form the fuzzy funnel. The suggested monopole construction takes the stack of  $N(k, n)$   $D1$ -branes and constructs a monopole defined on a stack of  $N(k-1, n+1)$   $D(2k+1)$ -branes. Recall that the reason for this was based on the fact that the dimension of the eigenspace of the matrix (4.14) with eigenvalue  $nf - r$  was  $N(k-1, n+1)$ . So we hope that the result of this charge calculation will also be  $N(k-1, n+1)$ . We are interested in the following Ramond-Ramond coupling [104–106]:

$$\begin{aligned} S_{wz} &= \frac{i^k \lambda^k \mu_1}{k!} \int \text{tr} P[(i_\Phi i_\Phi)^k C^{2k+2}] \\ &= \frac{i^k \lambda^{k+1} \mu_1}{k!} \int dt ds \text{tr} \left( \epsilon_{i_1 \dots i_{2k+1}} \Phi_{i_1} \dots \Phi_{i_{2k}} \frac{d\Phi_{i_{2k+1}}}{ds} \right) C_{0 \dots 2k+1}^{2k+2} \end{aligned} \quad (4.57)$$

To calculate the charge associated with this coupling, we first consider the matrix:

$$A = \epsilon_{i_1 \dots i_{2k+1}} \Phi_{i_1} \dots \Phi_{i_{2k}} \frac{d\Phi_{i_{2k+1}}}{ds} \quad (4.58)$$

where the fuzzy funnel is given by

$$\Phi_i(s) = f(s)X_i(k, n) \quad (4.59)$$

the definition of the ‘Physical radius’  $F$  is given by

$$f = \frac{F}{\lambda c(k, n)^{\frac{1}{2}}} \quad (4.60)$$

where the definition of  $c(k, n)$  is in (4.9). Now we use equation (4.44) from the appendix to [116] to give:

$$A = C(k, n)c(k, n)^{-k+\frac{1}{2}}\lambda^{-2k-1}F^{2k}\frac{dF}{ds}1_{N(k, n)} \quad (4.61)$$

now we use

$$\mu_1 = (2\pi\lambda)^k\mu_{2k+1} \quad (4.62)$$

and the volume of the  $2k$ -sphere from equation (4.47) to write the action  $S_{wz}$  as:

$$\frac{i^k}{2k!}C(k, n)c(k, n)^{-k+\frac{1}{2}}N(k, n)\prod_{l=1}^k(2l-1)\int dt dF F^{2k}\Omega_{2k}C_{0\dots 2k+1}^{2k+2} \quad (4.63)$$

The integral part of the above equation represents a single  $D(2k+1)$ -brane, so the number of branes is give by:

$$\begin{aligned} \text{number of branes} &= \frac{i^k}{2k!}C(k, n)c(k, n)^{-k+\frac{1}{2}}N(k, n)\prod_{l=1}^k(2l-1) \\ &= 2^{k-1}N(k, n)\left(\prod_{l=1}^k(2l-1)\right)c(k, n)^{-k+\frac{1}{2}}\left(\prod_{l=1}^{k-1}(n+2l)\right) \\ &= N(k-1, n+1)c(k, n)^{-k+\frac{1}{2}}\prod_{l=1}^{2k-1}(n+l) \end{aligned} \quad (4.64)$$

We had hoped that the number of branes would be precisely  $N(k-1, n+1)$ , but there is only agreement for large  $n$ :

$$\begin{aligned} c(k, n)^{-k+\frac{1}{2}}\prod_{l=1}^{2k-1}(n+l) &= 1 + \left[2k\left(-k + \frac{1}{2}\right) + \sum_{l=1}^{2k-1}l\right]\frac{1}{n} + \mathcal{O}\left(\frac{1}{n^2}\right) \\ &= 1 + \mathcal{O}\left(\frac{1}{n^2}\right) \end{aligned} \quad (4.65)$$

Thus, we have agreement with  $N(k-1, n+1)$  for the first two orders:

$$\text{number of branes} = N(k-1, n+1)\left[1 + \mathcal{O}\left(\frac{1}{n^2}\right)\right] \quad (4.66)$$

#### 4.4 Symmetrised trace calculations

As we have seen, it is possible to view the fuzzy sphere matrices  $X_i$  as the transverse coordinates of the world-volume theory of a stack of  $D1$ -branes expanding into a stack of  $D(2k + 1)$ -branes. There is also a dual realisation of this system in which the  $D1$ -branes appear as a monopole in the world-volume theory of the  $D(2k + 1)$ -brane. One can use the ADHM construction to construct the Monopole dual to the fuzzy sphere transverse coordinates. If one takes the  $N(k, n)$ -dimensional fuzzy sphere matrices representing a stack of  $N(k, n)$   $D1$ -branes as ADHM data for a monopole then one naturally constructs a monopole defined on a stack of  $N(k - 1, n + 1)$   $D(2k + 1)$ -branes. Reassuringly when you then calculate the charge of the monopole you have just constructed you get the answer  $N(k, n)$ . This is a nice consistency check of the ADHM construction.

As demonstrated in the last section, it is also possible to calculate the charge of the fuzzy sphere transverse coordinates, by looking at the RR coupling, but in this case you do not get  $N(k - 1, n + 1)$  as you would hope,

$$\text{number of } D(2k + 1)\text{-branes} = N(k - 1, n + 1) \frac{\prod_{i=1}^{2k-1} (n + i)}{c^{k-\frac{1}{2}}} \quad (4.67)$$

but there is agreement for the first two orders in the large  $n$  expansion:

$$\text{number of } D(2k + 1)\text{-branes} = N(k - 1, n + 1) \left[ 1 + \mathcal{O}\left(\frac{1}{n^2}\right) \right] \quad (4.68)$$

We now consider this RR charge calculation more carefully. First we consider the  $k = 1$  case. Based on the ADHM construction we expect the number of  $D3$ -branes to be  $N(0, n + 1) = 1$ . However, equation (4.67) suggests:

$$\text{number of } D3\text{-branes} = \frac{n + 1}{c^{\frac{1}{2}}} \quad (4.69)$$

Suppose that the numerator in the above is correct, but that the denominator is correct only at large  $n$  and that it receives corrections at lower order to make the number of  $D3$ -branes exactly one. Then these corrections need to satisfy:

$$1 = (n + 1)(c^{-\frac{1}{2}} + x_1 c^{-\frac{3}{2}} + x_2 c^{-\frac{5}{2}} + \dots) \quad (4.70)$$

It is easy to show that we need  $x_1 = -\frac{1}{2}$  and  $x_2 = \frac{3}{8}$ , by Taylor expanding and using that  $c = n(n + 2)$  for  $k = 1$ . Therefore, we would like to have a group theoretic justification for the series:

$$c^{-\frac{1}{2}} - \frac{1}{2}c^{-\frac{3}{2}} + \frac{3}{8}c^{-\frac{5}{2}} + \dots \quad (4.71)$$

There exists a formula for the first three terms in the large  $n$  expansion of the  $k = 1$

symmetrised trace operator [140], namely

$$\frac{1}{N(1, n)} \text{Str}(X_i X_i)^m = c^m - \frac{2}{3} m(m-1) c^{m-1} + \frac{2}{45} m(m-1)(m-2)(7m-1) c^{m-2} + \dots \quad (4.72)$$

Now, if we make the choice  $m = -\frac{1}{2}$  in (4.72) we get precisely (4.71). However, this suggests that if this choice is correct, then we should have an all orders prediction for the action of the symmetrised trace operator. Thus, for  $k=1$  we predict that

$$\frac{1}{N(1, n)} \text{Str}(X_i X_i)^m \Big|_{m=-\frac{1}{2}} \simeq \frac{1}{(n+1)} \quad (4.73)$$

where for future reference we consider the left hand side to be equal to the symmetrised trace in a large- $n$  series expansion, as appeared in [140].

Checking the conjecture (4.73) beyond the first three terms in a straightforward fashion, by techniques similar to those employed in [140], proves difficult. This involves either adding up a large number of chord diagrams, or complicated combinatorics if one uses the highest weight method.

An alternative approach involves first writing down the conjecture based on brane counting for general  $k$ , since the methods of [140] turn out to generalise from the  $k=1$  to the general  $k$  case. The conjecture for general  $k$ , based on the brane counting, follow immediately from (4.67) is:

$$\frac{1}{N(k, n)} \text{Str}(X_i X_i)^m \Big|_{m=-k+\frac{1}{2}} \simeq \prod_{i=1}^{2k-1} \frac{1}{(n+i)} \quad (4.74)$$

Note that the right hand side of this equation appears in the factor outside the sum in (4.100) and (4.101). Notice also that the above expression concerns the large  $n$  expansion of the symmetrised trace considered at  $m = -k + \frac{1}{2}$ .

One can then repeat the  $k=1$  calculation of [140] for general  $k$ , to check the first three terms of this conjecture. The details of these chord diagram calculations appear in the next section. We first calculated  $\text{Str}(X_i X_i)^m$  for  $m=2, 3, 4$ . Then we find the first three terms in the symmetrised trace, large  $n$  expansion using these results. We can check that the conjecture (4.74) is true for the first three terms in the symmetrised trace large  $n$  expansion, for general  $k$  as well as for  $k=1$ .

As the first three terms of (4.74) matched for general  $k$ , we then performed the long calculation to check the fourth term in the expansion, for general  $k$ . This calculation involves evaluating  $\text{Str}(X_i X_i)^m$  for  $m=5, 6$ . The result of this calculation shows that there is also agreement for the fourth term in the large  $n$  expansion of (4.74).

## 4.4.1 Chord diagram calculations

In this section we calculate the  $\text{Str}(X_i X_i)^m$  quantity for  $m = 1, 2, 3, 4, 5, 6$ . The fuzzy two-sphere case  $k = 1$  appeared in [140] for  $m = 1, 2, 3, 4$ . Just as in [140] it is convenient to summarise the algebra involved in these calculation using chord diagrams. Chord diagrams are constructed from the following vertex description of a matrix.

$$(X_i)_{ab} = \begin{array}{c} i \\ | \\ \hline a \quad b \end{array}$$

Where  $i = 1, \dots, 2k + 1$  and  $a, b = 1, \dots, N$ . The chord diagrams are then made by joining legs corresponding to the the summed indices of the matrices. The circle round the outside of a chord diagram joins up the  $a, b$  type indices and the chords across the circle join  $i, j$  type indices. The simplest example of a chord diagram is the one with a single chord.

$$\begin{array}{c} \bullet \\ | \\ \circ \\ | \\ \bullet \end{array} = \text{tr}(X_i X_i) = cN \quad (4.75)$$

To calculate  $\text{Str}(X_i X_i)^m$  we need to calculate the chord diagrams with  $m$  chords. For  $m = 2$  there are just two of these diagrams. The simplest chord diagram with two chords is given by:

$$\begin{array}{c} \bullet \\ | \\ \circ \\ | \\ \bullet \end{array} = \text{tr}(X_i X_i X_j X_j) = c^2 N \quad (4.76)$$

To evaluate the other chord diagram with two chords the following identity is useful:

$$[X_i, X_j] X_j = 4k X_i \quad (4.77)$$

The second chord diagram with two chords is given by:

$$\begin{aligned} \begin{array}{c} \bullet \\ | \\ \circ \\ | \\ \bullet \end{array} &= \text{tr}(X_i X_j X_i X_j) \\ &= \text{tr}(X_i X_i, X_j X_j) - \text{tr}(X_i [X_i, X_j] X_j) \\ &= c^2 N - 4k \text{tr}(X_i X_i) \\ &= c^2 N - 4kcN \\ &= c(c - 4k)N \end{aligned} \quad (4.78)$$

Finally we need to find the multiplicity with which each chord diagram appears in the quantity  $\text{Str}(X_i X_i)^m$ . Using the cyclic property of the trace we do not have to consider the full set of  $(2m)!$  permutations of  $2m$  objects, but we can just consider strings of numbers which contain the numbers  $(1, 1, 2, 2, 3, 3, \dots, m, m)$  with a special type of ordering. For a given  $m$ , one writes down strings working from left to right using the rule that one is not

allowed to write down the first copy of the number  $j$  until at least one copy of each of the numbers less than  $j$  has been written down. For  $m = 2$  the set of these strings is:

$$\{(1122), (1212), (1221)\} \quad (4.79)$$

These strings of numbers are turned into chord diagrams by writing the numbers in the string round the outer circle of the chord diagram and joining the two copies of each number with a chord. The first string (1122) corresponds to the chord diagram (4.76). The second string (1212) corresponds to chord diagram (4.78) and the final string (1221) corresponds to another copy of the first chord diagram (4.76). Thus we have

$$\begin{aligned} \frac{1}{N} \text{Str}(X_i X_i)^2 &= \frac{1}{N} \left( \frac{2}{3} \left( \text{Chord Diagram 1} \right) + \frac{1}{3} \left( \text{Chord Diagram 2} \right) \right) \\ &= \frac{1}{N} \left( \frac{2}{3} c^2 N + \frac{1}{3} (c - 4k) c N \right) \\ &= c^2 - \frac{4}{3} k c \end{aligned} \quad (4.80)$$

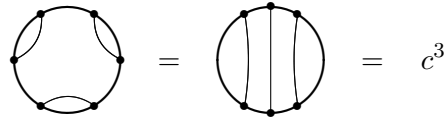
For  $k = 1$  this is in agreement with the calculations of [140].

The calculation of  $\text{Str}(X_i X_i)^m$  rapidly increases in complexity as  $m$  increases. For  $m = 3$  there are 5 different chord diagrams.



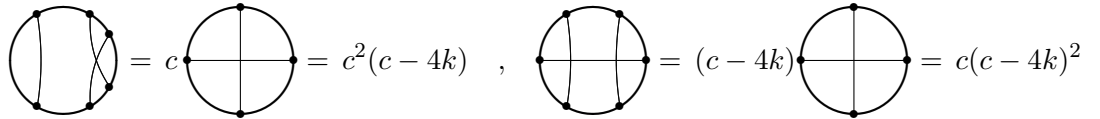
$$(4.81)$$

The first two diagrams are easily evaluated



$$= c^3$$

The third and fourth diagrams are evaluated using the identity (4.77):



$$= c \left( \text{Chord Diagram 4} \right) = c^2 (c - 4k) \quad , \quad \left( \text{Chord Diagram 3} \right) = (c - 4k) \left( \text{Chord Diagram 4} \right) = c (c - 4k)^2$$

To evaluate the final chord diagram we use the identity:

$$[X_k, [X_i, X_j]] = 4(\delta_{ki} X_j - \delta_{kj} X_i) \quad (4.82)$$

We evaluate the final star shaped chord diagram using the string of numbers notation

$$\begin{aligned} 123123 &= [1, 2]3123 + 213123 \\ &= [[1, 2], 3]123 + 3[1, 2]123 + 213123 \\ &= 4 \times (1122 - 2121) + 312123 - 321123 + 213123 \end{aligned} \quad (4.83)$$

In chord diagram notation the previous relation is:

$$\begin{aligned}
 \text{Diagram 1} &= 4 \text{Diagram 2} - 4 \text{Diagram 3} + \text{Diagram 4} - \text{Diagram 5} + \text{Diagram 6} \\
 &= c^3 - 12kc^2 + 16k(k+1)c
 \end{aligned}$$

We now calculate the multiplicity of these 5 chord diagrams in the  $\text{Str}(X_i X_i)^3$ . This involves the following 15 strings.

$$\begin{aligned}
 &\{(112233), (112323), (112332), (121233), (121323), \\
 &\quad (121332), (122133), (122313), (122331), (123123), \\
 &\quad (123132), (123231), (123213), (123312), (123321)\}
 \end{aligned} \tag{4.84}$$

Putting these calculations together yields the answer to  $\frac{1}{N}\text{Str}(X_i X_i)^3$ :

$$\begin{aligned}
 &= \frac{1}{N} \left( \frac{2}{15} \text{Diagram 1} + \frac{6}{15} \text{Diagram 2} + \frac{3}{15} \text{Diagram 3} + \frac{3}{15} \text{Diagram 4} + \frac{1}{15} \text{Diagram 5} \right) \\
 &= c^3 - 4kc^2 + \frac{16}{15}k(4k+1)c
 \end{aligned} \tag{4.85}$$

For  $m=4$  the calculation is much more tricky as there are 105 different strings and 18 different chord diagrams<sup>3</sup>. 11 of the 18 chord diagrams have one chord which does not cross any of the others. The contribution to  $\text{Str}(X_i X_i)^4$  from these diagrams is given by:

$$\begin{aligned}
 &= \frac{2}{105} \text{Diagram 1} + \frac{8}{105} \text{Diagram 2} + \frac{8}{105} \text{Diagram 3} + \frac{8}{105} \text{Diagram 4} \\
 &\quad + \frac{8}{105} \text{Diagram 5} + \frac{8}{105} \text{Diagram 6} + \frac{8}{105} \text{Diagram 7} + \frac{8}{105} \text{Diagram 8} \\
 &\quad + \frac{8}{105} \text{Diagram 9} + \frac{4}{105} \text{Diagram 10} + \frac{4}{105} \text{Diagram 11} \\
 &= \frac{14}{105}c^4 + \frac{28}{105}c^2 \text{Diagram 12} + \frac{24}{105}c \text{Diagram 13} + \frac{8}{105}c \text{Diagram 14}
 \end{aligned} \tag{4.86}$$

There are 4 chord diagrams in which all the chords cross at least one other chord, but there is at least one chord that crosses just a single other chord. These 4 diagrams can

<sup>3</sup>Thanks to Simon Nickerson for a computer program that computes the multiplicities of the various chord diagrams in the quantity  $\text{Str}(X_i X_i)^m$

be simplified using the identity (4.77). The contribution to  $\text{Str}(X_i X_i)^4$  from these 4 chord diagrams is given by:

$$\begin{aligned}
 &= \frac{4}{105} \text{CD}_1 + \frac{8}{105} \text{CD}_2 + \frac{8}{105} \text{CD}_3 + \frac{4}{105} \text{CD}_4 \\
 &= (c - 4k) \left( \frac{4}{105} \text{CD}_1 + \frac{8}{105} \text{CD}_2 + \frac{8}{105} \text{CD}_3 + \frac{4}{105} \text{CD}_4 \right) \quad (4.87)
 \end{aligned}$$

The 3 remaining chord diagrams can be evaluated using (4.82)

$$\begin{aligned}
 \text{CD}_1 &= 12314234 \\
 &= [1, 2]314234 + 21314234 \\
 &= [[1, 2], 3]14234 + 3[1, 2]14234 + 21314234 \\
 &= 4 \times (114224 - 214214) + 31214234 - 32114234 \\
 &= 4 \text{CD}_2 - 4 \text{CD}_3 + \text{CD}_4 - \text{CD}_5 + \text{CD}_6 \\
 &= 4c^3 + (c - 4(k + 1))(c^3 - 12kc^2 + 16k(k + 1)c) - 4kc(c - 4k)^2
 \end{aligned}$$

$$\begin{aligned}
 \text{CD}_2 &= 12314324 \\
 &= [1, 2]314324 + 21314324 \\
 &= [[1, 2], 3]14324 + 4[1, 2]14324 + 21314324 \\
 &= 4 \times (114224 - 214124) + 31214324 - 32114324 + 21314324 \\
 &= 4 \text{CD}_7 - 4 \text{CD}_8 + \text{CD}_4 - \text{CD}_5 + \text{CD}_6 \\
 &= 4c^3 - 4k(c^3 - 12kc^2 + 16k(k + 1)c) + c(c - 4(k + 1))(c - 4k)^2
 \end{aligned}$$

$$\begin{aligned}
 \text{CD}_3 &= 12341234 \\
 &= [1, 2]341234 + 21341234 \\
 &= [[1, 2], 3]41234 + 3[1, 2]41234 + 21341234 \\
 &= 4 \times (141224 - 241214) + 31241234 - 32141234 + 21341234 \\
 &= 4 \text{CD}_9 - 4 \text{CD}_8 + \text{CD}_4 - \text{CD}_7 + \text{CD}_6 \\
 &= 96kc^2 - 256ck^2 - 24kc^3 + c^4 + 112c^2k^2 - 128ck^3 - 64ck
 \end{aligned}$$

These last 3 chord diagrams appear in the quantity  $\text{Str}(X_i X_i)^4$  with multiplicity  $\frac{4}{105}$ ,  $\frac{2}{105}$  and  $\frac{1}{105}$  respectively.

The final answer for  $m=4$  is:

$$\frac{1}{N}\text{Str}(X_i X_i)^4 = c^4 - 8kc^3 + \frac{16}{5}k(7k+2)c^2 - \frac{64}{105}k(34k^2+24k+5)c \quad (4.88)$$

The cases  $m=5, 6$  are very long calculations. Instead of presenting the details we just present the answers<sup>4</sup>. For  $m=5$  there are 945 different strings and 105 different chord diagrams.

$$\begin{aligned} \frac{1}{N}\text{Str}(X_i X_i)^5 = & c^5 \\ & -\frac{40}{3}kc^4 \\ & +\frac{16}{3}(13k+4)kc^3 \\ & -\frac{64}{63}(158k^2+126k+31)kc^2 \\ & +\frac{256}{945}(496k^3+672k^2+344k+63)kc \end{aligned} \quad (4.89)$$

For  $m=6$  there are 10395 different strings and 902 different chord diagrams.

$$\begin{aligned} \frac{1}{N}\text{Str}(X_i X_i)^6 = & c^6 \\ & -20kc^5 \\ & +\frac{16}{3}(31k+10)kc^4 \\ & -\frac{64}{63}(677k^2+582k+157)kc^3 \\ & +\frac{256}{315}(1726k^3+2616k^2+1541k+336)kc^2 \\ & -\frac{1024}{10395}(11056k^4+24256k^3+22046k^2+9476k+1575)kc \end{aligned} \quad (4.90)$$

#### 4.4.2 The large $n$ expansion of $\text{Str}(X_i X_i)^m$

In this section we use the results of the previous section for specific values of  $m$  to calculate the first four terms in the large  $n$  expansion of  $\text{Str}(X_i X_i)^m$  for arbitrary  $m$ . The first three terms in the large  $n$  expansion of  $\text{Str}(X_i X_i)^m$  for arbitrary  $m$  and  $k=1$  appeared in [140]. The fourth term in the large  $n$  expansion and the generalisation of all these terms to  $k > 1$  which are calculated here are new results.

We guess that the coefficient of  $c^{m-i}$  term in  $\text{Str}(X_i X_i)^m$  is a polynomial in  $m$  of order  $2i$ , but we cannot prove this. If this is true, then we have the following simple ansatz involving polynomials where there are some known factors and some unknown factors. The

---

<sup>4</sup>Thanks to Simon Nickerson for a computer program that writes many of the six chord diagrams in terms of five chord diagrams

known factors in these polynomials come from the fact that the series has to terminate so that there are never negative powers of  $c$  for  $m = 1, 2, 3, \dots$ . The remaining unknown functions of  $k$  can then be found using the results from the last section of  $\text{Str}(X_i X_i)^m$  for  $m = 1, 2, 3, 4, 5, 6$ .

$$\begin{aligned} \frac{1}{N} \text{Str}(X_i X_i)^m &= c^m \\ &+ y_1(k) m(m-1) c^{m-1} \\ &+ (y_2(k)m + y_3(k)) m(m-1)(m-2) c^{m-2} \\ &+ (y_4(k)m^2 + y_5(k)m + y_6(k)) m(m-1)(m-2)(m-3) c^{m-3} \\ &+ \mathcal{O}(c^{m-4}) \end{aligned}$$

We now find the unknown functions  $y_1(k), y_2(k) \dots y_6(k)$  using the results of  $\text{Str}(X_i X_i)^m$  for  $m = 2, 3, 4, 5, 6$  calculated in the previous section. The answer for  $\text{Str}(X_i X_i)^2$  in (4.80) gives an equation for the unknown function  $y_1(k)$ .

$$y_1(k) = -\frac{2}{3}k \quad (4.91)$$

The calculations of  $\text{Str}(X_i X_i)^m$  for  $m = 3, 4$  give 2 equations for the unknowns  $y_2(k)$  and  $y_3(k)$ .

$$\begin{aligned} \mathcal{O}(c^1) \text{ term in (4.85)} \quad 3!(3y_2 + y_3) &= \frac{16}{15}k(4k+1) \\ \mathcal{O}(c^2) \text{ term in (4.88)} \quad 4!(4y_2 + y_3) &= \frac{16}{5}k(7k+2) \end{aligned}$$

The solution is

$$\begin{aligned} \begin{pmatrix} y_2 \\ y_3 \end{pmatrix} &= \begin{pmatrix} 3 & 1 \\ 4 & 1 \end{pmatrix}^{-1} \begin{pmatrix} \frac{8}{45}(4k+1)k \\ \frac{2}{15}(7k+2)k \end{pmatrix} \\ &= \frac{2}{45} \begin{pmatrix} (5k+2)k \\ (k-2)k \end{pmatrix} \end{aligned} \quad (4.92)$$

The calculation of  $\text{Str}(X_i X_i)^m$  for  $m = 4, 5, 6$  gives 3 equations for the unknowns  $y_4(k), y_5(k)$  and  $y_6(k)$ .

$$\begin{aligned} \mathcal{O}(c) \text{ term in (4.88)} \quad 4!(16y_4^2 + 4y_5 + y_6) &= -\frac{64}{105}(34k^2 + 24k + 5)k \\ \mathcal{O}(c^2) \text{ term in (4.89)} \quad 5!(25y_4^2 + 5y_5 + y_6) &= -\frac{64}{63}(158k^2 + 126k + 31)k \\ \mathcal{O}(c^3) \text{ term in (4.90)} \quad \frac{6!}{2}(36y_4^2 + 6y_5 + y_6) &= -\frac{64}{63}(677k^2 + 582k + 157)k \end{aligned}$$

So we need to calculate:

$$\begin{pmatrix} y_4 \\ y_5 \\ y_6 \end{pmatrix} = \begin{pmatrix} 16 & 4 & 1 \\ 25 & 5 & 1 \\ 36 & 6 & 1 \end{pmatrix}^{-1} \begin{pmatrix} -\frac{8}{315}(34k^2 + 24k + 5)k \\ -\frac{8}{945}(158k^2 + 126k + 31)k \\ -\frac{8}{2835}(677k^2 + 582k + 157)k \end{pmatrix}$$

The solution is

$$\begin{pmatrix} y_4 \\ y_5 \\ y_6 \end{pmatrix} = \frac{1}{2835} \begin{pmatrix} (-140k^2 - 168k - 64)k \\ (-84k^2 + 216k + 192)k \\ (128k^2 + 96k - 104)k \end{pmatrix} \quad (4.93)$$

It is now easy to check the original conjecture (4.74). The left hand side of (4.74) involves the large  $n$  expansion of  $\text{Str}(X_i X_i)^m$  evaluated at  $m = -k + \frac{1}{2}$ . Thus, the first three terms in the left had side of (4.74) are:

$$\frac{1}{N} \text{Str}(X_i X_i)^m \Big|_{m=-k+1/2} = c^{-k+\frac{1}{2}} \sum_{j=0}^{\infty} \frac{f_j}{c^j}$$

where the coefficients  $f_1, f_2$  and  $f_3$  are given explicitly by:

$$\begin{aligned} f_1 &= y_1(k)m(m-1) \Big|_{m=-k+\frac{1}{2}} \\ &= -\frac{2}{3}k\left(k-\frac{1}{2}\right)\left(k+\frac{1}{2}\right) \\ f_2 &= \left(y_2(k)m + y_3(k)\right)m(m-1)(m-2) \Big|_{m=-k+\frac{1}{2}} \\ &= \frac{1}{45}(10k^2 - 3k + 2)k\left(k-\frac{1}{2}\right)\left(k+\frac{1}{2}\right)\left(k+\frac{3}{2}\right) \\ f_3 &= \left(y_4(k)m^2 + y_5(k)m + y_6(k)\right)m(m-1)(m-2)(m-3) \Big|_{m=-k+\frac{1}{2}} \\ &= \frac{1}{2835}(-24 + 34k - 61k^2 + 56k^3 - 140k^4) \\ &\quad \times \left(k-\frac{1}{2}\right)\left(k+\frac{1}{2}\right)\left(k+\frac{3}{2}\right)\left(k+\frac{5}{2}\right) \end{aligned} \quad (4.94)$$

To check (4.74) we must expand the right hand side of (4.74) as a function of  $c$ :

$$\prod_{l=1}^{2k-1} \frac{1}{n+l} = \frac{1}{\sqrt{(k^2+c)}} \prod_{l=1}^{k-1} \frac{1}{c+2kl-l^2} = c^{-k+\frac{1}{2}} \sum_{j=0}^{\infty} \frac{g_j}{c^j} \quad (4.95)$$

where the coefficients  $g_j$  are easily calculated and given by:

$$\begin{aligned} g_1 &= -\frac{2}{3}k\left(k-\frac{1}{2}\right)\left(k+\frac{1}{2}\right) \\ g_2 &= \frac{1}{45}(10k^2 - 3k + 2)k\left(k-\frac{1}{2}\right)\left(k+\frac{1}{2}\right)\left(k+\frac{3}{2}\right) \\ g_3 &= \frac{1}{2835}(-24 + 34k - 61k^2 + 56k^3 - 140k^4) \\ &\quad \times k\left(k-\frac{1}{2}\right)\left(k+\frac{1}{2}\right)\left(k+\frac{3}{2}\right)\left(k+\frac{5}{2}\right) \end{aligned} \quad (4.96)$$

Thus there is precise agreement between the coefficients  $f_j$  in and  $g_j$ , so equation (4.74) holds for the first three terms.

## 4.4.3 An exact formula for the symmetrised trace

The simple answer for the symmetrised trace in (4.74) is totally hidden by the complexity of the chord diagram calculations. This suggested that the general formula for the symmetrised trace could also be simple. By looking at the result of  $\text{Str}(X_i X_i)^m$  for  $m = 1, 2, 3, 4, 5, 6$  calculated in the previous section and setting  $k = 1$  it is easy to come up with a simple guess for the answer:

$$\frac{1}{N} \text{Str}(X_i X_i)^m = \begin{cases} \frac{2(2m+1)}{n+1} \sum_{i=1}^{\frac{n}{2}} (2i)^{2m} & \text{for } n \text{ even} \\ \frac{2(2m+1)}{n+1} \sum_{i=1}^{\frac{n+1}{2}} (2i-1)^{2m} & \text{for } n \text{ odd} \end{cases} \quad (4.97)$$

Unfortunately we have been unable to prove this formula. However, this formula agrees with the chord diagram calculations from the last chapter which is a good check. The existence of a systematic construction of the symmetrised trace was anticipated on page 9 of [104].

The formula (4.97) is remarkable because, for example, it reduces the long calculations of the large  $n$  expansion in [140] and the last section of this thesis to a very simple expansion based on the Euler Maclaurin formula. The Euler Maclaurin formula approximates a sum by an integral, plus an infinite series of corrections involving the Bernoulli numbers  $B_{2i}$ :

$$\begin{aligned} \sum_{i=1}^p f(i) &= \int_0^{p+1} dx f(x) - \frac{1}{2} (f(p+1) + f(0)) \\ &+ \sum_{i=1}^j \frac{1}{(2i)!} B_{2i} (f^{(2i-1)}(p+1) - f^{(2i-1)}(0)) \\ &- \frac{1}{(2j)!} \int_0^1 dx B_{2j}(x) \sum_{\nu=0}^p f^{(2j)}(x+\nu) \end{aligned} \quad (4.98)$$

We now use this formula and the guess (4.97) to calculate the large  $n$  expansion of the symmetrised trace:

$$\begin{aligned} \frac{1}{N} \text{Str}(X_i X_i)^m &= \frac{n^{2m+1}}{n+1} \left[ \left(1 + \frac{2}{n}\right)^{2m+1} - (2m+1) \frac{1}{n} \left(1 + \frac{2}{n}\right)^{2m} \right. \\ &+ \frac{1}{3} (2m+1)(2m) \frac{1}{n^2} \left(1 + \frac{2}{n}\right)^{2m-1} \\ &\left. - \frac{1}{45} (2m+1)(2m)(2m-1)(2m-2) \frac{1}{n^4} \left(1 + \frac{2}{n}\right)^{2m-3} + \dots \right] \end{aligned} \quad (4.99)$$

This expansion in  $n$  can easily be rewritten in terms of  $c = n(n+2k)$  to reproduce the

functions  $y_i(k)$ , which were calculated in the last section. Calculating the terms of the expansion in this way is far simpler than performing the chord diagram calculations. The agreement of the answer (4.99) with the chord diagram answer is convincing evidence that the guess (4.97) is true.

This success of the guess (4.97) for the case  $k = 1$  led the following guess for  $k \geq 1$ . The formula for the symmetrised trace for all  $m, k$  and  $n$  even is:

$$\frac{1}{N} \text{Str}(X_i X_i)^m = \frac{2^k \prod_{i_1=1}^k (2m - 1 + 2i_1)}{(k-1)! \prod_{i_2=1}^{2k-1} (n + i_2)} \sum_{i_3=1}^{\frac{n}{2}} \left[ \prod_{i_4=1}^{k-1} \left( \left( \frac{n}{2} + i_4 \right)^2 - i_3^2 \right) (2i_3)^{2m} \right] \quad (4.100)$$

where the  $k = 1$  case is given above (in this case the product over  $i_4 = 1, \dots, k - 1$  is just defined to be the number 1).

Similarly for all  $m, k$  and  $n$  odd we have:

$$\frac{1}{N} \text{Str}(X_i X_i)^m = \frac{2^k \prod_{i_1=1}^k (2m - 1 + 2i_1)}{(k-1)! \prod_{i_2=1}^{2k-1} (n + i_2)} \sum_{i_3=1}^{\frac{n+1}{2}} \left[ \prod_{i_4=1}^{k-1} \left( \left( \frac{n}{2} + i_4 \right)^2 - \left( i_3 - \frac{1}{2} \right)^2 \right) (2i_3 - 1)^{2m} \right] \quad (4.101)$$

This formula can again be checked against the chord diagram calculations. In the next chapter we will use the formula (4.97) to study the collapse of a fuzzy spheres.

# CHAPTER 5

## FINITE $N$ EFFECTS ON THE COLLAPSE OF FUZZY SPHERES

### 5.1 Introduction

A new formula for the symmetrised trace was presented in the last Chapter. In this chapter we use this new formula to study the finite  $n$  effects on the collapse of a spherical bound state of  $D0$ -branes described by a fuzzy sphere. The symmetrised trace prescription for the non-Abelian action of multiple  $D0$ -branes was proposed in [141] and extended to include background RR fluxes in [109]. An interesting time dependent system, in which the need for an exact prescription arises, is a spherical bound state of  $N$   $D0$ -branes with a spherical  $D2$ -brane, for finite values of  $N$ . This can be studied both from the point of view of the Abelian  $D2$  DBI action and the non-Abelian  $D0$ -DBI action. The latter configuration also has an M-theory analogue, that of a time dependent spherical  $M2$ -brane, which has been studied in the context of matrix theory [143, 144]. In [140] it was shown that the  $D0$ -brane construction, based on the fuzzy 2-sphere, agrees with the Abelian  $D2$ -construction at large  $N$ .  $1/N$  corrections coming from the symmetrised trace and a finite  $N$  example were also studied. Here we develop further the study of finite  $N$ . The need for the non-linear DBI action as opposed to the Yang-Mills limit of the lower dimensional brane was recognised in a spatial  $D1 \perp D3$  analog of the  $D0 - D2$  system [104].

In this chapter we extend the calculation of symmetrised traces from the spin half example of [140] to general representations of  $SO(3)$ . These results allow us to study in detail the finite  $N$  physics of the time-dependent fuzzy two-sphere. We begin our finite  $N$  analysis with a careful discussion on how to extract the physical radius from the matrices of the non-Abelian ansatz. The standard formula used in the Myers effect is  $R^2 = \text{Tr}(\Phi_i \Phi_i)/N$ . Requiring consistency with a constant speed of light, independent of  $N$ , leads us to propose an equation in section 5.2, which agrees with the standard formula in large  $N$  commutative limits, but disagrees in general. Section 5.3 gives finite  $N$  formulae for the energy and Lagrangian of the time-dependent fuzzy two-sphere. We also give the conserved pressure which is relevant for the  $D1 \perp D3$  system. In section 4, we study the time of collapse as a function of  $N$ . In the region of large  $N$ , for fixed initial radius  $R_0$ , the time decreases as  $N$  decreases. However, at some point there is a turn-around in this trend and the time of collapse for spin half is actually larger than at large  $N$ . We also investigate the quantity

$E^2 - p^2$ , where  $E$  is the energy and  $p$  the momentum. This quantity is of interest when we view the time-dependent  $D$ -brane as a source for space-time fields.  $E$  is the  $T^{00}$  component of the stress tensor, and  $p$  is the  $T^{0r}$  component as we show by a generalisation of arguments previously used in the context of BFSS matrix theory. For the large  $N$  formulae,  $E^2 - p^2$  is always positive. At finite  $N$ , this can be negative, although the speed of radial motion is less than the speed of light. Given the relation to the stress tensor, we can interpret this as a violation of the dominant energy condition. The other object of interest is the proper acceleration along the trajectory of a collapsing  $D2$ -brane. We find analytic and numerical evidence that there are regions of both large  $R$  and small  $R$ , with small and relativistic velocities respectively, where the proper accelerations can be small. This is intriguing since the introduction of stringy and higher derivative effects in the small velocity region can be done with an adiabatic approximation, but it is interesting to consider approximation methods for the relativistic region.

In section 5.5, we discuss the higher fuzzy sphere case [115, 116, 118, 145–149]. We give a general formula for  $\text{STr}(X_i X_i)^m$ , in general irreducible, representations of  $SO(2k+1)$ . This formula is motivated by some considerations surrounding  $D$ -brane charges and the ADHM construction, which were discussed in more detail in the previous chapter. This allows us a partial discussion of finite  $N$  effects for higher fuzzy spheres. We are able to calculate the physical radius following the argument of section 5.2; however, in general one needs other symmetrised traces involving elements of the Lie algebra  $SO(2k+1)$ .

The symmetrised trace prescription, which we study in detail in this paper, is known to correctly match open string calculations up to the first two orders in an  $\alpha'$  expansion, but the correct answer deviates from the  $(\alpha')^3$  term onwards [150–153]. It is possible however that for certain special symmetric background configurations, it may give the correct physics to all orders. The  $D$ -brane charge computation discussed in the last chapter can perhaps be viewed as a possible indication in this direction. In any case, it is important to study the corrections coming from this prescription to all orders, in order to be able to systematically modify it, if that becomes necessary when the correct non-Abelian  $D$ -brane action is known. Conversely the physics of collapsing  $D$ -branes can be used to constrain the form of the non-Abelian Dirac-Born-Infeld action.

## 5.2 Lorentz invariance and the physical radius

We will study the collapse of a cluster of  $N$   $D0$ -branes in the shape of a fuzzy  $S^{2k}$ , in a flat background. This configuration is known to have a large- $N$  dual description in terms of spherical  $D(2k)$  branes with  $N$  units of flux. The microscopic  $D0$  description can be obtained from the non-Abelian action for a number of coincident branes, proposed

in [109, 141]

$$S_0 = -\frac{1}{g_s \ell_s} \int dt \text{STr} \sqrt{-\det(M)}, \quad (5.1)$$

where

$$M = \begin{pmatrix} -1 & \lambda \partial_t \Phi_j \\ -\lambda \partial_t \Phi_i & Q_{ij} \end{pmatrix}. \quad (5.2)$$

Here  $a, b$  are world-volume indices, the  $\Phi$ 's are world-volume scalars,  $\lambda = 2\pi \ell_s^2$  and

$$Q_{ij} = \delta_{ij} + i\lambda[\Phi_i, \Phi_j]. \quad (5.3)$$

We will consider the time dependent ansatz

$$\Phi_i = \hat{R}(t) X_i, \quad (5.4)$$

The  $X_i$  are matrices obeying some algebra. The part of the action that depends purely on the time derivatives and survives when  $\hat{R} = 0$  is

$$S_{D0} = \int dt \text{STr} \sqrt{1 - \lambda^2 (\partial_t \Phi_i)^2} = \int dt \text{STr} \sqrt{1 - \lambda^2 (\partial_t \hat{R})^2 X_i X_i}. \quad (5.5)$$

For the fuzzy  $S^2$ , the  $X_i = \alpha_i$ , for  $i = 1, 2, 3$ , are generators of the irreducible spin  $n/2$  matrix representation of  $su(2)$ , with matrices of size  $N = n + 1$ . In this case the algebra is

$$[\alpha_i, \alpha_j] = 2i\epsilon_{ijk} \alpha_k \quad (5.6)$$

and following [140], the action for  $N$  D0-branes can be reduced to

$$S_0 = -\frac{1}{g_s \ell_s} \int dt \text{STr} \sqrt{1 + 4\lambda^2 \hat{R}^4 \alpha_i \alpha_i} \sqrt{1 - \lambda^2 (\partial_t \hat{R})^2 \alpha_i \alpha_i}. \quad (5.7)$$

If we define the physical radius using

$$R_{phys}^2 = \lambda^2 \lim_{m \rightarrow \infty} \frac{\text{STr}(\Phi_i \Phi_i)^{m+1}}{\text{STr}(\Phi_i \Phi_i)^m} = \lambda^2 \hat{R}^2 \lim_{m \rightarrow \infty} \frac{\text{STr}(\alpha_i \alpha_i)^{m+1}}{\text{STr}(\alpha_i \alpha_i)^m}, \quad (5.8)$$

we will find that the Lagrangian will be convergent for speeds between 0 and 1. The radius of convergence will be exactly one - this follows by applying the ratio test to the series expansion of

$$\text{STr} \sqrt{1 - \lambda^2 \dot{\hat{R}}^2 \alpha_i \alpha_i}, \quad (5.9)$$

where a dot indicates differentiation with respect to time. This leads to

$$R_{phys}^2 = \lambda^2 \hat{R}^2 n^2. \quad (5.10)$$

Using explicit formulae for the symmetrised traces we will also see that, with this definition of the physical radius, the formulae for the Lagrangian and energy will have a first singularity at  $\dot{R}_{phys} = 1$ . In the large  $n$  limit, the definition of physical radius in (5.10) agrees with [109], where  $R_{phys}$  is defined by  $R_{phys}^2 = \frac{1}{N} Tr \Phi_i \Phi_i$ . Note that this definition of the physical radius will also be valid for the higher dimensional fuzzy spheres, and more generally in any matrix construction, where the terms in the non-Abelian DBI action depending purely on the velocity, are of the form  $\sqrt{1 - \lambda^2 X_i X_i (\partial_t \hat{R})^2}$ .

In what follows, the sums we get in expanding the square root are conveniently written in terms of  $r, s$ , defined by  $r^4 = 4\lambda^2 \hat{R}^4$  and  $s^2 = \lambda^2 \hat{R}^2$ . It is also useful to define

$$\begin{aligned} L^2 &= \frac{\lambda n}{2}, \\ \hat{r}^2 &= \frac{R_{phys}^2}{L^2} = r^2 n, \\ \hat{s}^2 &= s^2 n^2. \end{aligned} \tag{5.11}$$

The  $\hat{r}$  and  $\hat{s}$  variables approach the variables called  $r, s$  in the large  $n$  discussion of [140]. Note, using (5.10), that

$$\dot{R}_{phys}^2 = s^2 n^2 = \hat{s}^2 \tag{5.12}$$

### 5.3 The fuzzy $S^2$ at finite $n$

For the fuzzy  $S^2$ , the relevant algebra is that of  $su(2)$ , equation (5.6) above. We also have the Casimir

$$c = \alpha_i \alpha_i = (N^2 - 1),$$

where the last expression gives the value of the Casimir in the  $N$ -dimensional representation where  $N = n + 1$ , and  $n$  is related to the spin  $J$  by  $n = 2J$ .

We present here the result of the full evaluation of the symmetrised trace for odd  $n$

$$C(m, n) \equiv \frac{1}{n+1} STr(\alpha_i \alpha_i)^m = \frac{2(2m+1)}{n+1} \sum_{i=1}^{(n+1)/2} (2i-1)^m, \tag{5.13}$$

whilst for even  $n$

$$C(m, n) \equiv \frac{1}{n+1} STr(\alpha_i \alpha_i)^m = \frac{2(2m+1)}{n+1} \sum_{i=1}^{n/2} (2i)^m. \tag{5.14}$$

For  $m = 0$  the second expression doesn't have a correct analytic continuation and we will impose the value  $STr(\alpha_i \alpha_i)^0 = 1$ . The expression for  $C(m, 1)$  was proved in [140]. A proof of (5.14) for  $n = 2$  is given in Appendix C. The general formulae given above are

conjectured on the basis of various examples, together with arguments related to  $D$ -brane charges. These were given in the last chapter. There is also a generalisation to the case of higher dimensional fuzzy spheres, described in section 5.6.

We will now use the results (5.13), (5.14), to obtain the symmetrised trace corrected energy for a configuration of  $N$  time dependent  $D0$ -branes blown up to a fuzzy  $S^2$ . The reduced action (5.7) can be expanded to give

$$\begin{aligned}\mathcal{L} &= -STr\sqrt{1+4\lambda^2\hat{R}^4\alpha_i\alpha_i}\sqrt{1-\lambda^2\dot{\hat{R}}^2\alpha_i\alpha_i} \\ &= -STr\sqrt{1+r^4\alpha_i\alpha_i}\sqrt{1-s^2\alpha_i\alpha_i}\end{aligned}\quad (5.15)$$

$$= -STr\sum_{m=0}^{\infty}\sum_{l=0}^{\infty}s^{2m}r^{4l}(\alpha_i\alpha_i)^{m+l}\binom{1/2}{m}\binom{1/2}{l}(-1)^m.\quad (5.16)$$

The expression for the energy then follows directly -

$$\mathcal{E} = -STr\sum_{m=0}^{\infty}\sum_{l=0}^{\infty}s^{2m}r^{4l}(2m-1)(\alpha_i\alpha_i)^{m+l}\binom{1/2}{m}\binom{1/2}{l}(-1)^m,\quad (5.17)$$

and after applying the symmetrised trace results given above we get the finite- $n$  corrected energy for any finite-dimensional irreducible representation of spin- $\frac{n}{2}$  for the fuzzy  $S^2$ .

For  $n = 1, 2$  one finds

$$\frac{1}{2}\mathcal{E}_{n=1}(r, s) = \frac{1+2r^4-r^4s^2}{\sqrt{1+r^4(1-s^2)^{3/2}}},\quad (5.18)$$

$$\frac{1}{3}\mathcal{E}_{n=2}(r, s) = \frac{2}{3}\frac{(1+8r^4-16r^4s^2)}{\sqrt{1+4r^4(1-4s^2)^{3/2}}} + \frac{1}{3}.\quad (5.19)$$

We note that both of these expressions provide equations of motion which are solvable by solutions of the form  $\hat{r} = t$ .

For the case of general  $n$ , it can be checked that the energy can be written

$$\mathcal{E}_n(r, s) = \sum_{l=1}^{\frac{n+1}{2}} \frac{2-2(2l-1)^2r^4((2l-1)^2s^2-2)}{\sqrt{1+(2l-1)^2r^4(1-(2l-1)^2s^2)^{3/2}}},\quad (5.20)$$

for  $n$ -odd, while for  $n$  even

$$\mathcal{E}_n(r, s) = 1 + \sum_{l=1}^{\frac{n}{2}} \frac{2-2(2l)^2r^4((2l)^2s^2-2)}{\sqrt{1+(2l)^2r^4(1-(2l)^2s^2)^{3/2}}}.\quad (5.21)$$

Equivalently, the closed form expression for the Lagrangian for  $n$ -odd is

$$\mathcal{L}_n(r, s) = -2 \sum_{l=1}^{\frac{n+1}{2}} \frac{1 - 2(2l-1)^2 s^2 + (2l-1)^2 r^4 (2 - 3(2l-1)^2 s^2)}{\sqrt{1 + (2l-1)^2 r^4} \sqrt{1 - (2l-1)^2 s^2}}, \quad (5.22)$$

whilst for  $n$ -even

$$\mathcal{L}_n(r, s) = -1 - 2 \sum_{l=1}^{\frac{n}{2}} \frac{1 - 2(2l)^2 s^2 + (2l)^2 r^4 (2 - 3(2l)^2 s^2)}{\sqrt{1 + (2l)^2 r^4} \sqrt{1 - (2l)^2 s^2}}. \quad (5.23)$$

It is clear from these expressions that the equations of motion in the higher spin case will also admit the  $\hat{r} = t$  solution. Note that, after performing the rescaling to physical variables (5.11) and (5.12), these energy functions and Lagrangians have no singularity for fixed  $r$ , in the region  $0 \leq \dot{R}_{phys} \leq 1$ . As  $s$  increases from 0 the first singularity is at  $s = \frac{1}{n}$ , which corresponds to  $\hat{s} = \dot{R}_{phys} = 1$ . In this sense they are consistent with a fixed speed of light. However, they do not involve, for fixed  $r$ , the form  $\sqrt{dt^2 - dr^2}$  and hence do not have an  $so(1,1)$  symmetry. It will be interesting to see if there are generalisations of  $so(1,1)$ , possibly involving non-linear transformations of  $dt, dr$ , which can be viewed as symmetries.

### 5.3.1 The $D1 \perp D3$ intersection at finite- $n$

The static  $D1 \perp D3$  system consists of a set of  $N$   $D$ -strings ending on an orthogonal  $D3$  [104]. Far away from the intersection, the valid description is in terms of the non-abelian  $D1$ -brane worldvolume action, describing a funnel of increasing fuzzy- $S^2$  cross-section. The abelian  $D3$  worldvolume picture is valid close to the intersection, describing a BPS magnetic monopole with its Higgs field interpreted as an infinite spike transverse to the brane. In the large- $N$  limit the two descriptions overlap significantly.

The relationship between the microscopic descriptions of the time dependent  $D0 - D2$  system and the static  $D1 \perp D3$  intersection was established in [154]. In that paper, the large- $n$  behaviour of both systems was described by a genus one Riemann surface, which is a fixed orbit in complexified phase space. This was done by considering the conserved energy and pressure and complexifying the variables  $r$  and  $\partial r = s$  respectively. Conservation of the energy-momentum tensor then yielded elliptic curves in  $r, s$ , involving a fixed parameter  $r_0$ , which corresponded to the initial radius of the configuration. The actions for the two systems were related by a Wick rotation.

We can apply the symmetrised trace formula to also get exact results for the corrected pressure of the fuzzy- $S^2$  funnel configuration at finite- $n$ . For our system we simply display

the general result and the first two explicit cases

$$\mathcal{P} = STr \sum_{m=0}^{\infty} \sum_{l=0}^{\infty} s^{2m} r^{4l} (2m-1) (\alpha_i \alpha_i)^{m+l} \binom{1/2}{m} \binom{1/2}{l} \quad (5.24)$$

$$\frac{1}{2} \mathcal{P}_{n=1}(r, s) = -\frac{1 + 2r^4 + r^4 s^2}{\sqrt{1 + r^4} (1 + s^2)^{3/2}} \quad (5.25)$$

$$\frac{1}{3} \mathcal{P}_{n=2}(r, s) = -\frac{2}{3} \frac{(1 + 8r^4 + 16r^4 s^2)}{\sqrt{1 + 4r^4} (1 + 4s^2)^{3/2}} - \frac{1}{3}. \quad (5.26)$$

Note that the above formulae are related to the energies in (5.18) and (3.7) by a Wick rotation  $s \rightarrow is$ . Similar results to those for the time dependent case hold for the exact expression of the pressure for the general spin- $\frac{n}{2}$  representation. Note again that these expressions will provide equations of motion which are solved by solutions of the form  $\hat{r} = 1/\sigma$ , where  $\sigma$  is the spatial  $D1$  worldvolume coordinate. An easy way to see this is to substitute  $s^2 = r^4$  in (5.25), (5.26), to find that the pressures becomes independent of  $r$  and  $s$ . Since the higher spin results for the pressure are sums of the  $n = 1$  or  $n = 2$  cases, the argument extends.

### 5.3.2 Finite $N$ dynamics as a quotient of free multi-particle dynamics

Using the formulae above, we can see that the fuzzy  $S^2$  energy for general  $n$  is determined by the energy at  $n = 1$ . In the odd  $n$  case

$$C(m, n) = \frac{2}{n+1} C(m, 1) \sum_{i_3=1}^{\frac{n+1}{2}} (2i_3 - 1)^{2m} = \frac{2}{n+1} (2m+1) \sum_{i_3=1}^{\frac{n+1}{2}} (2i_3 - 1)^{2m}.$$

Using this form for  $C(m, n)$  in the derivation of the energy, we get

$$\mathcal{E}_n(r, s) = \sum_{i_3=1}^{\frac{n+1}{2}} \mathcal{E}_{n=1} \left( r \sqrt{(2i_3 - 1)}, s(2i_3 - 1) \right). \quad (5.27)$$

Similarly, in the even  $n$  case, we find

$$\mathcal{E}_n(r, s) = \sum_{i_3=1}^{\frac{n}{2}} \mathcal{E}_{n=2}(r\sqrt{i_3}, s(i_3)). \quad (5.28)$$

It is also possible to write  $C(m, 2)$  in terms of  $C(m, 1)$  as (for  $m \neq 0$ )

$$C(m, 2) = \frac{2^{2m+1}}{3} C(m, 1) = \frac{2^{2m+1}}{3} (2m+1). \quad (5.29)$$

Thus we can write  $\mathcal{E}_n(r, s)$ , for even  $n$ , in terms of the basic  $\mathcal{E}_{n=1}(r, s)$  as

$$\mathcal{E}_n(r, s) = 1 + \sum_{i_3=1}^{\frac{n}{2}} \mathcal{E}_{n=1}(r\sqrt{(2i_3)}, s(2i_3)). \quad (5.30)$$

These expressions for the energy of spin  $n/2$  can be viewed as giving the energy in terms of a quotient of a multi-particle system, where the individual particles are associated with the spin half system. For example, the energy function for  $(n+1)/2$  free particles with dispersion relation determined by  $\mathcal{E}_{n=1}$  is  $\sum_i \mathcal{E}_{n=1}(r_i, s_i)$ . By constraining the particles by  $r_i = r\sqrt{2i+1}, s_i = s(2i+1)$  we recover precisely (5.27).

We can now use this result to resolve a question raised by [140] on the exotic bounces seen in the Lagrangians obtained by keeping a finite number of terms in the  $1/n$  expansion. With the first  $1/n$  correction kept, the bounce appeared for a class of paths involving high velocities with  $\gamma = \frac{1}{\sqrt{1-s^2}} \sim c^{1/4}$ , near the limit of validity of the  $1/n$  expansion. The bounce disappeared when two orders in the expansion were kept. It was clear that whether the bounces actually happened or not could only be determined by finite  $n$  calculations. These exotic bounces would be apparent in constant energy contour plots for  $r, s$  as a zero in the first derivative  $\partial r/\partial s$ . In terms of the energies, this translates into the presence of a zero of  $\partial E/\partial s$  for constant  $r$ . It is easy to show from the explicit forms of the energies that these quantities are strictly positive for  $n=1$  and  $n=2$ . Since the energy for every  $n$  can be written in terms of these, we conclude that there are no bounces for any finite  $n$ . This resolves the question raised in [140] about the fate at finite  $n$  of these bounces.

We note that the large- $n$  limit of the formula for the energy provides us with a consistency check. In the large  $n$ -limit the sums above become integrals. For the odd- $n$  case (even- $n$  can be treated in a similar fashion), define  $x = \frac{2i_3-1}{n} \sim \frac{2i_3}{n}$ . Then the sum in (5.27) goes over to the integral

$$\frac{n}{2} \int_0^1 dx \frac{2 - 2x^2 n^2 r^4 (x^2 n^2 s^2 - 2)}{\sqrt{1 + x^2 n^2 r^4 (1 - x^2 s^2)}^{3/2}} = \frac{n\sqrt{1 + r^4 n^2}}{\sqrt{1 - s^2 n^2}}. \quad (5.31)$$

By switching to the  $\hat{r}, \hat{s}$  parameters the energy can be written as  $\frac{n\sqrt{1+\hat{r}^4}}{\sqrt{1-\hat{s}^2}}$ . This matches exactly the large  $n$  limit used in [140].

## 5.4 Physical properties of the finite $N$ solutions

### 5.4.1 Special limits where finite $n$ and large $n$ formulae agree

In the above we compared the finite  $n$  formula with the large  $n$  limit. Here we consider the comparison between the fixed  $n$  formula and the large  $n$  one in some other limits. On physical grounds we expect some agreement. The  $D0 - D2$  system at large  $\hat{r}$  and small

velocity  $\hat{s}$  is expected to be correctly described by the  $D2$  equations. These coincide with the large  $n$  limit of the  $D0$ . In the  $D1 \perp D3$  system, the large  $\hat{r}$  limit with large imaginary  $\hat{s}$  is also described by the  $D3$ .

Such an argument should extend to the finite- $n$  case. In [154], these systems were simply described by a genus one Riemann surface. However, in this case the energy functions are more complicated and the resulting Riemann surfaces are of higher genus. We still expect the region of the finite  $n$  curve, with large  $r$  and small, real  $s$ , to agree with the same limit of the large  $n$  curve. We also expect the region of large  $r$  and large imaginary  $s$  to agree with large  $n$ .

For concreteness consider odd  $n$ . Indeed for large  $r$ , small  $s$ , (5.20) gives

$$\sum_{l=1}^{\frac{n+1}{2}} 4(2l-1)r^2 \sim n^2 r^2 = n\hat{r}^2 \quad (5.32)$$

This agrees with the result obtained from the  $D2$ -brane Lagrangian [140] using (5.11) and (5.12). In this limit, both the genus one curve and the high genus finite  $n$  curves degenerate to a pair of points. Now consider the energy functions in the limit of large  $\hat{r}$  and large imaginary  $\hat{s}$ . This is the right regime for comparison with the  $D1 \perp D3$  system since this is described, at large  $n$  and in the region of large  $\hat{r}$ , by  $\hat{r} \sim \frac{1}{\sigma}$ . This means that  $\hat{r}$  is large at small  $\sigma$ , where  $\frac{d\hat{r}}{d\sigma} \rightarrow i\hat{s}$  is large. Using the Wick rotation  $s \rightarrow is$  (which takes us from the time-dependent system to the space-dependent system)

$$\mathcal{E} \rightarrow \mathcal{P} \sim \frac{nr^2}{s} = n\frac{\hat{r}^2}{\hat{s}}, \quad (5.33)$$

which agrees with the same limit of the large  $n$  curve. In this limit, both the large  $n$  genus one curve and the finite  $n$  curves of large genus degenerate to a genus zero curve.

The agreement in (5.32) between the  $D0$  and  $D2$  pictures is a stringy phenomenon. It follows from the fact that there is really one system, a bound state of  $D0$  and  $D2$  branes. A boundary conformal field theory would have boundary conditions that encode the presence of both the  $D0$  and  $D2$ . In the large  $N$  limit, the equations of motion coming from the  $D0$ -effective action agree with the  $D2$ -effective action description at all  $R_{phys}$ . This is because at large  $N$  it is possible to specify a DBI-scaling where the regime of validity of both the  $D0$  and  $D2$  effective actions extends for all  $R_{phys}$ . This follows because the DBI scaling has  $\ell_s \rightarrow 0$  [155]. Indeed it is easy to see that the effective open string metric discussed in [155] has the property that  $\ell_s^2 G^{-1} = \frac{\ell_s^2 R_{phys}^2}{R_{phys}^4 + L^4}$  goes to zero when  $N \rightarrow \infty$  with  $L = \ell_s \sqrt{\pi N}$ ,  $R_{phys}$  fixed. This factor  $\ell_s^2 G^{-1}$  controls higher derivative corrections for the open string degrees of freedom. At finite  $N$ , we can keep  $\ell_s^2 G^{-1}$  small, either when  $R_{phys} \ll L$  or  $R_{phys} \gg L$ . Therefore, there are two regimes where the stringy description reduces to an effective field theory, where higher derivatives can be neglected. The agreement holds for specified regions

of  $R_{phys}$  as well as  $\dot{R}_{phys}$ , because the requirement  $\ell_s^2 G^{-1} \ll 1$  is not the only condition needed to ensure that higher derivatives can be neglected. We also require that the proper acceleration is small. At large  $R_{phys}$ , the magnetic flux density is small (as well as the higher derivatives being small) and the  $D2$ -brane without non-commutativity is a good description. This is why the finite  $N$  equations derived from the  $D0$ -brane effective field theory agree with the Abelian  $D2$ -picture. For small  $R_{phys}$ , small  $\dot{R}_{phys}$ , we can also neglect higher derivatives. This is the region where the  $D0$ -Yang-Mills description is valid, or equivalently a strongly non-commutative  $D2$ -picture.

#### 5.4.2 Finite $N$ effects

We will consider the time of collapse as a function of  $n$  using the definition of the physical radius given in section (2). In order to facilitate comparison with the large  $n$  system, we will be using  $\hat{r}, \hat{s}$  variables. To begin with, consider the dimensionless acceleration, which can be expressed as

$$-\hat{s} \frac{\partial_s \mathcal{E}|_{\hat{r}}}{\partial_{\hat{r}} \mathcal{E}|_{\hat{s}}}, \quad (5.34)$$

with  $\gamma = 1/\sqrt{(1 - \hat{s}^2)}$ . As the sphere starts collapsing from  $\hat{r} = \hat{r}_0$  down to  $\hat{r} = 0$ , the speed changes from  $\hat{s} = 0$  to a value less than  $\hat{s} = 1$ . It is easy to see that the acceleration does not change sign in this region. Using the basic energy  $\hat{\mathcal{E}} = \mathcal{E}/N$  from (5.18), we can write

$$\begin{aligned} \frac{\partial \hat{\mathcal{E}}_{n=1}(\hat{r}, \hat{s})}{\partial \hat{s}} &= \hat{s} \frac{(3(1 + \hat{r}^4) + \hat{r}^4(1 - \hat{s}^2))}{\sqrt{(1 + \hat{r}^4)(1 - \hat{s}^2)}^{\frac{5}{2}}}, \\ \frac{\partial \hat{\mathcal{E}}_{n=1}(\hat{r}, \hat{s})}{\partial \hat{r}} &= \frac{2\hat{r}^3}{(1 + \hat{r}^4)^{\frac{3}{2}}(1 - \hat{s}^2)^{\frac{3}{2}}} \left( (1 + \hat{r}^4) + (1 - \hat{s}^2)(2 + \hat{r}^4) \right). \end{aligned} \quad (5.35)$$

Neither of the partial derivatives change sign in the range  $\hat{s} = 0$  to 1. Hence the speed  $\hat{s}$  increases monotonically. The same result is true for  $n > 1$ , since the energy functions for all these cases can be written as a sum of the energies at  $n = 1$ .

In the  $n = 1$  case,  $\hat{r} = r$ ,  $\hat{s} = s$ . For fixed  $r_0$  the speed at  $r = 0$  is given by

$$(1 - s^2|_{n=1}) = \frac{(1 + r_0^4)^{\frac{1}{3}}}{(1 + 2r_0^4)^{\frac{2}{3}}}. \quad (5.36)$$

Comparing this with the large  $n$  formula

$$(1 - s^2|_{n=\infty}) = (1 + r_0^4)^{-1}, \quad (5.37)$$

it is easy to see that

$$\left( \frac{(1-s^2)|_{n=\infty}}{(1-s^2)|_{n=1}} \right)^3 = \frac{(1+2r_0^4)^2}{(1+r_0^4)^4} < 1, \quad (5.38)$$

which establishes that the speed at  $r = 0$  is larger for  $n = \infty$ .

We can strengthen this result to show that the speed of collapse at all  $r < r_0$  is smaller for  $n = 1$  than at  $n = \infty$ . For any  $r < r_0$  we evaluate this energy function with the speed of collapse evaluated at  $s^2 = \frac{r_0^4 - r^4}{r_0^4 + 1}$ , which is the speed at the same  $r$  in the large  $n$  problem. Let us define  $F(r, r_0) = \hat{\mathcal{E}}_{n=1} \left( r, s = \sqrt{\frac{r_0^4 - r^4}{r_0^4 + 1}} \right)$ . We compare this with  $\hat{\mathcal{E}}_{n=1}(r, s)$  for  $s$  appropriate for the  $n = 1$  problem, which is just  $\frac{1+2r_0^4}{\sqrt{1+r_0^4}} \equiv G(r_0)$  by conservation of energy. We now use the fact, established above, that  $\frac{\partial \hat{\mathcal{E}}_{n=1}}{\partial s}$  is positive for any real  $r$ . This means that we can show  $s|_{n=1} < \sqrt{\frac{r_0^4 - r^4}{r_0^4 + 1}}$  by showing that  $F(r, r_0) > G(r_0)$ . A short calculation gives

$$F(r, r_0) - G(r_0) = \frac{r_0^4}{\sqrt{1+r_0^4}(1+r^4)}(r_0^4 - r^4). \quad (5.39)$$

It is clear that we have the desired inequality, showing that, at each  $r$ , the speed  $s$  in the  $n = 1$  problem is smaller than the speed in the  $n = \infty$  system. Hence the time of collapse is larger at  $n = 1$ . In the  $n = 2$  case, we find that an exactly equivalent treatment proves again that the collapse is slower than at large  $n$ . However, this trend is not a general feature for all  $n$ . In the leading large- $N$  limit, the time of collapse is given by the formula

$$\frac{T}{L} = \int dr \frac{\sqrt{1+r_0^4}}{\sqrt{r_0^4 - r^4}} = \frac{K(\frac{1}{\sqrt{2}}) \sqrt{R^4 + L^4}}{\sqrt{2} R} \quad (5.40)$$

For fixed  $\ell_s$ ,  $L$  decreases with decreasing  $N$  and as a result  $T$  decreases. When we include the first  $1/N$  correction the time of collapse is [140]

$$\frac{T}{L} = \int dr \left[ \frac{\sqrt{1+r_0^4}}{\sqrt{r_0^4 - r^4}} + \frac{r_0^8}{6N^2(1+r_0^4)^{3/2}\sqrt{r_0^4 - r^4}} - \frac{r_0^4(1+3(1+r_0^4))}{6N^2(1+r_0^4)\sqrt{1+r_0^4}\sqrt{r_0^4 - r^4}} \right]. \quad (5.41)$$

By performing numerical integration of the above for several values of the parameter  $r_0$  and some large but finite values of  $N$ , we see that the time of collapse is smaller for the  $1/N$  corrected case. This means that, in the region of large  $N$  the time of collapse decreases as  $N$  decreases, with both the leading large  $N$  formula and the  $1/N$  correction being consistent with this trend. However, as we saw above the time of collapse at  $n = 1$  and  $n = 2$  are larger than at  $n = \infty$ . This means that there are one or more turning points in the time of collapse as a function of  $n$ .

The deceleration effect that arises in the comparison of  $n = 1$  and  $n = 2$  with large  $n$  may have applications in cosmology. Deceleration mechanisms coming from DBI actions have been studied in the context of bulk causality in AdS/CFT [156, 157] and applied in

the problem of satisfying slow roll conditions in stringy inflation [158]. Here we see that the finite  $n$  effects result in a further deceleration in the region of small  $n$ .

We turn to the proper acceleration which is important in checking the validity of our action. Since the DBI action is valid when higher derivatives are small, it is natural to demand that the proper acceleration, should be small (see for example [156]). The condition is  $\gamma^3 \ell_s \partial_t^2 R_{phys} \ll 1$ . In terms of the dimensionless variables it is  $\gamma^3 (\partial_{\hat{r}}^2 \hat{r}) \ll \sqrt{N}$ . If we want a trajectory with initial radius  $\hat{r}_0$  such that the proper acceleration always remains less than one through the collapse, then there is an upper bound on  $\hat{r}_0$  (see for example section 8 of [140]). The corresponding upper bound on the physical radius goes to infinity as  $N \rightarrow \infty$ , since  $R_{phys} \sim \hat{r} \sqrt{\lambda N}$ . For small  $\hat{r}_0$  we are in the matrix theory limit and the effective action is valid. For large  $\hat{r}_0$  and  $\hat{r}$ -large, the acceleration is under control,  $\alpha \sim 1/\hat{r}$  and the velocity will be close to zero. Interestingly, there will also be a class of trajectories parametrised by large  $\hat{r}_0$ , which admit relativistic motion. Consider for example the  $n = 1$  case (where  $\hat{r} = r, \hat{s} = s$ ). The proper acceleration can be written as

$$\alpha = -\frac{2r^3}{1+r^4} \frac{-3+2s^2+r^4(s^2-2)}{\sqrt{1-s^2}(r^4(s^2-4)-3)}. \quad (5.42)$$

For  $s \sim 1$  and small  $r$ , this becomes

$$\alpha \simeq -\frac{2r^3}{3\sqrt{1-s^2}} \quad (5.43)$$

and  $\sqrt{1-s^2}$  can be found from the energy at the same limits, in which (5.18) becomes

$$\sqrt{1-s^2} \simeq \frac{1}{(2r_0^2)^{1/3}}. \quad (5.44)$$

Therefore, we can identify a region where the proper acceleration is small by restricting it to be of order  $1/r_0$  for example

$$\alpha \simeq \frac{2r^3}{3} (2r_0^2)^{1/3} \sim \frac{1}{r_0}. \quad (5.45)$$

This means that in regions where  $r \sim r_0^{-5/9}$ , we will have a relativistic limit described by the DBI, where stringy corrections can be neglected. This result also holds in the large- $N$  limit. It will be interesting to develop a perturbative approximation which systematically includes stringy effects away from this region.

Another quantity of interest is the effective mass squared  $E^2 - p^2$ , where  $p = \partial \mathcal{L} / \partial s$  is the radial conjugate momentum. It becomes negative for sufficiently large velocities. This includes the above regime of relativistic speeds and small radii. It is straightforward to see that if our collapsing configuration is considered as a source for spacetime gravity, this implies a violation of the dominant energy condition. In the context of the BFSS

matrix model, it has been shown that for an action containing a background spacetime  $G_{IJ} = \eta_{IJ} + h_{IJ}$ , in the linearised approximation, linear couplings in the fluctuation  $h_{0I}$  correspond to momentum in the  $X^I$  direction [159]. The same argument can be developed here for the non-Abelian DBI. We couple a small fluctuation  $h_{0r}$ , which in classical geometry we can write as  $h_{0i} = h_{0r}x_i$  for the unit sphere. We replace  $x_i$  by  $\alpha_i/n$ . The action for  $D0$ -branes [109,141] is generalised from (5.1) by replacing  $\dot{R}$  in  $\lambda\partial_t\Phi_i = \lambda(\dot{R})\alpha_i = \frac{\dot{R}}{n}\alpha_i$  with  $(\dot{R} + h_{0r})$ . It is then clear that the variation with respect to  $\dot{R}$ , which gives  $p$ , is the same as the variation with respect to  $h_{0r}$ , which gives  $T^{0r}$ . Hence, the dominant energy condition will be violated, since  $E < |p|$  is equivalent to  $T^{00} < T^{0r}$ . The violation of this condition by stringy  $D$ -brane matter can have profound consequences. For a discussion of possible consequences in cosmology see [160]. In this context, it is noteworthy that the violation can occur near a region of zero radius, which could be relevant to a near-big-bang region in a braneworld scenario.

### 5.4.3 Distance to blow-up in $D1 \perp D3$

Comparisons between the finite and large  $N$  results can be made in the spatial case using the conserved pressure. The arguments are similar to what we used for the time of collapse using the energy functions. Consider the case  $n = 1$ , and let  $\hat{P} = P/N$ . First calculate the derivative of the pressure -

$$\frac{\partial \hat{P}}{\partial s} = \frac{s(4r^4 + r^4s^2 + 3)}{\sqrt{1 + r^4(1 - s^2)^{5/2}}}. \quad (5.46)$$

This is clearly always positive. Now evaluate

$$\hat{P} \left( r, s = \frac{\sqrt{r^4 - r_0^4}}{\sqrt{1 + r_0^4}} \right) = -\frac{(1 + r_0^4)^{1/2}}{1 + r^4} (1 + r_0^4 + r^4). \quad (5.47)$$

This should be compared with  $\hat{P}(r, s)$ , evaluated for the value of  $s$  which solves the  $n = 1$  equation of motion, which by conservation of pressure is  $-\frac{(1+2r_0^4)}{\sqrt{1+r_0^4}}$ . Take the difference to find

$$\hat{P} \left( r, s = \frac{\sqrt{r^4 - r_0^4}}{\sqrt{1 + r_0^4}} \right) + \frac{(1 + 2r_0^4)}{\sqrt{1 + r_0^4}} = \frac{r_0^4(r^4 - r_0^4)}{\sqrt{1 + r_0^4}(1 + r^4)}. \quad (5.48)$$

Thus at fixed  $r_0$  and  $r$ ,  $\hat{P}_{n=1}$ , when evaluated for the value of  $s$  which solves the large  $n$  problem, is larger than when it is evaluated for the value of  $s$  which solves the  $n = \infty$  problem. Since  $\hat{P}$  increases monotonically with  $s$  for fixed  $r$ , this shows that for fixed  $r_0$ , and any  $r$ ,  $s$  is always larger in the large  $N$  problem. Since  $\Sigma = \int dr/s$ , this means the distance to blow-up is smaller for  $n = \infty$ . Hence for fixed  $r_0$ , the distance to blow-up is larger at  $n = 1$ .

## 5.5 Towards a generalisation to higher even-dimensional fuzzy-spheres

For generalisations to higher dimensional brane systems, and to higher dimensional fuzzy spheres [115, 118, 147, 148], it is of interest to derive an extension of the expressions for the symmetrised traces given above. In the general case, we define  $N(k, n)$  to be the dimension of the irreducible representation of  $SO(2k+1)$  with highest weight state  $(\frac{n}{2}, \frac{n}{2}, \dots, \frac{n}{2})$  which contains  $k$  entries. We then take  $C(m, k, n)$  to be the action of the symmetrised trace on  $m$  pairs of matrices  $X_i$ , where  $i = 1, \dots, 2k+1$

$$C(m, k, n) = \frac{1}{N(k, n)} STr(X_i X_i)^m. \quad (5.49)$$

Finding an expression for  $C(m, k, n)$  is non-trivial. Investigations based upon intuition from the ADHM construction lead us to conjecture that for  $n$  odd

$$C(m, k, n) = \frac{2^k \prod_{i_1=1}^k (2m-1+2i_1)}{(k-1)! \prod_{i_2=1}^{2k-1} (n+i_2)} \sum_{i_3=1}^{\frac{n+1}{2}} \left[ \prod_{i_4=1}^{k-1} \left( \left( \frac{n}{2} + i_4 \right)^2 - \left( i_3 - \frac{1}{2} \right)^2 \right) (2i_3-1)^{2m} \right], \quad (5.50)$$

while for  $n$  even<sup>1</sup>

$$C(m, k, n) = \frac{2^k \prod_{i_1=1}^k (2m-1+2i_1)}{(k-1)! \prod_{i_2=1}^{2k-1} (n+i_2)} \sum_{i_3=1}^{\frac{n}{2}} \left[ \prod_{i_4=1}^{k-1} \left( \left( \frac{n}{2} + i_4 \right)^2 - i_3^2 \right) (2i_3)^{2m} \right]. \quad (5.51)$$

We gave arguments leading to the expressions above in the previous chapter.

For higher even spheres there will be extra complications at finite- $n$ . Consider the case of the fuzzy  $S^4$  for concreteness. The evaluation of the higher dimensional determinant in the corresponding non-Abelian brane action will give expressions with higher products of  $\partial_t \Phi_i$  and  $\Phi_{ij} \equiv [\Phi_i, \Phi_j]$

$$\begin{aligned} S = & -T_0 \int dt STr \left\{ 1 + \lambda^2 (\partial_t \Phi_i)^2 + 2\lambda^2 \Phi_{ij} \Phi_{ji} + 2\lambda^4 (\Phi_{ij} \Phi_{ji})^2 - 4\lambda^4 \Phi_{ij} \Phi_{jk} \Phi_{kl} \Phi_{li} + \right. \\ & \left. + 2\lambda^4 (\partial_t \Phi_i)^2 \Phi_{jk} \Phi_{kj} - 4\lambda^4 \partial_t \Phi_i \Phi_{ij} \Phi_{jk} \partial_t \Phi_k + \frac{\lambda^6}{4} (\epsilon_{ijklm} \partial_t \Phi_i \Phi_{jk} \Phi_{lm})^2 \right\}^{1/2}. \quad (5.52) \end{aligned}$$

The ansatz for the transverse scalars will still be

$$\Phi_i = \hat{R}(t) X_i,$$

where now  $i = 1, \dots, 5$  and the  $X^i$ 's are given by the action of  $SO(5)$  gamma matrices on the totally symmetric  $n$ -fold tensor product of the basic spinor. After expanding the square root, the symmetrisation procedure should take place over all the  $X_i$ 's and  $[X_i, X_j]$ 's.

<sup>1</sup>For  $m = 0$  the value  $STr(X_i X_i)^0 = 1$  is once again imposed.

However, the commutators of commutators  $[[X, X], [X, X]]$  will give a nontrivial contribution, as opposed to what happens in the large- $n$  limit where they are sub-leading and are taken to be zero. Therefore, in order to uncover the full answer for the finite- $n$  fuzzy  $S^4$  it is not enough to just know the result of  $STr(X_i X_i)^m$  - we need to know the full  $STr((X X)^{m_1}([X, X][X, X]))^{m_2}$  with all possible contractions among the above. It would be clearly interesting to have the full answer for the fuzzy  $S^4$ . A similar story will apply for the higher even-dimensional fuzzy spheres.

Note, however, that for  $\hat{R} = 0$  in (5.52) all the commutator terms  $\Phi_{ij}$  will vanish, since they scale like  $\hat{R}^2$ . This reduces the symmetrisation procedure to the one involving  $X_i X_i$  and yields only one sum for the energy. The same will hold for any even-dimensional  $S^{2k}$ , resulting in the following general expression

$$\begin{aligned} \mathcal{E}_{n,k}(0, s) &= -STr \sum_{m=0}^{\infty} (-1)^m s^{2m} (2m-1) (X_i X_i)^m \binom{1/2}{m} \\ &= -N(k, n) \sum_{m=0}^{\infty} (-1)^m s^{2m} (2m-1) C(m, k, n) \binom{1/2}{m}. \end{aligned} \quad (5.53)$$

Using (5.50), notice that in the odd  $n$  case

$$C(m, k, n) = \prod_{i_2=1}^{2k-1} \frac{(1+i_2)}{(n+i_2)} C(m, k, 1) \sum_{i_3}^{\frac{n+1}{2}} \frac{f_{odd}(i_3, k, n)}{f_{odd}(1, k, 1)} (2i_3-1)^{2m}. \quad (5.54)$$

The factor  $f_{odd}$  is

$$f_{odd}(i_3, k, n) = \prod_{i_4=1}^{k-1} \left( \left( \frac{n}{2} + i_4 \right)^2 - \left( i_3 - \frac{1}{2} \right)^2 \right). \quad (5.55)$$

Inserting this form for  $C(m, k, n)$  in terms of  $C(m, k, 1)$  we see that

$$\mathcal{E}_{n,k}(0, s) = N(n, k) \prod_{i_2=1}^{2k-1} \frac{(1+i_2)}{(n+i_2)} \sum_{i_3=1}^{\frac{n+1}{2}} \frac{f_{odd}(i_3, k, n)}{f_{odd}(1, k, 1)} \hat{\mathcal{E}}_{n=1,k}(0, s(2i_3-1)) \quad (5.56)$$

Similarly we derive, in the even  $n$  case, that

$$\mathcal{E}_{n,k}(0, s) = N(n, k) \prod_{i_2=1}^{2k-1} \frac{(2+i_2)}{(n+i_2)} \sum_{i_3=1}^{\frac{n}{2}} \frac{f_{even}(i_3, k, n)}{f_{even}(1, k, 2)} \hat{\mathcal{E}}_{n=2,k}(0, s(i_3)) \quad (5.57)$$

where

$$f_{even}(i_3, k, n) = \prod_{i_4=1}^{k-1} \left( \left( \frac{n}{2} + i_4 \right)^2 - i_3^2 \right) \quad (5.58)$$

and  $\hat{\mathcal{E}}$  is the energy density, i.e. the energy divided a factor of  $N(n, k)$ .

It is also possible to write  $C(m, k, 2)$  in terms of  $C(m, k, 1)$

$$\begin{aligned} C(m, k, 2) &= 2^{2m} C(m, k, 1) \prod_{i_4=1}^{k-1} \frac{i_4(i_4+2)}{i_4(i_4+1)} \prod_{i_2=1}^{2k-1} \frac{(i_2+1)}{(i_2+2)} \\ &= 2^{2m} C(m, k, 1) \frac{f_{\text{even}}(1, k, 2)}{f_{\text{odd}}(1, k, 1)} \prod_{i_2=1}^{2k-1} \frac{(i_2+1)}{(i_2+2)}, \end{aligned} \quad (5.59)$$

which is valid for all values of  $m \neq 0$ .

It turns out to be possible to give explicit forms for the energy for the  $n = 1$  and  $n = 2$  case. Since the definition of the physical radius in section 2 is also valid for higher dimensional fuzzy spheres, we can express the results in terms of the rescaled variables  $\hat{r}$  and  $\hat{s}$

$$\begin{aligned} \hat{\mathcal{E}}_{n=1,k}(0, \hat{s}) &= \frac{1}{(1 - \hat{s}^2)^{\frac{2k+1}{2}}} \\ \hat{\mathcal{E}}_{n=2,k}(0, \hat{s}) &= \frac{1}{(1 - \hat{s}^2)^{\frac{2k+1}{2}}} \frac{(k+1)}{(2k+1)}. \end{aligned} \quad (5.60)$$

When plugged into (5.56), (5.57) the above results provide a closed form for the energy at  $\hat{r} = 0$ , for any  $n$  and any  $k$ . A complete study of the time dependent dynamics requires the evaluation of the energy functions for all  $\hat{r}$ , but the relative simplicity of (5.60) suggests that the computation of the required additional symmetrised traces might reveal a tractable extension.

## 5.6 Summary and Outlook

In this chapter we have given a detailed study of the finite  $N$  effects for the time dependent  $D0 - D2$  fuzzy sphere system and the related  $D1 \perp D3$  funnel. This involved calculating symmetrised traces of  $SO(3)$  generators. The formulae have a surprising simplicity.

The energy function  $E(r, s)$  in the large  $N$  limit looks like a relativistic particle with position dependent mass. This relativistic nature is modified at finite  $N$ . Nevertheless our results are consistent with a fixed relativistic upper speed limit. This is guaranteed by an appropriate definition of the physical radius which relies on the properties of symmetrised traces of large numbers of generators. We showed that the exotic bounces found in the large  $N$  expansion in [140] do not occur. It was previously clear that these exotic bounces happened near the regime where the  $1/N$  expansion was breaking down. The presence or absence of these could only be settled by a finite  $N$  treatment, which we have provided in this chapter. We also compared the time of collapse of the finite  $N$  system with that of the large  $N$  system and found a finite  $N$  deceleration effect for the first small values of  $N$ . The modified  $E(r, s)$  relation allows us to define an effective squared mass which depends on

both  $r, s$ . For certain regions in  $(r, s)$  space, it can be negative. When the  $D0 - D2$  system is viewed as a source for gravity, a negative sign of this effective mass squared indicates that the brane acts as a gravitational source which violates the dominant energy condition.

We have extended some of our discussion to the case of higher even fuzzy spheres with  $SO(2k + 1)$  symmetry. The results for symmetrised traces that we obtain can be used in a proposed calculation of charges in the  $D1 \perp D(2k + 1)$  system. They also provide further illustrations of how the correct definition of physical radius using symmetrised traces of large powers of Lie algebra generators gives consistency with a constant speed of light. A more complete discussion of the finite  $N$  effects for the higher fuzzy spheres could start from these results. Generalisations of the finite  $N$  considerations to fuzzy spheres in more general backgrounds [161] will be interesting to consider, with a view to possible applications in cosmology.

# APPENDIX A

## INTEGRAL IDENTITIES

In this appendix we summarise the tensor bubble, tensor triangle and tensor box integrals used in chapter 2.

### A.1 Scalar box, triangle and bubble integrals

The scalar  $n$ -point integral functions in  $D = 4 + 2m - 2\epsilon$  dimensions are defined as

$$\begin{aligned} I_n^D \equiv I_n^D[1] &= i(-1)^{n+1} (4\pi)^{D/2} \int \frac{d^D L}{(2\pi)^D} \frac{1}{L^2 (L-p_1)^2 \cdots (L - \sum_{i=1}^{n-1} p_i)^2} \\ &= \frac{i(-1)^{n+1}}{\pi^{2+m-\epsilon}} \int \frac{d^{4+2m} l d^{-2\epsilon} \mu}{(l^2 - \mu^2)((l-p_1)^2 - \mu^2) \cdots ((l - \sum_{i=1}^{n-1} p_i)^2 - \mu^2)} \end{aligned} \quad (\text{A.1})$$

The higher dimensional integral functions are related to  $4 - 2\epsilon$  dimensional integrals with a factor  $\mu^{2m}$  inserted in the integrand. For  $m = 1, 2$  one finds

$$I_n[\mu^2] \equiv J_n = (-\epsilon) I_n^{6-2\epsilon} \quad (\text{A.2})$$

$$I_n[\mu^4] \equiv K_n = (-\epsilon)(1-\epsilon) I_n^{8-2\epsilon} \quad (\text{A.3})$$

In chapter 2 we encounter bubble functions with  $m = 0, 1$ , triangles with one massive external line and  $m = 0, 1$ , and boxes with four massless external lines and  $m = 0, 1, 2$ :

$$\begin{aligned} I_2(P^2) &= \frac{r_\Gamma}{\epsilon(1-2\epsilon)} (-P^2)^{-\epsilon}, & I_2^{6-2\epsilon}(P^2) &= -\frac{r_\Gamma}{2\epsilon(1-2\epsilon)(3-2\epsilon)} (-P^2)^{1-\epsilon}, \\ I_3(P^2) &= \frac{r_\Gamma}{\epsilon^2} (-P^2)^{-1-\epsilon}, & I_3^{6-2\epsilon}(P^2) &= \frac{r_\Gamma}{2\epsilon(1-\epsilon)(1-2\epsilon)} (-P^2)^{-\epsilon}, \\ I_4 &= -\frac{r_\Gamma}{st} \left\{ -\frac{1}{\epsilon^2} [(-s)^{-\epsilon} + (-t)^{-\epsilon}] + \frac{1}{2} \log^2 \left( \frac{s}{t} \right) + \frac{\pi^2}{2} \right\} + \mathcal{O}(\epsilon), \\ (-\epsilon) I_4^{6-2\epsilon} &= 0 + \mathcal{O}(\epsilon), & (-\epsilon)(1-\epsilon) I_4^{8-2\epsilon} &= -\frac{1}{6} + \mathcal{O}(\epsilon). \end{aligned} \quad (\text{A.4})$$

Note that the expressions for the bubbles and triangles are valid to all orders in  $\epsilon$ , whereas for the box functions we have only kept the leading terms which contribute up to  $\mathcal{O}(\epsilon^0)$  in the amplitudes.

## A.2 Scalar Integral Identities

The following identities between integral functions which appear in appendix A of [59] are used in chapter 2. They are useful for comparison with the known answer and identifying quadratic divergences.

$$J_4 = -\frac{st}{4u}I_4 - \frac{s}{2u}I_3(s) - \frac{t}{2u}I_3(t) - \frac{1}{2}I_4^{6-2\epsilon} \quad (\text{A.5})$$

$$J_3(s) = \frac{1}{2}I_2(s) - I_3^{6-2\epsilon}(s) \quad (\text{A.6})$$

$$J_2(s) = \frac{s}{4}I_2(s) - \frac{3}{2}I_2^{6-2\epsilon}(s) \quad (\text{A.7})$$

These three identities for  $J_4, J_3$  and  $J_2$  are derived from the following general identity relating  $6 - 2\epsilon$  dimensional integrals to  $4 - 2\epsilon$  dimensional integrals for  $n$  point kinematics:

$$I_n^{6-2\epsilon} = \frac{1}{(n-5+2\epsilon)c_0} \left[ 2I_n - \sum_{i=1}^n c_i I_{n-1}^{(i)} \right] \quad (\text{A.8})$$

where the integral  $I_{n-1}^{(i)}$  is obtained from the integral  $I_n$  by removing the propagator between leg  $i-1 \pmod n$  and  $i$ . The  $c_i$  are defined by

$$c_i = -2 \sum_{j=1}^n (p_{ij})^{-1} \quad , \quad c_0 = \sum_{i=1}^n c_i \quad (\text{A.9})$$

The matrix  $p_{ij}$  is defined by

$$p_{ii} = 0 \quad \text{and} \quad p_{ij} = p_{ji} = k_i + k_{i+1} + \dots + k_{j-1} \quad \text{for} \quad i < j \quad (\text{A.10})$$

These  $c_i$  are easily found for small  $n$ . For example consider the case of four-point massless box kinematics

$$p^2 = \begin{pmatrix} 0 & 0 & s & 0 \\ 0 & 0 & 0 & t \\ s & 0 & 0 & 0 \\ 0 & t & 0 & 0 \end{pmatrix} \quad , \quad (p^2)^{-1} = \begin{pmatrix} 0 & 0 & \frac{1}{s} & 0 \\ 0 & 0 & 0 & \frac{1}{t} \\ \frac{1}{s} & 0 & 0 & 0 \\ 0 & \frac{1}{t} & 0 & 0 \end{pmatrix}$$

thus in this case the  $c_i$  are given by

$$\begin{aligned} c_1 = c_3 &= -\frac{2}{s} \quad , \quad I_3^{(1)} = I_3^{(3)} = I_3(t) \\ c_2 = c_4 &= -\frac{2}{t} \quad , \quad I_3^{(2)} = I_3^{(4)} = I_3(s) \end{aligned}$$

and  $c_0 = \frac{4u}{st}$ . So finally the identity for  $J_4$  is

$$\begin{aligned}
 J_4 &= (-\epsilon)I_4^{6-2\epsilon} \\
 &= -\frac{1}{2}(-1 + 2\epsilon)I_4^{6-2\epsilon} - \frac{1}{2}I_4^{6-2\epsilon} \\
 &= -\frac{1}{2c_0} \left( 2I_4 - c_1 I_3^{(1)} - c_2 I_3^{(2)} - c_3 I_3^{(3)} \right) - \frac{1}{2}I_4^{6-2\epsilon} \\
 &= -\frac{st}{4u}I_4 - \frac{s}{2u}I_3(s) - \frac{t}{2u}I_3(t) - \frac{1}{2}I_4^{6-2\epsilon}
 \end{aligned}$$

which is the identity (A.5) for  $J_4$ . The identities for  $J_3$  and  $J_2$  are similar

### A.3 PV reduction

In this section we present the result of the Passarino Veltman (PV) reduction for various tensor integrals which are relevant for the triple cut calculations of the  $--++$  and  $-+-+$  amplitudes in chapter 2.

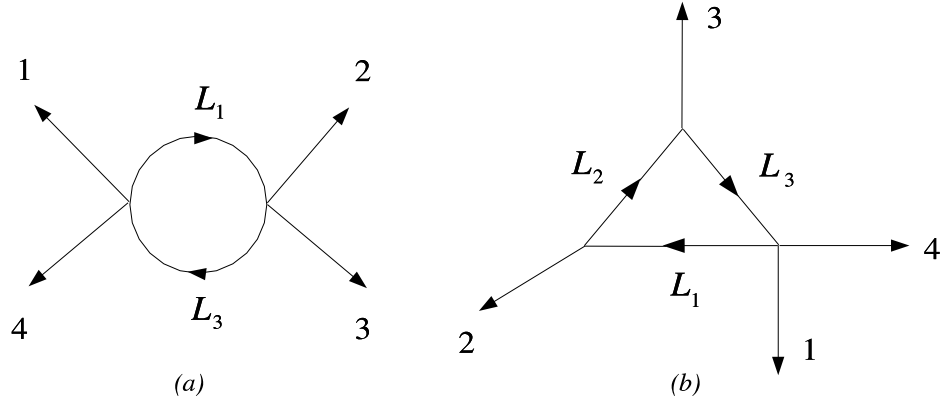


Figure A.1: *Kinematics of the bubble and triangle integral functions studied in this Appendix.*

For the linear and two-tensor bubbles we have (see Figure 10a):

$$I_2[L_3^\mu] = -\frac{1}{2}I_2(p_2 + p_3)^\mu \quad (\text{A.11})$$

$$I_2[L_3^\mu L_3^\nu] = -\frac{1}{2}I_2^{6-2\epsilon} \delta_{[4-2\epsilon]}^{\mu\nu} + \left( \frac{1}{4}I_2 + \frac{1}{2t}I_2^{6-2\epsilon} \right) (p_2 + p_3)^\mu (p_2 + p_3)^\nu \quad (\text{A.12})$$

For the linear, two- and three-tensor triangles (see Figure 10b):

$$I_3[L_3^\mu] = -\frac{1}{t}I_2p_2^\mu + \left(-I_3 + \frac{1}{t}I_2\right)p_3^\mu \quad (\text{A.13})$$

$$\begin{aligned} I_3[L_3^\mu L_3^\nu] &= \frac{1}{2t}I_2p_2^\mu p_2^\nu + \left(\frac{1}{t}I_3^{6-2\epsilon} + \frac{1}{2t}I_2\right)\left(p_2^\mu p_3^\nu + p_2^\nu p_3^\mu\right) \\ &\quad + \left(-\frac{3}{2t}I_2 + I_3\right)p_3^\mu p_3^\nu - \frac{1}{2}I_3^{6-2\epsilon}\delta_{[4-2\epsilon]}^{\mu\nu} \end{aligned} \quad (\text{A.14})$$

$$\begin{aligned} I_3[L_3^\mu L_3^\nu L_3^\rho] &= -\left(\frac{1}{4t}I_2 + \frac{1}{2t^2}I_2^{6-2\epsilon}\right)\left(p_2^\mu p_2^\nu p_2^\rho\right) \\ &\quad - \left(\frac{1}{4t}I_2 + \frac{3}{2t^2}I_2^{6-2\epsilon}\right)\left(p_2^\mu p_2^\nu p_3^\rho + p_2^\mu p_3^\nu p_2^\rho + p_3^\mu p_2^\nu p_2^\rho\right) \\ &\quad + \left(-\frac{1}{4t}I_2 + \frac{3}{2t^2}I_2^{6-2\epsilon} - \frac{2}{t}I_3^{6-2\epsilon}\right)\left(p_2^\mu p_3^\nu p_3^\rho + p_3^\mu p_3^\nu p_2^\rho + p_3^\mu p_2^\nu p_3^\rho\right) \\ &\quad + \left(\frac{7}{4t}I_2 + \frac{1}{2t^2}I_2^{6-2\epsilon} - I_3\right)\left(p_3^\mu p_3^\nu p_3^\rho\right) + \frac{1}{2t}I_2^{6-2\epsilon}\left(\delta^{\mu\nu}p_2^\rho + \delta^{\mu\rho}p_2^\nu + \delta^{\rho\nu}p_2^\mu\right) \\ &\quad + \left(-\frac{1}{2t}I_2^{6-2\epsilon} + \frac{1}{2}I_3^{6-2\epsilon}\right)\left(\delta^{\mu\nu}p_3^\rho + \delta^{\mu\rho}p_3^\nu + \delta^{\rho\nu}p_3^\mu\right) \end{aligned} \quad (\text{A.15})$$

Finally, for the linear box:

$$\begin{aligned} I_4[L_3^\mu] &= \left(\frac{t}{2u}I_4 - \frac{1}{u}(I_3(t) - I_3(s))\right)p_1^\mu - \frac{1}{2}I_4p_2^\mu \\ &\quad + \left(\frac{t-u}{2u}I_4 - \frac{1}{u}(I_3(t) - I_3(s))\right)p_3^\mu \end{aligned} \quad (\text{A.16})$$

where, as usual,  $s := (p_1 + p_2)^2$ ,  $t := (p_2 + p_3)^2$ ,  $u := (p_1 + p_3)^2$ .

Note that the above expressions are presented in terms of scalar  $n$ -point integral functions  $I_n^{\mathcal{D}}$  in various dimensions  $\mathcal{D}$ , specifically in terms of  $I_n$ ,  $I_n^{6-2\epsilon}$  and  $I_n^{8-2\epsilon}$  in  $4-2\epsilon$ ,  $6-2\epsilon$  and  $8-2\epsilon$  dimensions, respectively. The expressions are valid to all orders in  $\epsilon$ , if  $I_n$ ,  $I_n^{6-2\epsilon}$  and  $I_n^{8-2\epsilon}$  are evaluated to all orders. In deriving these formulae it is important to remember that massless bubbles vanish in dimensional regularisation (see page 36 of [14]). This is interpreted as the cancelling of a UV and an IR divergence. The PV reductions above have been performed in a fashion that naturally leads to coefficients without explicit  $\epsilon$  dependence. See [96]. We now illustrate this procedure by considering the explicit reduction of the tensor bubble integral

$$I_2[L_3^\mu L_3^\nu] = B_1\delta_{[4-2\epsilon]}^{\mu\nu} + B_2(p_2 + p_3)^\mu (p_2 + p_3)^\nu \quad (\text{A.17})$$

To obtain  $B_1$  and  $B_2$ , the conventional reduction procedure would be to trace over the indices  $\delta_{[4-2\epsilon]}^{\mu\nu}$  and contract with  $(p_2 + p_3)^\mu (p_2 + p_3)^\nu$  to obtain the following two equations:

$$(4 - 2\epsilon)B_1 + tB_2 = 0 \quad , \quad (B_1 + tB_2) = \frac{1}{4}I_2 \quad (\text{A.18})$$

Solving these two equations gives

$$B_1 = -\frac{1}{4t} \frac{1}{3 - 2\epsilon} I_2 \quad , \quad B_2 = \frac{1}{2} \frac{2 - \epsilon}{3 - 2\epsilon} I_2 \quad (\text{A.19})$$

which contain explicit  $\epsilon$  dependence. However it is simple to avoid this  $\epsilon$  dependence by using a modified procedure which involves the use of a  $6 - 2\epsilon$  dimensional bubble. Instead of first contracting with  $\delta_{[4-2\epsilon]}^{\mu\nu}$  we contract with  $\delta_{[-2\epsilon]}^{\alpha\beta}$ . Recall the following formulae

$$\delta_{\alpha\beta}^{[-2\epsilon]} l^\alpha l^\beta = -\mu^2 \quad \text{and} \quad \delta_{\alpha\beta}^{[-2\epsilon]} \delta_{[-2\epsilon]}^{\alpha\beta} = -2\epsilon \quad (\text{A.20})$$

So contracting with  $\delta_{[-2\epsilon]}^{\alpha\beta}$  gives

$$B_1 = \frac{1}{2\epsilon} I_2 [\mu^2] = -\frac{1}{2} I_2^{6-2\epsilon} \quad (\text{A.21})$$

To determine  $B_2$  we again use  $(B_1 + tB_2) = \frac{1}{4}I_2$  to give

$$B_2 = \frac{1}{4}I_2 + \frac{1}{2t} I_2^{6-2\epsilon} \quad (\text{A.22})$$

See Appendix I of [96] for more details on this particular variant of PV reductions.

# APPENDIX B

## GRAVITY AMPLITUDE CHECKS

### B.1 The VegasShift[n] Mathematica command

The following Mathematica code can be used to compare amplitudes numerically. There are two different commands `evalshift[X]` which puts random numbers into the shifted amplitude and `evalnormal[X]` which puts random numbers into the unshifted amplitude. `evalshift[X]` in conjunction with the standard Mathematica command `Apart[X]` can be used to check the residues of a shifted amplitude one by one.

```
VegasShift[nn_] := (
  rand := Random[Integer, {-100, 100}]/100;
  angle[ii1_,ii2_] := la[ii1][[1]] la[ii2][[2]] - la[ii1][[2]] la[ii2][[1]];
  square[ii1_,ii2_] := lat[ii1][[1]] lat[ii2][[2]] - lat[ii1][[2]] lat[ii2][[1]];
  Do[(la[ii] = {rand, rand};
    lat[ii] = {rand, rand}), {ii, 1, nn - 2}];
  P = Sum[Transpose[{la[ii]}].{lat[ii]}, {ii, 1, nn - 2}];
  la[nn - 1] = {1, 0};
  lat[nn - 1] = -P[[1]];
  la[nn] = {0, 1};
  lat[nn] = -P[[2]];
  Sum[Transpose[{la[ii]}].{lat[ii]}, {ii, 1, nn}];

  lat[1] = lat[1] - z lat[2];
  la[2] = la[2] + z la[1];

  replist = {};
  Do[replist = Union[replist, {ang[xx1, yy1] -> angle[xx1, yy1],
    sqr[xx1, yy1] -> square[xx1, yy1]}], {xx1, 1, nn}, {yy1, 1, nn}];
  evalshift[expression_] := expression /. replist;
  evalnormal[expression_] := expression /. replist /. z -> 0;)
```

## B.2 Other shifts of the $-++++$ gravity amplitude

### B.2.1 The $|4\rangle, |5\rangle$ shifts

In this section we consider  $M_5^{(1)}(1^-, 2^+, 3^+, 4^+, 5^+)$  with the following shifts which have both nonstandard factorisations and presumably also have a boundary term.

$$\begin{aligned}
 \lambda_4 &\rightarrow \lambda_4 \\
 \tilde{\lambda}_4 &\rightarrow \tilde{\lambda}_4 - z\tilde{\lambda}_5 \\
 \lambda_5 &\rightarrow \lambda_5 + z\lambda_4 \\
 \tilde{\lambda}_5 &\rightarrow \tilde{\lambda}_5
 \end{aligned} \tag{B.1}$$

We will calculate as many terms as we can.

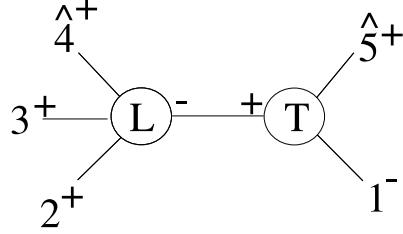


Figure B.1: *The diagram associated with  $\langle 1\hat{5} \rangle = 0$ , with shifts on  $|4\rangle, |5\rangle$ .*

The diagram in Figure B.1 gives:

$$\frac{i}{(4\pi)^2} \frac{1}{180} \frac{\langle 12 \rangle^2 \langle 13 \rangle^2 [23]^4 [15]}{\langle 23 \rangle^2 \langle 24 \rangle^2 \langle 45 \rangle^2 \langle 34 \rangle^2 \langle 15 \rangle} \left( \langle 12 \rangle^2 \langle 34 \rangle^2 - \langle 12 \rangle \langle 34 \rangle \langle 13 \rangle \langle 24 \rangle + \langle 13 \rangle^2 \langle 24 \rangle^2 \right) \tag{B.2}$$

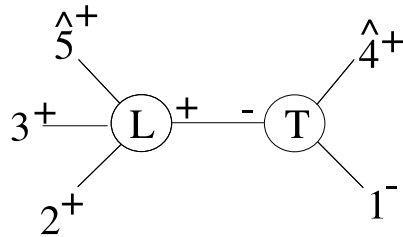


Figure B.2: *The diagram associated with  $[1\hat{4}] = 0$ , with shifts on  $|4\rangle, |5\rangle$ .*

The diagram in Figure B.2 gives:

$$\frac{i}{(4\pi)^2} \frac{3}{180} \frac{\langle 14 \rangle [45]^6}{\langle 23 \rangle^2 [14] [15]^4} \left( [23]^2 [15]^2 + [23][12][35][15] + [12]^2 [35]^2 \right) \tag{B.3}$$

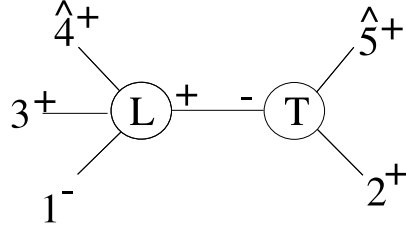


Figure B.3: *The standard factorisation diagram associated with  $\langle 2\hat{5} \rangle = 0$ , with shifts on  $|4\rangle, |5\rangle$ .*

The diagram in Figure B.3 gives:

$$\frac{i}{(4\pi)^2} \frac{1}{180} \frac{\langle 12 \rangle^2 \langle 13 \rangle^2 \langle 14 \rangle^2 [13]^4 [25]}{\langle 23 \rangle^2 \langle 24 \rangle^4 \langle 34 \rangle^2 \langle 25 \rangle \langle 45 \rangle^2} (\langle 13 \rangle^2 \langle 24 \rangle^2 + \langle 12 \rangle \langle 24 \rangle \langle 43 \rangle \langle 13 \rangle + \langle 34 \rangle^2 \langle 12 \rangle^2) \quad (\text{B.4})$$

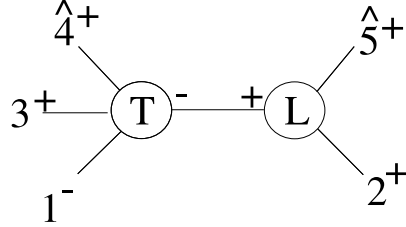


Figure B.4: *The nonstandard factorisation diagram associated with  $\langle 2\hat{5} \rangle = 0$ , with shifts on  $|4\rangle, |5\rangle$ .*

The diagram in Figure B.4 is a non standard factorisation. The double pole term associated with this diagram is

$$\frac{i}{(4\pi)^2} \frac{1}{180} \frac{\langle 12 \rangle^7 \langle 45 \rangle^2 [25]^4 [13]}{\langle 13 \rangle \langle 14 \rangle \langle 34 \rangle \langle 23 \rangle \langle 25 \rangle^2 \langle 24 \rangle^4} \quad (\text{B.5})$$

Just as in the  $|1\rangle, |2\rangle$  shifts the ‘single pole under this double pole’ term is mysterious. The other two diagrams corresponding to  $\langle 3\hat{5} \rangle = 0$  can be obtained from the results to Figure B.3 and Figure B.4 by swapping 2 and 3.

It is perhaps interesting to note that if we take some of the above terms in the  $|4\rangle, |5\rangle$  shifts, and apply the  $|1\rangle, |2\rangle$  shifts to the answers, and use partial fractions to extract the pole from the term, then there is agreement with the recursive diagrams in section 3.4. Thus the recursion relation is self consistent. For example, if you apply the  $|1\rangle, |2\rangle$  shifts to (B.3) and extract the  $1/[\hat{1}, 4]$  pole then this agrees with (3.52) after the legs 4 and 5 have been swapped. The results (B.4) and (B.5) can similarly be checked against (3.55) and (3.58) respectively.

B.2.2 The  $|2\rangle, |1\rangle$  shifts

In this section we again consider  $M_5^{(1)}(1^-, 2^+, 3^+, 4^+, 5^+)$ , but with the following shifts which have no nonstandard factorisations, but do presumably have a boundary term:

$$\begin{aligned}
 \lambda_1 &\rightarrow \lambda_1 + z\lambda_2 \\
 \tilde{\lambda}_1 &\rightarrow \tilde{\lambda}_1 \\
 \lambda_2 &\rightarrow \lambda_2 \\
 \tilde{\lambda}_2 &\rightarrow \tilde{\lambda}_2 - z\tilde{\lambda}_1
 \end{aligned} \tag{B.6}$$

As there are no nonstandard factorisations we can calculate all the diagrams.

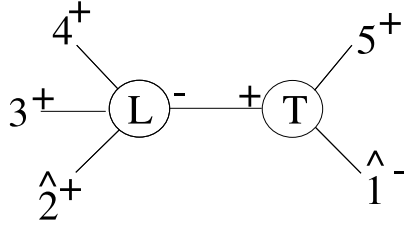


Figure B.5: *The diagram associated with  $\langle \hat{1}5 \rangle = 0$  with shifts on  $|2\rangle, |1\rangle$ .*

The diagram in Figure B.5 gives

$$\frac{i}{(4\pi)^2} \frac{1}{180} \frac{\langle 12 \rangle^6 \langle 35 \rangle^2 \langle 45 \rangle^2 [34]^4 [15]}{\langle 25 \rangle^8 \langle 23 \rangle^2 \langle 34 \rangle^2 \langle 24 \rangle^2 \langle 15 \rangle} (\langle 34 \rangle^2 \langle 25 \rangle^2 - \langle 34 \rangle \langle 24 \rangle \langle 35 \rangle \langle 25 \rangle + \langle 24 \rangle^2 \langle 35 \rangle^2) \tag{B.7}$$

The other diagrams that occur with these shifts correspond to poles located at  $\langle \hat{1}4 \rangle = 0$  and  $\langle \hat{1}3 \rangle = 0$  and can be obtained from Figure B.5 by swapping legs.

As there are no nonstandard factorisations in these shifts there is a possibility that the shifts on  $|2\rangle, |1\rangle$  could be used as the primary shift in an attempt to avoid non standard factorisations along the lines of section 3.6, however we have been unable to find an accompanying auxiliary shift that satisfies (3.82).

# APPENDIX C

## STR CALCULATIONS USING THE HIGHEST WEIGHT METHOD

Results on finite  $n$  symmetrised traces can be obtained by generalising the highest weight method of [140]. For the  $SO(3)$  representations used in fuzzy 2-spheres we have

$$\frac{1}{2}STr_{J=1/2}(\alpha_i\alpha_i)^m = (2m + 1) \quad (\text{C.1})$$

where the  $1/2$  comes from dividing with the dimension of the spin-1/2 representation. A similar factor will appear in all of the results below. The above result was derived in [140]. For the spin one case, we will obtain

$$\frac{1}{3}STr_{J=1}(\alpha_i\alpha_i)^m = \frac{2^{2m+1}(2m + 1)}{3} \quad (\text{C.2})$$

These results can be generalised to representations of  $SO(2l + 1)$  relevant for higher fuzzy spheres. The construction of higher dimensional fuzzy spheres uses irreducible representations of highest weight  $(\frac{n}{2}, \dots, \frac{n}{2})$ , as we have noted. For the minimal representation with  $n = 1$  we have

$$\frac{1}{D_{n=1}}STr_{n=1}(X_iX_i) = \frac{(2l + 2m - 1)!!}{(2m - 1)!!(2l - 1)!!} \quad (\text{C.3})$$

Notice the interesting symmetry under the exchange of  $l$  and  $m$ . For the next-to-minimal irreducible representation with  $n = 2$  we obtain:

$$\frac{1}{D_{n=2}}STr_{n=2}(X_iX_i) = 2^{2m}(l + 1)\frac{(2l + 2m - 1)!!}{(2m - 1)!!(2l + 1)!!} \quad (\text{C.4})$$

This is a generalisation of the spin 1 case to higher orthogonal groups. It agrees with the formulae in the chord diagram section of chapter 4, with  $l \rightarrow k$ .

### C.1 Review of spin half for $SO(3)$

We will begin by recalling some facts about the derivation of the  $n = 1$  case in [140]. The commutation relations can be expressed in terms of  $\alpha_3, \alpha_{\pm}$

$$\begin{aligned}\alpha_{\pm} &= \frac{1}{\sqrt{2}}(\alpha_1 \pm i\alpha_2), \\ [\alpha_3, \alpha_{\pm}] &= 2\alpha_{\pm}, \\ [\alpha_+, \alpha_-] &= 2\alpha_3, \\ c &= \alpha_+\alpha_- + \alpha_-\alpha_+ + \alpha_3^2\end{aligned}\tag{C.5}$$

With these normalisations, the eigenvalues of  $\alpha_3$  in the spin half representation are  $\pm 1$  and  $\alpha_+\alpha_-$  is 1 on the highest weight state.

It is useful to define a quantity  $\tilde{C}(p, q)$  which depends on two natural numbers  $p, q$  and counts the number of ways of separating  $p$  identical objects into  $q$  parts

$$\tilde{C}(p, q) = \frac{(p+q-1)!}{p!(q-1)!}\tag{C.6}$$

We begin by a review of the spin half case, establishing a counting which will be used again in more complicated cases below. This relies on a sum

$$2^k \sum_{\hat{i}_{2k}}^{2n-2k} \cdots \sum_{\hat{i}_2=0}^{\hat{i}_3} \sum_{\hat{i}_1=0}^{\hat{i}_2} (-1)^{\hat{i}_1+\hat{i}_2+\cdots+\hat{i}_{2k}} = 2^k \frac{n!}{(n-k)!k!}$$

Recall that this sum was obtained by evaluating a sequence of generators of  $SO(3)$  consisting of  $k$  pairs  $\alpha_-\alpha_+$  and with powers of  $\alpha_3$  between these pairs -

$$\alpha_3^{2J_{2k+1}} \alpha_+ \alpha_3^{2J_k} \alpha_- \cdots \alpha_- \alpha_3^{J_3} \alpha_+ \alpha_3^{J_2} \alpha_- \alpha_3^{J_1}\tag{C.7}$$

We can move the powers of  $\alpha_3$  to the left to get factors  $(\alpha_3 - 2)^{J_2+J_4+\cdots+J_{2k}}$ . Moving the  $\alpha_3$  with powers  $J_1, J_3, \dots$  gives  $\alpha_3^{J_1+J_3+\cdots}$ . The  $k$  powers of  $\alpha_-\alpha_+$  gives  $2^k$ . The above sum can be rewritten

$$2^k \sum_{J_{2k+1}=0}^{2m-2k} \cdots \sum_{J_2=0}^{2m-2k-J_3+\dots+J_{2k+1}} \sum_{J_1=0}^{2m-2k-J_2-\dots-J_{2k+1}} (-1)^{J_2+J_4+\dots+J_{2k}} = 2^k \frac{n!}{(n-k)!k!}\tag{C.8}$$

This includes a sum over  $J_e = J_2 + J_4 + \dots + J_{2k}$ . The summand does not depend on the individual  $J_2, J_4, \dots$  only on the sum  $J_e$  which ranges from 0 to  $2m - 2k$ . The sum over  $J_2, J_4, \dots$  is the combinatoric factor, introduced above, which is the number of ways of splitting  $J_e$  identical objects into  $k$  parts, i.e.  $\tilde{C}(J_e, k)$ . The remaining  $2m - 2k - J_e$  powers of  $\alpha_3$  are distributed in  $k + 1$  slots in  $\tilde{C}(2m - 2k - J_e, k + 1)$  ways. Hence the sum (C.8)

can be written more simply as

$$2^k \sum_{J_e=0}^{2m-2k} (-1)^{J_e} \tilde{C}(J_e, k) \tilde{C}(2m-2k-J_e, k+1) = 2^k \frac{m!}{(m-k)!k!} \quad (\text{C.9})$$

Then there is a sum over  $k$  from 0 to  $m$ , with weight

$$C(k, m) = \frac{2^k k! (2m-2k)! m!}{(m-k)! (2m)!} \quad (\text{C.10})$$

which gives the final result  $2m+1$  [140]. Similar sums arise in the proofs below. In some cases, closed formulae for the sums are obtained experimentally.

## C.2 Derivation of symmetrised trace for minimal $SO(2l+1)$ representation

The Casimir of interest here is

$$X_\mu X_\mu = X_{2l+1}^2 + \sum_{i=1}^l \left( X_-^{(i)} X_+^{(i)} + X_+^{(i)} X_-^{(i)} \right) \quad (\text{C.11})$$

The patterns are similar to those above, with  $\alpha_3$  replaced by  $X_{2l+1}$ , and noting that here there are  $l$  ‘‘colours’’ of  $\alpha_\pm$  which are  $X_\pm^{(l)}$ . All the states in the fundamental spinor are obtained by acting on a vacuum which is annihilated by  $l$  species of fermions. Generally we might expect patterns

$$\dots X_{2l+1}^{i_1} X_-^{(j_1)} X_{2l+1}^{i_2} X_+^{(j_2)} \dots \quad (\text{C.12})$$

In evaluating these, we can commute all the  $X_{2l+1}$  to the left. This results in shifts which do not depend on the value of  $j$ . It is easy to see that whenever  $X_+^{(1)}$  is followed by  $X_+^{(1)}$  we get zero because of the fermionic construction of the gamma matrices.  $X_+^{(1)}$  cannot also be followed by  $X_+^{(2)}$  because  $X_+^{(1)} X_+^{(2)} + X_+^{(2)} X_+^{(1)} = 0$ . So the pairs have to take the form  $X_-^{(j)} X_+^{(j)}$  for fixed  $j$ . The sum we have to evaluate is

$$\begin{aligned} & \sum_{k=0}^m \sum_{J_e=0}^{2m-2k} (-1)^{J_e} \tilde{C}(J_e, k) \tilde{C}(2m-2k-J_e, k) \tilde{C}(k, l) 2^k C(k, m) \\ &= \sum_{k=0}^m \binom{m}{k} 2^k C(k, m) \tilde{C}(k, l) \\ &= \frac{(2l+2m-1)!!}{(2m-1)!!(2l-1)!!} \end{aligned} \quad (\text{C.13})$$

The factors  $\tilde{C}(J_e, k)$  and  $\tilde{C}(2m - 2k - J_e, k)$  have the same origin as in the spin half case. The factor (C.10) is now generalised to an  $l$ -colour version

$$C(k_1, k_2 \dots k_l; m) = 2^k \frac{(2m - 2k)!}{(2m)!} \frac{m!}{(m - k)!} k_1! k_2! \dots k_l! \quad (\text{C.14})$$

This has to be summed over  $k_1, \dots, k_l$ . For fixed  $k = k_1 + \dots + k_l$  we have

$$\sum_{k_1 \dots k_l} C(k_1 \dots k_l, m) \frac{k!}{k_1! \dots k_l!} = \sum_{k_1 \dots k_l} C(k, m) = C(k, m) \tilde{C}(k, l) \quad (\text{C.15})$$

The combinatoric factor  $\frac{k!}{k_1! \dots k_l!}$  in the second line above comes from the different ways of distributing the  $k_1 \dots k_l$  pairs of  $(-+)$  operators in the  $k$  positions along the line of operators. The subsequent sum amounts to calculating the number of ways of separating  $k$  objects into  $l$  parts which is given by  $\tilde{C}(k, l)$ . The  $C(k, m)$  is familiar from (C.10). This sum can be done for various values of  $k, m$  and gives agreement with (C.3).

### C.3 Derivation of spin one symmetrised trace for $SO(3)$

For the spin one case more patterns will arise. After an  $\alpha_-$  acts on the highest weight, we get a state with  $\alpha_3 = 0$  so that we have, for any positive  $r$

$$\alpha_3^r \alpha_- |J = 1, \alpha_3 = 2 \rangle = 0, \quad \forall r > 0 \quad (\text{C.16})$$

Hence any  $\alpha_-$  can be followed immediately by  $\alpha_+$ . These neutral pairs of  $(\alpha_+ \alpha_-)$  can be separated by powers of  $\alpha_3$ . Alternatively an  $\alpha_-$  can be followed immediately by  $\alpha_-$ . The effect of  $\alpha_-^2$  is to change the highest weight state to a lowest weight state. In describing the patterns we have written the ‘‘vacuum changing operator’’ on the second line, with the first line containing only neutral pairs separated by  $\alpha_3$ ’s. Let there be  $J_1$  neutral pairs in this first line and  $L_1$  powers of  $\alpha_3$  distributed between them. After the change of vacuum, we can have a sequence of  $(\alpha_- \alpha_+)$  separated by powers of  $\alpha_3$ . Let there be a total of  $J_2$  neutral pairs and  $L_2$   $\alpha_3$ ’s in the second line. At the beginning of the third line we have another vacuum changing operator  $\alpha_+^2$  which takes us back to the highest weight state. In the third line, we have  $J_3$  neutral pairs and  $L_3$  powers of  $\alpha_3$ . The equation below describes a general pattern with  $p$  pairs of vacuum changing operators. The total number of neutral pairs is  $2p + J$  where  $J = J_1 + J_2 + \dots + J_{2p+1}$ . The general pattern of operators acting on



As usual  $X_i$  are expressed as operators acting on an  $n$ -fold tensor product, and

$$X_{\pm}^{(i)} = \sum_r \rho_r(\Gamma_{\pm}^{(i)}) . \quad (\text{C.18})$$

Some useful facts are

$$\begin{aligned} X_{2l+1}^r X_+ |0\rangle &= 0, & X_{2l+1}^r X_+^2 |0\rangle &= (-2)^r X_+^2 |0\rangle, \\ X_{2l+1}^r X_- X_+ |0\rangle &= X_- X_+ X_{2l+1}^r |0\rangle = (2)^r X_- X_+ |0\rangle, \\ X_- X_+ X_{2l+1}^r X_+^2 |0\rangle &= 0, & Y_+ X_+^2 + X_+^2 Y_+ |0\rangle &= 0, \\ X_+ Y_+ X_+ |0\rangle &= 0, & X_- Y_+ X_+ |0\rangle &= 0, \\ X_+ X_- X_+^2 |0\rangle &= Q(2,1) X_+^2 |0\rangle, & X_+ X_- X_+ Y_+ |0\rangle &= Q(2,1) X_+ Y_+ |0\rangle, \\ X_-^2 X_+^2 |0\rangle &= Q(2,2) |0\rangle, & Y_- X_- X_+ Y_+ |0\rangle &= Q(2,2) |0\rangle \end{aligned}$$

It is significant that the same  $Q(2,1), Q(2,2)$  factors appear in the different places in the above equation. In the above  $X_+$  stands for any of the  $l$   $X_+^{(i)}$ 's. Any equation containing  $X_{\pm}$  and  $Y_{\pm}$  stands for any pair  $X_{\pm}^{(i)}$  and  $X_{\pm}^{(j)}$  for  $i, j$  distinct integers from 1 to  $l$ .

The general pattern is similar to (C.17) with the only difference that the  $(\alpha_- \alpha_+)$  on the first line is replaced by any one  $(X_-^{(i)} X_+^{(i)})$  for  $i = 1, \dots, l$ . The positive vacuum changing operators can be  $(X_+^{(i)} X_+^{(j)})$ , where  $i, j$  can be identical or different. For every such choice the allowed neutral pairs following them are  $X_+^{(j)} X_-^{(i)}$  and the dual vacuum changing operator is  $(X_-^{(j)} X_-^{(i)})$ .

The summation we have to do is:

$$\begin{aligned} \sum_{p=0}^{[m/2]} \sum_{J=0}^{m-2p} \sum_{L_e=0}^{2m-4p-2J} \sum_{J_e=0}^J & \left( C(2p+J, m) \tilde{C}(2p+J, l) \tilde{C}(J_e, p) \tilde{C}(J-J_e, p+1) \times \right. \\ & (-1)^{L_e} \tilde{C}(L_e, J_e+p) \tilde{C}(2m-2J-4p-L_e, J-J_e+p+1) \times \\ & \left. 2^{2m-2J-4p} Q(1,1)^{J-J_e} Q(2,1)^{J_e} Q(2,2)^p \right) \end{aligned}$$

The  $Q$ -factors can be easily evaluated on the highest weight and then inserted into the above

$$Q(1,1) = 4, \quad Q(2,1) = 4 \quad Q(2,2) = 16 . \quad (\text{C.19})$$

By computing this for several values of  $m, l$ , we obtain (C.4). Note that both the  $l = 1$  and the general  $l$  case will yield the correct value for  $m = 0$ , which is 1.

# References

- [1] A. Brandhuber, S. McNamara, B. J. Spence and G. Travaglini, *Loop amplitudes in pure Yang-Mills from generalised unitarity*, JHEP **0510**, 011 (2005), [hep-th/0506068](#).
- [2] S. McNamara, C. Papageorgakis, S. Ramgoolam and B. Spence, *Finite  $N$  effects on the collapse of fuzzy spheres*, JHEP **0605**, 060 (2006), [hep-th/0512145](#).
- [3] G. 't Hooft, *A Planar Diagram Theory for Strong Interactions* Nucl. Phys. B **72**, 461 (1974).
- [4] J. M. Maldacena, *The large  $N$  limit of superconformal field theories and supergravity*, Adv. Theor. Math. Phys. **2**, 231 (1998), [Int. J. Theor. Phys. **38**, 1113 (1999)], [hep-th/9711200](#).
- [5] E. Witten, *Perturbative gauge theory as a string theory in twistor space*, Commun. Math. Phys. **252**, 189 (2004), [hep-th/0312171](#).
- [6] R. Penrose, *Twistor algebra*, J. Math. Phys. **8**, 345 (1967).
- [7] S. J. Parke and T. R. Taylor, *An Amplitude For  $N$  Gluon Scattering*, Phys. Rev. Lett. **56**, 2459 (1986).
- [8] F. Cachazo, P. Svrcek and E. Witten, *MHV vertices and tree amplitudes in gauge theory*, JHEP **0409**, 006 (2004), [hep-th/0403047](#).
- [9] F. A. Berends and W. Giele, *The Six Gluon Process As An Example Of Weyl-Van Der Waerden Spinor Calculus*, Nucl. Phys. B **294**, 700 (1987).
- [10] M. L. Mangano, S. J. Parke and Z. Xu, *Duality and Multi - Gluon Scattering*, Nucl. Phys. B **298**, 653 (1988).
- [11] N. Berkovits and E. Witten, *Conformal supergravity in twistor-string theory*, JHEP **0408**, 009 (2004), [hep-th/0406051](#).
- [12] A. Brandhuber, B. J. Spence and G. Travaglini, *One-loop gauge theory amplitudes in  $N = 4$  super Yang-Mills from MHV vertices*, Nucl. Phys. B **706**, 150 (2005), [hep-th/0407214](#).

- 
- [13] Z. Bern, L. J. Dixon, D. C. Dunbar and D. A. Kosower, *One loop  $n$  point gauge theory amplitudes, unitarity and collinear limits*, Nucl. Phys. B **425**, 217 (1994), [hep-ph/9403226](#).
- [14] Z. Bern, L. J. Dixon, D. C. Dunbar and D. A. Kosower, *Fusing gauge theory tree amplitudes into loop amplitudes*, Nucl. Phys. B **435**, 59 (1995), [hep-ph/9409265](#).
- [15] R. Britto, F. Cachazo and B. Feng, *Generalized unitarity and one-loop amplitudes in  $N = 4$  super-Yang-Mills*, Nucl. Phys. B **725**, 275 (2005), [hep-th/0412103](#).
- [16] R. Britto, F. Cachazo and B. Feng, *New recursion relations for tree amplitudes of gluons*, Nucl. Phys. B **715**, 499 (2005), [hep-th/0412308](#).
- [17] R. Britto, F. Cachazo, B. Feng and E. Witten, *Direct proof of tree-level recursion relation in Yang-Mills theory*, Phys. Rev. Lett. **94**, 181602 (2005), [hep-th/0501052](#).
- [18] Z. Bern, L. J. Dixon and D. A. Kosower, *On-shell recurrence relations for one-loop QCD amplitudes*, Phys. Rev. D **71**, 105013 (2005), [hep-th/0501240](#).
- [19] D. J. Gross and F. Wilczek, *Ultraviolet Behaviour of Non-Abelian Gauge Theories*, Phys. Rev. Lett. **30**, 1343 (1973).
- [20] H. D. Politzer, *Reliable Perturbative Results for Strong Interactions?*, Phys. Rev. Lett. **30**, 1346 (1973).
- [21] M. L. Mangano, *The Color Structure Of Gluon Emission*, Nucl. Phys. B **309**, 461 (1988).
- [22] Z. Bern and D. A. Kosower, *Color Decomposition Of One Loop Amplitudes In Gauge Theories*, Nucl. Phys. B **362**, 389 (1991).
- [23] R. Gastmans and T. T. Wu, *The Ubiquitous Photon: Helicity Method For QED And QCD*.
- [24] M. T. Grisaru, H. N. Pendleton and P. van Nieuwenhuizen, *Supergravity And The S Matrix*, Phys. Rev. D **15**, 996 (1977).
- [25] M. T. Grisaru and H. N. Pendleton, *Some Properties Of Scattering Amplitudes In Supersymmetric Theories*, Nucl. Phys. B **124**, 81 (1977).
- [26] M. Abou-Zeid, C. M. Hull and L. J. Mason, *Einstein supergravity and new twistor string theories*, [hep-th/0606272](#).
- [27] R. Roiban, M. Spradlin and A. Volovich, *A googly amplitude from the B-model in twistor space*, JHEP **0404**, 012 (2004), [hep-th/0402016](#).
- [28] R. Roiban and A. Volovich, *All googly amplitudes from the B-model in twistor space*, Phys. Rev. Lett. **93**, 131602 (2004), [hep-th/0402121](#).

- 
- [29] R. Roiban, M. Spradlin and A. Volovich, *On the tree-level S-matrix of Yang-Mills theory*, Phys. Rev. D **70**, 026009 (2004), [hep-th/0403190](#).
- [30] S. Gukov, L. Motl and A. Neitzke, *Equivalence of twistor prescriptions for super Yang-Mills*, [hep-th/0404085](#).
- [31] C. J. Zhu, *The googly amplitudes in gauge theory*, JHEP **0404**, 032 (2004), [hep-th/0403115](#).
- [32] G. Georgiou and V. V. Khoze, *Tree amplitudes in gauge theory as scalar MHV diagrams*, JHEP **0405**, 070 (2004), [hep-th/0404072](#).
- [33] J. B. Wu and C. J. Zhu, *MHV vertices and scattering amplitudes in gauge theory*, JHEP **0407**, 032 (2004), [hep-th/0406085](#).
- [34] J. B. Wu and C. J. Zhu, *MHV vertices and fermionic scattering amplitudes in gauge theory with quarks and gluinos*, JHEP **0409**, 063 (2004), [hep-th/0406146](#).
- [35] G. Georgiou, E. W. N. Glover and V. V. Khoze, *Non-MHV tree amplitudes in gauge theory*, JHEP **0407**, 048 (2004), [hep-th/0407027](#).
- [36] L. J. Dixon, E. W. N. Glover and V. V. Khoze, *MHV rules for Higgs plus multi-gluon amplitudes*, JHEP **0412**, 015 (2004), [hep-th/0411092](#).
- [37] Z. Bern, D. Forde, D. A. Kosower and P. Mastrolia, *Twistor-inspired construction of electroweak vector boson currents*, Phys. Rev. D **72**, 025006 (2005), [hep-ph/0412167](#).
- [38] K. Risager, *A direct proof of the CSW rules*, JHEP **0512**, 003 (2005), [hep-th/0508206](#).
- [39] F. Cachazo, P. Svrcek and E. Witten, *Twistor space structure of one-loop amplitudes in gauge theory*, JHEP **0410**, 074 (2004), [hep-th/0406177](#).
- [40] F. Cachazo, P. Svrcek and E. Witten, *Gauge theory amplitudes in twistor space and holomorphic anomaly*, JHEP **0410**, 077 (2004), [hep-th/0409245](#).
- [41] I. Bena, Z. Bern, D. A. Kosower and R. Roiban, *Loops in twistor space*, Phys. Rev. D **71**, 106010 (2005), [hep-th/0410054](#).
- [42] F. Cachazo, *Holomorphic anomaly of unitarity cuts and one-loop gauge theory amplitudes*, [hep-th/0410077](#).
- [43] R. Britto, F. Cachazo and B. Feng, *Computing one-loop amplitudes from the holomorphic anomaly of unitarity cuts*, Phys. Rev. D **71** (2005) 025012, [hep-th/0410179](#).
- [44] Z. Bern, V. Del Duca, L. J. Dixon and D. A. Kosower, *All non-maximally-helicity-violating one-loop seven-gluon amplitudes in  $N = 4$  super-Yang-Mills theory*, Phys. Rev. D **71** (2005) 045006, [hep-th/0410224](#).

- 
- [45] S. J. Bidder, N. E. J. Bjerrum-Bohr, L. J. Dixon and D. C. Dunbar,  *$N = 1$  supersymmetric one-loop amplitudes and the holomorphic anomaly of unitarity cuts*, Phys. Lett. B **606** (2005) 189, hep-th/0410296.
- [46] A. Brandhuber, B. Spence and G. Travaglini, *From trees to loops and back*, JHEP **0601**, 142 (2006), hep-th/0510253.
- [47] C. Quigley and M. Rozali, *One-loop MHV amplitudes in supersymmetric gauge theories*, JHEP **0501**, 053 (2005), hep-th/0410278.
- [48] J. Bedford, A. Brandhuber, B. J. Spence and G. Travaglini, *A twistor approach to one-loop amplitudes in  $N = 1$  supersymmetric Yang-Mills theory*, Nucl. Phys. B **706**, 100 (2005), hep-th/0410280.
- [49] J. Bedford, A. Brandhuber, B. J. Spence and G. Travaglini, *Non-supersymmetric loop amplitudes and MHV vertices*, Nucl. Phys. B **712**, 59 (2005), hep-th/041210.
- [50] P. Mansfield, *The Lagrangian origin of MHV rules*, JHEP **0603**, 037 (2006), hep-th/0511264.
- [51] A. Gorsky and A. Rosly, *From Yang-Mills Lagrangian to MHV diagrams*, JHEP **0601**, 101 (2006), hep-th/0510111.
- [52] J. H. Eittle and T. R. Morris, *Structure of the MHV-rules Lagrangian*, JHEP **0608**, 003 (2006), hep-th/0605121.
- [53] L. D. Landau, *On analytic properties of vertex parts in quantum field theory*, Nucl. Phys. **13**, 181 (1959).
- [54] S. Mandelstam, *Determination Of The Pion - Nucleon Scattering Amplitude From Dispersion Relations And Unitarity. General Theory*, Phys. Rev. **112**, 1344 (1958).
- [55] S. Mandelstam, *Analytic Properties Of Transition Amplitudes In Perturbation Theory*, Phys. Rev. **115**, 1741 (1959).
- [56] R. E. Cutkosky, *Singularities and discontinuities of Feynman amplitudes*, J. Math. Phys. **1**, 429 (1960).
- [57] R.J. Eden, P.V. Landshoff, D.I. Olive, J.C. Polkinghorne, *The Analytic S-Matrix*. Cambridge University Press 1966.
- [58] W. L. van Neerven, *Dimensional Regularization Of Mass And Infrared Singularities In Two Loop On-Shell Vertex Functions*, Nucl. Phys. B **268** (1986) 453.
- [59] Z. Bern and A. G. Morgan, *Massive Loop Amplitudes from Unitarity*, Nucl. Phys. B **467** (1996) 479, hep-ph/9511336.

- 
- [60] Z. Bern, L. J. Dixon, D. C. Dunbar and D. A. Kosower, *One-loop self-dual and  $N = 4$  super Yang-Mills*, Phys. Lett. B **394** (1997) 105, [hep-th/9611127](#).
- [61] S. D. Badger, E. W. N. Glover, V. V. Khoze and P. Svrcek, *Recursion relations for gauge theory amplitudes with massive particles*, JHEP **0507**, 025 (2005), [hep-th/0504159](#).
- [62] Z. Bern, L. J. Dixon and D. A. Kosower, *One-loop amplitudes for  $e^+ e^-$  to four partons*, Nucl. Phys. B **513** (1998) 3, [hep-ph/9708239](#).
- [63] Z. Bern, L. J. Dixon and D. A. Kosower, *A two-loop four-gluon helicity amplitude in QCD*, JHEP **0001** (2000) 027, [hep-ph/0001001](#).
- [64] Z. Bern, L. J. Dixon and D. A. Kosower, *Two-loop  $g \rightarrow g g$  splitting amplitudes in QCD*, JHEP **0408** (2004) 012, [hep-ph/0404293](#).
- [65] C. Anastasiou, Z. Bern, L. J. Dixon and D. A. Kosower, *Planar amplitudes in maximally supersymmetric Yang-Mills theory*, Phys. Rev. Lett. **91**, 251602 (2003), [hep-th/0309040](#).
- [66] C. Anastasiou, L. J. Dixon, Z. Bern and D. A. Kosower, *Cross-order relations in  $N = 4$  supersymmetric gauge theories*, [hep-th/0402053](#).
- [67] Z. Bern, L. J. Dixon and V. A. Smirnov, *Iteration of planar amplitudes in maximally supersymmetric Yang-Mills theory at three loops and beyond*, Phys. Rev. D **72**, 085001 (2005), [hep-th/0505205](#).
- [68] Z. Bern, M. Czakon, D. A. Kosower, R. Roiban and V. A. Smirnov, *Two-loop iteration of five-point  $N = 4$  super-Yang-Mills amplitudes*, [hep-th/0604074](#).
- [69] S. J. Bidder, N. E. J. Bjerrum-Bohr, D. C. Dunbar and W. B. Perkins, *One-loop gluon scattering amplitudes in theories with  $N \leq 4$  supersymmetries*, Phys. Lett. B **612**, 75 (2005), [hep-th/0502028](#).
- [70] R. Britto, E. Buchbinder, F. Cachazo and B. Feng, *One-loop amplitudes of gluons in SQCD*, Phys. Rev. D **72**, 065012 (2005), [hep-ph/0503132](#).
- [71] M. x. Luo and C. k. Wen, *Recursion relations for tree amplitudes in super gauge theories*, JHEP **0503**, 004 (2005), [hep-th/0501121](#).
- [72] M. x. Luo and C. k. Wen, *Compact formulas for all tree amplitudes of six partons*, Phys. Rev. D **71**, 091501 (2005), [hep-th/0502009](#).
- [73] J. Bedford, A. Brandhuber, B. J. Spence and G. Travaglini, *A recursion relation for gravity amplitudes*, Nucl. Phys. B **721**, 98 (2005), [hep-th/0502146](#).
- [74] F. Cachazo and P. Svrcek, *Tree level recursion relations in general relativity*, [hep-th/0502160](#).

- 
- [75] Z. Bern, L. J. Dixon and D. A. Kosower, *The last of the finite loop amplitudes in QCD*, Phys. Rev. D **72**, 125003 (2005), [hep-ph/0505055](#).
- [76] Z. Bern, L. J. Dixon and D. A. Kosower, *Bootstrapping multi-parton loop amplitudes in QCD*, Phys. Rev. D **73**, 065013 (2006), [hep-ph/0507005](#).
- [77] C. F. Berger, Z. Bern, L. J. Dixon, D. Forde and D. A. Kosower, *Bootstrapping one-loop QCD amplitudes with general helicities*, [hep-ph/0604195](#).
- [78] C. F. Berger, Z. Bern, L. J. Dixon, D. Forde and D. A. Kosower, *All one-loop maximally helicity violating gluonic amplitudes in QCD*, [hep-ph/0607014](#).
- [79] Z. Bern, N. E. J. Bjerrum-Bohr, D. C. Dunbar and H. Ita, *Recursive calculation of one-loop QCD integral coefficients*, JHEP **0511**, 027 (2005), [hep-ph/0507019](#).
- [80] H. Kawai, D. C. Lewellen and S. H. H. Tye, *A Relation Between Tree Amplitudes Of Closed And Open Strings*, Nucl. Phys. B **269**, 1 (1986).
- [81] N. E. J. Bjerrum-Bohr, D. C. Dunbar, H. Ita, W. B. Perkins and K. Risager, *MHV-vertices for gravity amplitudes*, JHEP **0601**, 009 (2006), [hep-th/0509016](#).
- [82] Z. Bern and D. A. Kosower, *The Computation of loop amplitudes in gauge theories*, Nucl. Phys. B **379**, 451 (1992).
- [83] Z. Bern, L. J. Dixon and D. A. Kosower, *New QCD Results From String Theory*, [hep-th/9311026](#).
- [84] Z. Bern, G. Chalmers, L. J. Dixon and D. A. Kosower, *One loop N gluon amplitudes with maximal helicity violation via collinear limits*, Phys. Rev. Lett. **72**, 2134 (1994), [hep-ph/9312333](#).
- [85] Z. Bern, L. J. Dixon and D. A. Kosower, *One loop corrections to five gluon amplitudes*, Phys. Rev. Lett. **70**, 2677 (1993), [hep-ph/9302280](#).
- [86] Z. G. Xiao, G. Yang and C. J. Zhu, *The rational part of QCD amplitude. III: The six-gluon*, [hep-ph/0607017](#).
- [87] S. Moch, J. A. M. Vermaseren and A. Vogt, *The three-loop splitting functions in QCD: The non-singlet case*, Nucl. Phys. B **688**, 101 (2004), [hep-ph/0403192](#).
- [88] A. V. Kotikov, L. N. Lipatov, A. I. Onishchenko and V. N. Velizhanin, *Three-loop universal anomalous dimension of the Wilson operators in N=4 SUSY Yang-Mills model*, Phys. Lett. B **595**, 521 (2004), [Erratum-ibid. B **632**, 754 (2006)], [hep-th/0404092](#).
- [89] N. Beisert, V. Dippel and M. Staudacher, *A novel long range spin chain and planar N = 4 super Yang-Mills*, JHEP **0407**, 075 (2004), [hep-th/0405001](#).
- [90] B. Eden and M. Staudacher, *Integrability and transcendentality*, [hep-th/0603157](#).

- 
- [91] S. Frolov and A. A. Tseytlin, *Semiclassical quantization of rotating superstring in  $AdS(5) \times S(5)$* , JHEP **0206**, 007 (2002), [hep-th/0204226](#).
- [92] H. Ooguri and C. Vafa, *Worldsheet derivation of a large  $N$  duality*, Nucl. Phys. B **641**, 3 (2002), [hep-th/0205297](#).
- [93] R. Gopakumar, *From free fields to  $AdS$* , Phys. Rev. D **70**, 025009 (2004), [hep-th/0308184](#).
- [94] G. 't Hooft and M. J. G. Veltman, *One Loop Divergences In The Theory Of Gravitation*, Annales Poincare Phys. Theor. A **20**, 69 (1974).
- [95] Z. Bern, *Perturbative quantum gravity and its relation to gauge theory*, Living Rev. Rel. **5**, 5 (2002), [gr-qc/0206071](#).
- [96] Z. Bern and G. Chalmers, *Factorization in one loop gauge theory*, Nucl. Phys. B **447**, 465 (1995), [hep-ph/9503236](#).
- [97] D. A. Kosower and P. Uwer, *One-loop splitting amplitudes in gauge theory*, Nucl. Phys. B **563**, 477 (1999), [hep-ph/9903515](#).
- [98] D. C. Dunbar and P. S. Norridge, *Calculation of graviton scattering amplitudes using string based methods*, Nucl. Phys. B **433**, 181 (1995), [hep-th/9408014](#).
- [99] Z. Bern, L. J. Dixon, M. Perelstein and J. S. Rozowsky, *One-loop  $n$ -point helicity amplitudes in (self-dual) gravity*, Phys. Lett. B **444**, 273 (1998), [hep-th/9809160](#).
- [100] Z. Bern, L. J. Dixon, M. Perelstein and J. S. Rozowsky, *Multi-leg one-loop gravity amplitudes from gauge theory*, Nucl. Phys. B **546**, 423 (1999), [hep-th/9811140](#).
- [101] C. F. Berger, *Bootstrapping one-loop QCD amplitudes*, [hep-ph/0608027](#).
- [102] W. Nahm, *A Simple Formalism For The Bps Monopole*, Phys. Lett. B **90**, 413 (1980),
- [103] M. F. Atiyah, N. J. Hitchin, V. G. Drinfeld and Y. I. Manin, *Construction Of Instantons*, Phys. Lett. A **65**, 185 (1978),
- [104] N. R. Constable, R. C. Myers and O. Tafjord, *The noncommutative bion core*, Phys. Rev. D **61**, 106009 (2000), [hep-th/9911136](#).
- [105] N. R. Constable, R. C. Myers and O. Tafjord, *Non-Abelian brane intersections*, JHEP **0106**, 023 (2001), [hep-th/0102080](#).
- [106] P. Cook, R. de Mello Koch and J. Murugan, *Non-Abelian BIon brane intersections*, Phys. Rev. D **68**, 126007 (2003), [hep-th/0306250](#).
- [107] E. Witten, *Bound states of strings and  $p$ -branes*, Nucl. Phys. B **460**, 335 (1996), [hep-th/9510135](#).

- 
- [108] W. I. Taylor and M. Van Raamsdonk, *Multiple Dp-branes in weak background fields*, Nucl. Phys. B **573**, 703 (2000), [hep-th/9910052](#).
- [109] R. C. Myers, *Dielectric-branes*, JHEP **9912**, 022 (1999), [hep-th/9910053](#).
- [110] R. C. Myers, “*Nonabelian phenomena on D-branes*”, Class. Quant. Grav. **20**, S347 (2003), [hep-th/0303072](#).
- [111] C. V. Johnson, *D-branes*, Cambridge University Press (2003).
- [112] J. Madore, *The fuzzy sphere*, Class. Quant. Grav. **9**, 69 (1992).
- [113] H. Grosse, C. Klimcik and P. Presnajder, *Finite quantum field theory in noncommutative geometry*, Commun. Math. Phys. **180**, 429 (1996), [hep-th/9602115](#).
- [114] J. Castelino, S. M. Lee and W. I. Taylor, *Longitudinal 5-branes as 4-spheres in matrix theory*, Nucl. Phys. B **526**, 334 (1998), [hep-th/9712105](#).
- [115] S. Ramgoolam, *On spherical harmonics for fuzzy spheres in diverse dimensions*, Nucl. Phys. B **610**, 461 (2001), [hep-th/0105006](#).
- [116] Y. Kimura, *On higher dimensional fuzzy spherical branes*, Nucl. Phys. B **664**, 512 (2003), [hep-th/0301055](#).
- [117] W. Fulton, J. Harris, *Representation theory*, Springer (1991).
- [118] P. M. Ho and S. Ramgoolam, *Higher dimensional geometries from matrix brane constructions*, Nucl. Phys. B **627**, 266 (2002), [hep-th/0111278](#).
- [119] H. B. Lawson, M. Michelson, *Spin Geometry*, Princeton University Press.
- [120] C. G. Callan and J. M. Maldacena, *Brane dynamics from the Born-Infeld action*, Nucl. Phys. B **513**, 198 (1998), [hep-th/9708147](#).
- [121] P. S. Howe, N. D. Lambert and P. C. West, *The self-dual string soliton*, Nucl. Phys. B **515**, 203 (1998), [hep-th/9709014](#).
- [122] G. W. Gibbons, *Born-Infeld particles and Dirichlet p-branes*, Nucl. Phys. B **514**, 603 (1998), [hep-th/9709027](#).
- [123] Y. Kimura, *Nonabelian gauge field and dual description of fuzzy sphere*, JHEP **0404**, 058 (2004), [hep-th/0402044](#).
- [124] E. Witten, *Sigma models and the ADHM construction of instantons*, J. Geom. Phys. **15**, 215 (1995), [hep-th/9410052](#).
- [125] E. Witten, *Small Instantons in String Theory*, Nucl. Phys. B **460**, 541 (1996), [hep-th/9511030](#).

- 
- [126] M. R. Douglas, *Gauge Fields and D-branes*, J. Geom. Phys. **28**, 255 (1998), hep-th/9604198.
- [127] M. R. Douglas and G. W. Moore, *D-branes, Quivers, and ALE Instantons*, hep-th/9603167.
- [128] D. E. Diaconescu, *D-branes, monopoles and Nahm equations*, Nucl. Phys. B **503**, 220 (1997), hep-th/9608163.
- [129] M. Bianchi, M. B. Green, S. Kovacs and G. Rossi, *Instantons in supersymmetric Yang-Mills and D-instantons in IIB superstring theory*, JHEP **9808**, 013 (1998), hep-th/9807033.
- [130] N. Dorey, T. J. Hollowood, V. V. Khoze, M. P. Mattis and S. Vandoren, *Multi-instanton calculus and the AdS/CFT correspondence in  $N = 4$  superconformal field theory*, Nucl. Phys. B **552**, 88 (1999), hep-th/9901128.
- [131] C. Bachas, J. Hoppe and B. Pioline, *Nahm equations,  $N = 1^*$  domain walls, and D-strings in  $AdS(5) \times S(5)$* , JHEP **0107**, 041 (2001), hep-th/0007067.
- [132] K. Hashimoto and S. Terashima, *Stringy derivation of Nahm construction of monopoles*, JHEP **0509**, 055 (2005), hep-th/0507078.
- [133] K. Hashimoto and S. Terashima, *ADHM is tachyon condensation*, JHEP **0602**, 018 (2006), hep-th/0511297.
- [134] T. Asakawa, S. Matsuura and K. Ohta, *Construction of Instantons via Tachyon Condensation*, hep-th/0604104.
- [135] N. R. Constable and N. D. Lambert, *Calibrations, monopoles and fuzzy funnels*, Phys. Rev. D **66**, 065016 (2002), hep-th/0206243.
- [136] A. Basu and J. A. Harvey, *The M2-M5 brane system and a generalized Nahm's equation*, Nucl. Phys. B **713**, 136 (2005), hep-th/0412310.
- [137] D. S. Berman and N. B. Copland, *Five-brane calibrations and fuzzy funnels*, Nucl. Phys. B **723**, 117 (2005), hep-th/0504044.
- [138] D. S. Berman and N. B. Copland, *A note on the M2-M5 brane system and fuzzy spheres*, hep-th/0605086.
- [139] D. J. Gross and N. A. Nekrasov, *Monopoles and strings in noncommutative gauge theory*, JHEP **0007**, 034 (2000), hep-th/0005204.
- [140] S. Ramgoolam, B. J. Spence and S. Thomas, *Resolving brane collapse with  $1/N$  corrections in non-Abelian DBI*, Nucl. Phys. B **703**, 236 (2004), hep-th/0405256.

- 
- [141] A. A. Tseytlin, *Born-Infeld action, supersymmetry and string theory*, hep-th/9908105.
- [142] P. M. Sutcliffe, *BPS monopoles*, Int. J. Mod. Phys. A **12**, 4663 (1997), hep-th/9707009.
- [143] T. Banks, W. Fischler, S. H. Shenker and L. Susskind, *M theory as a matrix model: A conjecture*, Phys. Rev. D **55** (1997) 5112, hep-th/9610043.
- [144] D. Kabat and W. I. Taylor, *Spherical membranes in matrix theory*, Adv. Theor. Math. Phys. **2** (1998) 181, hep-th/9711078.
- [145] H. Grosse, C. Klimcik and P. Presnajder, *Finite quantum field theory in noncommutative geometry*, Commun. Math. Phys. **180** (1996) 429, hep-th/9602115.
- [146] J. Castelino, S. M. Lee and W. I. Taylor, *Longitudinal 5-branes as 4-spheres in matrix theory*, Nucl. Phys. B **526** (1998) 334, hep-th/9712105.
- [147] Y. Kimura, *Noncommutative gauge theory on fuzzy four-sphere and matrix model*, Nucl. Phys. B **637** (2002) 177, hep-th/0204256.
- [148] T. Azuma and M. Bagnoud, *Curved-space classical solutions of a massive supermatrix model*, Nucl. Phys. B **651** (2003) 71, hep-th/0209057.
- [149] B. P. Dolan, D. O'Connor and P. Presnajder, *Fuzzy Complex Quadrics and Spheres*, JHEP **0402** (2004) 055, hep-th/0312190.
- [150] A. Hashimoto and W. I. Taylor, *Fluctuation spectra of tilted and intersecting D-branes from the Born-Infeld action*, Nucl. Phys. B **503** (1997) 193, hep-th/9703217.
- [151] A. Sevrin, J. Troost and W. Troost, *The non-Abelian Born-Infeld action at order  $F^*F^6$* , Nucl. Phys. B **603** (2001) 389, hep-th/0101192.
- [152] A. Sevrin and A. Wijns, *Higher order terms in the non-Abelian D-brane effective action and magnetic background fields*, JHEP **0308** (2003) 059, hep-th/0306260.
- [153] D. Oprisa and S. Stieberger, *Six gluon open superstring disk amplitude, multiple hypergeometric series and Euler-Zagier sums*, hep-th/0509042.
- [154] C. Papageorgakis and S. Ramgoolam, *Large-small dualities between periodic collapsing / expanding branes and brane funnels*, Nucl. Phys. B **731** (2005) 45, hep-th/0504157.
- [155] C. Papageorgakis, S. Ramgoolam and N. Toumbas, *Noncommutative geometry, quantum effects and DBI-scaling in the collapse of D0-D2 bound states*, hep-th/0510144.
- [156] E. Silverstein and D. Tong, *Scalar speed limits and cosmology: Acceleration from D-acceleration*, Phys. Rev. D **70** (2004) 103505, hep-th/0310221.

- 
- [157] A. Hamilton, D. Kabat, G. Lifschytz and D. A. Lowe, *Local bulk operators in AdS/CFT: A boundary view of horizons and locality*, hep-th/0506118.
- [158] M. Alishahiha, E. Silverstein and D. Tong, *DBI in the sky*, Phys. Rev. D **70** (2004) 123505, hep-th/0404084.
- [159] W. I. Taylor and M. Van Raamsdonk, *Supergravity currents and linearized interactions for matrix theory configurations with fermionic backgrounds*, JHEP **9904** (1999) 013, hep-th/9812239.
- [160] G. W. Gibbons, *Thoughts on tachyon cosmology*, Class. Quant. Grav. **20** (2003) S321, hep-th/0301117.
- [161] S. Thomas and J. Ward, *Fuzzy sphere dynamics and non-Abelian DBI in curved backgrounds*, hep-th/0508085.